Anders Thorstensen

2D and 3D echocardiography during inotropic alterations and after recent myocardial infarction

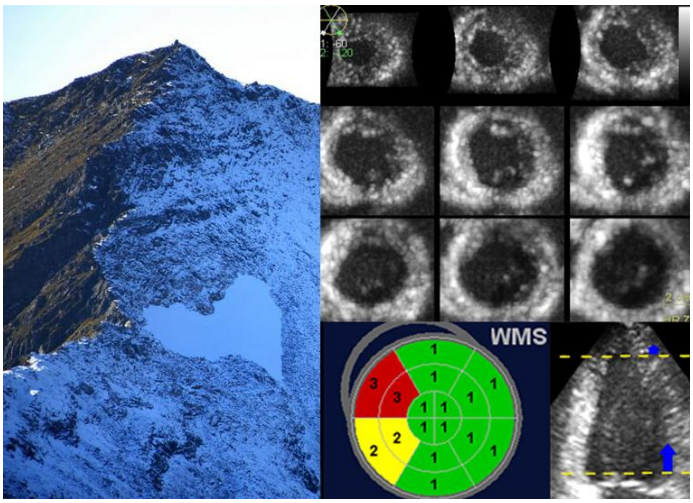

Thesis for the degree of Philosophiae Doctor

Trondheim, December 2012

MI Lab and Department of Circulation and Medical Imaging,

Norwegian University of Science and Technology

Trondheim, Norway

Department of Cardiology

St Olavs Hospital/Trondheim University Hospital,

Trondheim, Norway

NTNU

Norwegian University of Science and Technology

Thesis for the degree of Philosophiae Doctor

Faculty of Medicine

MI Lab and Department of Circulation and Medical Imaging,

Trondheim, Norway

2012:378 ISBN 978-82-471-4094-9 (printed ver.)

2012:378 ISBN 978-82-471-4095-6 (electronic ver.)

Norsk Sammendrag

Vurdering av venstre ventrikkels størrelse og funksjon er helt sentral ved enhver ekkokardiografisk undersøkelse og den vanligste kliniske indikasjon for å utføre ultralyd av hjertet. I dette prosjektet ble hjertefunksjonen hovedsakelig undersøkt ved hjelp av todimensjonal og tredimensjonal beregning av ejeksjonsfraksjon, hastighetsmålinger i hjertemuskelen ved hjelp av vevsdoppler, todimensjonal og tredimensjonal speckle tracking (mønsterfølging) og visuell vurdering av veggfortykkelse i gråtonebildet. Et viktig mål med prosjektet var å evaluere tradisjonelle og moderne ekkokardiografiske metoders repeterbarhet og evne til å detektere endringer i hjertets kontraktilitet. Et annet hovedmål var å validere nøyaktigheten av direkte ekkokardiografisk beregning av hjerteinfarktstørrelse, og å evaluere nytteverdien av 3D ekkokardiografi hos pasienter med hjerteinfarkt.

Artikkel 1:

10 friske forsøkspersoner ble undersøkt med ekkokardiografi av 2 ulike leger, som hver for seg analyserte ulike mål på hjertefunksjon både på sine egne opptak (2 ganger) og på den andre legens ultralydopptak. Repeterbarheten av målingene ble analysert. Alle mål hadde akseptabel repeterbarhet, men målinger som var gjennomsnitt av flere enkeltmålinger hadde best repeterbarhet. Repeterbarheten var bedre når det samme ultralydopptaket ble analysert 2 ganger, sammenlignet med når legene analyserte to ulike ultralydopptak.

Artikkel 2:

33 friske forsøkspersoner ble undersøkt med ekkokardiografi i hvile, under medikamentstress med lavdose dobutamin og etter injeksjon av beta-blocker. Ulike ekkokardiografiske metoders relative endring fra hvile til stress og fra hvile til beta-blokker påvirkning ble undersøkt. Studien viste at det var et markert skille mellom hastighetsrelaterte målinger tidlig i hjertets

sammentrekningsfase (systolen) og slagvolumrealterte ende-systoliske målinger. Hastighetsrelaterte målinger som klaffeplanhastighet, strain rate og blodstrømshastighet i utløpstraktus var mest følsomme for endringer i kontraktilitet, noe som kan indikere at disse målingene også er best egnet for å påvise endringer i hjertefunksjonen i klinisk praksis.

Artikkel 3:

I studien valideres direkte automatisert ekkokardiografisk beregning av hjerteinfarktstørrelse, som er en ny metode utviklet ved vårt institutt, på 58 pasienter med gjennomgått førstegangs hjerteinfarkt og 35 kjønns- og aldersmatchede friske fra Helseundersøkelsen i Nord Trøndelag. Den nye metoden er basert på fargekodet vevsdoppler strain rate med manuell korreksjon ut i fra visuell vurdering av veggfortykkelse i gråtonebildet. Metoden skilte best mellom små og store infarkter når infarktstørrelse på 12% ble benyttet som cut-off, og hadde høyere korrelasjon med kontrast-MR sammenliknet med ejeksjonsfraksjon, speckle tracking basert global strain, visuell vurdering av veggfortykkelse, langakseforkortning og klaffeplanhastighet. Rapportering av prosentvis infarktstørrelse i stedet for funksjonelle mål vil være enklere å forstå for pasienter og helsepersonell uten kjennskap til avansert ekkokardiografisk terminologi.

Artikkel 4:

I denne studien ble de samme personene som deltok i studie 3 undersøkt med 2D og 3D ekkokardiografi. Visuell vurdering av veggfortykkelsen med 3D ekkokardiografi var spesielt nyttig ved undersøkelse av pasienter med godt akustisk vindu fra hjertets apex. Totalt sett var visuell vurdering av veggfortykkelsen med 2D og 3D ekkokardiografi og 2D speckle tracking basert strain mer nøyaktig enn måling av ejeksjonsfraksjonen og 3D speckle tracking basert strain ved måling av global og regional funksjon, når kontrast-MR ble benyttet som referansemetode.

Content

page

Acknowledgements

The research has been funded by the Norwegian Research Council, through the Centre for Research-based Innovation, Medical Imaging Laboratory (MI Lab). There are several public health-care partners as well as industry partners in MI lab. The research was carried out at the Department of Circulation and Medical Imaging, NTNU. Associate Professor Asbjørn Støylen, Department of Circulation and Medical Imaging, NTNU has been my main supervisor and the architect of this project. I am grateful for his contribution to this thesis and for guiding me into the world of research. Learning from his excellent expertise of both technical and clinical echocardiography has been a privilege. I have learnt a lot from his comments and advices. In addition, Asbjørn has been my teacher in clinical stress echocardiography.

I also want to express my gratitude to my co-supervisors Brage Amundsen and Professor Hans Torp, both at the Department of Circulation and Medical Imaging, NTNU. Brage has recorded and analysed the magnetic resonance imaging (MRI) recordings. He has shared his excellent knowledge of cardiac imaging and has really impressed me when it comes to the art of writing. Hans has been my technical supervisor. He is a brilliant researcher and I really appreciate his useful comments and advices. Thus, thanks to both of you for the significant contribution to this work.

My co-authors Håvard Dalen, Svein Arne Aase, Pavel Hala, Gabriel Kiss and Jan D'hooge also deserve a huge thank. Many meaningful discussions have improved this work with regard to both technical and clinical aspects. I owe a special thank to Håvard, my colleague, fellow PhD student, co-author and friend who has significantly contributed to this thesis. We have shared office, joy and frustrations during several years of research. I admire

Håvards tremendous working energy and excellent skills in echocardiography and many other topics. It has been a great pleasure to collaborate with him.

I also gratefully acknowledge the technical support from the GE Vingmed Ultrasound staff in Trondheim, with Svein Arne Aase and Vidar Lundberg specially mentioned. During my years of research I have had the pleasure of sharing office with Siri Ann Nyrnes, who among other things has inspired me to go more cross country skiing (even in bad weather). All my present and previous colleagues at the Department of Cardiology Trondheim University Hospital deserves a great thank as well. In particular I am grateful for the helpfulness and assistance of research nurses Ann-Elise Antonsen and Eli Granviken in two of my clinical studies. Olav Haraldseth, Øyvind Ellingsen and Rune Wiseth each deserves a special thank for making it possible to combine clinical work and work with this thesis. I would also like to thank all my former colleagues at Innlandet Hospital, division Hamar and Elverum who introduced me to the exciting world of cardiology.

A special thanks to all my friends who still are my friends, even though I have turned down most invitations in the recent time period. I want to thank my parents for showing interest in my work. Finally, I will thank Wenche for always being there, for always claiming that I will make it, and for ignoring some research-related frustrations. More important you have given birth to two children during the work with this thesis. Now, we have three fantastic children who have been very lucky in their choice of mother. Magnus, Julie and Sondre, thanks for bringing joy and happiness into our lives.

List of papers

Paper 1:

Thorstensen A, Dalen H, Amundsen BH, Aase SA, Støylen A.

Reproducibility in echocardiographic assessment of the left ventricular global and regional function, the HUNT study. Eur J Echocardiogr 2010; 11:149-56.

Paper 2:

Thorstensen A, Dalen H, Amundsen BH, Støylen A.

Peak systolic velocity indices are more sensitive than end-systolic indices in detecting contraction changes assessed by echocardiography in young healthy humans. Eur J Echocardiogr 2011; 12:924-30.

Paper 3:

Thorstensen A, Amundsen BH, Dalen H, Hala P, Kiss G, Aase SA, Torp H, Støylen A.

Strain rate imaging combined with wall motion analysis gives incremental value in direct quantification of myocardial infarct size. Eur Heart J Cardiovasc Imaging. 2012 Apr 12

Paper 4:

Thorstensen A, Dalen H, Hala P, Kiss G, D'hooge J, Torp H, Støylen A Amundsen BH.

Diagnostic accuracy of 3D echocardiography in patients with recent myocardial infarction - a comparison with magnetic resonance imaging.

Manuscript submitted Echocardiography 2012

Abbreviation list

A = mitral flow late atrial filling velocity

a`= peak late annular diastolic velocity

AUC = area under the receiver operating characteristic curves

B-mode = brightness mode

E = mitral flow early diastolic filling velocity

e′ = peak early diastolic annular velocity

FPS = frames per second

LE-MRI = late enhancement magnetic resonance imaging

LV = left ventricular

LVEF = left ventricular ejection fraction

LVOT = left ventricular outflow tract

MRI = magnetic resonance imaging

MAE = mitral annular excursion

MI = myocardial infarction

M-mode = motion-mode

S' = peak systolic mitral annulus velocity

SD = standard deviation

TD = tissue Doppler

WMS(I) = wall motion score (index)

2D = two-dimensional

3D = three-dimensional

1 Introduction

1.1 Echocardiography

Echocardiography is the most widely used method for assessing left and right ventricular function, valvular disease and cardiac abnormalities (1).

1.1.1 Selected history of cardiac ultrasound in Trondheim

The history of cardiac ultrasound started in Sweden with Edlers description of cardiac structures by the ultrasound reflectoscope already in 1953 (2). Subsequent pioneer research led to the development of continuous and pulsed wave Doppler and the first presentation of real-time two-dimensional (2D) real-time cardiac images by Hertz and Asberg in 1967. However, invasive catheterization remained the main method to assess cardiac function for still some years. Further development and validation of cardiac ultrasound was necessary, and in Trondheim, Liv Hatle and Bjørn Angelsen made important contributions in validating the Doppler methods as tools for diagnosing and monitoring cardiac diseases. Angelsen and colleagues developed the pulsed echo Doppler flow velocity meter (PEDOF) which was the basis for the first publication of non-invasive assessment of pressure gradient in mitral stenosis by Holen in 1976 (3). Subsequently, several pioneering studies were conducted by Hatle, Angelsen, Brubakk, Skjærpe and colleagues on the clinical use of Doppler showing that non-invasive Doppler examination could replace cardiac catheterization in diagnosing different non-coronary cardiac diseases (4-8). These developments were followed by new important studies for the diagnosis of cardiac disease by the Trondheim group. Estimation of the valve area in patients with aortic stenosis and hemodynamic evaluation of aortic prostheses by Doppler ultrasound and 2D echocardiography were described (9-11). The Trondheim group contributed to better understanding of the diastolic function and showed

that left ventricular (LV) diastolic pressures could be estimated by pulmonary venous flow Doppler (12). The technical – clinical cooperation continued, with Hans Torp as an important contributor on the technical (software) side. The aortic and mitral blood flow profiles were described in detail by 2D and three-dimensional (3D) colour flow Doppler (13, 14). Contributions to better understanding of the LV function and the ventriculo-arterial interaction in patients with hypertension were published (15, 16). The accuracy of contrast echocardiography compared with magnetic resonance imaging has been evaluated (17). Pioneer research and validation of strain and strain rate by tissue Doppler (TD) in Trondheim started a new international era in cardiac research (18-21). Validation of new methodology based on tissue Doppler and 3D endocardial surface reconstruction in patients undergoing dobutamine stress echocardiography were performed (22, 23), and the feasibility of automated analysis of myocardial deformation was demonstrated (24, 25). More recently, strain measurements by speckle tracking have been validated against magnetic resonance imaging (26), and reference values for strain, strain rate and annular velocities have been established (27, 28). The ultrasound research group is currently part of the department of Circulation and Medical Imaging, NTNU, and a substantial part of ultrasound research in fields like 3D-echocardiography, high frame rate in 2D tissue Doppler imaging, handhold ultrasound (29) and blood flow imaging (30), is done in collaboration with MI-lab.

1.1.2 Grey scale and Doppler echocardiography

Ultrasound is generated by piezoelectric crystals that vibrate when being compressed and decompressed. The same crystals can act as receivers of reflected ultrasound from reflecting structures, usually termed scatters. The amplitude of the reflected ultrasound pulse and the distance from the probe can be displayed on monitors as brightness-points as in M-mode (motion-mode) or B-mode (brightness mode) images. Grey scale echocardiography by M-mode was the first ultrasound modality that displayed moving echoes from the heart and is

still an important tool in clinical practice. Cardiac structures are displayed on the vertical axis corresponding to the distance from the transducer while the horizontal axis gives the time period. The high resolution of M-mode (up to 1000 FPS (frames per second)) is favourable in the timing of events in the cardiac cycle. M-mode is also frequently used for estimation of chamber sizes and the long axis function.

Grey scale echocardiography by B-mode is the most important ultrasound mode for visual evaluation of cardiac anatomy and function, and is also used as underlying guiding tool when cardiac function is quantified. Visualization of the endocardial surface in B-mode recordings enables measurements of chamber volumes and ejection fraction. Left ventricular ejection fraction (LVEF) is the most widely used measurement of global LV systolic function. B-mode recordings also allow judgement of the regional function by visual judgement of wall thickening during the cardiac cycle, but the temporal resolution is far lower than M-mode. The frame rate depends on the sector width and depth, as well as the line density (lateral resolution). Typically, a 2D sector covering the left ventricle has a frame rate of about 50 FPS.

The Doppler methods are based on detection of the Doppler shift from moving scatters (31). The frequency of reflected ultrasound is altered by moving targets (red blood cells or myocardium). The Doppler shift for reflected ultrasound ($f_d = f - f_0$) and subsequently the velocity (v) of the moving target (blood cells or myocardium) are given (*Eq. 1 and Eq. 2*):

Eq. 1: $$f_d \approx 2 * f_o * v * \cos(\theta) / c$$

$$\Downarrow$$

Eq. 2: $$v \approx f_d * c / 2 * f_o * \cos(\theta)$$

where f_d = Doppler shift, f_o = transmitted frequency, v = target (blood or myocardium) velocity, θ = insonation angle (between ultrasound beam and velocity vector) and c = velocity of sound in tissue (≈1540 m/s).

The alignment between the ultrasound beam and velocity direction is a crucial point in all Doppler analyses. Misalignment less than ±15 degrees will cause ≤3.5% error in the measurement and misalignment more than ±30 degrees will cause ≥13% error.

Blood flow velocity can be measured within a specific site (sample volume) by pulsed wave Doppler or all velocities along the ultrasound beam by continuous wave Doppler. By continuous wave Doppler the beam is transmitted continuously, and the received echoes are sampled continuously. Thus, there is no information about the depth of the different signal components. In pulsed wave Doppler, a new pulse cannot be transmitted before the last signal has returned. In clinical practice this means that for pulsed wave Doppler, the ability to measure high velocities decreases when the distance to the sampled volume is increased. Thus, both methods have limitations: pulsed wave Doppler has velocity ambiguity at high velocities, and continuous wave Doppler has depth or range ambiguity. Spectral Doppler has an effective frame rate of about 300 FPS.

Pulsed and continuous waved Doppler is displayed in spectral analyzers according to the velocity (amplitude), intensity and timing of the reflected ultrasound frequencies *(Figure 1)*. Gain settings are important for optimal measurements in the Doppler spectrum both for pulsed and continuous wave Doppler. The reflected signal of tissue echoes has high intensity but low velocity. Blood has high velocity with a wider distribution, but lower intensity. For blood flow Doppler, a high pass filter (low velocity reject) is applied to suppress the tissue echoes. A low pass filter (high velocity reject) may be applied to suppress noise above the velocity range. In tissue Doppler, the high pass filter can be removed, or at least partially, to allow the low velocities from the tissue (usually on the order of 1/10 of flow). The blood signal can be removed both by reducing the gain, and by applying a low pass filter (high velocity reject).

In colour TD each Doppler signal consists of fewer samples per time unit than in pulsed wave spectral TD, and the mean Doppler frequency is estimated by the autocorrelation technique, causing lower absolute velocities compared with the spectral TD method. Each pixel in the ultrasound image is colour coded according to the velocity, and the B-mode and colour TD images are displayed superposed, but with multiple of colour Doppler images hidden between each B-mode frame. By off-line post processing, either semi quantitative analysis in curved anatomical M-mode or quantitative data may be extracted. When picking one region of interest, corresponding velocity, motion, and strain rate data are presented in time trace *(Figure 1)*.

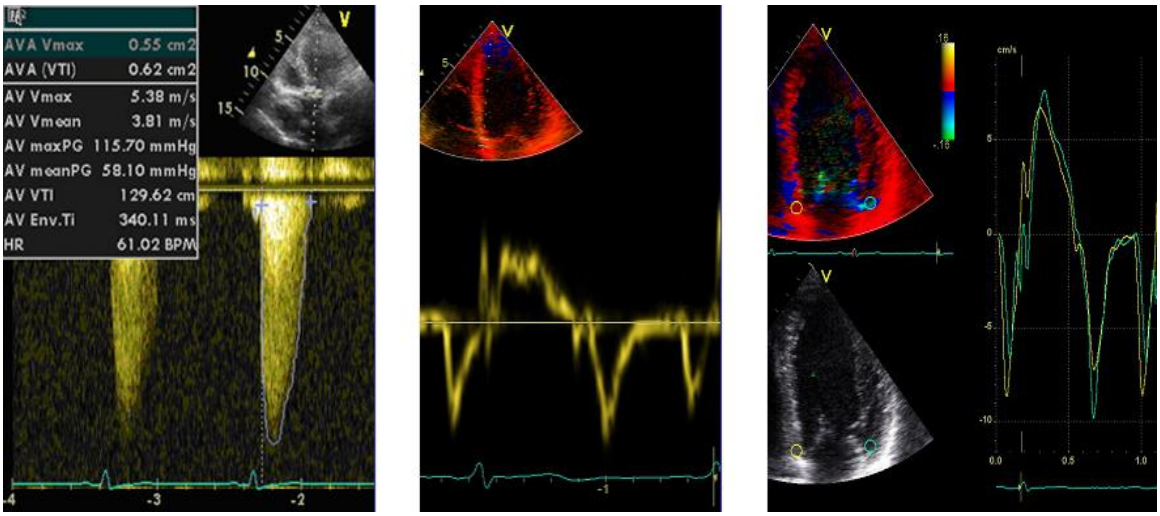

Figure 1. *Spectral land trace analyses of flow and tissue Doppler velocity curves with velocity shown on the y-axis and time on the x-axis. Left figure: maximal velocity through a stenotic aortic valve assessed by continuous wave Doppler. Mid figure: Pulsed wave spectral TD curve with sample volume in the base of the inferioseptal wall showing systolic and diastolic mitral annular velocities. Right figure: Off-line colour TD trace analyses with systolic and diastolic mitral annular velocities of the base of the inferioseptal and anterolateral wall.*

1.1.3 Ejection fraction versus longitudinal function

Quantification of LV systolic function has traditionally been based on measurements of changes in cavity volumes during systole (i.e. stroke volume and ejection fraction). LVEF is the most widely used measurement of LV systolic function and is a key functional and prognostic marker of heart disease, due to the huge amount of studies supporting the prognostic information and the guidance of therapeutic interventions linked to LVEF. However, LVEF may overestimate the myocardial function in small hypertrophic hearts (32), has limited reproducibility and is not an optimal indicator of the contractile properties of the myocardium (33).

The concept of the heart functioning as a double pump, with the atrioventricular plane as a piston, was described already by Leonardo da Vinci (34). The basis for all measurements of longitudinal function is the understanding of the relatively fixed apex and the displacement of the atrioventricular plane towards apex during systole. Annular measurements reflect the total shortening of the ventricle, and are measurements of global longitudinal function. The mitral annular excursion (MAE) was first measured directly by M-mode (35). The correlation between MAE and LVEF is strong in dilated ventricles. In normal ventricles, the MAE is related to the stroke volume (36). In LV hypertrophy, MAE is reduced despite preserved LVEF and the correlation is poor (37). MAE is also reduced in patients with heart failure and preserved ejection fraction (38). The displacement of the atrioventricular plane is influenced by the total ventricular size, and smaller ventricles have lower MAE than healthy larger ventricles. Thus, variations in MAE are caused by both variations in size and function of the heart. Correcting MAE for the heart size has so far only been proven useful in children where LV size varies considerably (39).

The peak velocity of the atrioventricular plane towards apex during systole is another measurement of the longitudinal function. The annular velocities can be measured by colour

tissue Doppler (TD) from high frame rate colour TD or by pulsed wave spectral TD measured at the outer edge of the band-shaped spectrum. By colour TD the mean velocities of the regions of interest are assessed (autocorrelation method), which will give lower values compared with pulsed wave spectral TD (40) (41). The peak systolic mitral annulus velocity (S') occurs early in systole, and is related to LV acceleration. S' has been validated as a measurement of global systolic function (42, 43). The correlation of S' with EF is weaker than for MAE, which is expected as EF and MAE are end-systolic measurements, reflecting the total systolic work (stoke volume) while S' is a peak systolic velocity measurement reflecting the peak systolic performance (contraction). S' is reduced in patients with heart failure with normal ejection fraction (44). S' can differentiate between pathologic and physiologic LV hypertrophy (43) and has been shown to be a sensitive marker for reduced function in mutation positive relatives of patients with manifest hypertrophic cardiomyopathy (45).

1.1.4 Regional function by deformation imaging

Deformation imaging is quantitative methods used to assess myocardial global and regional deformation, most often used as measurements of systolic function. Visual evaluation of wall motion is a robust and quick way to evaluate regional myocardial function, but WMS is semi-quantitative. With the introduction of tissue Doppler echocardiography in the 1990s, it was possible to quantify regional myocardial deformation as strain and strain rate, mainly along the long-axis of the left ventricle (18). Semi quantitative assessment of wall shortening by colour strain rate imaging was shown to be equivalent to B-mode wall motion scoring by wall thickening (20).

Systolic longitudinal strain is the systolic shortening of a myocardial segment relative to the end diastolic length ($S_{es} = \frac{L - L_0}{L_0}$), i.e. relative deformation, expressed in percent, with negative values indicating shortening. Likewise, circumferential systolic strain is

circumferential shortening, and is negative. Transmural (radial) systolic strain is wall thickening, and is positive. Strain rate means deformation rate, expressed in s^{-1}. Experimental studies have shown that end-systolic strain is highly influenced by afterload, while peak systolic strain rate, most often occurring on the early 1/3 of systole, is more closely linked to the regional contractile function (46, 47). However, clinical usefulness of these methods has been limited due to problems with noise and artefacts (48). The technique of speckle tracking is based on the interference of the reflected ultrasound as well as uneven reflection properties of the myocardium, giving rise to a unique irregular random speckled pattern in the myocardium. Kernels corresponding to myocardial areas are tracked forwards and backwards during the cardiac cycle. By the speckle tracking method it is possible to measure the percentage shortening of a myocardial segment during systole (strain), and by temporal derivation strain rate can be calculated. Speckle tracking echocardiography has gained more widespread acceptance than TD based deformation imaging, mainly because it has been implemented with a more user friendly user interface (26). However, definite proof of added diagnostic value over conventional wall motion score index is still scarce. In addition, the regional speckle tracking values are normally highly influenced by spline smoothing, and thus, substantially depended of the MAE, which is a global index of LV performance. In the recent versions of commercial speckle tracking software, the smoothing is adjustable, but it remains to be proven whether a lower degree of smoothing might increase diagnostic accuracy in conditions with regional dysfunction.

Deformation analyses were developed to assess segmental myocardial function, but the average of these segmental data is commonly used to assess global ventricular function. Global strain corresponds to displacement of the atrioventricular plane corrected for LV length, while global strain rate corresponds to the spatial derivative of myocardial velocity *(Figure 2)*. Thus, MAE divided by LV length is a measurement of LV global longitudinal

strain. However, normal values differ due to different post processing and because MAE/LV length is measured along a straight line while longitudinal strain is measured along a curved line. Global average of segmental speckle tracking based longitudinal strain has shown better prediction of long term mortality compared with LVEF and WMSI (49).

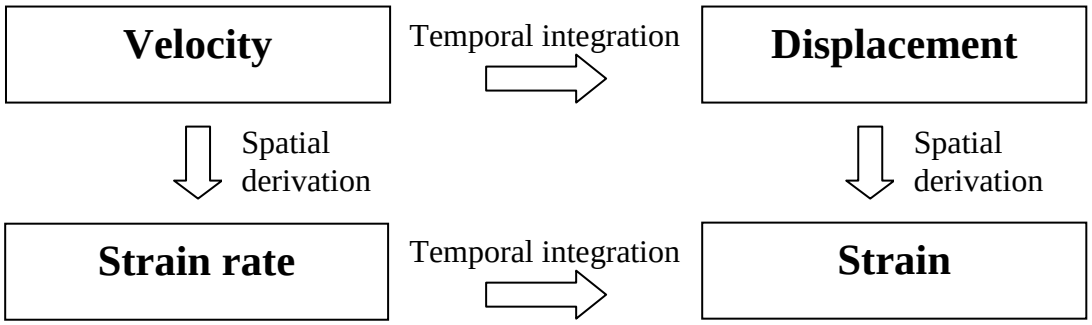

Figure 2. *Strain rate is equal to the velocity gradient (spatial derivative of velocity), and strain is the displacement gradient (spatial derivative of displacement). Velocity and displacement are global measures (measures the whole ventricle apical to the localization of the measurement), while strain and strain rate measures regional deformation. Courtesy: Asbjørn Støylen (http://folk.ntnu.no/stoylen).*

Cardiac deformation is 3D with longitudinal and circumferential shortening and transmural (radial) thickening during systole. With speckle tracking, the different deformation components can be approximated, and this has led to a search for "the most sensitive direction". However, the different myocardial layers are tightly connected which indicates that the accuracy of the measurement is most crucial for detecting dysfunction regardless of which direction being measured. Due to the principle of incompressibility of the myocardium the systolic wall thickening has to follow systolic shortening (20, 32). However, concentric myocardial hypertrophy will reduce the luminal diameter of the LV, and thus, the percentage fractional or radial shortening and ejection fraction will increase (32), even when the longitudinal shortening decreases. There is a common misconception that reduced systolic

longitudinal function is compensated by increased radial function (32). This is due to the fact that longitudinal function is measured in the myocardium, while radial function is measured in the cavity (50).

1.1.5 Three-dimensional echocardiography

The evolution of 3D echocardiography from slow and labour-intense offline reconstruction to real-time volumetric imaging has been one of the most significant developments in ultrasound imaging of the last decade. The clinical acceptance of this new tool has broadened significantly. A firmly established advantage of 3D compared with 2D echocardiography is the improvement in the accuracy and the reproducibility of the evaluation of LV volumes and LVEF demonstrated by multiple studies with widely accepted reference techniques, including magnetic resonance imaging (MRI) (51, 52). In contrast to 3D echocardiography, quantification of chamber volumes by 2D echocardiography is based on assumption of the LV shape, but the LV geometry has considerable individual variations particularly in the presence of aneurysms, asymmetrical ventricles, or wall motion abnormalities. Errors caused by apical foreshortening are also more common in 2D echocardiography. Despite the high correlation with the MRI, several studies have reported that 3D echocardiography significantly underestimate LV volumes compared with MRI. This may be explained by differences in the separation between myocardial tissue and trabeculae of the two imaging techniques (53). Three-dimensional echocardiography may also be useful in the assessment of atrial and right ventricular volumes and function and the evaluation of LV dyssynchrony (53).

The standard planes of 2D echocardiography do not encompass the entire left ventricle, resulting in a potential risk of missing deformation abnormalities between the planes. The ability of 3D echocardiography to cover the entire heart in one data set from which the ventricle can be viewed in any plane orientation, suggests that 3D echocardiography have the potential to overcome errors caused by misalignment and out-of-

plane motion in 2D wall motion analysis. Three-dimensional echocardiography can display multiple 2D short-axis slices simultaneously, and automated tracking of the long-axis motion can reduce out-of-plane motion, which may cause misinterpretations in 2D analysis. So far there is little evidence of incremental diagnostic value of 3D wall motion analysis compared with deformation imaging by 2D echocardiography (53). Therefore the aim of paper 4 was to compare the accuracy of 3D and 2D echocardiography in the evaluation of the global and regional myocardial function following acute MI.

Recent improvements in 3D matrix array transducers have enabled real-time visualization of valves and subvalvular anatomic features with improved resolution and more realistic imaging of valves. Real-time 3D transesophageal echocardiography plays an increasingly important role in the management of valvular heart disease and can be used in the intraoperative evaluation of patients undergoing mitral valve repair (54). Three-dimensional transesophageal echocardiography has been shown to be highly accurate and reproducible in localizing prolapsing segments of the mitral valve (55), and the determination of aortic valve area by the continuity equation is more accurate when 2D LVOT measurements are substituted by 3D planimetered LVOT measurements (56). In prosthetic valve endocarditis, 3D transesophageal echocardiography has been shown to correlate well with surgical findings, may identify additional vegetations not seen on 2D, and can assist in differentiating vegetations from loose suture material (57). However, because of frame rate limitations in 3D echocardiography 2D echocardiography remains superior for the identification of small mobile vegetations (54).

1.2 Cardiac magnetic resonance imaging

Cardiac MRI is an attractive imaging modality due to its non-radiation nature and its high image quality. The availability of the method has increased, and cardiac MRI is now an important tool in the guidance of therapy in many patients.

1.2.1 Left ventricular function by cardiac MRI

Cardiac MRI is generally recognized as the most accurate and reproducible technique for assessing LV volume, mass and ejection fraction owing to its high spatial resolution, excellent signal-to-noise ratio, and the possibility to acquire images in any orientation of the heart. Therefore cardiac MRI is considered as the reference standard for these purposes (58-60), although definite proofs of incremental prognostic value compared with LVEF by echocardiography are still lacking (61). Cardiac MRI will continue to be an invaluable research tool, and sample sizes can be smaller with MRI than with echocardiography for assessing changes in ventricular volumes, mass, and function in the evaluation of pharmacologic treatment in heart disease (62). Cardiac MRI examinations should follow a protocol that includes assessment of left and right ventricular volumes and function as well as evaluation of wall thickness, valvular function, atrial dimensions, the pericardium, and myocardial tissue characterization.

1.2.2 Cardiac MRI in ischemic heart disease

The development of late enhancement magnetic resonance imaging (LE-MRI) has offered the opportunity to characterise the myocardial tissue in an entirely new way. By using the extracellular contrast agent gadolinium, LE-MRI takes advantage of the delayed wash-in and wash-out of contrast in areas with increased extracellular volume; i.e. scar or fibrosis. In addition, an inversion-recovery sequence magnifies the difference between healthy and infarcted tissue. This gives a method with high accuracy and reproducibility, and LE-MRI is established as the reference standard for the quantification of myocardial scars (60, 63). The pattern of hyperenhancement can provide additional information about etiology of the scars. In coronary artery disease the expansion of the ischemic injury is starting from the subendocardium and progressing toward the epicardium located in a region that is consistent with a perfusion territory of an epicardial coronary artery (64) *(Figure 3)*. Subendocardial

hyperenhancement may also be seen in amyloidosis, systemic sclerosis and after cardiac transplantation, but in these conditions the hyperenhancement does not correspond to the perfusion territories of the epicardial coronary arteries (59). Midwall or epicardial hyperenhancement is common in myocarditis, hypertrophic cardiomyopathy and Fabry′s disease (59).

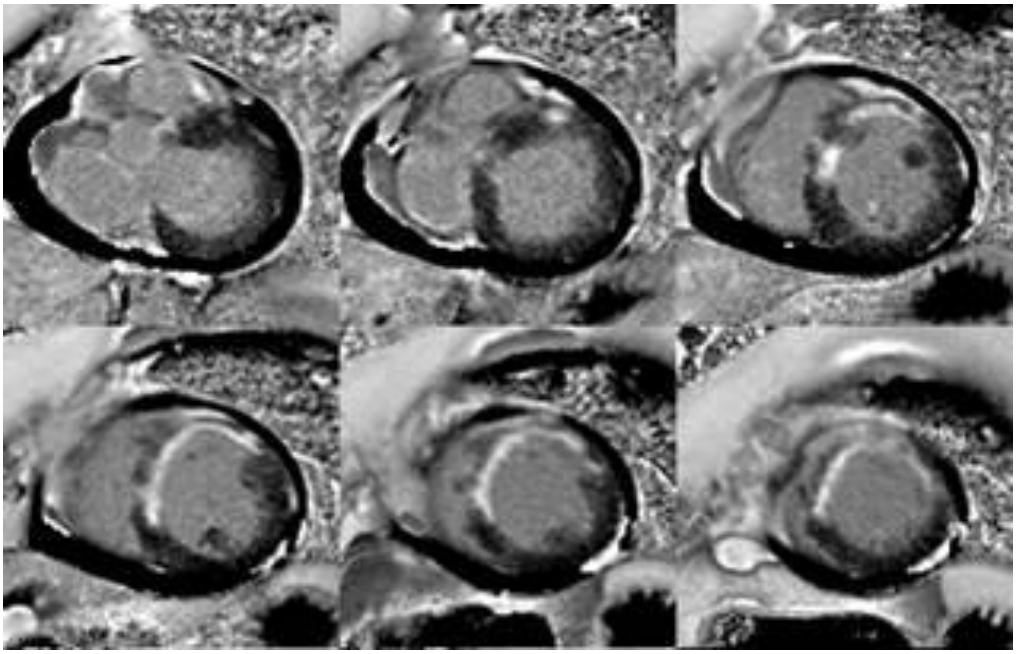

Figure 3. *Scar visualization by late enhancement magnetic resonance imaging. White hyperenhanced areas in the septal and anterior wall corresponding to the left anterior descending coronary artery. The expansion of the ischemic injury is starting from the subendocardium and progressing almost to the epicardium, indicating transmural infarction (segmental infarct volume fraction >50%).*

Hibernating myocardium refers to a dynamic condition of chronic abnormally contracting myocardium, with function that improves after revascularization. Low-dose dobutamine stress MRI is accurate in the assessment of contractile reserve and in the detection of hibernating myocardium. However, wall thickening in cardiac MRI may be difficult to quantify due to the effects of trabeculae that are merging in end-systole, and incremental prognostic value compared with radionuclide methods and dobutamine stress

echocardiography needs to be confirmed. LE-MRI can determine the transmural extent of scar and the remaining viable rim. Increasing segmental infarct transmurality assessed by LE-MRI showed a gradual decreasing likelihood of response to revascularisation (65). However, the prediction of recovery is not accurate in the segments with 25-75% infarction.

1.3 Reproducibility in medical imaging

Reproducibility is the degree of agreement between measurements or observations preferably conducted in different locations by different observers. Reproducibility is part of the precision of a test method. Repeatability or test-retest reliability is often defined as the variation in measurements taken by a single person or instrument on the same item and under the same conditions (66).

Accuracy and reproducibility of echocardiographic measurements is essential for addressing correct diagnosis, decision making and reduce the frequency of unnecessary, repeated examinations. Reproducibility is also fundamental in cardiac research as echocardiography is widely applied in clinical trials in order to identify potential mechanisms of clinical end-points or to assess surrogate end-points.

1.3.1 Estimation of reproducibility in medical imaging

The reproducibility is often reported as different variants of correlation coefficients. The Pearson correlation coefficient is sometimes misapplied in agreement studies. It describes the closeness of the linear relationship between two variables, but the test is potentially misleading as there may be a strong correlation between two variables but poor agreement, and there might be an undetected systematic error. The intraclass correlation coefficient (ICC) and Lin's concordance correlation coefficient avoid the problem of linear relationship being mistaken for agreement. The intraclass correlation coefficient is centred and scaled using a pooled mean and SD, whereas the Pearson correlation coefficient is centred and scaled by its

own mean and SD. The Lin's concordance correlation coefficient assesses the closeness of the data about the line of best fit in the scatter plot by taking into account how far the line of best fit is to the line of equality. However, all correlation coefficients are highly influenced by the range of measurements, and the correlation coefficients tell us little about the size of errors between the methods. If the range of measurements is wide, the correlation coefficients might be high despite moderate agreement between the methods. If the range of measurements is small, the correlation coefficients might be low despite moderate or good agreement between the methods. Thus, comparing correlation coefficients of different study populations is totally misleading. Furthermore, the correlation coefficients may be difficult to interpret, as consensus regarding clinical acceptable levels is lacking (67).

Bland and Altman recognised the limitations of using correlation coefficients in the clinical comparison of the agreement between two measurement methods, and in their landmark paper they elegantly describe why two methods may have strong correlation but poor agreement (66). They introduced the "95% limits of agreement" which gives a much better description on how much two methods differ and whether two methods may be used interchangeably or a new method may replace an old method. Their approach has been used extensively for the assessment of agreement between two methods and repeated measurements of a single measurement by one or two observers. The method can easily be interpreted in a clinical context as 95 percent of repeated measurements are expected to be within the interval given by the 95% limits of agreement. If the difference between two methods is not significantly different from zero, the 95% limits of agreement is equivalent to the coefficient of repeatability (66).

The 95% limits of agreement is based on a linear relationship between the errors, but echocardiographic measurements may have errors that are proportional to the magnitude, especially when they are collected over a large physiological range. This can be overcome by

logarithmic transformation, which gives a different coefficient of repeatability at different measurement magnitudes (66, 68). An alternative approach is to divide the error with the mean to get the mean absolute error, which is a dimensionless ratio. The percentage error is calculated as the absolute difference between the two sets of observations, divided by the mean of the observations. Expressing the error in per cent allows direct comparisons between methods with different measurement units and is frequently used in the assessment of reproducibility in cardiac imaging (69-71). A similar approach is to calculate the coefficient of variation as the within-subject SD divided by the mean of the observations. When only two repeated measurements are measured, the coefficient of variation is directly proportional to the mean error, and their relation is given by the following equations:

<u>Eq. 3:</u> $COV = \frac{SD}{\bar{x}} = \frac{\sqrt{\frac{1}{n-1}\sum_{i=1}^{n}(x_i - \bar{x})^2}}{\bar{x}}$ <u>Eq. 4:</u> $\%Error = \frac{|x_1 - x_2|}{\bar{x}} = \sqrt{2} \times COV$

The mean error is more easily interpreted as it directly describes the percentage difference between two methods. The coefficient of variation is in contrast to the mean error also possible to calculate when more than two repeated measurements are measured.

For non-parametric data, different statistics are required. A commonly used and valid statistic with categorical data is Cohen's kappa coefficient. The kappa coefficient has the added advantage that is takes into account the agreement occurring by chance. However, the kappa coefficient has some of the same limitations as the intraclass correlation coefficient. A non-parametric variant of the limits of agreement method has been described, where data can be ranked with a range of data reported within centiles (72). If 95th percentiles are used, including presentation on a difference plot, this approach resembles 95% limits of agreement.

1.4 Contraction and contractility of the left ventricle

1.4.1 Different phases during systole

The opening and the closure of the cardiac valves divide the cardiac cycle into different phases. The phases of the cardiac cycle can also be described by the volume changes and the pressure changes during the heart cycle (50). The flow is a result of the pressure differences, and the volume changes are a direct result of flow (the volume is the integrated flow rate). The isovolumic contraction phase is the first part of systole, and ventricular contraction after mitral valve closure is characterised by increase in tension and pressure, but no volume changes (no flow in or out of the ventricle), although there may be small changes in ventricular shape. In the ejection phase, there is ejection of the stroke volume (flow), and a corresponding decrease in ventricular volume *(Figure 4A)*. The ejection phase can be divided into the rapid ejection during the last part of myocardial contraction and the reduced ejection during the first part of relaxation, both belonging to the ventricular systole *(Figure 4B)*. In the last part of ejection there is decrease of myocardial tension - relaxation, but continuing outflow of blood and volume decrease due to the inertia of blood. In the isovolumic relaxation phase, which is the first part of diastole, there is decrease in tension, but no volume change. In the early filling phase, there is continuing ventricular pressure decrease and filling flow, and a corresponding increase of ventricular volume. In the subsequent diastasis, there is little or no flow and volume change. In the last part of diastole, the late filling phase, there is flow into the ventricle and increase in ventricular volume due to atrial contraction.

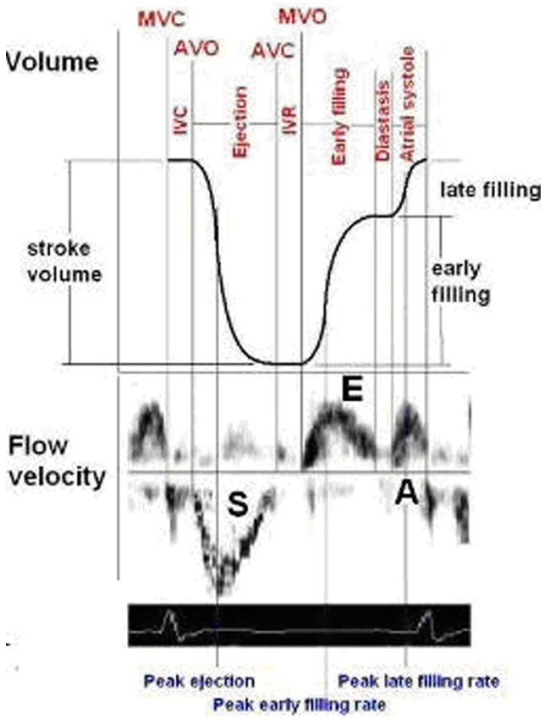

Figure 4A

Top, Ventricular volume curve, during the different phases of the cardiac cycle. Below, composite Doppler flow velocity curve showing both LVOT outflow and mitral inflow to the left ventricle. The flow velocity curve is an approximation to flow rate, and hence, similar to the temporal derivative of the volume curve, or, conversely, the volume changes are the integrated flow rate. The isovolumic phases are exaggerated. Courtesy: Asbjørn Støylen (http://folk.ntnu.no/stoylen).

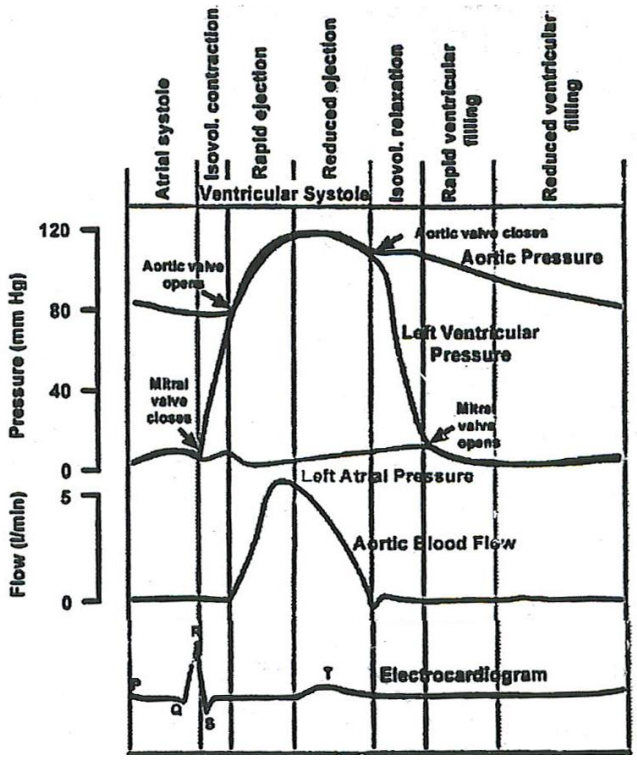

Figure 4B

The Wiggers cycle. The pressure changes are indications of myocardial tension. The decline in tension (i.e. relaxation of the myocardium) starts close to mid ejection, but the ejection of flow and volume reduction still continues. Thus the ejection phase can be divided into the rapid ejection during the last part of myocardial contraction and the reduced ejection during the first part of relaxation, but both ejection phases and the isovolumic contraction belong to the ventricular systole. After: McGill Faculty of Medicine e-curriculum (http://alexandria.healthlibrary.ca).

1.4.2 Estimation of contraction and contractility in medical imaging

The assessment of LV dysfunction is a frequent indication for echocardiography. However, LV dysfunction is a general and non-specific entity that is defined depending on the context (33). For instance are the LVEF and the diastolic assessment highly dependent on loading and may produce abnormal results under unusual loading conditions. Although the value of LVEF for assessing LV dysfunction is unquestionable, the referring clinician is often also requesting an assessment of the nature of the underlying myocardial tissue. Intrinsic cardiac function implies the assessment of true contractility (73). True contractility of the myocardium is

currently not measurable non-invasively in clinical practice (33), but detecting the best non-invasive surrogate for true contractility has been an important task in cardiac research for decades.

Contraction is generation of tension, and contractility is the intrinsic ability of the muscle to generate force independently of load (50). When an isolated myocyte is under no influence of load, the generated tension corresponds to shortening and the contraction equals contractility. In the intact heart, there is external load, and deformation is a consequence of tension and load. If the load is greater than the tension developed, the contraction is isometric, i.e. contraction with tension development without shortening. If the tension exceeds the load (and the load is constant) the contraction is isotonic (shortening at constant load). In the heart, the load and the tension changes during the cardiac cycle and causing a mix between isometric and isotonic contraction.

During the systole, there is active contraction only during isovolumic contraction and the first part of the ejection period (until peak ventricular pressure). Thus, a considerable part of the energy from myocyte contraction is used to build up the ventricular pressure from the low filling pressures of the left atrium to the high ejection pressures of the aorta. Therefore the ejection do not correspond to myocyte contraction, and force development (contraction of the myocytes) which generates sufficient pressure to open the cardiac valves should be distinguished from deformation (shortening of the myocytes) which gives rise to the actual volume ejection. In the last part of ejection, there is myocyte relaxation, but still flow and volume reduction due to the inertia of the blood. Cardiac imaging can visualise wall motion, wall-deformation, cavity deformation or flow but only a part of myocyte contraction.

It is still questionable whether some echocardiographic indices are more closely related to contraction than others, but in an experimental study, beta blocker and dobutamine, strain rate was most closely related to the maximal first derivative of LV pressure (peak

dP/dt), while strain and displacement were more closely related to stroke volume and EF (47). Myocyte contraction occurs in the first part of systole, which corresponds well to the timing of the echocardiographic peak systolic velocity indices like peak systolic annulus tissue velocities, peak ejection velocity and peak systolic strain rate. These measurements may also be less load dependent, as maximum afterload is reached later in systole. Peak velocity is also related to acceleration, which is a direct measure of force, and thus to contraction. In contrast to force development, deformation and volume ejection continue until the end of systole, and end-systolic echocardiographic indices like ejection fraction, fractional shortening, systolic mitral annulus displacement, global strain and the ejection velocity time integral are measurements of the total work performed by the left ventricle during ejection (47).

1.5 Myocardial infarction

1.5.1 LV function and prognosis after acute myocardial infarction

The goal of risk stratification after MI is to identify patients whose outcomes can be improved through specific medical interventions. Previous studies have established LVEF as an important predictor for mortality with therapeutic implications in patients with coronary artery disease (74). In patients with coronary artery disease and severely depressed LV function, the mortality is high and progressive pump failure is the main cause of death (74). In patients with coronary artery disease and preserved or moderately depressed LVEF the overall annual mortality ranges from 5% to 15%, with a relatively high percentage of sudden cardiac deaths (75, 76). Although the precise cause of sudden cardiac deaths may be uncertain, it has been demonstrated that scar tissue may serve as a substrate for lethal arrhythmias (77). Quantification of scar tissue gives incremental prognostic value beyond LVEF and may be superior to LVEF for prediction of all-cause mortality in patients with preserved or moderately depressed LV function (78, 79).

Myocardial ischemia rapidly impairs contractile function, which may persist for several hours after reperfusion (myocardial stunning), or might lead to chronic dysfunction even when perfusion are re-established. The pathophysiological substrate of chronic dysfunction is heterogeneous, varying from predominantly hibernating myocardium to irreversible scarring. Hibernating myocardium is most commonly defined as dysfunctional but viable myocardium with the potential to regain contractility after revascularization (80). This definition is retrospective and thus not useful for clinical decision making. Patients with hibernating myocardium have been shown to have a significant survival advantage following revascularization (60, 81). In fact, the meta-analysis by Allman (82) seemed to show no prognostic benefit of revascularisation at all, if there was no viability. However, in a recently published substudy of the STICH trial, myocardial viability assessed by single photon emission computed tomography or dobutamine echocardiography, did not identify patients with survival benefit from coronary arterial bypass grafting (83). The study has several important limitations (84), but it questions the benefit of viability imaging and whether surgery could be refused on the basis of imaging alone. Other studies have indicated that assessment of myocardial viability is superior to regional scar quantification by LE-MRI in prediction of improvement in myocardial dysfunction after revascularization (85, 86).

1.5.2 Quantification of myocardial infarct size

Evaluation of the regional myocardial function following acute MI is of major importance as the morbidity and mortality are closely related to infarct size and location (60). Prognosis is progressively worse with increasing amounts of scar, and scar quantification by LE-MRI may be a stronger predictor of adverse clinical outcome than LVEF and volumes in the presence of healed myocardial infarctions (87-89), but LE-MRI is less available than echocardiography in most clinical settings. Echocardiographic measurements of the LV function have been extensively validated in patients with MI (20, 90, 91), and a good agreement with LE-MRI

has been demonstrated (92, 93). However, most echocardiographic methods are measurements of global LV function, where the degree of function reduction may serve as an indirect estimate of infarct size. In paper 3 we present a new method for direct quantification of infarct size, and the accuracy of echocardiography in predicting myocardial infarct size is one of the aims of this thesis.

The transmural extent of scar assessed by LE-MRI can predict the likelihood of functional recovery after revascularization. The initial landmark study by Kim et al showed a gradual decreasing likelihood of response to revascularisation with increasing segmental infarct transmurality (65). Scars with <25% transmural extent had 72% likelihood of functional recovery, whereas scars with >75% transmural extent had <2% likelihood of functional recovery. However, in the large group of segments with 25-75% infarction, the prediction of recovery was not very accurate. In a study by Kelle et al (94) the presence of scar on LE-MRI images was more accurate for predicting events than hibernating myocardium assessed by low-dose stress MRI in patients with <6 scarred segments. Conversely, hibernating myocardium assessed by low-dose stress MRI was a better predictor of events than scar tissue on LE-MRI in patients with >6 scarred segments (94). In a recent review paper regarding the management of ischemic cardiomyopathy, combined scar imaging and contractile reserve assessment by MRI is suggested as a future gold standard (60). However the costs are high and the evidence is sparse for recommending these examinations in everyday clinical practice, and a substantial part of the MI patients has contraindications to MRI. Echocardiography is widely available, harmless, fast, relatively cheap, and therefore more suitable as first line imaging modality. It remains to be proven whether recent technological improvements in echocardiography provide increased diagnostic accuracy. Therefore the aim of paper 3 and 4 was to compare the accuracy of new and traditional

echocardiographic methods in the evaluation of the global and regional myocardial function following acute MI.

Many clinicians use values of biomarkers to provide a rough estimate of infarct size. Recent data suggest that peak cardiac troponin T values or the 72 to 96 hour values correlate well with infarct size by LE-MRI (95-97). The slope of the relationship is different with and without reperfusion as reperfusion leads to an earlier and higher maximum. The correlation is less robust with NSTEMI than with STEMI (95). However, it has been suggested that patients with small infarcts have different cardiac troponin T release time curves than patients with large myocardial infarction. Therefore, it cannot be excluded that in patients with NSTEMI, an earlier cardiac troponin T sampling time point would result in better correlation with infarct size by LE-MRI. Nonetheless, correlations of cardiac troponins in these studies are better than the correlations reported for creatine kinase-MB and N-terminal brain-type natriuretic peptide (95, 96). The cardiac troponin T value after 96 hours has been suggested as the best single-point value and was as effectively as the peak cardiac troponin T and the areas under the receiver operating characteristic curves (AUC) of cardiac troponin T over 96 hours (95). For the latter, it is reasonable to speculate that performance of cumulative measurements could be improved by expansion of serial measurements beyond 96 hours. However, prolongation of sampling is likely to reduce the attractiveness and acceptance of the method.

2 Aims

2.1 General aims

The overall aim of the thesis is to compare new and traditional ultrasound methodology in the assessment of systolic function during inotropic alterations and after recent MI.

2.2 Specific aims

1) To study and compare the reproducibility of new and conventional measurements of the LV global and regional function, and to test whether the reproducibility data based on repeated measurements of single datasets underestimate the more clinically relevant inter-observer reproducibility based on separate recordings.

2) To compare the ability of different echocardiographic methods in detecting contraction changes of the LV, and to test whether the peak systolic velocity indices better reflect changes in contraction compared with the end systolic indices.

3) To validate a new method for direct quantification of infarct size based on area measurement by tissue Doppler based colour coded strain rate data and wall motion analysis, and to test whether this method gives higher diagnostic accuracy compared with other echocardiographic techniques.

4) To compare the diagnostic accuracy of 3D wall motion analysis, 3D speckle tracking echocardiography and 2D echocardiography in patients with recent myocardial infarctions, using LE-MRI as reference method in order to test whether 3D echocardiography gives added diagnostic value in this population.

3 Study population characteristics

3.1 The reproducibility study (study 1)

The study population consisted of ten (7 men and 3 women) healthy volunteers (30 ± 6 years). The subjects were free from medications, known cardiovascular disease, structural heart disease, diabetes or hypertension. None were excluded due to inadequate echocardiographic images.

3.2 The contraction study (study 2)

The study population consisted of 33 (25 males and 8 women) healthy volunteers (20-32 years). Thirty subjects were medical students. Two subjects were recruited among the staff of the faculty of medicine, and one of the volunteers was an engineer student. The subjects were free from medications, known cardiovascular disease, structural heart disease, diabetes or hypertension. None were excluded due to inadequate echocardiographic images. Table 1 shows the basic characteristics of the study population.

Table 1 Characteristics of the study population of study 2.

Variable	**Mean (SD)**
Age (years)	25 (2.9)
Height (cm)	179 (6.5)
Weight (kg)	75 (12)
BMI (kg/m^2)	23 (3)
BSA (m^2)	1.9 (0.2)
LV mass (g)	180 (27)
LV volume (ml)	134 (27)

Table 1: *The parameters are displayed as mean (standard deviation). BMI = body mass index; BSA = body surface area; LV = left ventricular. LV mass and volume were obtained from real-time 3D echocardiography.*

3.3 The patients with recent myocardial infarction (study 3 and 4)

The final infarct population of study three and four consisted of 58 patients with first time MI. None were excluded due to inadequate echocardiographic images. Forty six (79%) had STEMI, while 12 (21 %) had NSTEMI. Coronary angiography identified a coronary culprit lesion in all patients. Percutaneous coronary intervention (PCI) of the culprit coronary lesion was performed during the hospital stay in all patients except three patients in whom the defined culprit lesion was not amenable to PCI. The median time from onset of symptoms to PCI was 3.0 hours (range 0.6-140 hours). PCI was performed within ≤ six hours from onset of symptoms in 39 patients. Additional patient characteristics are listed in Table 2.

3.4 The sex and age matched healthy volunteers (study 3 and 4)

The control group of study three and four consisted of 35 age- and sex-matched participants in the Echocardiography in the Nord-Trøndelag Health Survey (HUNT). None were excluded due to inadequate echocardiographic images. Patient characteristics are listed in Table 2.

Table 2 Patient characteristics, risk factors, angiographic findings and medications of study 3 and 4.

	Infarct Size >12% (n=25)	Infarct Size <12% (n=33)	Healthy controls (n=35)
LE-MRI infarct size (infarct volume fraction)	19.5 ± 5.7% *	5.3 ± 3.2%	not available
Age, years	56.7 ± 13.6	54.9 ± 12.9	56.9 ± 13.0
BMI, kg/m2	26.1 ± 6.0	25.4 ± 5.4	26.1 ± 5.2
Male sex, n (%)	19 (76)	25 (76)	28 (80)
Heart rate, bpm	64 (11)	60 (11) †	67 (11)
Current smoker, n (%)	12 (48)	17 (52)	-
Creatinine, µmol/L	68.5 1 ± 7.1 ‡	70.5 ± 17.2 †	88.0 ± 19.1
Peak Troponin T, µg/L	7.7 ± 5.7 *	3.2 ± 2.4	not available
Hypertension, n (%)	5 (20)	5 (15)	-
Diabetes mellitus, n (%)	4 (16)	2 (6)	-
STEMI, n (%)	22 (88)	24 (73)	-
Single vessel disease, n (%)	14 (56)	25 (76)	not available
LAD culprit, n (%)	10 (40)	13 (39)	-
CX culprit, n (%)	7 (28)	6 (18)	-
RCA culprit, n (%)	8 (32)	14 (42)	-
Aspirin, n (%)	25 (100)	33 (100)	-
Clopidogrel, n (%)	25 (100)	33 (100)	-
Beta-blocker, n (%)	23 (92)	29 (88)	-
Statin, n (%)	25 (100)	33 (100)	-
ACEi or ARB, n (%)	7 (28)	8 (24)	-

Table 2: *Continuous variables displayed as mean ± SD. Categorical variables are displayed as numbers (percentage). * P<0.001 for large MIs vs. small MIs; † P<0.05 for small MIs vs. healthy controls; ‡ P<0.001 for large MIs vs. healthy controls. Abbreviations: ACEi = angiotensin-converting enzyme inhibitors; ARB = angiotensin II receptor blockers; bpm = beats per minute; BMI = body mass index; LE-MRI = late enhancement magnetic resonance imaging; CX = circumflex coronary artery; LAD = left anterior descending coronary artery; RCA = right coronary artery; STEMI = ST-segment–elevation myocardial infarction.*

4 Methods

4.1 Inclusion and exclusion

4.1.1 The reproducibility study (study 1)

In this echocardiographic study 10 healthy volunteers were prospectively recruited among the staff at the Department of Circulation and Medical Imaging at the Norwegian University. Validation of the normality of the study population was performed by careful medical history and examinations by the physician echocardiographers (AT and HD).

4.1.2 The contraction study (study 2)

The participants were recruited after local advertisement broadcasted on the main website of the faculty of medicine. Healthy students free from medications were encouraged to contact the responsible investigator (AT) by e-mail. Three candidates refused to participate after more detailed information of the study protocol. Written informed consent was obtained from the final study population of 33 (25 males and 8 women) healthy volunteers (20-32 years). Validation of the normality was performed by careful medical history and examinations including electrocardiogram and echocardiogram at rest. None were excluded due to inadequate echocardiographic image quality.

4.1.3 The patients with recent myocardial infarction (study 3 and 4)

The study was conducted at St Olavs University Hospital, which is a tertiary coronary care centre in Trondheim, Norway. The responsible investigator (AT) consecutively considered all the discharged patients at the department of cardiology from April 2008 to June 2009 for possible participation, by reading the discharge summaries. Exclusion criteria were peak cardiac troponin T measurement <0.5 µg/L, prior MI, bundle-branch block with QRS duration >130 ms, significant valvular disease, previous heart surgery, age above 75 years, extensive co-morbidity with short life expectancy, chronic atrial fibrillation and contraindications to LE-MRI. All patients with estimated glomerular filtration rate <60 ml/min per 1.73m^2 or temporary increase in creatinine during the hospital stay were excluded form the study. Patients who had >100 kilometers driving distance to the hospital were also excluded. Of the 82 patients eligible for participation, we were able to reach 77 patients by mail. After reading the informed consent and receiving further information by phone, six patients denied participating due to fear of discomfort during the MRI examination. Thus, 71 consecutive patients with documented first time non–ST-segment–elevation myocardial infarction (NSTEMI) or ST-segment–elevation myocardial infarction (STEMI) and peak cardiac troponin T measurement >0.5 µg/L were prospectively enrolled from April 2008 to June 2009. No patients were excluded because of impaired echocardiographic image quality. Written informed consent was obtained. Five patients were excluded because they were not able to complete the LE-MRI examinations due to claustrophobia. Another eight patients were excluded due to sub-optimal LE-MRI image quality. Thus the final patient population was 58.

4.1.4 The sex and age matched healthy volunteers (study 3 and 4)

In the third wave of the HUNT Study a total of 93,210 people were invited, and 50,839 (54%) participated from autumn 2006 to June 2008. The selection of healthy participants was based

on the self-administered main questionnaire of the HUNT Study, where participants were not eligible if they answered 'Yes' to any of the questions about 'having' or 'ever had' cardiovascular disease, hypertension or diabetes. Participants were then selected by randomization. Validation of the normality was performed by careful medical history and examinations by the physician echocardiographer (HD). After exclusion of 30 subjects due to significant pathology on echocardiography, electrocardiogram or clinical examination, the final study population consisted of 1266 subjects in the HUNT echocardiography study. No patients were excluded because of impaired echocardiographic image quality. Written informed consent was obtained. From this study population, 35 subjects matched for age and sex with the infarct population of study three and four, were randomly selected as healthy control group.

4.2 Study design

4.2.1 The reproducibility study (study 1)

Two experienced physician echocardiographers (AT and HD), blinded to each other's recordings, performed separate complete echocardiographic examinations on all the participants (20 examinations in total). The recordings on the same subject were separated by a time interval of approximately 30 minutes. Both echocardiographers analysed all measurements. Inter-observer reproducibility was defined as the reproducibility calculated by separate recordings. Inter-analyser reproducibility was defined as the reproducibility calculated by the two echocardiographers' analyses of the same set of recordings. Intra-analyser reproducibility was defined as the reproducibility calculated by one of the echocardiographers reanalyses of his own recordings. The reanalyses were done in random order after a period of approximately three weeks. In all, 20 examinations and 50 analyses

were obtained. The study was approved by the Regional Committee for Medical Research Ethics, and conducted according to the second Helsinki Declaration.

4.2.2 The contraction study (study 2)

All examinations were conducted by one experienced physician echocardiographer (AT). A complete echo/Doppler study at rest was performed in all the participants. Low-dose dobutamine stress echocardiography was performed in 13 subjects. Both low-dose dobutamine stress echocardiography and echocardiography after intravenous administration of metoprolol were performed in seven subjects. Echocardiography after intravenous administration of metoprolol was performed on 13 subjects. In total 20 paired rest-dobutamine recordings and 20 paired rest-metoprolol recordings were obtained and the subsequent measurements were categorised into three contractile states: beta-blocker, rest or dobutamine.

Dobutamine was initially infused at 5 mcg/kg/min for three minutes, before the infusion rate was increased to 10 mcg/kg/min. The recordings were obtained after additional three minutes of continuously infusion of 10 mcg/kg/min. dobutamine (steady state). All the analyses were based on apical recordings, which were obtained in less than one minute for each contractile state. For the beta-blocker study, 15 mg of metoprolol was injected over 10 minutes, and a new complete echo/Doppler study started 10 minutes after the last injection of metoprolol. Thus, for those who received both dobutamine and metoprolol, the recordings after infusion of metoprolol started more than 20 minutes after the infusion of dobutamine was ended.

Recordings of the 20 subjects were compared during resting conditions and under influence of dobutamine (paired recordings). Correspondingly, recordings of the 20 subjects (with 7 overlapping the dobutamine group) were compared during resting conditions and under influence of metoprolol (paired recordings). All participants completed their pre-

specified protocol. The study was approved by the Regional Committee for Medical Research Ethics, and conducted according to the second Helsinki Declaration.

4.2.3 The infarction studies (study 3 and 4)

Echocardiograms were performed within three hours before or after the LE-MRI examinations and in average 31 ± 11 days after the index MI. Different indices of LV global and regional function were obtained from the echocardiographic recordings of the patients and healthy controls. LE-MRI was used as a reference method, but the control group was not examined by LE-MRI and their infarction size was assumed to be 0%. The correlations between global and segmental percentage infarct volume fraction assessed by LE-MRI and each global and segmental echocardiographic index were calculated.

The study population was divided in three; healthy controls, patients with infarct size <12%, and patients with infarct size >12%. Furthermore, segments with percentage infarct volume fraction <1% were classified as not infarcted, segments with percentage infarct volume fraction >1% were classified as infarcted, and segments with percentage infarct volume fraction >50% were classified as transmurally infarcted. AUC of each echocardiographic method for identification of small MI, large MI, infarcted segments, and transmurally infarcted segments were calculated. Thus, study three and four compared different echocardiographic methods in the assessment of global and regional LV function in patients with recent MI, using LE-MRI as reference method. In study three we tested out whether a new method for direct quantification of infarct size based on area measurement by TD based colour coded SRs data corrected by visual wall motion analysis gave incremental diagnostic value compared with other 2D echocardiographic methods. In study four we tested whether 3D dynamic multi-slice echocardiography and 3D speckle gave incremental diagnostic value compared with 2D echocardiography. The studies were approved by the

Regional Committee for Medical Research Ethics, and conducted according to the second Helsinki Declaration.

4.3 Echocardiographic acquisition and analysis

4.3.1 Echocardiographic image acquisition

In study one all the participants were examined with a Vivid 7 scanner (GE Vingmed, Horten, Norway) with a phased-array (M3S) transducer. All participants in study two and 46 patients and the healthy controls in study three and four were examined with a Vivid 7 scanner with a M3S transducer for the 2D recordings and a matrix-array (3V) transducer for the 3D recordings. Fourteen patients in study three and four were examined with a E9 scanner (GE Vingmed, Horten, Norway) with a M3S transducer for the 2D recordings and a 3V transducer for the 3D recordings.

All the participants in the four studies were examined in the left lateral decubitus position. The recordings were obtained during quiet respiration or breath-hold. Three consecutive cycles in B-mode acquisitions and colour tissue Doppler mode were recorded from the three apical views (4-chamber, 2-chamber and long-axis), and three consecutive cycles were recorded in B-mode acquisitions from three parasternal views (mitral valve, papillary muscle, and apical short-axis planes). In study one and two colour tissue Doppler acquisitions were recorded at a mean frame rate of 110 $s^{-1,}$ and the B-mode recordings were recorded at a mean frame rate of 44 s^{-1} in study one and a mean frame rate of 50 s^{-1} in study two. In study three and four colour tissue Doppler acquisitions were recorded at a mean frame rate of 123 s^{-1}, and the B-mode recordings were recorded with a mean frame rate 61 s^{-1}.

Pulsed wave Doppler mitral flow velocities were recorded from the apical four-chamber view with the sample volume between the leaflet tips. The left ventricular outflow tract (LVOT) velocity was recorded from the apical five-chamber view with the sample

volume positioned about five mm proximal to the aortic valve. Spectral TD mitral annular velocities were acquired with a 6 mm sample volume positioned at the base of the septal, lateral, inferior and anterior walls. Recording for isovolumic relaxation time measurement was obtained by simultaneous recording of the aortic and mitral flows. Pulmonary venous flow velocities were recorded with the sample volume approximately one cm into the right upper pulmonary vein.

Real-time 3D echocardiography recordings were preformed immediately after the 2D examination. From the apical approach four to six consecutive ECG-gated subvolumes were acquired during end-expiratory apnoea to generate full volume data sets (mean frame rate 26 s^{-1}). Care was taken to encompass the entire LV cavity and, if unsatisfactory, the data set was re-acquired (98). All echocardiographic data were stored digitally and analyzed subsequently.

4.3.2 Analysis of B-mode and Doppler echocardiography

LV volumes and LVEF were measured by biplane Simpson's rule from the apical four- and two-chamber views (98). End-diastolic volume was measured at the time of mitral valve closure, and end-systolic volume was measured on the image with the smallest LV cavity. LV internal end-diastolic and end-systolic dimensions, the inter ventricular septal wall thickness, and the posterior wall thickness were measured perpendicular to the long axis of the ventricle at the mitral valve leaflet tips in the parasternal long-axis view, using anatomical M-mode echocardiography. The fractional shortening of the myocardium in short axis was calculated as the difference between the LV internal end-diastolic and end-systolic dimension divided by the LV internal end-diastolic dimension. LVEF was also obtained from the 3D recordings (four-dimensional auto LV quantification, version BT11, GE Vingmed Ultrasound, Horten, Norway). End-diastolic and end-systolic volumes were measured after manual alignment followed by automatic detection of endocardial surface, which was manually adjusted by placing as many additional points as needed in three dimensions at both end-diastole and end-

systole. Finally the automatically detected epicardial borders were manually adjusted in three dimensions at end-diastole in order to calculate LV mass.

The mitral flow early diastolic filling velocity (E), late atrial filling velocity (A), E-wave deceleration time, and E/A-ratio were measured. Isovolumic relaxation time was measured from the start of the aortic valve closure signal to the start of mitral flow. The LVOT peak velocity was measured from the LVOT spectrum using low gain setting. The LVOT velocity time integral was measured by tracing the modal velocity throughout systole. From the pulmonary venous flow waveforms, peak systolic velocity, peak antegrade diastolic velocity.

From the pulsed wave spectral TD recordings peak systolic mitral annular velocity (S′), peak early diastolic annular velocity (e′), and late diastolic velocity (a′) were measured at the peak of the Doppler spectrum with low gain setting *(figure 5A)*. S′ were also measured at the peak of the curve obtained from colour TD *(figure 5B*). MAE was measured using anatomical M-mode echocardiography from the apical position *(figure 5C)* and from colour TD by integration of the TD velocity curves *(figur 5C)*. Measurements of the septal, lateral, inferior and anterior walls were averaged for S′, e′, a′, MAE and LV length. E/e′ ratio was calculated by dividing E by the average e′(spectral TD) of the septal, lateral, inferior and anterior walls. In study three, S′ corrected for the ventricle length (S´/LV length) and the fractional shortening of the myocardium in long axis were calculated by dividing spectral TD S′ by spectral TD and M-mode MAE by the end-diastolic length of the left ventricle (99). All measurements reflected the average of three cardiac cycles during quiet respiration.

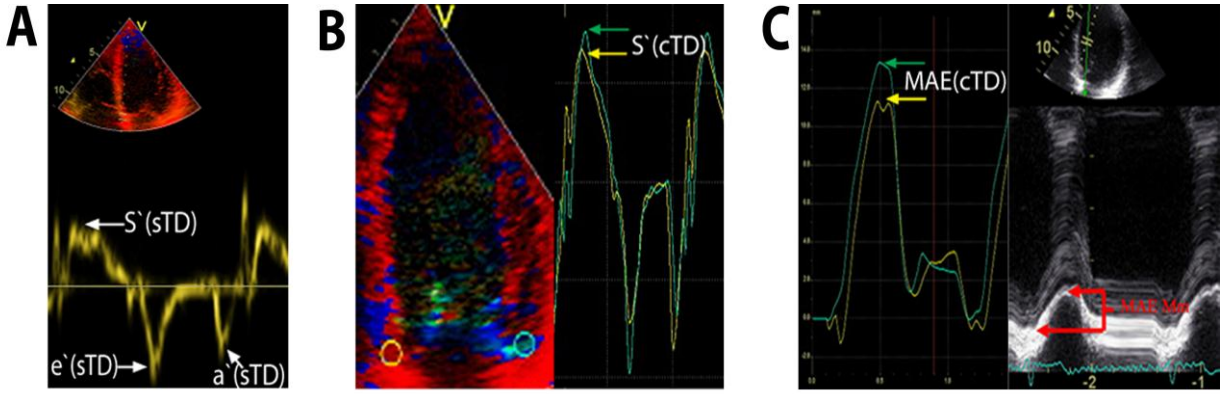

Figure 5: *A: Spectral tissue Doppler (sTD) derived septal mitral annulus velocities. Peak systolic velocity S'(sTD), early diastolic velocity (e'(sTD)) and late diastolic velocity a'(sTD) measured at the maximum of the Doppler spectrum with low gain setting. B: Velocity curves from colour tissue Doppler (cTD). Peak systolic mitral annulus velocity S'(cTD) measured at the peaks. C: Measurements of systolic mitral annular excursion (MAE) by integrated velocity curves from colour tissue Doppler MAE(cTD) and by reconstructed M-mode MAE(Mm).*

4.3.3 2D and 3D wall motion analysis

Two-dimensional wall motion score (WMS) was based on combined judgement of three apical views (4-chamber, 2-chamber and long-axis) and three parasternal views (mitral valve, papillary muscle, and apical short-axis planes), all recorded in B-mode. Three-dimensional WMS was analyzed in dynamic multi-slice view, obtained from the apex *(figure 6).* According to the American Society of Echocardiography recommendations, the LV was divided in a 16-segment model defined by various landmarks (1). Segmental WMS was graded as 1; normal, 2; hypokinetic, 3; akinetic, and 4; dyskinetic. The WMS was based on qualitative frame-by-frame judgement of the wall thickening of each segment. Segments with only passive movement or only post-systolic thickening were considered as akinetic. Wall motion score index (WMSI) was calculated by averaging the scored segments when ≥12 segments were accepted for analysis.

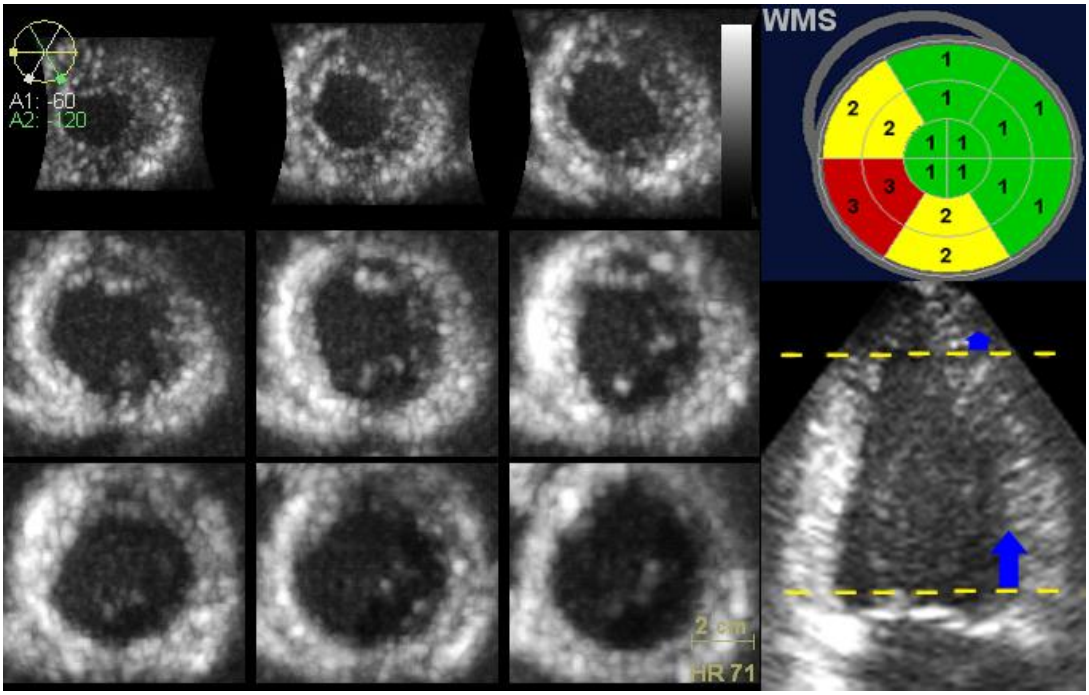

Figure 6: *Left: Three-dimensional wall motion analysis performed by dynamic multi-slice short axis views. Upper right: Bulls-eye presentation of wall motion scores (WMS) indicating inferoseptal myocardial infarction in a 16-segment model. Lower right: Two-chamber view with blue arrows indicating correction for out-of-plane motion caused by longitudinal shortening, which is more prominent at the basal level.*

4.3.4 Direct echocardiographic quantification of infarct size

Longitudinal strain rate was obtained from colour TD recordings by calculating the velocity gradient. The cine loops were post-processed by in-house software (GC lab, ELVIZ). The regions of interest were tracked with TD along the ultrasound beam and grey-scale speckles perpendicular to the ultrasound beam, and the velocity gradient was sampled along curved M-modes drawn along the LV walls. Strain rate data in the areas between the three standard planes were applied by cubic spline interpolation, assuming 60° rotation angle between the three apical planes and displayed as semi quantitative colour coded strain rate in a conventional bull's eye view, as comprehensively described previously (21). The mid-systolic frame was selected for analysis, and on the sub segmental level, areas with mid-systolic strain

rate <-0.5 s^{-1} were automatically marked as normal, areas with mid-systolic strain rate -0.5 s^{-1} to -0.25 s^{-1} were automatically marked as hypokinesia and areas with mid-systolic strain rate >-0.25 s^{-1} were automatically marked as akinesia (21, 100). Strain rate data in the apical ¼ of the apical segments were automatically discarded. Based on combined judgement of the colour coded strain rate data and wall motion analyses in the grey-scale recordings, the areas with marked hypokinesia and akinesia were manually corrected, but in the apical ¼ of the apical segments or in case of obvious artefacts in the strain rate analysis, the judgement of LV function was based on wall motion analyses in grey-scale recordings only. The areas of all the sub segments with hypokinesia and akinesia were divided by the total myocardial area and the total segmental area for estimation of global and segmental area fractions of hypokinesia and akinesia *(Figure 7).* Based on the previously reported relationship between infarct size and WMSI (91) and the relationship between the estimated infarct percentage obtained from peak TnT and the infarcted areas of the 13 patients without satisfactory LE-MRI. (101), the transmurality of the hypokinetic and akinetic areas were defined as 50% and 100%, respectively. Thus, the described area-based method gives a direct estimate of infarct size by echocardiography which can be directly compared to the infarct volume fraction given by LE-MRI.

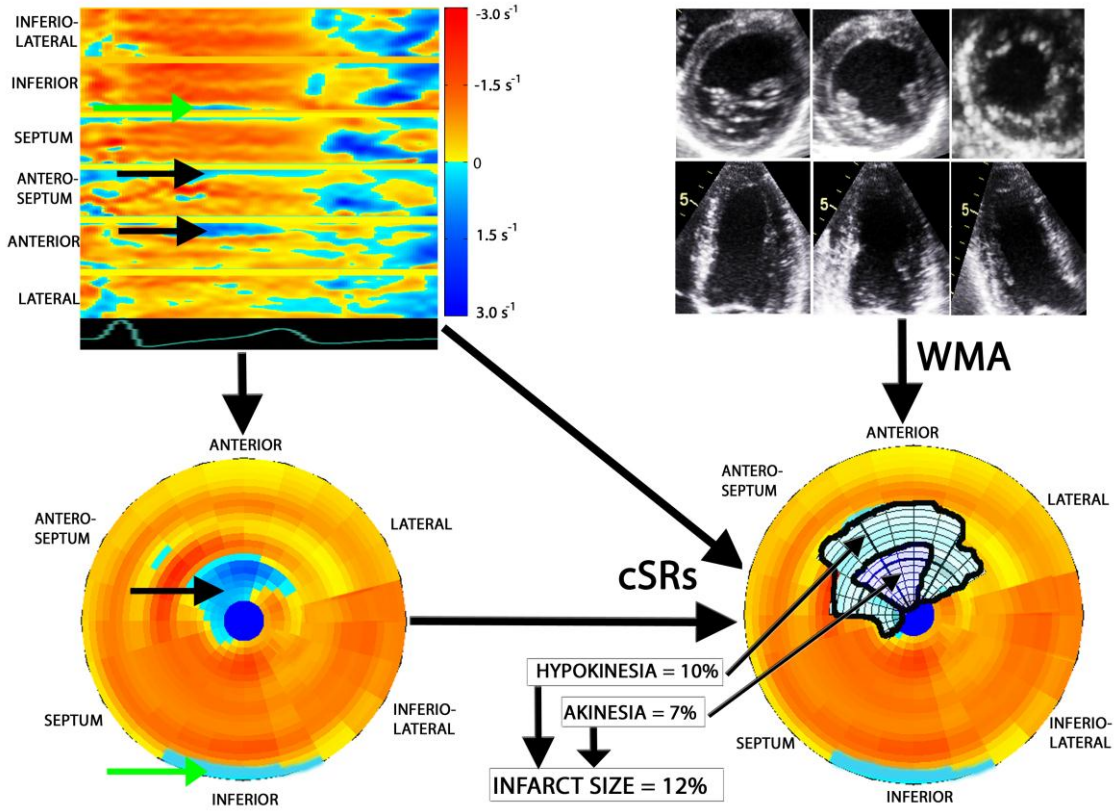

Figure 7: *Composite figure displaying the direct quantification of infarct size by cSRs combined with WMA. Upper left: curved anatomic motion mode of cSRs during systole and early diastole. Lower left: bull's eye view of cSRs during mid-systole. Arrows are indicating areas of suspected artefact and akinesia. Upper right: Three short axis views and three apical views of the left ventricle in B-mode recordings indicating WMA. Lower right: Based on combined judgement of cSRs and WMA, areas of hypokinesia and akinesia are marked and displayed as percentages of the total left ventricle area. Infarct size estimated assuming 50% infarct volume fraction in the hypokinetic areas and 100 % infarct volume fraction in the akinetic areas. Abbreviations: cSRs = tissue Doppler based colour coded systolic strain rate data; WMA = wall motion analysis.*

4.3.5 2D Echocardiographic quantitative deformation analysis

Two-dimensional longitudinal strain and strain rate were obtained by three different methods. For all the 4 studies, longitudinal strain was obtained by 2D speckle tracking in B-mode recordings (Automated Function Imaging; EchoPAC PC version BT 09-11, GE Vingmed, Horten, Norway). The regions of interest were manually adjusted to include the entire LV myocardium and simultaneously avoid the pericardium. Location of end-systole was manually corrected if necessary. The smoothing of the Automated Function Imaging EchoPAC software was not adjusted (i.e. default smoothing was used) in the first set of analyses. In study three and four a second set of longitudinal strain values were obtained by using exactly the same regions of interest, but with minimum smoothing in the adjustable post processing parameters of the Automated Function Imaging EchoPAC software. In study one the 2D speckle tracking method was also used to obtain segmental systolic and diastolic strain rate values. Peak systolic strain rate was measured as the maximal negative strain rate value during ejection time, early diastolic peak strain rate was measured as the maximal positive strain rate during the first part of diastole, and late diastolic peak strain rate was measured as the maximal positive strain rate during the last part of diastole.

In study one and four 2D longitudinal strain and strain rate were also obtained from a semi automatic combination of TD and speckle tracking by customized software (GcMat; GE Vingmed Ultrasound, Horten, Norway) that runs on a MATLAB platform (MathWorks, Inc., Natick, MA, USA) (28). The kernels at the segmental borders were tracked with TD along the ultrasound beam and grey-scale speckles perpendicular to the ultrasound beam. Strain was calculated from the variation of segment length, and strain rate was calculated as the temporal derivative of strain, with correction to Eulerian strain rate. End-systolic strain was measured at aortic valve closure (25), and peak systolic strain rate was measured as the maximal negative strain rate value during ejection time. In study one this method was also used to

measure early diastolic peak strain rate as the maximal positive strain rate during the first part of diastole and late diastolic peak strain rate as the maximal positive strain rate during the last part of diastole.

In study three longitudinal strain rate was calculated from colour tissue Doppler recordings, using the tissue Doppler velocity gradient along the ultrasound beam (Q-Analysis; EchoPAC PC version BT 09, GE Vingmed, Horten, Norway). For each segment a stationary region of interest with offset length 12 mm was manually positioned in the middle of the myocardium. The region of interest was adjusted up to 10 mm longitudinally and 5 mm laterally in order to avoid noise. Peak systolic strain rate was measured as the maximal negative value during ejection.

For the three quantitative deformation methods, segments with poor tracking were excluded manually, and segmental values were obtained for each segment in the standard American Association of Echocardiography 16 segment model of the LV (1). Global averages of the segmental strain and strain rate values were calculated by averaging all the accepted segmental values, but in study three and four global averages were only calculated if at least 12 segmental values were accepted for analyses.

4.3.6 3D Echocardiographic quantitative deformation analysis

Three-dimensional strain analysis was conducted using auto LV quantification (version BT11, GE Vingmed Ultrasound, Horten, Norway) *(Figure 8).* After manual alignment of the three apical views and the short axis view, points were placed in the mitral annulus plane and at the apex, in end-diastole and end-systole. End systole, which was defined as the frame with the smallest LV cavity, was automatically detected by the software, but manually corrected if necessary. End-diastolic and end-systolic volumes were measured by semi-automatic detection of the endocardial surface, with manual adjustment, and 3D LVEF was calculated. The epicardial border was automatically detected by the software and manually adjusted, in

order to delineate the region of interest for the analysis of end-systolic 3D longitudinal, circumferential, transmural and area strain. The strain values were obtained by a midwall tracking algorithm, based on frame-to-frame block matching in three dimensions. Area strain was calculated as the percentage variation in the midwall surface area. Finally, the tracking of each segment was manually controlled, and segments with sub-optimal tracking were manually rejected. Measurements of 3D global longitudinal strain, 3D global circumferential strain, 3D global transmural strain, and 3D global area strain were calculated by averaging the end-systolic segmental values when ≥12 segments had acceptable tracking (1).

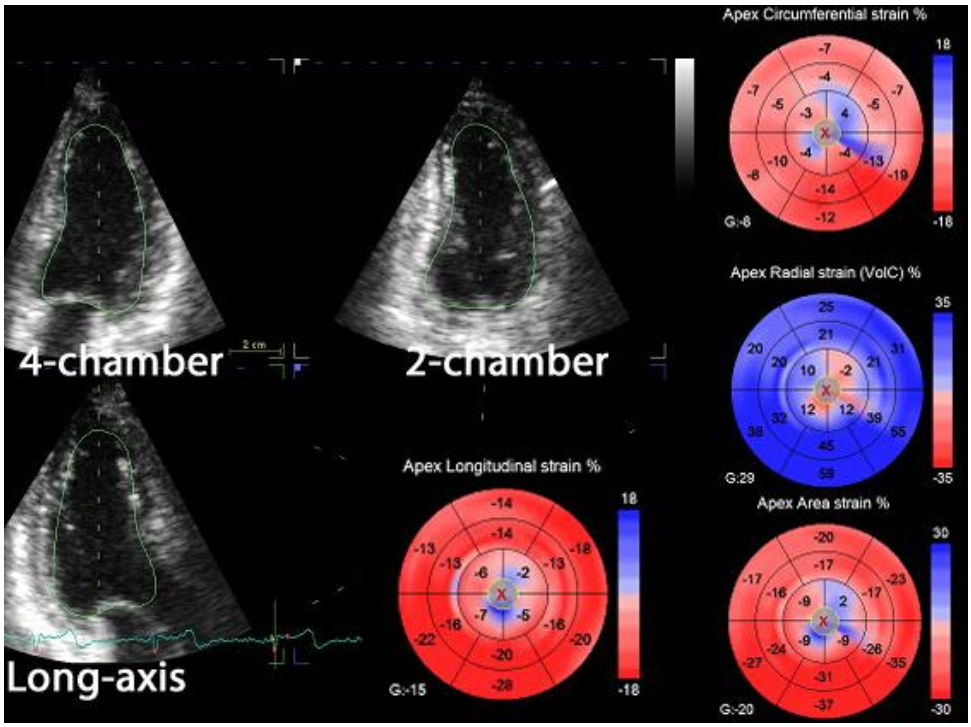

Figure 8: *Analyses of global and segmental three-dimensional longitudinal, circumferential, radial (transmural), and 3D area strain in a patient with an apical anterior myocardial infarction. The regions of interest were delineated after semi-automatic detection of the endocardial surface and the epicardial borders in end-diastole and end-systole.*

4.4 MRI acquisition and analysis

4.4.1 MRI acquisition

Examinations were performed on a 1.5 T Siemens Avanto (Siemens Medical, Erlangen, Germany) with a six-element body matrix coil. Late-enhancement images were obtained 10-20 minutes after intravenous injection of 0.15 mmol/kg gadodiamide (Omniscan, GE Healthcare, Oslo, Norway) in multiple short-axis slices covering the LV. A balanced steady-state free precision inversion recovery sequence was used, with ECG-triggered data acquisition in mid-diastole. Typical image parameters were: matrix 176x256, in-plane resolution 1.3x1.3 mm, slice thickness 8 mm, gap 2 mm, flip angel^{o}, and inversion time 280-350 ms.

4.4.2 MRI analysis

The LE-MRI analyses were performed by two operators (PH and BHA), using Segment v1.7 (102). On each short-axis image, the total myocardial area as well as the area of infarcted myocardium was semi-automatically drawn. Areas with signal intensity more than two SDs above normal myocardium were considered infarcted. The infarct size was calculated as infarct volume in percentage of total myocardial volume. As short- and long-term mortality rates have been demonstrated to be increased in patients with infarct size >12% (103), patients were divided in small and large MI, using 12% as cut-off. Segments with infarct volume fraction >50% were classified as transmurally infarcted, while segments with infarct volume 1-50% were classified as sub-endocardially infarcted (65, 91).

All echocardiographic and LE-MRI analyses were performed separately and blinded to other analyses and participant's data.

4.5 Statistical analyses.

Continuous variables are presented as mean ± SD. Categorical variables are presented as numbers (%). In study one the coefficient of repeatability was calculated according to the method of Bland and Altman as 2×SD of the differences in repeated measurements (66). The percentage error was derived as the absolute difference between the two sets of observations, divided by the mean of the observations (69, 71), and the mean error was defined as the average percentage error of each echocardiographic measurement. For comparison of the mean errors, one-way analysis of variance with post-hoc least significant difference (104) was used.

In study two the relative changes between different contractile states were calculated as the measured difference between rest and the contractile state, divided by the measurement at rest. For multiple comparisons, one-way ANOVA with post-hoc Tukey correction were used. The area under the receiver operating characteristic curve (AUC) for detection of different contractile states was also used for comparison of the methods. We also calculated the intervals given by mean ± 2SD for indices at rest and during the different contractile states, and compared the percentage overlap relative to the mean at rest of these intervals.

In study three and four differences between small and large MIs and the healthy controls were analyzed by independent samples *t*-test. For the global indices, the relationship between the infarct size assessed by LE-MRI and each echocardiographic index was analyzed by bivariate correlation based on normal distribution among the final 58 patients and reported as Pearson's correlation coefficient (*r*). For the segmental indices, the relationship between each echocardiographic index and the segmental percentage infarct volume fraction assessed by LE-MRI was analyzed by bivariate rank correlations and reported as Spearman's correlation coefficient (*r*). Correlation coefficients were compared according to the method described by Meng et al (105). The area under the receiver-operating characteristic curves

(AUC) for the identification of small and large MIs is reported. AUC for the different methods was compared according to the method described by Hanley and McNeil (106). Cut-off values giving the largest sum of sensitivity and specificity are reported. Statistical analyses were performed in SPSS version 17 (SPSS Inc, Chicago, Ill)

5 Summary of results

5.1 Feasibility (all studies)

Estimation of biplane 2D and 3D LVEF, mitral annulus velocity and -motion indices, and flow Doppler indices were feasible in all recordings. On the segmental level the feasibility was 98% (1455 accepted segments out of 1488 segments) for 2D wall motion score, and 95% (1405 accepted segments out of 1488 segments) for 3D wall motion score, 99% (1469 accepted segments out of 1488 segments) for direct quantification of infarct size by tissue Doppler strain rate and wall motion analyses (GC lab, ELVIZ), 83% (2932 accepted segments out of 3522 segments) for the 2D speckle tracking (Automated Function Imaging; EchoPAC), 81% (1210 accepted segments out of 1488 segments) for the combined 2D TD and speckle tracking method (GcMat), 85 % (1120 accepted segments out of 1314 segments) for the tissue Doppler velocity gradient method (Automated Function Imaging; EchoPAC), and 71% (1050 accepted segments out of 1488 segments) for the 3D speckle tracking (Auto LVQ EchoPAC).

5.2 The reproducibility study (study 1)

In study one, the MAE by M-mode showed the best reproducibility with an inter-observer mean error of 4% and coefficient of repeatability of 1.6 mm. After correcting for multiple comparisons of the systolic indices in table 3, the inter-observer mean error of the MAE by M-mode was significantly lower ($P<0.05$) than the inter-observer mean error of the interventricular septal and posterior wall thickness, the fractional shortening of the

myocardium in short axis, the biplane end-diastolic and end-systolic volumes, the LVOT peak velocity, and the global peak systolic strain rate obtained by 2D speckle tracking.

Table 3: Reproducibility of measurements of dimensions and global systolic function

Method	**Mean** inter-observer	**COR** inter-observer	**Mean Error** inter-observer	**Mean Error** inter-analyser	**Mean Error** intra-analyser
IVSd (Mm)	8.5 (1.1) mm	1.8 mm	12 %	10 %	10 %
LVPWd (Mm)	7.7 (1.1) mm	2.4 mm	12 %	10 %	10 %
LVIDd (Mm)	50 (5.3) mm	5.4 mm	5 %	5 %	3 %
MAE (Mm)	17 (1.1) mm	1.6mm	4 %	3 %	3 %
MAE (cTD)	15 (1.1) mm	2.2mm	7 %	4 %	2 %
S′(sTD)	9.1 (2.0) cm/s	1.7 cm/s	8 %	3 %	2 %
S′(cTD)	7.7 (1.4) cm/s	1.6 cm/s	7 %	3 %	2 %
EDV biplane	108 (24) ml	14ml	12 %	8 %	8 %
ESV biplane	44 (9) ml	9ml	9 %	10 %	9 %
LVEF biplane	0.59 (0.05)	0.07	6 %	6 %	5 %
FS	0.33 (0.06)	0.11	14 %	16 %	13 %
LVOT peak	1.0 (0.1) m/s	0.2m/s	10 %	3 %	3 %
Global S_{ES} (2D-St)	0.21 (0.02)	0.02	6 %	6 %	3%
Global SR_S (2D-St)	-1.1 (0.01) s^{-1}	$0.2s^{-1}$	9%	5%	5%

Table 3: *Mean (standard deviation), coefficient of repeatability (COR) and mean error of systolic indices. IVSd (Mm) = end-diastolic interventricular septal thickness by M-mode, LVPWd (Mm) = left ventricular end-diastolic posterior wall thickness by M-mode, LVIDd (Mm) = left ventricular end-diastolic internal diameter by M-mode MAE(Mm) = systolic mitral annulus excursion by M-mode, MAE(cTD) = systolic mitral annulus excursion by colour tissue Doppler, S'(sTD) = peak systolic annulus velocity by pulsed wave spectral tissue Doppler, S'(cTD) = peak systolic annulus velocity by colour tissue Doppler, EDV = end-diastolic volume, ESV = end-systolic volume, EF = ejection fraction, FS = fractional shortening of the myocardium in short axis, LVOT peak = left ventricular outflow tract peak velocity, S_{ES} (2D-ST) = end-systolic strain by the 2D-strain application, SR_S (2D-ST) = peak systolic strain rate by the 2D-strain application, both measured by the 2D-strain application.*

After correcting for multiple comparisons of the diastolic indices in table 4 the inter-observer mean errors of the E, e′, a′ and the global early diastolic peak strain rate obtained by 2D speckle tracking were significantly (P<0.04) lower than the A, the E deceleration time, the E/A ratio, and the peak systolic and diastolic pulmonary venous flow velocity.

Table 4: Reproducibility of global diastolic measurements

Method	**Mean** inter-observer	**COR** inter-observer	**Mean Error** Inter-observer	**Mean Error** inter-analyser	**Mean Error** intra-analyser
e′	14 (1.0) cm/s	3.4 cm/s	8%	3%	2%
a′	8.5 (2.5) cm/s	2.1 cm/s	9%	9%	2%
E	74 (13) cm/s	12 cm/s	8%	5%	2%
DT	175 (33) cm/s	10 cm/s	20%	17%	8%
A	41 (12) cm/s	14 cm/s	18%	10%	4%
E/A	2.0 (0.6)	0.35	22%	10%	5%
IVRT	83 (9) ms	13 ms	17%	7%	3%
E/e′	5.4 (1.0)	1.3	11%	7%	3%
PV S	55 (12) cm/s	12 cm/s	15%	4%	5%
PV D	54 (7) cm/s	20 cm/s	16%	4%	4%
PV S/D	1.0 (0.2)	0.38	12%	6%	6%
Global SR_E (2D-St)	1.6 (0.1) s^{-1}	0.3s^{-1}	7%	8%	7%
Global SR_A (2D-St)	0.8 (0.1) s^{-1}	0.3s^{-1}	13%	8%	12%

Table 4: *Mean (standard deviation), coefficient of repeatability (COR) and mean error of systolic indices, e′ = mean peak early diastolic velocity by pulsed wave spectral tissue Doppler, a′ = mean peak late diastolic velocity by pulsed wave tissue Doppler imaging, E = mitral flow peak early diastolic filling velocity, A = mitral flow peak late diastolic filling velocity, DT = E-wave deceleration time, IVRT = isovolumic relaxation time, PV S = pulmonary venous flow peak systolic velocity, PV D = pulmonary venous flow peak diastolic velocity diastolic, Global SR_E = peak early diastolic strain rate, Global SR_A = Peak late diastolic strain rate, both measured by the 2D-strain application.*

Another important finding of study one is that repeated analyses of the same recordings underestimate the clinically more relevant inter-observer reproducibility obtained by separate examinations by approximately 40% for most measurements of LV systolic function and approximately 50% for most measurements of LV diastolic function. Furthermore, the inter-

observer mean errors of e′ and a′ were reduced by 40% and 31% (P<0.022), respectively when 4 instead of 2 walls were averaged. This corresponds to a reduction in the inter-observer mean error from 15% to 8% and the coefficient of repeatability from 4.9 cm/s to 3.4 cm/s for e′, and a reduction in the inter-observer mean error from 13% to 9% and the coefficient of repeatability from 2.7 cm/s to 2.2 cm/s for the a′. The mean error and the coefficient of repeatability of the S' were reduced from 11% to 8% and 2.3 cm/s to 1.7 cm/s when 4 instead of 2 walls were averaged.

The inter-observer mean error and the coefficient of repeatability were 14% and 7.1% (percentage points) for segmental strain by 2D speckle tracking and 17% and 0.52 s^{-1} for peak systolic strain rate by 2D speckle tracking. When segmental strain and strain were averaged into global indices of LV performance, there were highly significant reductions of the mean errors by 60% for segmental strain and 44% for peak systolic strain rate. There were no significant differences in the reproducibility of 2D speckle tracking compared with the combined 2D tissue Doppler and speckle tracking method at the global level, but the inter-observer mean error of segmental strain by 2D speckle tracking was significantly lower (P=0.03) than segmental strain by the combined 2D tissue Doppler and speckle tracking method.

5.3 The contraction study (study 2)

The systolic measurements were divided into peak systolic velocity indices (occurring during the rapid ejection phase) and end-systolic indices (reflecting the total work performed by the left ventricle during the ejection). S′ by spectral TD, S′ by colour TD, LVOT peak velocity and peak systolic strain rate by TD were defined as peak systolic velocity indices. Two-dimensional and 3D LVEF, fractional shortening of the short axis, MAE by M-mode, MAE by colour TD, global longitudinal strain by 2D speckle tracking, and the LVOT velocity time integral, were defined as end-systolic velocity indices.

During stress the relative increase of the peak velocity indices ranged from 51% to 62%, and these changes were significantly higher (all P<0.05) than the relative changes of all end-systolic indices which ranged from 21% to 31%. The range and the mean ± 2SD at rest and during stress overlapped for all indices except S′ by spectral TD, S′ by colour TD and peak systolic strain rate by TD (*Figure 9 and Table 5*).

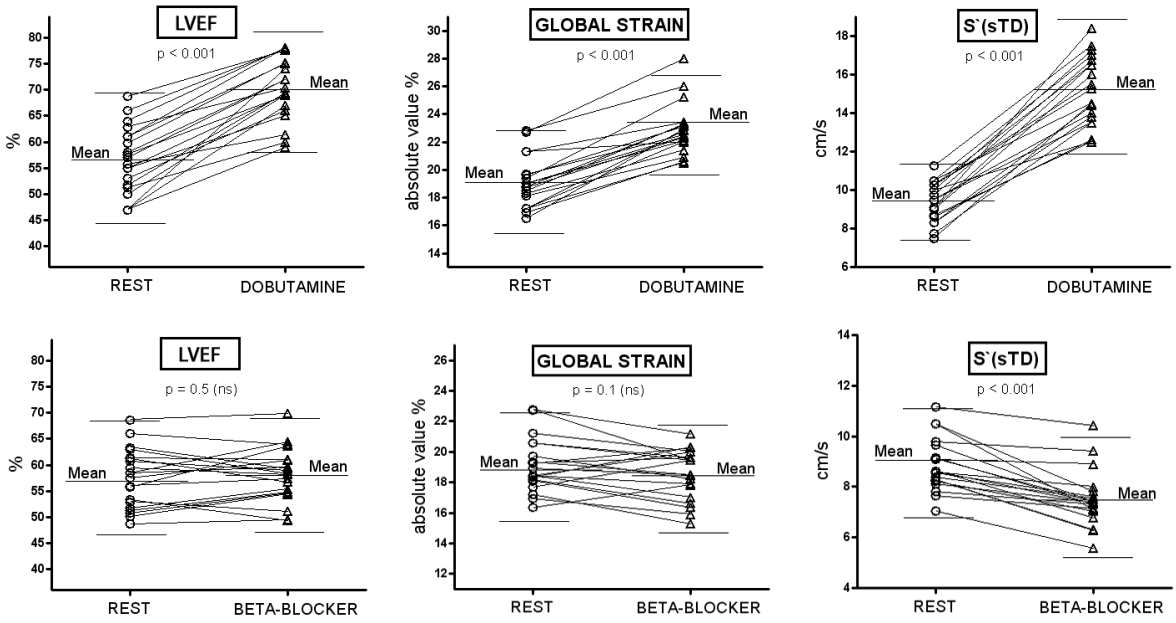

Figure 9: *Individual changes of left ventricular ejection fraction (EF, global strain, and peak systolic velocity spectral tissue Doppler mitral annulus velocities (S`(sTD)) at rest, during low-dose dobutamine (upper panels) and after injection of metoprolol (lower panels). The mean (wide line), the mean ±2SD (narrow line) and the p-value of the change are displayed for each variable. The relative change during stress and after injection of metoprolol was highest for S`(sTD).*

Table 5: Systolic echocardiographic indices at rest and during dobutamine.

	Mean (SD) at rest	Mean (SD) during stress	Mean change (95% CI)	Mean ±2SD overlap rest vs dobutamine (% overlap)	AUC (95% CI)
Peak systolic velocity indices					
S′(spectral TD)	9.4 (1.0) cm/s	15.1 (1.8) cm/s	62% (53 - 71)%	-0.10 cm/s (no overlap)	1.00 (1.00 – 1.00)
S′(colour TD)	7.6 (0.9) cm/s	11.5 (1.0) cm/s	52% (43 - 62)%	-0.06 cm/s (no overlap)	1.00 (1.00 – 1.00)
LVOT peak	1.0 (0.1) m/s	1.7 (0.2) m/s	60% (48 - 73)%	0.11 m/s (11%)	0.99 (0.99 – 1.00)
Global SRs (TD)	-1.2 (0.1) s^{-1}	-1.8 (0.1) s^{-1}	56% (50 - 61)%	0.2 s^{-1} (no overlap)	1.00 (1.00 – 1.00)
End-systolic indices					
Global strain (2D-ST)	-0.19 (0.02)	-0.23 (0.02)	21% (17 - 25)%	3.4 (18%)	0.95 (0.86 – 1.00)
LVOT vti	21 (4) cm	27 (4) cm	30% (20 - 40)%	8.6 cm (41%)	0.89 (0.79 – 1.00)
MAE(M-mode)	15 (2) mm	20 (2) mm	30% (25 - 36)%	2.8 (18%)	0.96 (0.91 – 1.00)
MAE(colour TD)	15 (2) mm	18 (2) mm	23% (17 - 29)%	3.4 mm (23%)	0.93 (0.85 – 1.00)
2D LVEF	0.57 (0.06)	0.70 (0.06)	25% (20 - 30)%	0.11 (21%)	0.95 (0.89 – 1.00)
3D LVEF	0.56 (0.04)	0.69 (0.04)	24% (21-27)%	0.03 (5%)	1.00 (1.00 – 1.00)
FS_S	0.32 (0.04)	0.42 (0.06)	31% (24 – 37)%	0.10 (32%)	0.89 (0.60 – 1.00)

Table 5: *AUC = area under the receiver operating characteristic curve for detection of increased contraction; CI = confidence interval; FS_S = fractional shortening of the short axis; LVEF = left ventricular ejection fraction; LVOT = left ventricular outflow tract; MAE = mitral annulus excursion; S′ = peak systolic mitral annulus velocity; SD = standard deviation; SRs = peak systolic strain rate; ST = speckle tracking echocardiography; vti = velocity time integral; TD = tissue Doppler; 2D = two dimensional; 3D = three dimensional.*

After injection of metoprolol, all indices decreased significantly (all P<0.05), except global strain, MAE by M-mode and 2D LVEF. The relative changes of the peak velocity indices ranged from -15 to -11 % and the relative changes of all end-systolic indices ranged from -5 to 1 %. There was a trend for all peak systolic indices to have higher AUC for detection of decreased contraction compared with the end-systolic indices, and this was significant for peak systolic strain rate by TD compared to all end-systolic indices and for S′(spectral TD) compared to global strain, MAE(M-mode) and 2D LVEF.

The relative changes of the diastolic indices during stress and after metoprolol were less pronounced than the changes of the peak systolic indices. During stress the relative change of the diastolic indices ranged from 4% to 31%, and after injection of metoprolol the relative changes ranged from -9% to 14%.

5.4 The infarction studies (study 3 and 4)

5.4.1 Infarct Size by LE-MRI

Evidence of MI was detected by LE-MRI in all patients. The mean (SD) infarct size was 11.4 (8.1)% of the total LV myocardial volume. Thirty-three patients (57%) had calculated the infarct size <12% and 25 patients (43%) had infarct size >12%. Evidence of infarction by LE-MRI was detected in 387 (42%) segments, with transmural extension (>50% late enhancement) in 74 (8%) segments *(Figure 10).*

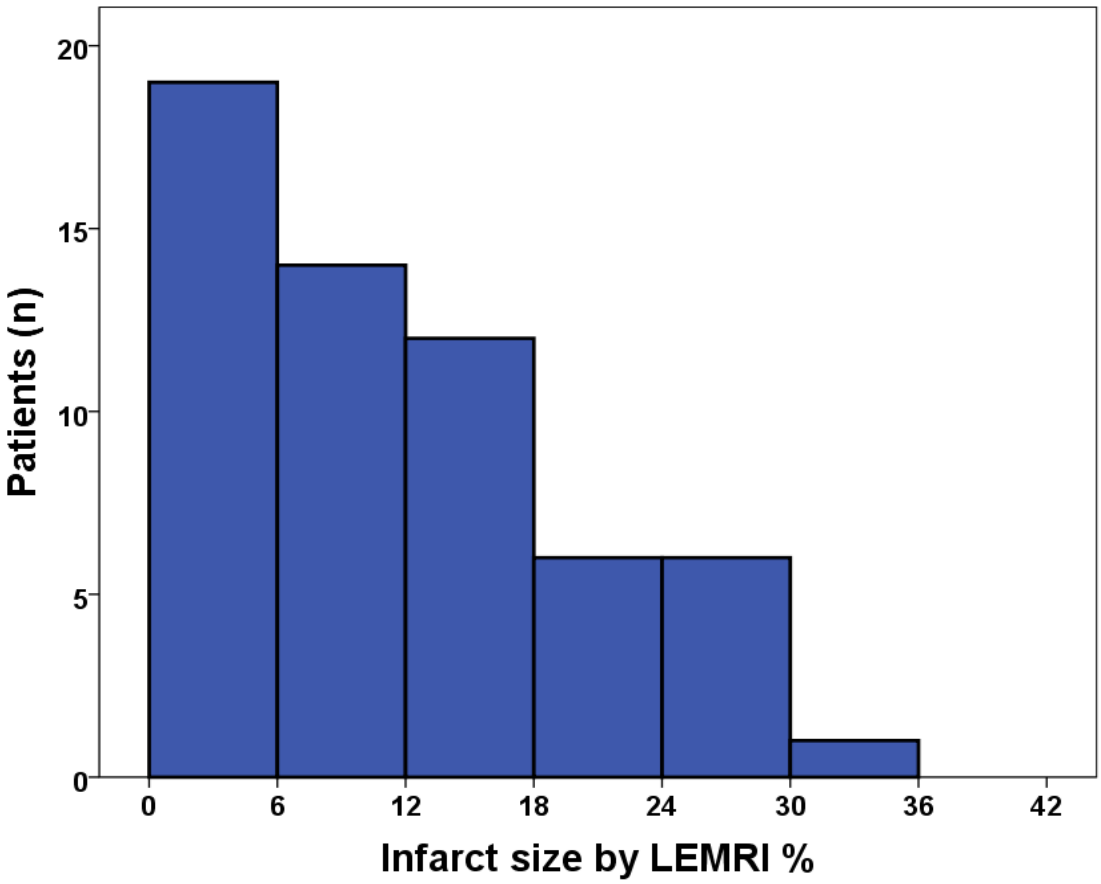

Figure 10: *Histogram demonstrating the distribution of infarct size by LE-MRI.*

Abbreviations: LE-MRI = late enhancement magnetic resonance imaging.

5.4.2 Echocardiography - Global indices

There were significant differences between the patients with large MIs compared with those with small MIs or healthy controls for all the indices (Table 6). In patients with small MIs, the 3D-LVEF was significantly lower (P<0.02) while direct echocardiographic quantification of infarct size and 2D- and 3D-WMSI were significantly higher (P<0.03) compared with the healthy controls. There were significant correlations between global infarct size assessed by LE-MRI and all the echocardiographic indices of LV global function with r = 0.51 for 3D-LVEF, 0.55 for 2D-LVEF, 0.61 for FS_L, 0.44 for S´/LV, 0.72 for 3D-WMSI, 0.74 for 2D-WMSI, 0.81 for direct echocardiographic quantification of infarct size, 0.67 for global longitudinal strain by 2D speckle tracking with default smoothing, 0.66 for global

longitudinal strain by 2D speckle tracking with minimum smoothing, 0.56 for global longitudinal strain by 2D TD and speckle tracking, 0.44 for global longitudinal strain rate by 2D TD and speckle tracking for 0.42 for global longitudinal strain by 3D speckle tracking, 0.47 for global circumferential strain by 3D speckle tracking, 0.48 for global transmural strain by 3D speckle tracking, and 0.50 for global area strain by 3D speckle tracking. The correlation coefficient of direct echocardiographic quantification of infarct size was significantly higher ($P<0.05$) than all the other echocardiographic indices.

The AUC for identification of large MIs ranged from 0.66 to 0.84 (Table 6). Direct echocardiographic quantification of infarct size demonstrated the highest AUC for separation of small vs. large MI, large MI vs. healthy controls and small MI vs. healthy controls, but the differences between methods were not statistical significant for most of the comparisons. A cut-off value of 7.0% by direct echocardiographic quantification of infarct size had a sensitivity of 72% and a specificity of 88% for separating small and large MI. Three-dimensional-WMSI of 1.11 and 2D-WMSI of 1.14 had a sensitivity of 76% and 72% and a specificity of 72% and 74%, respectively, to separate small and large MI, while global longitudinal strain by 2D speckle tracking of 16.5% had a sensitivity of 68% and a specificity of 85% to separate small and large MIs.

The correlation coefficient of the peak cardiac troponin T with global infarct size assessed by LE-MRI was $r = 0.66$ ($P<0.001$). The AUC of the peak cardiac troponin T for separation of small vs. large MI was 0.79. Peak cardiac troponin T of 3.0 µg/L had a sensitivity of 92% and a specificity of 64% to separate small and large MIs.

Table 6 AUC for identification of large MI and transmurally infarcted segments of the different echocardiographic indices of global and segmental LV function

	AUC (95% CI) of global indices for separation of large and small MIs	AUC (95 % CI) of segmental indices for identification of transmurally infarcted segments
Infarct size by the new method	0.84 * (0.73-0.94)	0.89 § (0.84-0.94)
2D WMS	0.79 (0.67-0.91)	-
3D-WMS	0.80 (0.68-0.91)	-
2D longitudinal speckle tracking strain, default smoothing	0.80 (0.68-0.92)	0.88 § (0.83-0.93)
2D longitudinal speckle tracking strain, minimum smoothing	0.79 (0.67-0.91)	0.87 § (0.82-0.92)
2D longitudinal strain by TD and speckle tracking	0.77 (0.65-0.90)	0.80 § (0.73-0.87)
2D longitudinal strain rate by TD and speckle tracking	0.70 (0.56-0.84)	0.79 § (0.73-0.86)
2D-LVEF	0.78 (0.66-0.89)	-
3D-LVEF	0.74 (0.62-0.87)	-
FS_L	0.78 (0.65-0.91)	-
S´/LV length	0.72 (0.57-0.85)	-
E/e′	0.66 (0.52-0.81)	-
3D longitudinal strain	0.72 (0.56-0.88)	0.73 (0.66-0.79)
3D area strain	0.72 (0.57-0.87)	0.85 § (0.80-0.89)
3D circumferential strain	0.69 (0.53-0.84)	0.87§ (0.83-0.92)
3D transmural strain	0.71 (0.56-0.86)	0.86 § (0.82-0.90)
Peak cardiac troponin T	0.79 (0.68-0.90)	-

Table 6: *Large MI: total infarct volume fraction >12% by LE-MRI. Small MI: total infarct volume fraction <12% by LE-MRI. Transmurally infarcted segments: segmental infarct*

*volume fraction >50%. * = AUC significantly (P≤0.05) higher than 2D longitudinal strain rate by TD and speckle tracking, S´/LV length, E/e', 3D longitudinal strain, 3D area strain, 3D circumferential strain and 3D transmural strain § = AUC significantly (P≤0.01) higher than 3D longitudinal strain; AUC = area under the receiver operating characteristic curve; CI = confidence interval; E = peak early diastolic velocity; e` = mean peak early diastolic mitral annular velocity; FS_L = fractional shortening of the longaxis; LV = left ventricular; LE-MRI = late enhancement magnetic resonance imaging; LVEF = left ventricular ejection fraction; MI = myocardial infarction; new method = combined judgement of colour coded strain rate data and wall motion analysis; S`= peak systolic mitral annulus velocity; WMS = wall motion score; 2D = two-dimensional; 3D = three-dimensional.*

Of the patients with LE-MRI infarct size <6%, hypokinetic or akinetic areas were only identified in 6 patients (32%) by the direct echocardiographic quantification of infarct size and in 5 patients (26%) by 2D and 3D WMS. The direct echocardiographic quantification of infarct size underestimated the infarct size by 4.2 % (95 % limits of agreement -14.3% to 5.9%) compared to LE-MR.

5.4.3 Echocardiography - Segmental indices

The mean segmental values of the non-infarcted, sub-endocardial infarcted and transmurally infarcted segments were significantly different for all the echocardiographic methods. There were significant correlations between segmental infarct volume fraction assessed by LE-MRI and all the segmental echocardiographic indices with r = 0.53 for 3D-WMS, 0.53 for 2D-WMS, 0.59 for direct echocardiographic quantification of infarct size, 0.48 for longitudinal strain by 2D speckle tracking with default smoothing, 0.46 for longitudinal strain by 2D speckle tracking with minimum smoothing, 0.39 for longitudinal strain by 2D TD and speckle tracking, 0.31 for longitudinal strain rate by 2D TD and speckle tracking, 0.25 for longitudinal

strain by 3D speckle tracking, 0.40 for circumferential strain by 3D speckle tracking, 0.40 for transmural strain by 3D speckle tracking, 0.40 for area strain by 3D speckle tracking.

The correlations of 3D-WMS, 2D-WMS, direct echocardiographic quantification of infarct size, and longitudinal strain by 2D speckle tracking with default and minimum smoothing with segmental infarct volume fraction were significantly higher compared to the other echocardiographic indices (all $P<0.05$). In addition, the correlation coefficients for longitudinal strain by 2D TD and speckle tracking and circumferential, transmural and area strain by 3D speckle tracking were significantly higher than for longitudinal strain by 3D speckle tracking (all $P<0.03$). The correlation coefficient between 3D-WMS and 2D-WMS was 0.74. The correlation coefficient between segmental longitudinal strain by 2D speckle tracking and longitudinal strain by 2D TD and speckle tracking were 0.74. The correlations between the four different measurements of segmental 3D strain were generally strong (all $r>0.79$), except the correlation between longitudinal and circumferential strain by 3D speckle tracking ($r = 0.43$).

All the segmental echocardiographic indices showed generally good ability to identify transmurally infarcted segments with more than 50% contrast enhancement by LE-MRI (Table 6). However, the AUC for longitudinal strain rate by 2D TD and speckle tracking and longitudinal strain by 3D speckle tracking was significant lower (all $P<0.01$) than the other echocardiographic indices. Otherwise, the differences in AUC of the echocardiographic indices were not statistically significant. Three-dimensional-WMS and 2D-WMS >1 had a sensitivity of 73% and 77% and a specificity of 95% and 94%, respectively, for identification of transmurally infarcted segments, while longitudinal strain by 2D speckle tracking with default smoothing of >-14.4% had a sensitivity of 80% and a specificity of 85% for identification of transmurally infarcted segments.

5.4.4 Data reproducibility

Reproducibility of study three and four was assessed by one of the co-authors reanalyses of 20 randomly selected recordings. For the global echocardiographic indices the coefficient of repeatability was 0.21 for 3D WMSI, 0.19 for 2D WMSI, 9.7% for direct echocardiographic quantification of infarct size, 2.2% for global longitudinal strain by 2D speckle tracking, 2.9% for global longitudinal strain by 2D TD and speckle tracking, 0.20 s^{-1} for global longitudinal strain rate by 2D TD and speckle tracking, 4.1% for global longitudinal strain by 3D speckle tracking, 5.7% for global circumferential strain by 3D speckle tracking, 12.2% for global transmural strain by 3D speckle tracking, and 6.1% for global area strain by 3D speckle tracking.

For the segmental echocardiographic indices the weighted kappa coefficient was 0.72 for 3D WMS and 0.67 for 2D WMS. The coefficient of repeatability was 33% for direct echocardiographic quantification of infarct size, 6.6% for longitudinal strain by 2D speckle tracking, 5.7% for global longitudinal strain by 2D TD and speckle tracking, 0.52 s^{-1} for longitudinal strain rate by 2D TD and speckle tracking, 8.3% for longitudinal strain by 3D speckle tracking, 10.3% for circumferential strain by 3D speckle tracking, 25.2% for transmural strain by 3D speckle tracking, and 11.9% for area strain by 3D speckle tracking.

6 Discussion

6.1 Main findings

As hypothesized in study one, repeated analyses of the same recordings severely underestimated the clinically more relevant inter-observer reproducibility obtained by separate examinations. MAE by M-mode seemed to show the best reproducibility.

In study two peak systolic velocity indices (mitral annulus tissue velocities, ejection velocities and strain rate) exhibited greater variation than end-systolic indices during inotropic

alterations, which supports the hypothesis that the peak systolic velocity indices better reflect changes in contraction compared to the end systolic indices.

In study three we were able to quantify the percentage infarct size by echocardiography with high accuracy. As hypothesized in study three, strain rate imaging adds incremental diagnostic value to wall motion score in B-mode, and this new method combining strain rate imaging and wall motion analysis showed better correlation to LE-MRI compared with other echocardiographic indices of global LV function.

In study four we hypothesized that 3D echocardiography would provide added diagnostic value in patients with recent myocardial infarctions. However, we could not prove better overall accuracy of 3D echocardiography compared with 2D echocardiography. WMS by dynamic multi-slice short-axis obtained from only one 3D recording gave a quick and reliable view of the LV regional function with added diagnostic value in several patients, particularly those with better apical acoustic window, but added diagnostic value of the tested implementation of 3D strain could not be proven.

6.2 Study population and study design

None were excluded due to inadequate echocardiographic images in the four papers, meaning that the results are not idealised.

6.2.1 The reproducibility study (study 1)

The study population of study one was selected among people who reported to be free from cardiovascular disease. The participants were fairly young, and had fair image quality. Reproducibility might be expected to be lower in a general patient population. In all 20 separate echocardiographic examinations (10 participants) were recorded. Thus, clinical important differences in reproducibility could be tested, but this study population had limited power to detect small differences in the reproducibility of different measurements. Those

differences however, can be assumed to be of less clinical importance. It is likely that the population of study one is representative for the population of study two. Thus, we assume that the reproducibility analyses of study one is representative for the reproducibility of the echocardiographic measurements of study two. The age, cardiac function and echocardiographic image quality of participants were significantly different in study one compared with study three and four. Thus, the reproducibility analyses of study one can not directly be generalized to study three and four.

The inter-observer reproducibility analyses of study one were based on different recordings obtained from different physician echocardiographers. Compared to repeated analyses of single recordings, test-retest analyses of separate recordings are more clinically relevant and better reflect the repeatability and imaging related variability of echocardiographic parameters in everyday clinical practice. Standard parameters for assessment of systolic function are strongly influenced by biological variation, and we sought to minimize these by repeating the study over a short time frame, so that the main source of variation was related to imaging per se.

6.2.2 The contraction study (study 2)

The study population of study two was selected among young people who reported to be free from cardiovascular disease. This relatively homogeneous population was chosen in order to induce uniform alterations in contraction in order to compare the ability of different echocardiographic methods in detecting contractility changes. Any unphysiological response to dobutamine or metoprolol, for instance due to ischemia, would have biased the results. We believe that the deliberate careful selection of a homogenous population of young and healthy subjects was favourable and may have contributed to clear and robust differences between the methods. However, detection of contraction changes in healthy subjects might be detection different from changes in cardiac function of patients with cardiac diseases.

The aim of the protocol was to obtain 20 paired rest-dobutamine recordings and 20 paired rest-metoprolol recordings, which were achieved without discontinuation or exclusion of any examination. However, in case of residual effects of dobutamine in the metoprolol study, we did preliminary analyses of the data of the seven first subjects who received both dobutamine and metoprolol. As there was a trend towards a smaller decrease in heart rate after injection of metoprolol of these subjects, we decided not to give both dobutamine and metoprolol to all the subjects. Thus only 7 of 33 underwent imaging in the basal state and after both dobutamine infusion and metoprolol infusion, whereas 13 patients underwent imaging in the basal state and during low-dose dobutamine stress, and another 13 patients underwent imaging in the basal state and after metoprolol infusion. The final analyses of the echocardiographic indices after metoprolol infusion did not indicate that the seven subjects who received dobutamine before metoprolol responded significantly differently from the 13 subjects who only received metoprolol.

The main effect of dobutamine at low dose is increased inotropy without a profound effect on heart rate (107), and it is thus well suited for studying changes in contraction and contractility. In line with previous studies, low-dose dobutamine increased the heart rate by 13 % (108, 109), and metoprolol reduced the heart rate by 12 %. No invasive reference method was used, but dobutamine and metoprolol have well-documented positive and negative inotropic effects, and has previously been used to define inotropic states in several studies (47, 107, 109, 110), and we therefore found it ethically unacceptable to let healthy subjects undergo an invasive procedure for this purpose. Low-dose dobutamine has previously induced >50 % increase in the maximal first derivative of left ventricular pressure (LV dP/dtmax) obtained by cardiac catheterization in different populations, (111-113) which is in the same range as the measured increase of peak systolic velocity indices during low-dose dobutamine in this study. Thus the “gold standard” is that the data belongs to one of three contractile

states, betablocker, baseline or dobutamine, and the aim of the study was to test the ability of different measurements to detect the contraction changes given á priori.

6.2.3 The infarction studies (study 3 and 4)

The study population consisted of patients with a mean age of 55 years, and approximately 75% were men. The predominance of males is in accordance with multicenter trials of patients with myocardial infarction in which about 25–30% of women were recruited (114, 115). Other studies have shown that women with first time myocardial infarction were older and had a higher prevalence of hypertension and kidney failure (116, 117) compared with men. There was much focus in medical literature and public media on the risks of development of nephrogenic systemic fibrosis induced by gadolinium-based contrast at the time of inclusion. Therefore we were particularly careful in the judgement of the renal function. Thus, it is likely that more women than men were excluded due to age >75 years and kidney failure. Furthermore 5 of the 11 drop outs were women. There was a balanced representation of all the three main coronary arteries identified as the culprit lesion. Although approximately 80% of the MI's was STEMI and only patients with peak troponin T levels below 0.5 µg/L were included, approximately 30% had infarct size below 6%. A subgroup of NSTEMI patients has substantial myocardial necrosis, but the majority of NSTEMI patients have small myocardial infarctions typically with peak troponin T levels below 0.5 µg/L troponin T (90, 118). There was a predominance of males, few patients with diabetes mellitus and hypertension in the study population, no unstable patients, and no patients with severe heart failure. Otherwise, the patients in study three and four in whom the majority were STEMI patients treated with acute PCI, may reflect the population of moderate to large first time MI in most coronary care units.

The sex and age matched healthy controls of study three and four were selected from the participants randomized to echocardiography in the third wave of the HUNT Study. Both

the cardiac risk factors and the echocardiographic indices of LV function of the participants of the HUNT3 Echocardiography sub-study followed a normal distribution (119). Nevertheless, all population studies are sensitive to a selection bias. For all participants simultaneous symptoms or knowledge of cardiac risk factors may increase the attendance rate in a cardiac ultrasound study as health examination may be more attractive to subjects with any symptoms or higher level of risk (120). However, the Echocardiography in HUNT3 was only one of many sub-studies. Both the randomization of participants to the different sub-studies, and the exclusion of participants with known cardiovascular disease, diabetes and hypertension may, at least partly, reduce this bias. The mean body mass index of the healthy controls of study three and four was 26.1 kg/m^2, which indicate that more than 50 percent of the healthy controls were classified as overweighed or obese (121, 122). However, with the today's epidemic of obesity in mind this may reflect normality, as it reflects the worldwide change in body mass index (123). Surprisingly, the creatinine level of the healthy controls was significantly lower than the patients with recent MI. This might be explained by the careful judgement of the renal function prior to inclusion of the MI patients.

6.3 Echocardiographic acquisition and analysis

6.3.1 Echocardiographic image acquisition.

In all four studies we used scanners, transducers and software from GE Vingmed, (Horten, Norway). As there are differences between, manufacturers, the results can not be unconditionally generalized to other manufacturers. We used clinical applicable wide sector acquisition as we sought to investigate the clinical use of grey scale and tissue Doppler echocardiography. The frame rate is inversely related to line density (number of lines in the scanner sector). As we used the default frame rate setting, the frame rate was only adjusted by adapting the width of the sector to encompass the LV walls. However, the recordings of the fourteen patients in study three and four who were examined with a newer scanner, had

significant higher frame rate compared with the other patients and the healthy controls. All the recordings of the four studies were obtained by two experienced echocardiographers (Anders Thorstensen and Håvard Dalen).

6.3.2 Analysis of B-mode and Doppler echocardiography.

Study one showed that a conventional method like MAE by M-mode was at least as good as global longitudinal strain by 2D speckle tracking or TD in terms of reproducibility. MAE by M-mode showed also good correlation with LE-MRI and good ability to separate small and large MIs. The correlation of MAE by M-mode with LE-MRI was higher than for LVEF and lower than for global longitudinal strain by 2D speckle tracking, but these differences were not statistically significant. Two dimensional and 3D LVEF showed fair correlation with LE-MRI and good ability to separate small and large MIs. Despite, the superior accuracy and reproducibility of 3D-LVEF compared to 2D-LVEF demonstrated in multiple studies (51, 52), added diagnostic value of 3D-LVEF could not been shown in this thesis. LVEF by either 2D or 3D echocardiography did not show the best reproducibility, showed limited ability to detect contraction changes and only moderate correlations with LE-MRI. Thus, the overall results of the thesis indicate that LVEF may not be the optimal measurement of LV function.

S′ is an attractive method in everyday clinical practice as it is easy and fast to obtain with low demand of post-processing. In study two S′ by spectral TD and S′ by colour TD averaged over four walls showed excellent ability to detect contraction changes induced by dobutamine and beta-blocker. S′ measures the peak velocity of the mitral annulus motion, occurring in the first part of systole, and in line with our hypothesis S′ better reflected the contraction changes compared with end-systolic indices like MAE by M-mode, global strain and LVEF. However, S′ by spectral TD showed weaker correlation with LE-MRI compared with MAE by M-mode, 2D and 3D WMS, and direct echocardiographic quantification of infarct size. Other studies of patients with MI have also shown that S′ had weaker correlation

with the reference methods compared to regional deformation indices (124-126), while experimental studies have shown that S′ better reflects myocardial contractility compared with end-systolic indices (47, 109, 110). Thus, the apparently contradictive results of study 2-4 might be explained by preserved LV global contractility of the patients with small or medium large MI. Furthermore, S′ is a measurement of LV global function due to tethering effects between LV walls (41), and global average of regional indices may be the best measurements in conditions with regional dysfunction.

E/e′ has been shown to be a useful prognostic index and is established as an index of LV filling pressure (127), but E/e′ showed weaker correlation than most other measured indices of LV performance. E/e′ is a combined measurement of two diastolic indices and diastolic indices might be inferior to systolic measurement in estimation of infarct size. In addition, E/e′ and other diastolic indices are very dynamic parameters and particularly sensitive to changes in loading conditions, and as shown in study one, E/e′ and other diastolic indices, were inferior to systolic indices in terms of reproducibility.

In order to avoid variability due to ventricular size, MAE and S′ were divided by the end-diastolic length of the left ventricle (128). However, correcting for the end-diastolic length led only to a trend towards increase in the diagnostic accuracy which was not statistically significant (data not shown). However, it may be noted that the variability in LV size was small, as 80% of the subjects were men. The fractional shortening of the myocardium in long axis is a measurement of LV global longitudinal strain, and as expected, the fractional shortening of the myocardium in long axis and global longitudinal strain by 2D speckle tracking showed high mutual correlation and similar diagnostic accuracy.

6.3.3 2D and 3D wall motion score

Two-dimensional and 3D-WMS showed strong correlation with LE-MRI and excellent ability to separate small and large MIs, and good ability to identify transmurally infarcted segments.

WMS showed better correlation with LE-MRI than the other measured indices of LV global performance, except longitudinal strain by 2D speckle tracking and direct quantification of infarct size. Similar diagnostic accuracy of WMS and 2D speckle tracking echocardiography in patients with MI has also been shown by others (90, 129).

The results of study three and four show that 3D-WMS by dynamic multi-slice obtained from only one 3D recording provides a quick and reliable view of the LV function. Wall motion score in 2D recordings can be difficult due to in- and out-of-plane motion, tethering and the limited coverage of the LV. Also, due to the longitudinal motion of even akinetic segments, the wall thickening is more difficult to discern visually. When looking at dynamic short axis slices, only wall thickening is seen. In some cases with better apical acoustic window, 3D-WMS showed added diagnostic value, but as 2D echocardiography performed better in subjects with better parasternal acoustic window, the overall accuracy of 3D-WMS and 2D echocardiography did not differ significantly. Comparing the entire LV circumference in dynamic short-axis slices from a 3D recording makes it easier to separate areas with reduced function, and this may compensate for the lower temporal resolution and larger voxel size in 3D. In daily routine, this would be a clear advantage in patients with limited parasternal acoustic window, where short-axis images are hard to get.

6.3.4 Direct echocardiographic quantification of infarct size

In study three, we present a new method for direct echocardiographic quantification of infarct size based on interpolation of semi quantitative colour coded strain rate in bull's eye views. On the sub segmental level, areas were automatically marked as normal, hypokinetic, or akinetic, and divided by the total myocardial area and the total segmental area for estimation of global and segmental area fractions. However, TD based strain rate is sensitive to signal noise and acoustic artefacts, and the accuracy of the automatic quantification of infarct size based on TD strain rate alone was unsatisfactory. Manual correction of the strain rate data by

wall motion analysis was necessary to achieve high accuracy. Thus, the method is not a replacement of wall motion score, which still can be said to be part of the method. Direct echocardiographic quantification infarct size by colour coded strain rate and wall motion analysis yields high diagnostic accuracy and better correlation to LE-MRI compared with the other measured indices of LV global performance. The strain rate data yielded additive diagnostic information to wall motion analysis. Similar results have been reported previously (22, 24) and underscore the versatility of echocardiography and the advantage of performing an integrated judgment, using more than one echocardiographic method. However, in a recent publication the combined use of WMS and longitudinal strain by 2D speckle tracking did not increase the diagnostic accuracy compared with the accuracy of the two methods used alone (90). This might indicate that strain rate data to a greater extent than speckle tracking echocardiography is helpful for counteracting misinterpretations due to passive motion caused by tethering in wall motion analyses. Although strain rate data is sensitive to signal noise and acoustic artefacts and the segmental 95% confidence interval of trace analysis is rather wide (28), identification of MI and artefacts are often easy when TD based strain rate is displayed as semi-quantitative colour information in curved M-mode. Direct quantification of percentage infarct size by echocardiography may be particularly attractive for patients and health workers who are not familiar with the terminology of advanced echocardiography. All the other methods, except WMSI which measure the extent of infarction semi-quantitatively, are measurements of global LV function, where the degree of reduced function only may serve as an indirect estimate of infarct size, and the units and magnitude these methods may be difficult to relate to infarct size and difficult to interpret for many patients and health workers.

6.3.5 2D echocardiographic quantitative deformation analysis

In study one, the test-retest variability reproducibility was good for global longitudinal strain by 2D speckle tracking, but the test-retest variability was high on the segmental level, suggesting use of clinical watchful approach when performing regional analyses. In study two, strain by 2D speckle tracking was clearly inferior to peak systolic velocity measurements in detecting contraction changes. Strain by 2D speckle tracking also showed weaker correlation with LV pressure development compared with S′ and strain rate in animal models (47, 109, 110). Thus, longitudinal strain by 2D speckle is probably not the optimal non-invasive index for measuring myocardial contractility. In study three and four, longitudinal strain by 2D speckle tracking had high correlation with LE-MRI, good ability to identify large MIs and transmurally infarcted segments. Although, direct echocardiographic quantification showed better correlation with LE-MRI the accuracy of 2D speckle tracking echocardiography was comparable. The correlation of 2D speckle tracking with LE-MRI was significantly better than for longitudinal strain rate and strain rate by 2D TD and speckle tracking, both on the global and the segmental level. Strain analyses by the speckle tracking method is less angle dependent and may be less sensitive to signal noise and acoustic artefacts compared with TD analyses, although this to at least some degree is due to a liberal amount of spatial smoothing. However, in line with other studies (90, 91, 129) the accuracy of 2D speckle tracking echocardiography was no better than wall motion score. Thus, there is still potential for further technological development of quantitative deformation imaging. The cut-off values longitudinal strain by 2D speckle tracking (-16.5%) for separation of small and large MI presented are in line with others (91, 93). Sjølie et al presented a cut-off value of -15.0% for identification of infarct size >20% in a study of 39 STEMI patients in whom echocardiography was performed approximately 10 days after hospital admittance (93). As expected due to acute stunning effects, the cut-off values were different in a study where

echocardiography was performed immediately before revascularization (90). There was no significant difference in the correlation with LE-MRI or the accuracy of detecting large MIs or transmural infarcted segments, when the regions of interest was reanalysed using minimum smoothing by the 2D speckle tracking method. However, the average end systolic strain values obtained by minimum smoothing were significant lower ($P < 0.001$) for small MIs, large MIs and healthy controls (in average 0.4% (percentage points) higher absolute strain values for the whole study population).

In study one, the test-retest reproducibility of global longitudinal strain and strain rate obtained from the combination of speckle tracking and TD was comparable to the commercially available speckle tracking strain method, but the test-retest variability was unsatisfactory high on the segmental level. TD imaging has a high component of random noise, which may lead to measurement at the top of noise spikes, which may incorporate a component of noise in the estimate of peak values. In study three and four, strain and strain rate obtained from the combination of speckle tracking and TD showed significantly lower correlation with infarct size by LE-MRI compared with longitudinal strain by speckle tracking both at the global and segmental level. However, TD based methods could provide additional information that is not present in grey-scale recordings. For instance, is the timing of events in the cardiac cycle more reliable in TD analyses, due to the much better temporal resolution.

In study two, we wanted to use only commercially available methods, and therefore we calculated the strain rate values from the tissue Doppler velocity gradient method. Peak systolic strain rate by TD showed excellent ability to detect contraction changes. However, in order to achieve reasonable strain rate values by the tissue Doppler velocity gradient method, the regions of interests had to be adjusted, and only minor adjustment of the regions of interest had huge impact on the strain rate values. In addition, it was easy for the analysers to recognise that the myocardium was influenced by Dobutamine. Thus, this method is probably

more subjective and operator depended than the other methods. In our opinion trace analyses by tissue Doppler velocity gradient method are accurate and useful in clinical practice in the timing of cardiac events (130), but when performing regional analyses we recommend that the trace analyses should be supplemented by semi-quantitative colour coded curved M-mode or bull's eye views in which identification of MI and artefacts are more easy.

6.3.6 3D echocardiographic quantitative deformation analysis

The four different measurements of 3D strain in study 4 were able to identify most patients with infarct size >12%, but considering the lower feasibility and more moderate correlations to LE-MRI of 3D strain compared with wall motion analysis and 2D speckle tracking echocardiography, added diagnostic value of the tested implementation of 3D strain could not be proven. ST-echocardiography and other quantitative deformation analyses are sensitive to low frame rate, signal noise, and artefacts. Despite acquiring the 3D recordings over four to six consecutive heart beats, both the temporal and spatial resolutions were considerably lower in 3D than in 2D. This is probably the cause of the low correlation between longitudinal 3D strain and LE-MRI; longitudinal motion is higher at the base, where resolution is lower. Furthermore, stitching artefacts in 3D recordings are more likely to cause misinterpretation in speckle tracking than in visual wall motion analysis. A recent publication reported accurate and reproducible 3D strain measurements in a study which mainly included healthy subjects and patients with ischemic and non-ischemic cardiomyopathy (131), but this study population was selected on the basis of image quality and their results were not validated by MRI.

6.3.7 Global versus segmental analyses

Segmental analyses are challenging. In Study 1 the test-retest variability, assessed by mean error (absolute difference divided by the mean of two observations) of global strain analyses by two different methods (AFI and GcMat) was 4-6%, compared to 14-18% in segmental

analyses. Previously it has been shown that the normal ranges are much wider for segmental indices compared with global indices. These findings indicate the main limitations of segmental analyses (28), and the need for special awareness of methodological and technical limitations of the method used. The results of study one and two showed that global indices of LV performance by conventional methods was comparable to methods based on global average of regional deformation indices. In addition, conventional methods like MAE by M-mode and S′ appear superior to deformation imaging with respect to feasibility and time efficiency, as deformation analysis for instance by speckle tracking echocardiography require experienced critical judgement of the tracking of each segment. However, in study three and four global average of regional deformation indices generally showed the strongest correlations with LE-MRI than conventional methods. Thus, regional indices seems to be preferable in conditions with regional dysfunction

6.3.8 Methodological differences - strengths and weaknesses

The different methods used in these studies illustrate to some degree the armamentarium of methods used in echocardiographic laboratories. Although, LVEF is the most commonly used measurement of LV function, the overall results of the thesis indicate that LVEF may not be the optimal measurement. LVEF is a key functional and prognostic marker of LV function. Low LVEF correlates well to mortality, but the method is inferior to the more modern methods with respect to quantification of LV function (49, 132). LVEF overestimates the myocardial function in small hypertrophic hearts, has limited reproducibility and is a poor indicator of the contractile properties of the myocardium (33). In line with previous studies peak cardiac Troponin T showed better correlation with infarct size by LE-MRI than LVEF (96).

The annular tissue velocity and motion measurements have shown ability to differentiate between sick and healthy myocardium, and as well predict mortality (133-136).

The pulsed wave spectral TD method is performed online, while the colour TD requires offline post-processing. The pulsed wave spectral TD method is recommended by the European and the American Associations of Echocardiography due to more validation studies than the colour TD method. (127). However, in the Copenhagen Heart Study colour TD systolic mitral annular velocity predicted mortality (133). As shown in this thesis the two tissue Doppler methods for assessing myocardial velocities differ with respect to methodology and the absolute values obtained, with lower values by the colour TD method. However, they seem equal with respect to reproducibility and identification of contraction changes. Controversies about correct gain settings and localization of the peak in the Doppler spectrum points is an important limitation of the spectral TD method *(Figure 11)*, but the colour TD method requires off-line post processing and is more prone to acoustic artefacts.

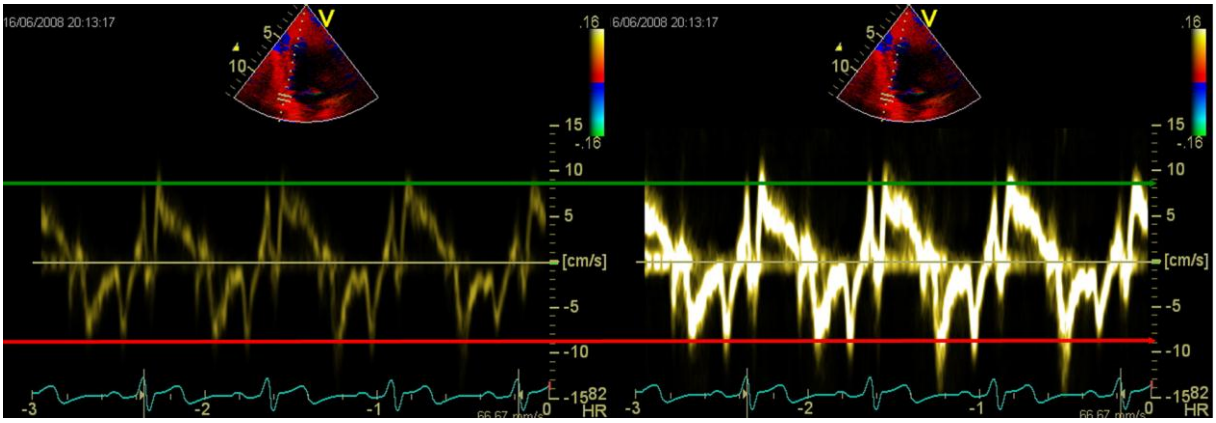

Figure 11. *Pulsed wave spectral TD assessed velocities from the base of the inferior LV wall with low gain settings in the left recording and the high gain settings in the same recording at right. Green line refers to peak systolic velocity measured at the outer edge of the Doppler spectrum at low gain, and with high gain it is obvious that similar method measure higher velocity. Red line refers to peak early diastolic velocity at low gain, and similarly it looks like the velocities are higher when gain is increased.*

WMSI is an established parameter of LV systolic function, validated as a prognostic indicator after MI. However, it is semi quantitative, experience dependent, and based on subjective interpretation of the wall thickening. Despite lower spatial and temporal resolution of 3D echocardiography, 3D WMS showed similar diagnostic accuracy as 2WMS. Analyses in short axis are often preferable when performing wall motion analysis as passive longitudinal motion caused by tethering of adjacent myocardium may cause misinterpretations in long axis views. Also, the longitudinal motion makes discernment of the wall thickening component visually challenging. Comparing the entire LV circumference in dynamic short-axis slices from a 3D recording makes it easier to separate areas with reduced function, and this may compensate for the lower temporal resolution and larger voxel size in 3D. In daily routine, this would be a clear advantage of 3D echocardiography in patients with limited parasternal acoustic window, where short-axis images are hard to get.

A possible explanation to the difference between 2D WMSI and direct echocardiographic quantification of infarct size is that the areas of hypokinesia and akinesia are classified on a sub-segment level and reported as continuous data by the new method. This may increase the diagnostic accuracy compared to WMSI, which dichotomize each segment into ordinal data. In addition, the new method corrects for the area distortion in the bull's eye view, while WMSI has no correction for unequal segment size, apart from the reduced number of segments in the apex. Echocardiographic measurements like LVEF, MAE S´, E/e, and global strain and strain rate, may yield measurements that are in the border zone between normal and decreased LV function, while direct echocardiographic quantification of infarct size and WMSI dichotomizes each segment or sub segment as either healthy or diseased. Thus, infarct size above 0 or WMSI above 1.0 are more conclusive indications of visible MI.

When comparing the quantitative deformation indices, the different methods differ with respect to the technological basis and how user-friendly the interface is. TD based

deformation indices have a high component of random noise, which may lead to measurement at the top of noise spikes, and this may incorporate component of noise in the estimate of peak values. The high SDs of the segmental TD values are an indication of this (3). The commercial available Automated Function Imaging and auto LV quantification methods for 2D and 3D speckle tracking strain have a user-friendly interface, but they are still very user dependent and require experienced critical judgement of the tracking of each segment. The 2D strain speckle tracking method has a high degree of spatial smoothing by polynomial or spline fitting along the regions of interest. This software, like other commercially available speckle tracking tools, has limited opportunities to change preferences, and the technology behind the analyses is hidden for the user. The speckle tracking methods are regularly improved by the manufacturers, and during the work of this thesis, we have recognized improvements in the software. However, the tested 3D speckle tracing strain method suffered from low temporal and spatial resolution in 3D acquisitions and was very sensitive to acoustic artefacts.

6.4 MRI acquisition and analysis

LE-MRI is established as the reference standard for the quantification of myocardial scars (60, 63). We used the usual cut-off of 2 SD above the mean pixel intensity for identification of infarcted myocardium by LE-MRI. However this cut-off is not thoroughly validated and may result in overestimation of the true infarct size (137).

7 Limitations

7.1 General limitations

All four studies were single centre studies, and the number of participants was low, particularly in study one. Thus, the studies have limited power to detect small differences

between methods. Those differences however, can be assumed to be of less clinical importance. In study two, three, and four all echocardiographic analyses were done by one single operator, but care was taken to achieve blinded measurements for all methods, with different id-numbers for the echocardiographic and LE-MRI analyses. In addition, a subset of the recordings was reanalysed by one of the co-authors in order to calculate inter-analyser reproducibility. The greatest current limitation of echocardiography is subjectivity. Echocardiographic acquisition and analyses are operator dependent, and in particular deformation imaging require experienced critical judgement. Use of customized software makes it difficult for other centra to use the same methods in studies with similar study design. However, the customized software was the only available software with full information about segmental borders and wide opportunities to change preferences, and the process used to calculate myocardial deformation was not hidden for the user.

Parameters of twist and torsion and 2D circumferential and radial strain were not analysed in any of the studies. Longitudinal strain tracks motion parallel to the ultrasound beam, where resolution is optimal in contrast to 2D circumferential and radial strain where motion is tracked in all directions. In addition, circumferential and radial strain is calculated from short-axis images, where image planes are not well standardized, and there is considerable through plane motion, especially in the basal parts of the heart. Thus, these methods might be less accurate due to methodological reasons as indicated by several studies (90, 91, 138), although one recent study has indicated added diagnostic value of 2D circumferential strain in patients with acute coronary syndromes (139).

A subset of the recordings of all four studies had below average image quality. In clinical practice, echocardiographers might have considered use of contrast to achieve better image quality in these patients. Use of contrast was not allowed by the study protocol as one of the primary aims of the thesis was to evaluate the diagnostic accuracy of quantitative

deformation imaging, and the use of contrast precludes TD based quantitative measurements (140), as well as speckle tracking. On the other hand, particularly the accuracy of WMS, which was one of the best methods even without contrast, might have been expected to increase with the use of contrast. However, with contrast one evaluates endocardial motion more than wall thickening, which might mask tethering. Direct wall motion scoring by colour strain rate was not studied here, but has been shown to be reasonably similar in accuracy to B-mode wall motion (19, 20).

7.2 Specific limitations

We sought to minimize biological variation by repeating the study over a short time frame, so that the main source of variation was related to imaging per se. However, biological variation over time is also clinically relevant, and performing repeated analyses with the same participants some weeks later would also have been valuable.

In study two, no patients with cardiac disease was included, and it remains to be tested whether our results could be extrapolated to a more general population of patients with heart disease, but we believe that the deliberate careful selection of a homogenous population of young and healthy students was favourable and may have contributed to clear and robust differences between the methods. On the other hand detection of inotropic alterations in healthy subjects is not the same as detection of cardiac dysfunction. Dobutamine and metoprolol were given to similar but not identical populations. However, the aim of the study was not to compare the effect of dobutamine against the effect of metoprolol as the effects of these drugs have been extensively studied previously. We gave dobutamine before metoprolol in seven subjects, and waited approximately 10 half lives before the subjects entered the metoprolol study, which should be enough to avoid residual effects among healthy subjects. However, there was a trend towards a smaller decrease in heart rate after injection of metoprolol among the 7 subjects who received dobutamine before metoprolol, but the

analyses of the echocardiographic indices did not indicate that these subjects responded significantly. No invasive reference method was used in study two and the subjects were not examined during changes in loading conditions (141). Furthermore, fully blinded analysis was not realistic in study two as the analyser easily could recognize if the myocardium was influenced by dobutamine.

In study three and four the healthy controls were not examined by LE-MRI. Therefore, the LE-MRI analyses were, in contrast to the echocardiographic analyses, performed without mixing healthy controls and MI patients. This might increase the prevalence of positive findings, as the MRI analyser had a priori knowledge that the patients actually had coronary artery disease. In study three and four, Anders Thorstensen examined the MI patients and Håvard Dalen examined the healthy controls. This might cause a systematic bias between the recordings of the MI patients and the healthy controls, but the extensive validation of the reproducibility between these echocardiographers showed excellent reproducibility for global indices and fair reproducibility for segmental indices. Although no patients were excluded due to poor image quality, there was probably a selection of patients with little co-morbidity mainly because of careful evaluation of the renal function prior to inclusion. In addition, prior MI and age >75 years were exclusion criteria. The 3D recordings were acquired with a 3V transducer. Later hardware versions have improved both volume rate and resolution, and this might have improved the 3D strain results.

8 Conclusions

Most traditional and newer echocardiographic indices of global LV function obtained with modern equipment allow reproducible measurements with moderate or strong correlations with LE-MRI in patients with recent MIs. Repeated analyses of the same recordings underestimate the clinically more relevant inter-observer reproducibility obtained by separate

examinations by approximately 40% for most measurements of LV function. Systolic annular excursion by M-mode and global average of segmental strain values showed the best inter-observer reproducibility. Annular tissue Doppler measurements should be averaged from four sites instead of two, in order to optimize reproducibility. A major limitation of segmental measurements is high test-retest variability.

Peak systolic velocity indices and end-systolic indices responded markedly different to inotropic alterations. Peak systolic velocity indices were most sensitive in detecting contraction changes, which indicates that peak systolic velocity indices might give important supplementary information to end-systolic indices like LVEF and global strain.

Echocardiography performed approximately one month after myocardial infarction did show ability to identify the patients with infarct size >12 %, while most patients with infarct size <6 % did not have echocardiographic indices of impaired LV function. TD based colour coded strain rate added incremental diagnostic value to wall motion analysis in B-mode, and underscore the advantage of performing an integrated judgment, using more than one echocardiographic method. Dynamic multi-slice short-axis obtained from only one 3D recording gives a quick and reliable view of the LV regional function. As 3D WMS was one of the best methods and direct echocardiographic quantification of infarct size, showed the highest diagnostic accuracy in patients with MI, an overall conclusion is that echocardiography in three dimensions increases diagnostic accuracy.

9 Future studies

Reproducibility studies are clinically very relevant and also very instructive for the echocardiographic centres participating. Performing a larger test retest reproducibility study including 3D echocardiography of patients with various cardiac diseases would be interesting. Infarct size by LE-MRI yields prognostic information beyond LVEF (79). Hopefully, the

method of direct echocardiographic quantification of infarct size can be commercialized with a more user-friendly interface, and evaluating the prognostic value of this method in a prospective study would be attractive. Use of contrast, particularly for the 3D wall motion analyses, would probably be included if we perform a new study of patients with MI. There are plans for a 3D stress echocardiography study of patients with suspected coronary artery disease. However, as the relative frame rate decreases during peak stress, improvement in software and hardware would probably be necessary to achieve reliable 3D strain results in stress echocardiography.

10 References

1. Lang RM, Bierig M, Devereux RB, Flachskampf FA, Foster E, Pellikka PA, et al. Recommendations for chamber quantification. Eur J Echocardiogr 2006;7:79-108.
2. Edler. I HC. The use of ultrasonic reflectoscope for the continuous recording of the movements of heart walls. Kungl Fysiogr Sallsk Lund Forh 1954;24:40.
3. Holen J, Aaslid R, Landmark K, Simonsen S. Determination of pressure gradient in mitral stenosis with a non-invasive ultrasound Doppler technique. Acta Med Scand 1976;199:455-60.
4. Hatle L, Angelsen B, Tromsdal A. Noninvasive assessment of atrioventricular pressure half-time by Doppler ultrasound. Circulation 1979;60:1096-104.
5. Hatle L, Angelsen BA, Tromsdal A. Non-invasive assessment of aortic stenosis by Doppler ultrasound. Br Heart J 1980;43:284-92.
6. Hatle L, Angelsen BA, Tromsdal A. Non-invasive estimation of pulmonary artery systolic pressure with Doppler ultrasound. Br Heart J 1981;45:157-65.
7. Hatle L, Brubakk A, Tromsdal A, Angelsen B. Noninvasive assessment of pressure drop in mitral stenosis by Doppler ultrasound. Br Heart J 1978;40:131-40.
8. Skjaerpe T, Hatle L. Noninvasive estimation of systolic pressure in the right ventricle in patients with tricuspid regurgitation. Eur Heart J 1986;7:704-10.
9. Hegrenaes L, Hatle L. Aortic stenosis in adults. Non-invasive estimation of pressure differences by continuous wave Doppler echocardiography. Br Heart J 1985;54:396-404.
10. Skjaerpe T, Hegrenaes L, Hatle L. Noninvasive estimation of valve area in patients with aortic stenosis by Doppler ultrasound and two-dimensional echocardiography. Circulation 1985;72:810-8.
11. Wiseth R, Levang OW, Sande E, Tangen G, Skjaerpe T, Hatle L. Hemodynamic evaluation by Doppler echocardiography of small (less than or equal to 21 mm) prostheses and bioprostheses in the aortic valve position. Am J Cardiol 1992;70:240-6.
12. Rossvoll O, Hatle LK. Pulmonary venous flow velocities recorded by transthoracic Doppler ultrasound: relation to left ventricular diastolic pressures. J Am Coll Cardiol 1993;21:1687-96.
13. Haugen BO, Berg S, Brecke KM, Samstad SO, Skjaerpe T, Slordahl SA, et al. Measurement of volumetric mitral and aortic blood flow based on a new freehand three-dimensional colour flow imaging method. An in vivo validation. Eur J Echocardiogr 2000;1:204-12.
14. Samstad SO, Rossvoll O, Torp HG, Skjaerpe T, Hatle L. Cross-sectional early mitral flow-velocity profiles from color Doppler in patients with mitral valve disease. Circulation 1992;86:748-55.
15. Soma J, Wideroe TE, Dahl K, Rossvoll O, Skjaerpe T. Left ventricular systolic and diastolic function assessed with two-dimensional and doppler echocardiography in "white coat" hypertension. J Am Coll Cardiol 1996;28:190-6.
16. Aakhus S, Soerlie C, Faanes A, Hauger SO, Bjoernstad K, Hatle L, et al. Noninvasive computerized assessment of left ventricular performance and systemic hemodynamics by study of aortic root pressure and flow estimates in healthy men, and men with acute and healed myocardial infarction. Am J Cardiol 1993;72:260-7.
17. Malm S, Frigstad S, Sagberg E, Larsson H, Skjaerpe T. Accurate and reproducible measurement of left ventricular volume and ejection fraction by contrast echocardiography: a comparison with magnetic resonance imaging. J Am Coll Cardiol 2004;44:1030-5.

18. Heimdal A, Stoylen A, Torp H, Skjaerpe T. Real-time strain rate imaging of the left ventricle by ultrasound. J Am Soc Echocardiogr 1998;11:1013-9.
19. Stoylen A, Heimdal A, Bjornstad K, Torp HG, Skjaerpe T. Strain Rate Imaging by Ultrasound in the Diagnosis of Regional Dysfunction of the Left Ventricle. Echocardiography 1999;16:321-9.
20. Stoylen A, Heimdal A, Bjornstad K, Wiseth R, Vik-Mo H, Torp H, et al. Strain rate imaging by ultrasonography in the diagnosis of coronary artery disease. J Am Soc Echocardiogr 2000;13:1053-64.
21. Stoylen A, Ingul CB, Torp H. Strain and strain rate parametric imaging. A new method for post processing to 3-/4-dimensional images from three standard apical planes. Preliminary data on feasibility, artefact and regional dyssynergy visualisation. Cardiovasc Ultrasound 2003;1:11.
22. Bjork Ingul C, Rozis E, Slordahl SA, Marwick TH. Incremental value of strain rate imaging to wall motion analysis for prediction of outcome in patients undergoing dobutamine stress echocardiography. Circulation 2007;115:1252-9.
23. Bjornstad K, Maehle J, Aakhus S, Torp HG, Hatle LK, Angelsen BA. Evaluation of reference systems for quantitative wall motion analysis from three-dimensional endocardial surface reconstruction: an echocardiographic study in subjects with and without myocardial infarction. Am J Card Imaging 1996;10:244-53.
24. Ingul CB, Stoylen A, Slordahl SA, Wiseth R, Burgess M, Marwick TH. Automated analysis of myocardial deformation at dobutamine stress echocardiography: an angiographic validation. J Am Coll Cardiol 2007;49:1651-9.
25. Aase SA, Stoylen A, Ingul CB, Frigstad S, Torp H. Automatic timing of aortic valve closure in apical tissue Doppler images. Ultrasound Med Biol 2006;32:19-27.
26. Amundsen BH, Helle-Valle T, Edvardsen T, Torp H, Crosby J, Lyseggen E, et al. Noninvasive myocardial strain measurement by speckle tracking echocardiography: validation against sonomicrometry and tagged magnetic resonance imaging. J Am Coll Cardiol 2006;47:789-93.
27. Dalen H, Thorstensen A, Vatten LJ, Aase SA, Stoylen A. Reference values and distribution of conventional echocardiographic Doppler measures and longitudinal tissue Doppler velocities in a population free from cardiovascular disease. Circ Cardiovasc Imaging 2010;3:614-22.
28. Dalen H, Thorstensen A, Aase SA, Ingul CB, Torp H, Vatten LJ, et al. Segmental and global longitudinal strain and strain rate based on echocardiography of 1266 healthy individuals: the HUNT study in Norway. Eur J Echocardiogr 2010;11:176-83.
29. Mjolstad OC, Dalen H, Graven T, Kleinau JO, Salvesen O, Haugen BO. Routinely adding ultrasound examinations by pocket-sized ultrasound devices improves inpatient diagnostics in a medical department. Eur J Intern Med 2012;23:185-91.
30. Nyrnes SA, Lovstakken L, Skogvoll E, Torp H, Haugen BO. Does a new ultrasound flow modality improve visualization of neonatal pulmonary veins? Echocardiography 2010;27:1113-9.
31. Doppler C. Über das farbige licht der Doppelsterne und einiger anderer Gestirne des Himmels. Abhandlungen der königl. böhm. Gesellschaft der Wissenschaften. 1843; 2:465-82.
32. Maciver DH, Townsend M. A novel mechanism of heart failure with normal ejection fraction. Heart 2008;94:446-9.
33. Bijnens BH, Cikes M, Claus P, Sutherland GR. Velocity and deformation imaging for the assessment of myocardial dysfunction. Eur J Echocardiogr 2009;10:216-26.
34. Wandt B. Long-axis contraction of the ventricles: a modern approach, but described already by Leonardo da Vinci. J Am Soc Echocardiogr 2000;13:699-706.

35. Zaky A, Grabhorn L, Feigenbaum H. Movement of the mitral ring: a study in ultrasoundcardiography. Cardiovasc Res 1967;1:121-31.
36. Carlhall CJ, Lindstrom L, Wranne B, Nylander E. Atrioventricular plane displacement correlates closely to circulatory dimensions but not to ejection fraction in normal young subjects. Clin Physiol 2001;21:621-8.
37. Wandt B, Bojo L, Tolagen K, Wranne B. Echocardiographic assessment of ejection fraction in left ventricular hypertrophy. Heart 1999;82:192-8.
38. Ren YQ, Feng W, Liu L, Xia W, Qu XF. [Reduced left ventricular systolic atrioventricular plane displacement in heart failure patients with preserved ejection fraction]. Zhonghua Xin Xue Guan Bing Za Zhi 2009;37:809-12.
39. Roberson DA, Cui W. Tissue Doppler Imaging Measurement of Left Ventricular Systolic Function in Children: Mitral Annular Displacement Index Is Superior to Peak Velocity. Journal of the American Society of Echocardiography 2009;22:376-82.
40. McDicken WN, Sutherland GR, Moran CM, Gordon LN. Colour Doppler velocity imaging of the myocardium. Ultrasound Med Biol 1992;18:651-4.
41. Stoylen A, Skjaerpe T. Systolic long axis function of the left ventricle. Global and regional information. Scand Cardiovasc J 2003;37:253-8.
42. Gulati VK, Katz WE, Follansbee WP, Gorcsan J, 3rd. Mitral annular descent velocity by tissue Doppler echocardiography as an index of global left ventricular function. Am J Cardiol 1996;77:979-84.
43. Vinereanu D, Florescu N, Sculthorpe N, Tweddel AC, Stephens MR, Fraser AG. Differentiation between pathologic and physiologic left ventricular hypertrophy by tissue Doppler assessment of long-axis function in patients with hypertrophic cardiomyopathy or systemic hypertension and in athletes. Am J Cardiol 2001;88:53-8.
44. Yip G, Wang M, Zhang Y, Fung JW, Ho PY, Sanderson JE. Left ventricular long axis function in diastolic heart failure is reduced in both diastole and systole: time for a redefinition? Heart 2002;87:121-5.
45. Nagueh SF, Bachinski LL, Meyer D, Hill R, Zoghbi WA, Tam JW, et al. Tissue Doppler imaging consistently detects myocardial abnormalities in patients with hypertrophic cardiomyopathy and provides a novel means for an early diagnosis before and independently of hypertrophy. Circulation 2001;104:128-30.
46. Ferferieva V, Van den Bergh A, Claus P, Jasaityte R, Veulemans P, Pellens M, et al. The relative value of strain and strain rate for defining intrinsic myocardial function. Am J Physiol Heart Circ Physiol 2012;302:H188-95.
47. Weidemann F, Jamal F, Sutherland GR, Claus P, Kowalski M, Hatle L, et al. Myocardial function defined by strain rate and strain during alterations in inotropic states and heart rate. Am J Physiol Heart Circ Physiol 2002;283:H792-9.
48. Støylen A. Strain rate imaging. 2012 [1.3.2012]; Available from: http://folk.ntnu.no/stoylen/strainrate/.
49. Stanton T, Leano R, Marwick TH. Prediction of all-cause mortality from global longitudinal speckle strain: comparison with ejection fraction and wall motion scoring. Circ Cardiovasc Imaging 2009;2:356-64.
50. Støylen A. Strain rate imaging. 2012. (Accessed 1.4.2012, at http://folk.ntnu.no/stoylen/strainrate/.).
51. Nikitin NP, Constantin C, Loh PH, Ghosh J, Lukaschuk EI, Bennett A, et al. New generation 3-dimensional echocardiography for left ventricular volumetric and functional measurements: comparison with cardiac magnetic resonance. Eur J Echocardiogr 2006;7:365-72.
52. Jenkins C, Moir S, Chan J, Rakhit D, Haluska B, Marwick TH. Left ventricular volume measurement with echocardiography: a comparison of left ventricular opacification,

three-dimensional echocardiography, or both with magnetic resonance imaging. Eur Heart J 2009;30:98-106.
53. Mor-Avi V, Sugeng L, Lang RM. Real-time 3-dimensional echocardiography: an integral component of the routine echocardiographic examination in adult patients? Circulation 2009;119:314-29.
54. Lang RM, Tsang W, Weinert L, Mor-Avi V, Chandra S. Valvular heart disease. The value of 3-dimensional echocardiography. J Am Coll Cardiol 2011;58:1933-44.
55. Chandra S, Salgo IS, Sugeng L, Weinert L, Tsang W, Takeuchi M, et al. Characterization of degenerative mitral valve disease using morphologic analysis of real-time three-dimensional echocardiographic images: objective insight into complexity and planning of mitral valve repair. Circ Cardiovasc Imaging 2011;4:24-32.
56. Khaw AV, von Bardeleben RS, Strasser C, Mohr-Kahaly S, Blankenberg S, Espinola-Klein C, et al. Direct measurement of left ventricular outflow tract by transthoracic real-time 3D-echocardiography increases accuracy in assessment of aortic valve stenosis. Int J Cardiol 2009;136:64-71.
57. Kort S. Real-time 3-dimensional echocardiography for prosthetic valve endocarditis: initial experience. J Am Soc Echocardiogr 2006;19:130-9.
58. Holman ER, Buller VG, de Roos A, van der Geest RJ, Baur LH, van der Laarse A, et al. Detection and quantification of dysfunctional myocardium by magnetic resonance imaging. A new three-dimensional method for quantitative wall-thickening analysis. Circulation 1997;95:924-31.
59. Kim YJ, Kim RJ. The role of cardiac MR in new-onset heart failure. Curr Cardiol Rep 2011;13:185-93.
60. Schuster A, Morton G, Chiribiri A, Perera D, Vanoverschelde JL, Nagel E. Imaging in the management of ischemic cardiomyopathy: special focus on magnetic resonance. J Am Coll Cardiol 2012;59:359-70.
61. Bingham SE, Hachamovitch R. Incremental prognostic significance of combined cardiac magnetic resonance imaging, adenosine stress perfusion, delayed enhancement, and left ventricular function over preimaging information for the prediction of adverse events. Circulation 2011;123:1509-18.
62. Bellenger NG, Davies LC, Francis JM, Coats AJ, Pennell DJ. Reduction in sample size for studies of remodeling in heart failure by the use of cardiovascular magnetic resonance. J Cardiovasc Magn Reson 2000;2:271-8.
63. Thiele H, Kappl MJ, Conradi S, Niebauer J, Hambrecht R, Schuler G. Reproducibility of chronic and acute infarct size measurement by delayed enhancement-magnetic resonance imaging. J Am Coll Cardiol 2006;47:1641-5.
64. Reimer KA, Lowe JE, Rasmussen MM, Jennings RB. The wavefront phenomenon of ischemic cell death. 1. Myocardial infarct size vs duration of coronary occlusion in dogs. Circulation 1977;56:786-94.
65. Kim RJ, Wu E, Rafael A, Chen EL, Parker MA, Simonetti O, et al. The use of contrast-enhanced magnetic resonance imaging to identify reversible myocardial dysfunction. N Engl J Med 2000;343:1445-53.
66. Bland JM, Altman DG. Statistical methods for assessing agreement between two methods of clinical measurement. Lancet 1986;1:307-10.
67. Kramer MS, Feinstein AR. Clinical biostatistics. LIV. The biostatistics of concordance. Clin Pharmacol Ther 1981;29:111-23.
68. Keyl C, Rodig G, Lemberger P, Hobbhahn J. A comparison of the use of transoesophageal Doppler and thermodilution techniques for cardiac output determination. Eur J Anaesthesiol 1996;13:136-42.

69. Nagueh SF, Middleton KJ, Kopelen HA, Zoghbi WA, Quinones MA. Doppler tissue imaging: a noninvasive technique for evaluation of left ventricular relaxation and estimation of filling pressures. J Am Coll Cardiol 1997;30:1527-33.
70. Soliman OI, Kirschbaum SW, van Dalen BM, van der Zwaan HB, Delavary BM, Vletter WB, et al. Accuracy and reproducibility of quantitation of left ventricular function by real-time three-dimensional echocardiography versus cardiac magnetic resonance. Am J Cardiol 2008;102:778-83.
71. van Dalen BM, Soliman OI, Vletter WB, Kauer F, van der Zwaan HB, Ten Cate FJ, et al. Feasibility and reproducibility of left ventricular rotation parameters measured by speckle tracking echocardiography. Eur J Echocardiogr 2009;10:669-76.
72. Bland JM, Altman DG. Measuring agreement in method comparison studies. Stat Methods Med Res 1999;8:135-60.
73. Carabello BA. Evolution of the study of left ventricular function: everything old is new again. Circulation 2002;105:2701-3.
74. Group TCTS. Effects of enalapril on mortality in severe congestive heart failure. Results of the Cooperative North Scandinavian Enalapril Survival Study (CONSENSUS). The CONSENSUS Trial Study Group. N Engl J Med 1987;316:1429-35.
75. Group M-HS. Effect of metoprolol CR/XL in chronic heart failure: Metoprolol CR/XL Randomised Intervention Trial in Congestive Heart Failure (MERIT-HF). Lancet 1999;353:2001-7.
76. Gradman A, Deedwania P, Cody R, Massie B, Packer M, Pitt B, et al. Predictors of total mortality and sudden death in mild to moderate heart failure. Captopril-Digoxin Study Group. J Am Coll Cardiol 1989;14:564-70; discussion 71-2.
77. Bolick DR, Hackel DB, Reimer KA, Ideker RE. Quantitative analysis of myocardial infarct structure in patients with ventricular tachycardia. Circulation 1986;74:1266-79.
78. Bello D, Einhorn A, Kaushal R, Kenchaiah S, Raney A, Fieno D, et al. Cardiac magnetic resonance imaging: infarct size is an independent predictor of mortality in patients with coronary artery disease. Magnetic Resonance Imaging 2011;29:50-6.
79. Wu E, Ortiz JT, Tejedor P, Lee DC, Bucciarelli-Ducci C, Kansal P, et al. Infarct size by contrast enhanced cardiac magnetic resonance is a stronger predictor of outcomes than left ventricular ejection fraction or end-systolic volume index: prospective cohort study. Heart 2008;94:730-6.
80. Patel MR, Dehmer GJ, Hirshfeld JW, Smith PK, Spertus JA. ACCF/SCAI/STS/AATS/AHA/ASNC 2009 Appropriateness Criteria for Coronary Revascularization: A Report of the American College of Cardiology Foundation Appropriateness Criteria Task Force, Society for Cardiovascular Angiography and Interventions, Society of Thoracic Surgeons, American Association for Thoracic Surgery, American Heart Association, and the American Society of Nuclear Cardiology: Endorsed by the American Society of Echocardiography, the Heart Failure Society of America, and the Society of Cardiovascular Computed Tomography. Circulation 2009;119:1330-52.
81. Camici PG, Prasad SK, Rimoldi OE. Stunning, hibernation, and assessment of myocardial viability. Circulation 2008;117:103-14.
82. Allman KC, Shaw LJ, Hachamovitch R, Udelson JE. Myocardial viability testing and impact of revascularization on prognosis in patients with coronary artery disease and left ventricular dysfunction: a meta-analysis. J Am Coll Cardiol 2002;39:1151-8.
83. Bonow RO, Maurer G, Lee KL, Holly TA, Binkley PF, Desvigne-Nickens P, et al. Myocardial viability and survival in ischemic left ventricular dysfunction. N Engl J Med 2011;364:1617-25.
84. Cortigiani L, Bigi R, Sicari R. Is viability still viable after the STICH trial? Eur Heart J Cardiovasc Imaging 2012;13:219-26.

85. Becker M, Altiok E, Lente C, Otten S, Friedman Z, Adam D, et al. Layer-specific analysis of myocardial function for accurate prediction of reversible ischaemic dysfunction in intermediate viability defined by contrast-enhanced MRI. Heart 2011;97:748-56.
86. Wellnhofer E, Olariu A, Klein C, Grafe M, Wahl A, Fleck E, et al. Magnetic resonance low-dose dobutamine test is superior to SCAR quantification for the prediction of functional recovery. Circulation 2004;109:2172-4.
87. Kelle S, Roes SD, Klein C, Kokocinski T, de Roos A, Fleck E, et al. Prognostic value of myocardial infarct size and contractile reserve using magnetic resonance imaging. J Am Coll Cardiol 2009;54:1770-7.
88. Roes SD, Kelle S, Kaandorp TA, Kokocinski T, Poldermans D, Lamb HJ, et al. Comparison of myocardial infarct size assessed with contrast-enhanced magnetic resonance imaging and left ventricular function and volumes to predict mortality in patients with healed myocardial infarction. Am J Cardiol 2007;100:930-6.
89. Cheong BY, Muthupillai R, Wilson JM, Sung A, Huber S, Amin S, et al. Prognostic significance of delayed-enhancement magnetic resonance imaging: survival of 857 patients with and without left ventricular dysfunction. Circulation 2009;120:2069-76.
90. Eek C, Grenne B, Brunvand H, Aakhus S, Endresen K, Hol PK, et al. Strain echocardiography and wall motion score index predicts final infarct size in patients with non-ST-segment-elevation myocardial infarction. Circ Cardiovasc Imaging 2010;3:187-94.
91. Gjesdal O, Helle-Valle T, Hopp E, Lunde K, Vartdal T, Aakhus S, et al. Noninvasive separation of large, medium, and small myocardial infarcts in survivors of reperfused ST-elevation myocardial infarction: a comprehensive tissue Doppler and speckle-tracking echocardiography study. Circ Cardiovasc Imaging 2008;1:189-96, 2 p following 96.
92. Montant P, Chenot F, Goffinet C, Poncelet A, Vancraeynest D, Pasquet A, et al. Detection and quantification of myocardial scars by contrast-enhanced 3D echocardiography. Circ Cardiovasc Imaging 2010;3:415-23.
93. Sjoli B, Orn S, Grenne B, Vartdal T, Smiseth OA, Edvardsen T, et al. Comparison of left ventricular ejection fraction and left ventricular global strain as determinants of infarct size in patients with acute myocardial infarction. J Am Soc Echocardiogr 2009;22:1232-8.
94. Kelle S, Roes SD, Klein C, Kokocinski T, de Roos A, Fleck E, et al. Prognostic Value of Myocardial Infarct Size and Contractile Reserve Using Magnetic Resonance Imaging. Journal of the American College of Cardiology 2009;54:1770-7.
95. Giannitsis E, Steen H, Kurz K, Ivandic B, Simon AC, Futterer S, et al. Cardiac magnetic resonance imaging study for quantification of infarct size comparing directly serial versus single time-point measurements of cardiac troponin T. J Am Coll Cardiol 2008;51:307-14.
96. Steen H, Futterer S, Merten C, Junger C, Katus HA, Giannitsis E. Relative role of NT-pro BNP and cardiac troponin T at 96 hours for estimation of infarct size and left ventricular function after acute myocardial infarction. J Cardiovasc Magn Reson 2007;9:749-58.
97. Steen H, Giannitsis E, Futterer S, Merten C, Juenger C, Katus HA. Cardiac troponin T at 96 hours after acute myocardial infarction correlates with infarct size and cardiac function. J Am Coll Cardiol 2006;48:2192-4.
98. Lang RM, Badano LP, Tsang W, Adams DH, Agricola E, Buck T, et al. EAE/ASE recommendations for image acquisition and display using three-dimensional echocardiography. Eur Heart J Cardiovasc Imaging 2012;13:1-46.
99. Emilsson K, Egerlid R, Nygren BM, Wandt B. Mitral annulus motion versus long-axis fractional shortening. Exp Clin Cardiol 2006;11:302-4.
100. Ingul CB, Stoylen A, Slordahl SA. Recovery of stunned myocardium in acute myocardial infarction quantified by strain rate imaging: a clinical study. J Am Soc Echocardiogr 2005;18:401-10.

101. Arruda-Olson AM, Roger VL, Jaffe AS, Hodge DO, Gibbons RJ, Miller TD. Troponin T Levels and Infarct Size by SPECT Myocardial Perfusion Imaging. JACC: Cardiovascular Imaging 2011;4:523-33.
102. Heiberg E, Engblom H, Engvall J, Hedstrom E, Ugander M, Arheden H. Semi-automatic quantification of myocardial infarction from delayed contrast enhanced magnetic resonance imaging. Scand Cardiovasc J 2005;39:267-75.
103. Miller TD, Christian TF, Hodge DO, Hopfenspirger MR, Gersh BJ, Gibbons RJ. Comparison of acute myocardial infarct size to two-year mortality in patients <65 to those >=65 years of age. The American Journal of Cardiology 1999;84:1170-5.
104. Palecek T, Skalicka L, Lachmanova J, Tesar V, Linhart A. Effect of preload reduction by hemodialysis on conventional and novel echocardiographic parameters of left ventricular structure and function. Echocardiography 2008;25:162-8.
105. Meng X-l, Rosenthal R, Rubin DB. Comparing correlated correlation coefficients. Psychological Bulletin 1992;111:172-5.
106. Hanley JA, McNeil BJ. A method of comparing the areas under receiver operating characteristic curves derived from the same cases. Radiology 1983;148:839-43.
107. Singer M, Allen MJ, Webb AR, Bennett ED. Effects of alterations in left ventricular filling, contractility, and systemic vascular resistance on the ascending aortic blood velocity waveform of normal subjects. Crit Care Med 1991;19:1138-45.
108. Gorcsan J, 3rd, Deswal A, Mankad S, Mandarino WA, Mahler CM, Yamazaki N, et al. Quantification of the myocardial response to low-dose dobutamine using tissue Doppler echocardiographic measures of velocity and velocity gradient. Am J Cardiol 1998;81:615-23.
109. Greenberg NL, Firstenberg MS, Castro PL, Main M, Travaglini A, Odabashian JA, et al. Doppler-derived myocardial systolic strain rate is a strong index of left ventricular contractility. Circulation 2002;105:99-105.
110. Vogel M, Cheung MM, Li J, Kristiansen SB, Schmidt MR, White PA, et al. Noninvasive assessment of left ventricular force-frequency relationships using tissue Doppler-derived isovolumic acceleration: validation in an animal model. Circulation 2003;107:1647-52.
111. Kobayashi M, Izawa H, Cheng XW, Asano H, Hirashiki A, Unno K, et al. Dobutamine stress testing as a diagnostic tool for evaluation of myocardial contractile reserve in asymptomatic or mildly symptomatic patients with dilated cardiomyopathy. JACC Cardiovasc Imaging 2008;1:718-26.
112. Lenihan DJ, Gerson MC, Dorn GW, 2nd, Hoit BD, Walsh RA. Effects of changes in atrioventricular gradient and contractility on left ventricular filling in human diastolic cardiac dysfunction. Am Heart J 1996;132:1179-88.
113. Mak S, Newton GE. Vitamin C augments the inotropic response to dobutamine in humans with normal left ventricular function. Circulation 2001;103:826-30.
114. Hailer B, Naber C, Koslowski B, van Leeuwen P, Schafer H, Budde T, et al. Gender-related differences in patients with ST-elevation myocardial infarction: results from the registry study of the ST elevation myocardial infarction network Essen. Clin Cardiol 2011;34:294-301.
115. Investigators TG. An international randomized trial comparing four thrombolytic strategies for acute myocardial infarction. The GUSTO investigators. N Engl J Med 1993;329:673-82.
116. Berger JS, Elliott L, Gallup D, Roe M, Granger CB, Armstrong PW, et al. Sex differences in mortality following acute coronary syndromes. JAMA 2009;302:874-82.
117. Hochman JS, Tamis JE, Thompson TD, Weaver WD, White HD, Van de Werf F, et al. Sex, clinical presentation, and outcome in patients with acute coronary syndromes. Global

Use of Strategies to Open Occluded Coronary Arteries in Acute Coronary Syndromes IIb Investigators. N Engl J Med 1999;341:226-32.
118. Kontos MC, Kurdziel KA, Ornato JP, Schmidt KL, Jesse RL, Tatum JL. A nonischemic electrocardiogram does not always predict a small myocardial infarction: Results with acute myocardial perfusion imaging. American Heart Journal 2001;141:360-6.
119. Dalen H, Thorstensen A, Romundstad PR, Aase SA, Stoylen A, Vatten LJ. Cardiovascular risk factors and systolic and diastolic cardiac function: a tissue Doppler and speckle tracking echocardiographic study. J Am Soc Echocardiogr 2011;24:322-32 e6.
120. Grimes DA, Schulz KF. Bias and causal associations in observational research. Lancet 2002;359:248-52.
121. Obesity WHOCo. Obesity: Preventing and Managing the Global Epidemic. Geneva, Switzerland: Division of Non-communicable Diseases, Programme of Nutrition, Family and Reproductive Health. WHO 1998.
122. Graham I, Atar D, Borch-Johnsen K, Boysen G, Burell G, Cifkova R, et al. European guidelines on cardiovascular disease prevention in clinical practice: executive summary. Eur Heart J 2007;28:2375-414.
123. Lavie CJ, Milani RV, Ventura HO. Obesity and cardiovascular disease: risk factor, paradox, and impact of weight loss. J Am Coll Cardiol 2009;53:1925-32.
124. Jamal F, Kukulski T, Sutherland GR, Weidemann F, D'Hooge J, Bijnens B, et al. Can changes in systolic longitudinal deformation quantify regional myocardial function after an acute infarction? An ultrasonic strain rate and strain study. J Am Soc Echocardiogr 2002;15:723-30.
125. Voigt JU, Arnold MF, Karlsson M, Hubbert L, Kukulski T, Hatle L, et al. Assessment of regional longitudinal myocardial strain rate derived from doppler myocardial imaging indexes in normal and infarcted myocardium. J Am Soc Echocardiogr 2000;13:588-98.
126. Zhang Y, Chan AK, Yu CM, Yip GW, Fung JW, Lam WW, et al. Strain rate imaging differentiates transmural from non-transmural myocardial infarction: a validation study using delayed-enhancement magnetic resonance imaging. J Am Coll Cardiol 2005;46:864-71.
127. Nagueh SF, Appleton CP, Gillebert TC, Marino PN, Oh JK, Smiseth OA, et al. Recommendations for the evaluation of left ventricular diastolic function by echocardiography. Eur J Echocardiogr 2009;10:165-93.
128. Nestaas E, Stoylen A, Brunvand L, Fugelseth D. Longitudinal strain and strain rate by tissue Doppler are more sensitive indices than fractional shortening for assessing the reduced myocardial function in asphyxiated neonates. Cardiol Young 2011;21:1-7.
129. Mistry N, Beitnes JO, Halvorsen S, Abdelnoor M, Hoffmann P, Kjeldsen SE, et al. Assessment of left ventricular function in ST-elevation myocardial infarction by global longitudinal strain: a comparison with ejection fraction, infarct size, and wall motion score index measured by non-invasive imaging modalities. Eur J Echocardiogr 2011;12:678-83.
130. Aase SA, Bjork-Ingul C, Thorstensen A, Torp H, Stoylen A. Aortic valve closure: relation to tissue velocities by Doppler and speckle tracking in patients with infarction and at high heart rates. Echocardiography 2010;27:363-9.
131. Reant P, Barbot L, Touche C, Dijos M, Arsac F, Pillois X, et al. Evaluation of Global Left Ventricular Systolic Function Using Three-Dimensional Echocardiography Speckle-Tracking Strain Parameters. J Am Soc Echocardiogr 2011.
132. Manisty CH, Francis DP. Ejection fraction: a measure of desperation? Heart 2008;94:400-1.
133. Mogelvang R, Sogaard P, Pedersen SA, Olsen NT, Marott JL, Schnohr P, et al. Cardiac dysfunction assessed by echocardiographic tissue Doppler imaging is an independent predictor of mortality in the general population. Circulation 2009;119:2679-85.

134. Mogelvang R, Sogaard P, Pedersen SA, Olsen NT, Schnohr P, Jensen JS. Tissue Doppler echocardiography in persons with hypertension, diabetes, or ischaemic heart disease: the Copenhagen City Heart Study. Eur Heart J 2009;30:731-9.
135. Vinereanu D, Florescu N, Sculthorpe N, Tweddel AC, Stephens MR, Fraser AG. Left ventricular long-axis diastolic function is augmented in the hearts of endurance-trained compared with strength-trained athletes. Clin Sci (Lond) 2002;103:249-57.
136. Alam M, Hoglund C, Thorstrand C, Philip A. Atrioventricular plane displacement in severe congestive heart failure following dilated cardiomyopathy or myocardial infarction. J Intern Med 1990;228:569-75.
137. Flett AS, Hasleton J, Cook C, Hausenloy D, Quarta G, Ariti C, et al. Evaluation of techniques for the quantification of myocardial scar of differing etiology using cardiac magnetic resonance. JACC Cardiovasc Imaging 2011;4:150-6.
138. Chan J, Hanekom L, Wong C, Leano R, Cho GY, Marwick TH. Differentiation of subendocardial and transmural infarction using two-dimensional strain rate imaging to assess short-axis and long-axis myocardial function. J Am Coll Cardiol 2006;48:2026-33.
139. Grenne B, Eek C, Sjoli B, Dahlslett T, Uchto M, Hol PK, et al. Acute coronary occlusion in non-ST-elevation acute coronary syndrome: outcome and early identification by strain echocardiography. Heart 2010;96:1550-6.
140. Malm S, Frigstad S, Stoylen A, Torp H, Sagberg E, Skjarpe T. Effects of ultrasound contrast during tissue velocity imaging on regional left ventricular velocity, strain, and strain rate measurements. J Am Soc Echocardiogr 2006;19:40-7.
141. Abali G, Tokgozoglu L, Ozcebe OI, Aytemir K, Nazli N. Which Doppler parameters are load independent? A study in normal volunteers after blood donation. J Am Soc Echocardiogr 2005;18:1260-5.

European Journal of Echocardiography (2010) **11**, 149–156
doi:10.1093/ejechocard/jep188

Reproducibility in echocardiographic assessment of the left ventricular global and regional function, the HUNT study

Anders Thorstensen[1]*, Havard Dalen[1,2], Brage Høyem Amundsen[1,3], Svein Arne Aase[1], and Asbjørn Stoylen[1,3]

[1]Department of circulation and medical imaging, Norwegian University of Science and Technology, N-7489 Trondheim, Norway; [2]Department of Medicine, Levanger Hospital, Nord-Trøndelag Health Trust, Norway; and [3]Department of Cardiology, St Olavs Hospital/Trondheim University Hospital, Trondheim, Norway

Received 16 July 2009; accepted after revision 4 November 2009; online publish-ahead-of-print 3 December 2009

Aims The study aimed to compare the inter-observer reproducibility of new and traditional measurements of the left ventricular (LV) global and regional function.

Methods and results Two experienced echocardiographers performed 20 complete echo/Doppler examinations and 50 analyses on ten healthy subjects. All recordings were analysed for systolic and diastolic conventional and deformation measurements by both echocardiographers. Inter-observer mean error (absolute difference divided by the mean) was 4% and lowest ($P = 0.001$) for systolic M-mode annulus excursion. Mean error for the regional deformation indices was significantly higher than for all the global measurements (all $P < 0.001$). Mean error for analyses of the same recording was 34% ($P = 0.002$) lower for global systolic indices and 44% ($P < 0.001$) lower for global diastolic indices than inter-observer mean error for analyses made in separate recordings.

Conclusion Systolic M-mode annulus excursion showed better inter-observer reproducibility than other traditional and newer measurements of LV systolic and diastolic function. Repeated analyses of the same recordings underestimate the more clinically relevant inter-observer reproducibility by ~40% for most measurements of LV function.

Keywords Repeatability • Myocardial deformation • Tissue Doppler • Speckle tracking • Systolic function • Diastolic function

Introduction

Left ventricular (LV) functional indices, including volumes, ejection fraction (EF), annular plane systolic displacement, annular plane velocity, and LV diastolic filling parameters have been shown to have prognostic value. Tissue Doppler imaging (TDI) and the technique of speckle tracking (ST)[1] have enabled reliable measurements of regional function, and global averages of segmental deformation indices are now alternative measurements of global LV performance.[2]

When new techniques are introduced in clinical practice, evaluation of the reproducibility in a realistic clinical setting is of major importance. A common limitation of validation studies is reporting of intra- and inter-observer reproducibility based on repeated measurements of the same recordings. Few studies report reproducibility based on repeated recordings, and even fewer studies compare the reproducibility of new parameters with the more established ones. We aimed to evaluate and compare the reproducibility of new and traditional measurements of the LV global and regional function based on both separate recordings and analyses.

Methods

Study population

This was a supplementary study of the population-based third wave of the Nord-Trøndelag Health study (HUNT-3) in which 1266 healthy participants were randomized to echocardiographic examination.[3] In this study, 10 healthy volunteers (7 men, age 30 ± 6 years) were

* Corresponding author. Tel: +47 73 59 50 00 or +47 97 69 07 31, Fax: +47 73 59 86 13, Email: anders.thorstensen@ntnu.no

prospectively recruited among the staff at the Department of Circulation and Medical Imaging at the Norwegian University of Science and Technology. None were excluded due to inadequate echocardiographic images. The study was approved by the Regional Committee for Medical Research Ethics, and conducted according to the Helsinki Declaration. Written informed consent was obtained.

Study design

Two experienced physician echocardiographers (A.T. and H.D.), blinded to each other's recordings, performed separate complete echo/Doppler studies on all the participants (20 examinations in total). The recordings on the same subject were separated by a time interval of ~30 min. Both echocardiographers analysed all measurements. Inter-observer reproducibility was defined as the reproducibility calculated by separate recordings. Inter-analyser reproducibility was defined as the reproducibility calculated by the two echocardiographers' analyses of the same set of recordings. Intra-analyser reproducibility was defined as the reproducibility calculated by one of the echocardiographers re-analyses of his own recordings. The re-analyses were done in random order after a period of approximately 3 weeks. In all, 20 examinations and 50 analyses were obtained.

Echocardiographic image acquisition

Examinations were performed in the left lateral decubitus position with a Vivid 7 scanner (version BT06, GE Vingmed Ultrasound, Horten, Norway) using a 2.0 MHz phased-array transducer (M3S). The echo/Doppler examination included parasternal long- and short-axis views and three standard apical views. For each view, three consecutive cardiac cycles were recorded during quiet respiration. From the three apical views, separate B-mode and colour tissue Doppler acquisitions were recorded. The Doppler pulse repetition frequency was 1 kHz. Colour tissue Doppler acquisitions were recorded at a mean frame rate of 110 s^{-1} with underlying grey-scale frame rate of 27 s^{-1}. B-mode recordings were optimized for evaluation of the LV at a mean frame rate of 44 s^{-1}.

The LV outflow tract velocity was recorded from the apical five-chamber view with the sample volume positioned about 5 mm proximal to the aortic valve.[4] Other Doppler flow recordings were taken from the apical four-chamber view. Pulsed wave Doppler mitral flow velocities were recorded with the sample volume between the leaflet tips.[5] Recording for isovolumic relaxation time measurement was obtained by simultaneous recording of the aortic and mitral flows. Pulmonary venous flow velocities were recorded with the sample volume approximately 1 cm into the right upper pulmonary vein.[5] Pulsed wave tissue Doppler imaging (pwTDI) mitral annular velocities were acquired from the base of the septal, lateral, inferior, and anterior walls[6] in the two- and four-chamber views. The sample volume was positioned within 1 cm of the insertion of the mitral leaflets and adjusted as necessary to cover the longitudinal excursion of the mitral annulus in both systole and diastole.[5]

Analysis of B-mode and Doppler echocardiography

Interventricular septal and posterior wall thickness, fractional shortening, and LV internal dimension were analysed on parasternal M-mode echocardiograms with the ultrasound beam at the tip of the mitral leaflet. Left ventricular volumes were measured by biplane Simpson's rule from the apical four- and two-chamber views.[7] End-diastolic volume was measured at the time of mitral valve closure, and end-systolic volume was measured on the image with the smallest LV cavity.

From the pwTDI spectral recordings, peak systolic mitral annular velocities S′(pwTDI), peak early diastolic annular velocities E′(pwTDI), and late diastolic velocities A′(pwTDI) were measured at the maximum of the Doppler spectrum with low gain setting (*Figure 1*). Peak systolic annular velocities were also measured at the peak of the curve obtained from colour tissue Doppler imaging S′(cTDI), which represents the average velocity of the sample volume (*Figure 1*). Systolic mitral annular excursion was measured in reconstructed longitudinal M-mode from the apical position (MAE Mm) (*Figure 2*) and from tissue Doppler by integration of the systolic cTDI velocity curves (MAE cTDI) (*Figure 2*). The annular plane motion and velocity measurements of the septal, lateral, inferior, and anterior walls were averaged to get measurements of global LV performance.

The transmitral early diastolic filling velocity (E), late atrial filling velocity (A), E-wave deceleration time (DT), and E/A-ratio were measured. Isovolumic relaxation time was measured from the start of the aortic valve closure signal to the start of mitral flow. E/E′(pwTDI) ratio was calculated by dividing E by the average E′(pwTDI) of the septal, lateral, inferior, and anterior walls. From the pulmonary venous flow waveforms, peak systolic (S) velocity, peak antegrade diastolic velocity (D), and S/D ratio were measured. All measurements reflected the average of three cardiac cycles during quiet respiration.[5]

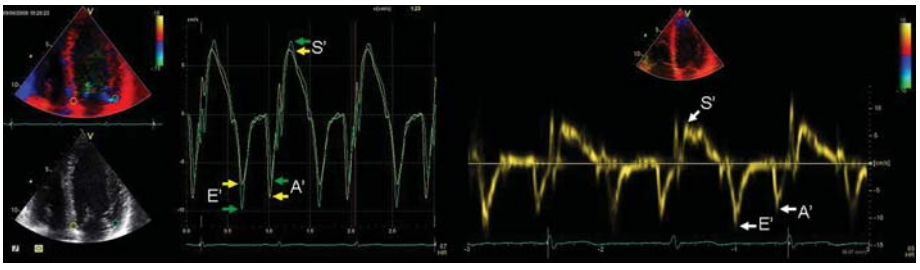

Figure 1 Left: velocity curves from colour Doppler tissue imaging in four-chamber view. Region of interest is positioned close to the septal and lateral insertion of the mitral leaflets, and peak systolic velocity (S′), early diastolic velocity (E′) and late diastolic velocity (A′) were measured at the peaks of the Doppler curve. Right: pulsed-waved tissue Doppler-derived septal annulus velocities with low gain setting in four-chamber long-axis view. S′, E′, and A′ were measured at the maximum of the Doppler spectrum.

Analysis of deformation indices

End-systolic strain (S_{ES}) was measured at aortic valve closure, peak systolic strain rate (SR_S) as the maximal negative value during ejection time, early diastolic peak strain rate (SR_E) as the maximal positive strain rate during the first part of diastole, and late diastolic peak strain rate (SR_A) as the maximal positive strain rate during the last part of diastole. Segmental longitudinal S_{ES}, SR_S, SR_E, and SR_A were measured in the three standard apical views.

Speckle tracking in B-mode recordings was done by 2D speckle tracking echocardiography (2D-ST) in commercially available software (Automated Function Imaging; EchoPAC PC version BT 09, GE Vingmed, Horten, Norway). The region of interest was manually adjusted to include the entire LV myocardium and simultaneously avoid the pericardium. The software automatically tracked speckles frame by frame throughout the cardiac cycle, and segments with poor tracking were excluded manually (*Figure 3*).

Combined tissue Doppler and B-mode recordings were analysed by a dedicated software in which the tracking is based on a combination of speckle tracking and tissue Doppler velocities (D + ST) (GcMat; GE Vingmed Ultrasound, Horten, Norway, running on a MATLAB platform; MathWorks, Inc., Natick, MA, USA). Seven kernels (chosen regions of the myocardium) sized 5 × 5 mm defining segment borders were tracked by tissue Doppler in the direction of the ultrasound beams and by gray-scale speckles in directions

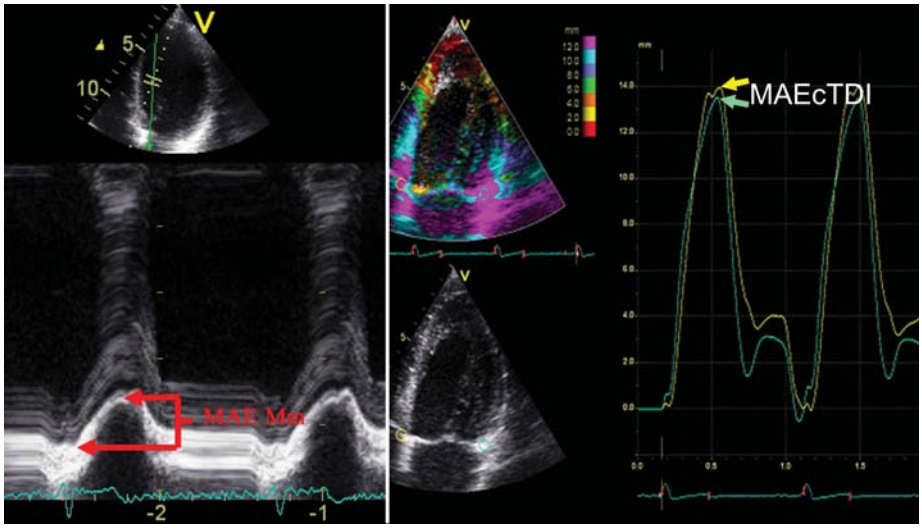

Figure 2 Measurements of systolic mitral annular excursion (MAE) obtained by two different methods in four-chamber view. To the left, systolic MAE is measured by reconstructed M-mode (Mm). To the right, MAE is measured at the top of the displacement curve obtained from integrated velocity colour tissue Doppler imaging (cTDI) recordings.

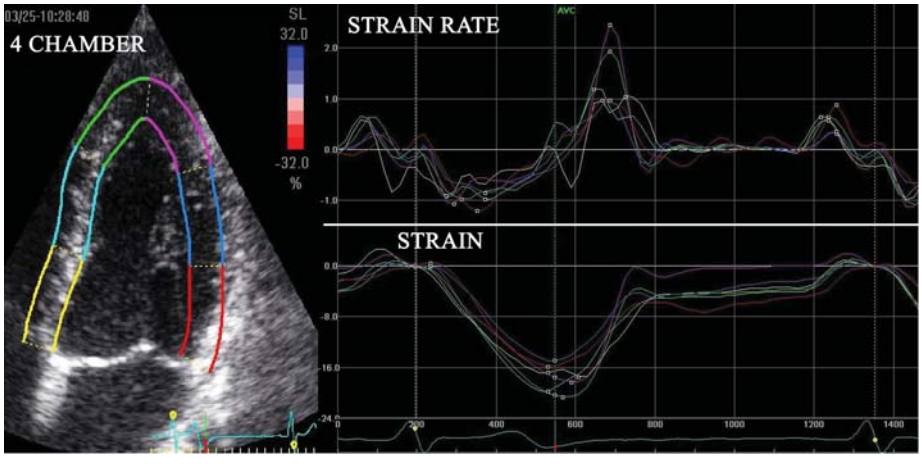

Figure 3 Composite figure showing segmental deformation indices obtained from commercially available 2D speckle tracking echocardiography. Region-of-interest (left side) of six segments in four-chamber long-axis view with the corresponding graphic depiction of longitudinal strain rate (upper right) and strain (lower right).

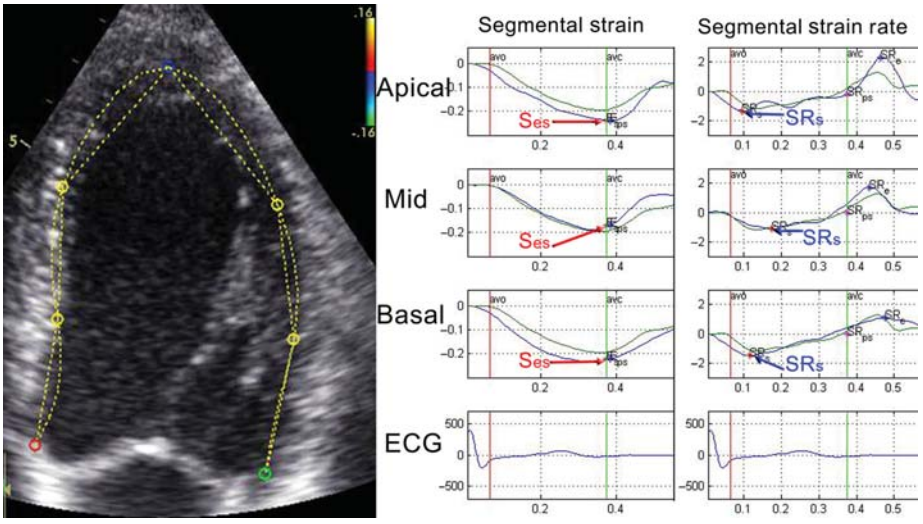

Figure 4 Composite figure showing segmental deformation indices obtained in customized semiautomatic software (GcMat). To the left, tracking points in four-chamber long-axis view, which defines the segment lengths at end-diastole. In the middle, strain curves of the three septal segments, end-systolic strain (SES) marked with red arrows. To the right strain rate curves of the same segments, peak systolic strain rate (SRS) marked with blue arrows.

perpendicular to the ultrasound beam. Lagrangian strain was calculated from the change of segment length, and strain rate was calculated as the temporal derivative of strain, with correction to Eulerian SR. This method has been described previously.[8–10] Aortic valve closure was automatically detected by tissue velocities.[11] Only segments with good tracking of the kernels assessed by visual evaluation were accepted (*Figure 4*).

Segmental longitudinal strain and SR were analysed in an 18 segment model of the left ventricle, i.e. three segments per wall. This model gives too much weight to the apex, compared with the actual amount of myocardium; therefore, global averages were calculated from the standard ASE 16 segment model, with only four segments at the apical level.[7]

Statistics

Values are reported as mean and standard deviation (SD). The reproducibility is expressed by the coefficient of repeatability (COR), and as the mean percent error (mean error). Coefficient of repeatability was calculated according to the method of Bland and Altman[12] as 2 × SD of the differences in repeated measurements. Mean error was derived as the absolute difference between the two sets of observations, divided by the mean of the observations.[13–16] For comparison of the mean errors of the global systolic and diastolic measurements of LV performance shown in *Tables 1 and 2*, one-way analysis of variance (ANOVA) was used. A two-sided $P < 0.05$ was considered a marker of statistical significance. All statistical analyses were performed using SPSS for Windows (version 15.0, SPSS Inc., Chicago, IL, USA).

Results

Estimation of biplane EF, mitral annulus velocity and motion measurements and all flow measurements were feasible in all recordings. 133/180 (74%) segments post-processed by 2D-ST and 114/180 (63%) post-processed by D + ST were accepted for inter-observer validation by both echocardiographers. The rest of the segments were excluded by at least one of the observers because of reverberations, valvular interference, tracking difficulties, or poor image quality.

Mean (SD) inter-observer COR and inter-observer, inter- and intra-analyser mean error of the global systolic and end-diastolic dimension measurements are shown in *Table 1*. There was an overall significant difference between the inter-observer mean errors of the measurements (ANOVA $P = 0.001$). MAE (Mm) showed the best reproducibility with an inter-observer mean error of 4% and COR 1.6 mm.

Mean (SD), the inter-observer COR and inter-observer, inter- and intra-analyser mean error of the LV diastolic measurements are shown in *Table 2*. There was an overall significant difference (ANOVA $P = 0.002$) between the inter-observer mean errors of the diastolic measurements. The inter-observer mean error seemed to be the lowest for global SR_E (2D-St), E′ (pwTDI), A′ (pwTDI), and mitral flow E.

By averaging S′(pwTDI) and E′(pwTDI) of the septal, lateral, inferior, and anterior walls, the mean error was reduced by 31 and 40% (*Tables 3 and 4*). For S′(pwTDI), the mean error was reduced from 11 to 8% ($P = 0.11$) when four instead of two walls were averaged. The corresponding reduction for E′(pwTDI) was 15–8% ($P < 0.001$).

Mean error of segmental S_{ES} and SR_S was significantly higher than all the respective global averages ($P < 0.001$ for all) (*Table 5*). The 2D-ST inter-observer segmental S_{ES} and SR_S mean error was 14 and 17% and the COR 7.1% and 0.52 s^{-1}. When the segmental S_{ES} and SR_S were averaged into global S_{ES} and SR_S, the strain inter-observer mean error was reduced by 60% and the SR mean error was reduced by 44%. There were no significant differences in the reproducibility of global S_{ES} and SR_S by

Table 1 Reproducibility of measurements of dimensions and global systolic function

Method	Mean, inter-observer	COR, inter-observer	Mean error, inter-observer (%)	Mean error, inter-analyser (%)	Mean error, intra-analyser (%)
IVSd (Mm)	8.5 (1.1) mm	1.8 mm	12	10	10
LVPWd (Mm)	7.7 (1.1) mm	2.4 mm	12	10	10
LVIDd (Mm)	50 (5.3) mm	5.4 mm	5	5	3
MAE (Mm) mean	17 (1.1) mm	1.6 mm	4	3	3
MAE (cTDI) mean	15 (1.1) mm	2.2 mm	7	4	2
S′(pwTDI) mean	9.1 (2.0) cm/s	1.7 cm/s	8	3	2
S′(cTDI) mean	7.7 (1.4) cm/s	1.6 cm/s	7	3	2
EDV biplane	108 (24) mL	14 mL	12	8	8
ESV biplane	44 (9) mL	9 mL	9	10	9
EF biplane	0.59 (0.05)	0.07	6	6	5
FS	0.33 (0.06)	0.11	14	16	13
LVOT peak	1.0 (0.1) m/s	0.2 m/s	10	3	3
Global S_{ES} (2D-St)	−0.21 (0.02)	0.02	6	6	3
Global SR_S (2D-St)	−1.1 (0.01) s^{-1}	0.2 s^{-1}	9	5	5

Mean (SD), coefficient of repeatability (COR), and mean error of systolic indices. IVSd (Mm), end-diastolic interventricular septal thickness by M-mode; LVPWd (Mm), left ventricular end-diastolic posterior wall thickness by M-mode; LVIDd (Mm), left ventricular end-diastolic internal diameter by M-mode; MAE(Mm), systolic mitral annulus excursion by reconstructed M-mode; MAE(cTDI), systolic mitral annulus excursion by tissue Doppler; S′(pwTDI), peak systolic annulus velocity by pulsed wave tissue Doppler imaging; S′(cTDI), peak systolic annulus velocity by colour tissue Doppler; EDV, end-diastolic volume; ESV, end-systolic volume; EF, ejection fraction; FS, fractional shortening; LVOT peak, left ventricular outflow tract peak velocity; S_{ES}, end-systolic strain; SR_S, peak systolic strain rate, both measured by the 2D-strain application.

Table 2 Reproducibility of global diastolic measurements

Method	Mean, inter-observer	COR, inter-observer	Mean error, inter-observer (%)	Mean error, inter-analyser (%)	Mean error, intra-analyser (%)
E′(pwTDI) mean	14 (1.0) cm/s	3.4 cm/s	8	3	2
A′(pwTDI) mean	8.5 (2.5) cm/s	2.1 cm/s	9	9	2
E	74 (13) cm/s	12 cm/s	8	5	2
DT	175 (33) cm/s	10 cm/s	20	17	8
A	41 (12) cm/s	14 cm/s	18	10	4
E/A	2.0 (0.6)	0.35	22	10	5
IVRT	83 (9) ms	13 ms	17	7	3
E/E′(pwTDI)	5.4 (1.0)	1.3	11	7	3
PV S	55 (12) cm/s	12 cm/s	15	4	5
PV D	54 (7) cm/s	20 cm/s	16	4	4
PV S/D	1.0 (0.2)	0.38	12	6	6
Global SR_E (2D-St)	1.6 (0.1) s^{-1}	0.3 s^{-1}	7	8	7
Global SR_A (2D-St)	0.8 (0.1) s^{-1}	0.3 s^{-1}	13	8	12

Mean (SD), coefficient of repeatability (COR), and mean error of systolic indices. E′(pwTDI), peak early diastolic velocity by pulsed wave tissue Doppler imaging; A′(pwTDI), peak late diastolic velocity by pulsed wave tissue Doppler imaging; E, mitral flow peak early diastolic filling velocity; A, mitral flow peak late diastolic filling velocity; DT, E-wave deceleration time; IVRT, isovolumic relaxation time; PV S, pulmonary venous flow peak systolic velocity; PV D, pulmonary venous flow peak diastolic velocity diastolic; Global SR_E, peak early diastolic strain rate; Global SR_A, peak late diastolic strain rate, both measured by the 2D-strain application.

the 2D-ST method compared with the ST + D method, but the inter-observer mean error of segmental S_{ES} was significantly lower ($P = 0.03$) for 2D-ST (*Table 5*).

The inter- and intra-analyser average mean error of the 10 global systolic measurements based on repeated measurements of the same recording was 34% ($P = 0.02$) and 43% ($P = 0.002$) lower than the average inter-observer mean error calculated by separate recordings and analyses. The corresponding reduction for the global diastolic measurements was 44% ($P < 0.001$) and 64% ($P < 0.001$).

Table 3 Reproducibility of S′(pwTDI)

Method	Mean, inter-observer	COR, inter-observer	Mean error, inter-observer (%)	Mean error, inter-analyser (%)	Mean error, intra-analyser (%)
S′(pwTDI) mean of 4	9.1 cm/s	1.7 cm/s	8	3	2
S′(pwTDI) mean of septal and lateral	9.2 cm/s	2.3 cm/s	11	2	3
S′(pwTDI) septal	8.4 cm/s	2.9 cm/s	13	4	2
S′(pwTDI) lateral	10.1 cm/s	2.1 cm/s	9	4	4
S′(pwTDI) inferior	8.7 cm/s	2.8 cm/s	15	4	2
S′(pwTDI) anterior	9.3 cm/s	2.7 cm/s	12	8	5

Mean, coefficient of repeatability (COR), and mean error of peak systolic annulus velocity by tissue Doppler imaging (S′(pwTDI)) measured at different walls and averaged.

Table 4 Reproducibility of E′(pwTDI)

Method	Mean, inter-observer	COR, inter-observer	Mean error, inter-observer (%)	Mean error, inter-analyser (%)	Mean error, intra-analyser (%)
E′(pwTDI) mean of 4	13.9 cm/s	3.4 cm/s	8	3	2
E′(pwTDI) mean of septal and lateral	14.1 cm/s	4.9 cm/s	15	3	3
E′(pwTDI) septal	12.8 cm/s	5.6 cm/s	19	6	4
E′(pwTDI) lateral	15.4 cm/s	5.5 cm/s	14	4	3
E′(pwTDI) inferior	13.6 cm/s	3.8 cm/s	10	5	3
E′(pwTDI) anterior	13.7 cm/s	3.6 cm/s	13	5	4

Mean, coefficient of repeatability (COR), and mean error of peak early diastolic annulus velocity by tissue Doppler imaging (E′(pwTDI)) measured at different walls and averaged.

Table 5 Reproducibility of systolic deformation indices obtained by two different applications

	Mean, inter-observer		COR, inter-observer		Mean Error, inter-observer	
Method	2D-St	D + St	2D-St	D + St	2D-St	D + St
Global S_{ES}	−0.21	−0.19	0.02	0.02	6%	4%
Global SR_S	$-1.1\ s^{-1}$	$-1.2\ s^{-1}$	$0.2\ s^{-1}$	$0.2\ s^{-1}$	10%	8%
Segmental S_{ES}	−0.21	−0.19	0.07	0.08	14%	18%
Segmental SR_S	$-1.1\ s^{-1}$	$-1.2\ s^{-1}$	$0.5\ s^{-1}$	$0.5\ s^{-1}$	17%	16%

Mean, coefficient of repeatability (COR), and mean error of global and segmental end-systolic strain (S_{ES}) and peak systolic strain rate (SR_S). 2D-St, measurements by 2D-strain; D + ST, measurements by GcMat.

Discussion

To our knowledge, the present study represents the first comparison of the test–retest reproducibility of different measurements of LV function, including newer ST-based methods, using the same data set. The study shows that for systolic function, a conventional method like systolic annular excursion by M-mode is equal or better in terms of reproducibility, compared with averaging segmental values from newer ST and tissue Doppler-based methods. Furthermore, we show that reproducibility data based on repeated measurements of single data sets severely underestimate the more clinically relevant inter-observer reproducibility based on separate recordings.

We evaluated reproducibility by using the COR and the mean error. The COR is related to the widely accepted Bland–Altman method for evaluation of agreement, and is based on a linear relationship between errors and measurements. The COR is expressed in the measurement units, and is the smallest significant difference between repeated measurements. It is directly related to the 95% limits of agreement.[13] However, repeated cardiac

measurements, especially when they are collected over a large physiological range, often have errors that are proportional to the magnitude. This can be overcome by logarithmic transformation, which gives different COR at different measurement-magnitudes within the same method.[13,17] An alternative approach is to divide the error with the mean to get the mean error, which is a dimensionless ratio. Expressing the error in per cent allows direct comparisons between methods with different measurement units.

In this study, there was a weak correlation between the absolute differences and the mean for some of the measurements. Therefore, the combination of inter-observer COR and mean error for each method should give a good description of the reproducibility.

The reproducibility of the traditional measurements tested in the present study is in the same range or slightly better than previously determined test–retest reproducibility based on older scanners and software.[18–20] In contrast to the commonly reported reproducibility based on single data sets in the majority of echo/Doppler studies, publications on test–retest reliability of new Echo/Doppler techniques are scarce.[21]

Systolic, diastolic, and end-diastolic dimension measurements

Superior reproducibility of MAE (Mm) compared to other methods has been described earlier.[22] As this study used reconstructed M-mode, temporal resolution seems to be of minor importance. The spatial resolution, however, is high, and the demand for post-processing is low by this technique. In addition, abnormalities of the mitral annular motion and velocity have been described in a variety of cardiac diseases[23–25] and have a high correlation to brain natriuretic peptide in patients with heart failure.[26,27]

In general, the reproducibility of LV global diastolic measurements was poorer than global LV systolic measurements. This finding is supported by previously published test–retest reproducibility studies based on older scanners and software.[18–20] However E′ (pwTDI), A′ (pwTDI), and mitral flow E showed fairly good reproducibility. The difference between systolic and diastolic measurements was less evident for inter- and intra-analyser reproducibility. This difference may indicate a higher short-term biological variation in diastolic flow measurements, which is hardly surprising, given the normal respiratory variation in diastolic filling.

Tissue Doppler measurements

This study shows that the reproducibility for S′(pwTDI) and E′(pwTDI) is much better when averaging four walls compared to single wall measurements, as shown also previously.[28] Although averaging the septal and lateral wall pwTDI velocities was recently recommended from the American and European Society of Echocardiography,[5] this study indicates that averaging four instead of two walls is superior in terms of reproducibility. The inter- and intra-analyser reproducibility of S′(pwTDI) and E′(pwTDI) was considerably better than the respective inter-observer reproducibility based on separate recordings. This suggests that these measurements are sensitive to differences in image acquisition techniques between echocardiographers and/or physiological variations in cardiac function over short time periods. However, when the analysers share common agreement on gain-setting, the reproducibility of S′(pwTDI) and E′(pwTDI) based on repeated analysis of the same recording is excellent.

Segmental myocardial function

The reproducibility of segmental deformation indices is significantly poorer than other measurements of systolic and diastolic function. As expected, the reproducibility improves when segmental deformation indices are averaged into global indices for LV performance, but as these measurements are time-consuming and depend on special awareness of both methodological and technical limitations, they are less attractive for clinical use, and there is no gain in terms of reproducibility compared with the other systolic measurements. The relatively high COR and mean error of the LV segmental S_{ES} and SR_S suggest use of clinical watchful approach when performing quantitative regional analyses of the left ventricle. The two described methods for segmental strain and strain-rate measurements had almost the same reproducibility. The slightly better reproducibility of segmental strain obtained by 2D-ST could be explained by a higher degree of spatial smoothing with this technique. A high degree of spatial smoothing will in theory give higher reproducibility, but could on the other hand reduce sensitivity for differences in deformation indices between myocardial segments.

Limitations

The present study is a comparison of reproducibility between methods, without any reference method. Thus, it gives no validity comparison.

The subjects were fairly young, and had fair image quality. Reproducibility might be expected to be lower in a general patient population. In all 20 separate echocardiographic examinations (10 participants) were recorded. Thus, clinical important differences in reproducibility could be tested, but this study population will have limited power to detect small differences in the reproducibility of different measurements. Those differences, however, can be assumed to be of less clinical importance.

Standard parameters for assessment of systolic function are strongly influenced by biological variation, and we sought to minimize these by repeating the study over a short time frame, so that the main source of variation was related to imaging *per se*.

Conclusion

Modern echocardiographic equipment allows reproducible measurements of most global indices of LV performance. Systolic annular excursion by M-mode shows better inter-observer reproducibility than other traditional and newer measurements of LV systolic function. Annular tissue Doppler measurements should be averaged from four sites instead of two, in order to optimize reproducibility. Global averages of segmental strain and strain rate have approximately the same reproducibility as other global measurements, but segmental measurements have high variability.

Repeated analyses of the same recordings underestimate the clinically relevant inter-observer reproducibility obtained by separate examinations by ~40% for most measurements of LV function.

Conflict of interest: none declared.

Funding

The study has been supported by a grant from the Norwegian Research Council, through the centre for research based innovation, MI-Lab.

References

1. Bohs LN, Trahey GE. A novel method for angle independent ultrasonic imaging of blood flow and tissue motion. *IEEE Trans Biomed Eng* 1991;**38**:280–6.
2. Reisner SA, Lysyansky P, Agmon Y, Mutlak D, Lessick J, Friedman Z. Global longitudinal strain: a novel index of left ventricular systolic function. *J Am Soc Echocardiogr* 2004;**17**:630–3.
3. Dalen H, Thorstensen A, Ingul CB, Aase SA, Stoylen A. Normal values for diastolic strain rate from combined speckle tracking and Doppler tissue imaging. Preliminary data from the HUNT3-study. *ESC CONGRESS 2009*. *Eur Heart J* 2009; **30**(Abstract Supplement):320.
4. Quinones MA, Otto CM, Stoddard M, Waggoner A, Zoghbi WA. Recommendations for quantification of Doppler echocardiography: a report from the Doppler Quantification Task Force of the Nomenclature and Standards Committee of the American Society of Echocardiography. *J Am Soc Echocardiogr* 2002;**15**: 167–84.
5. Nagueh SF, Appleton CP, Gillebert TC, Marino PN, Oh JK, Smiseth OA *et al.* Recommendations for the evaluation of left ventricular diastolic function by echocardiography. *Eur J Echocardiogr* 2009;**10**:165–93.
6. Gottdiener JS, Bednarz J, Devereux R, Gardin J, Klein A, Manning WJ *et al.* American Society of Echocardiography recommendations for use of echocardiography in clinical trials. *J Am Soc Echocardiogr* 2004;**17**:1086–119.
7. Lang RM, Bierig M, Devereux RB, Flachskampf FA, Foster E, Pellikka PA *et al.* Recommendations for chamber quantification. *Eur J Echocardiogr* 2006;**7**:79–108.
8. Amundsen BH, Crosby J, Steen PA, Torp H, Slordahl SA, Stoylen A. Regional myocardial long-axis strain and strain rate measured by different tissue Doppler and speckle tracking echocardiography methods: a comparison with tagged magnetic resonance imaging. *Eur J Echocardiogr* 2009;**10**:229–37.
9. Ingul CB, Stoylen A, Slordahl SA, Wiseth R, Burgess M, Marwick TH. Automated analysis of myocardial deformation at dobutamine stress echocardiography: an angiographic validation. *J Am Coll Cardiol* 2007;**49**:1651–9.
10. Ingul CB, Torp H, Aase SA, Berg S, Stoylen A, Slordahl SA. Automated analysis of strain rate and strain: feasibility and clinical implications. *J Am Soc Echocardiogr* 2005;**18**:411–8.
11. Aase SA, Stoylen A, Ingul CB, Frigstad S, Torp H. Automatic timing of aortic valve closure in apical tissue Doppler images. *Ultrasound Med Biol* 2006;**32**:19–27.
12. Bland JM, Altman DG. Statistical methods for assessing agreement between two methods of clinical measurement. *Lancet* 1986;**1**:307–10.
13. Soliman OI, Kirschbaum SW, van Dalen BM, van der Zwaan HB, Delavary BM, Vletter WB *et al.* Accuracy and reproducibility of quantitation of left ventricular function by real-time three-dimensional echocardiography versus cardiac magnetic resonance. *Am J Cardiol* 2008;**102**:778–83.
14. Nagueh SF, Middleton KJ, Kopelen HA, Zoghbi WA, Quinones MA. Doppler tissue imaging: a noninvasive technique for evaluation of left ventricular relaxation and estimation of filling pressures. *J Am Coll Cardiol* 1997;**30**:1527–33.
15. Sugeng L, Mor-Avi V, Weinert L, Niel J, Ebner C, Steringer-Mascherbauer R *et al.* Quantitative assessment of left ventricular size and function: side-by-side comparison of real-time three-dimensional echocardiography and computed tomography with magnetic resonance reference. *Circulation* 2006;**114**:654–61.
16. van Dalen BM, Soliman OI, Vletter WB, Kauer F, van der Zwaan HB, Ten Cate FJ *et al.* Feasibility and reproducibility of left ventricular rotation parameters measured by speckle tracking echocardiography. *Eur J Echocardiogr* 2009;**10**: 669–76.
17. Keyl C, Rodig G, Lemberger P, Hobbhahn J. A comparison of the use of transoesophageal Doppler and thermodilution techniques for cardiac output determination. *Eur J Anaesthesiol* 1996;**13**:136–42.
18. Gottdiener JS, Livengood SV, Meyer PS, Chase GA. Should echocardiography be performed to assess effects of antihypertensive therapy? Test-retest reliability of echocardiography for measurement of left ventricular mass and function. *J Am Coll Cardiol* 1995;**25**:424–30.
19. Himelman RB, Cassidy MM, Landzberg JS, Schiller NB. Reproducibility of quantitative two-dimensional echocardiography. *Am Heart J* 1988;**115**:425–31.
20. Vinereanu D, Khokhar A, Fraser AG. Reproducibility of pulsed wave tissue Doppler echocardiography. *J Am Soc Echocardiogr* 1999;**12**:492–9.
21. Jenkins C, Bricknell K, Hanekom L, Marwick TH. Reproducibility and accuracy of echocardiographic measurements of left ventricular parameters using real-time three-dimensional echocardiography. *J Am Coll Cardiol* 2004;**44**:878–86.
22. Emilsson K, Egerlid R, Nygren BM, Wandt B. Mitral annulus motion versus long-axis fractional shortening. *Exp Clin Cardiol* 2006;**11**:302–4.
23. Alam M, Hoglund C, Thorstrand C. Longitudinal systolic shortening of the left ventricle: an echocardiographic study in subjects with and without preserved global function. *Clin Physiol* 1992;**12**:443–52.
24. Alam M, Wardell J, Andersson E, Nordlander R, Samad B. Assessment of left ventricular function using mitral annular velocities in patients with congestive heart failure with or without the presence of significant mitral regurgitation. *J Am Soc Echocardiogr* 2003;**16**:240–5.
25. Vinereanu D, Florescu N, Sculthorpe N, Tweddel AC, Stephens MR, Fraser AG. Differentiation between pathologic and physiologic left ventricular hypertrophy by tissue Doppler assessment of long-axis function in patients with hypertrophic cardiomyopathy or systemic hypertension and in athletes. *Am J Cardiol* 2001;**88**: 53–8.
26. Vinereanu D, Lim PO, Frenneaux MP, Fraser AG. Reduced myocardial velocities of left ventricular long-axis contraction identify both systolic and diastolic heart failure—a comparison with brain natriuretic peptide. *Eur J Heart Fail* 2005;**7**: 512–9.
27. Elnoamany MF, Abdelhameed AK. Mitral annular motion as a surrogate for left ventricular function: correlation with brain natriuretic peptide levels. *Eur J Echocardiogr* 2006;**7**:187–98.
28. Stoylen A, Skjaerpe T. Systolic long axis function of the left ventricle. Global and regional information. *Scand Cardiovasc J* 2003;**37**:253–8.

European Journal of Echocardiography Advance Access published September 22, 2011

European Journal of Echocardiography
doi:10.1093/ejechocard/jer178

Peak systolic velocity indices are more sensitive than end-systolic indices in detecting contraction changes assessed by echocardiography in young healthy humans

Anders Thorstensen[1,2]*, Håvard Dalen[1,3], Brage H. Amundsen[1,2], and Asbjørn Støylen[1,2]

[1]MI Lab and Department of Circulation and Medical Imaging, Norwegian University of Science and Technology, Trondheim, Norway; [2]Department of Cardiology, St Olavs Hospital/Trondheim University Hospital, Trondheim, Norway; and [3]Department of Medicine, Levanger Hospital, Nord-Trøndelag Health Trust, Levanger, Norway

Received 19 April 2011; accepted after revision 1 September 2011

Aims It remains to be proven whether left ventricular (LV) peak systolic velocity indices (peak systolic annulus tissue velocities, ejection velocity, and strain rate) are more closely related to contraction than LV end-systolic echocardiographic indices (ejection fraction, fractional shortening, systolic annulus displacement, global strain, and ejection velocity time integral). The study aimed to compare the ability of different echocardiographic methods in detecting contraction changes of the LV.

Methods and results Thirty-three healthy volunteers (20–32 years) were examined by echocardiography at rest, during 10 μg/kg/min dobutamine ($n = 20$), and after injection of 15 mg metoprolol ($n = 20$). The effects of dobutamine and metoprolol on peak systolic velocity indices and end-systolic indices were compared. The relative increase from rest to dobutamine stress and the relative decrease after injection of metoprolol were 62 and −15% for peak systolic annulus tissue velocity, 60 and −11% for LV outflow tract (LVOT) peak velocity, 56 and −11% for peak systolic strain rate, 25 and 1% for ejection fraction, 30 and −1% for systolic mitral annulus displacement, 30 and −5% for LVOT velocity time integral, and 21 and −3% for global strain, respectively. The changes of the peak systolic indices were significantly higher (all $P < 0.05$) than the changes of the end-systolic indices.

Conclusion Peak systolic velocity indices (mitral annulus tissue velocities, ejection velocities, and strain rate) exhibited greater variation than end-systolic indices during inotropic alterations from which it is assumed that they better reflected LV contraction.

Keywords β-Blocker • contractility • dobutamine • myocardial deformation • speckle tracking • strain

Introduction

Myocardial systolic function depends upon the interaction of myocardial contractility, preload, and afterload. Force development (contractility of the myocytes) which generates sufficient pressure to open the cardiac valves should be distinguished from deformation (shortening of the myocytes) which gives rise to the actual volume ejection.[1] True contractility of the myocardium is currently not measurable non-invasively in clinical practice.[1] However, myocyte contraction occurs in the first part of systole, which corresponds well to the timing of the echocardiographic peak systolic velocity indices such as peak systolic annulus tissue velocities, ejection velocity, and peak systolic strain rate, but it is still questionable whether these indices are closely related to contraction. In contrast to force development, deformation and volume ejection continue until the end of systole, and end-systolic

* Corresponding author: Department of Circulation and Medical Imaging, NTNU, MTFS, Postboks 8905, NO-7491 Trondheim, Norway. Tel: +47 72 82 85 46 or +47 97 69 07 31; fax: +47 72 82 83 72, Email: anders.thorstensen@ntnu.no

echocardiographic indices such as ejection fraction, fractional shortening (FS), systolic mitral annulus displacement, global strain and the ejection velocity time integral have been shown to be closely related to deformation and stroke volume.[2,3]

We hypothesized that peak systolic velocity indices better reflect changes in contraction compared with end-systolic indices and aimed to test whether these indices responded differently to inotropic alterations.

Methods

Study population

After local advertisement, we prospectively recruited 33 (25 males and 8 women) healthy volunteers (20–32 years), height 179 [standard deviation (SD 8)] cm and weight 75 (SD 12) kg. The study was approved by the Regional Committee for Medical Research Ethics and conducted according to the Helsinki Declaration. Written informed consent was obtained. The subjects were free from medications, known cardiovascular disease, structural heart disease, diabetes, or hypertension. All participants had normal electrocardiogram (ECG) and echocardiogram at rest. None were excluded due to inadequate echocardiographic image quality.

Study design

All examinations were conducted by one experienced physician echocardiographer (A.T.). A complete echo/Doppler study at rest was performed in all the participants. Low-dose dobutamine stress echocardiography was performed in 13 subjects. Both low-dose dobutamine stress echocardiography and echocardiography after intravenous administration of metoprolol were performed in seven subjects. Echocardiography after intravenous administration of metoprolol was performed on 13 subjects. In total, 20 paired rest-dobutamine recordings and 20 paired rest-metoprolol recordings were obtained and the subsequent measurements were categorized into three contractile states: β-blocker, rest, or dobutamine.

The low-dose dobutamine protocol started with a dose of 5 μg/kg/min for 3 min, followed by 10 μg/kg/min until the recordings were completed. The recordings during 10 μg/kg/min dobutamine infusion started after 3 min of steady state. For the β-blocker study, 15 mg of metoprolol was injected over 10 min, and a new complete echo/Doppler study started 10 min after the last injection. For those who received both dobutamine and metoprolol, the recordings after infusion of metoprolol started 20 min after the infusion of dobutamine was ended.

Echocardiographic image acquisition

All examinations were performed in the left lateral decubitus position with a Vivid 7 scanner (version BT09, GE Vingmed Ultrasound, Horten, Norway) using a 2.0 MHz phased-array matrix transducer (M3S) for the two-dimensional (2D) recordings and a 2.0 MHz vector-array transducer (3V) for the three-dimensional (3D) recordings. For each 2D view, three consecutive cardiac cycles were recorded during quiet respiration. From the three apical views, separate B-mode acquisitions (mean frame rate 50 s^{-1}) and colour tissue Doppler (TD) acquisitions (mean frame rate 110 s^{-1}) were recorded.

The left ventricular outflow tract (LVOT) velocity was recorded from the apical five-chamber view with the sample volume positioned about 5 mm proximal to the aortic valve. Pulsed-wave Doppler mitral flow velocities were recorded from the apical four-chamber view with the sample volume between the leaflet tips. Spectral TD mitral annular velocities were acquired from the base of the septal, lateral, inferior, and anterior walls in the four- and two-chamber views. A 6 mm sample volume was positioned within 1 cm of the insertion of the mitral leaflets.[4]

Real-time 3D echocardiography recordings were preformed immediately after the 2D examination. From the apical approach, four to six consecutive ECG-gated subvolumes were acquired during end-expiratory apnoea to generate full-volume data sets (mean frame rate 26 s^{-1}). Care was taken to encompass the entire LV cavity and, if unsatisfactory, the data set was re-acquired.

Analysis of B-mode and Doppler echocardiography

LV volumes and LV ejection fraction (LVEF) were measured by biplane Simpson's rule from the apical four- and two-chamber views. End-diastolic volume was measured at the time of mitral valve closure, and end-systolic volume was measured on the image with the smallest LV cavity. LV internal end-diastolic and end-systolic dimensions were measured perpendicular to the long axis of the ventricle at the mitral valve leaflet tips in the parasternal long-axis view, using anatomical M-mode echocardiography. The FS was calculated as the difference between LV internal end-diastolic and end-systolic dimensions divided by the LV internal end-diastolic dimension.

LVEF was also obtained from the 3D recordings (4D auto LV quantification, version BT11, GE Vingmed Ultrasound). End-diastolic and end-systolic volumes were measured after manual alignment followed by automatic detection of endocardial surface which were manually adjusted by placing as many additional points as needed in 3D at both end-diastole and end-systole. Finally, the automatically detected epicardial borders were manually adjusted in 3D at end-diastole in order to calculate LV mass.

From the spectral TD recordings, peak systolic mitral annular velocities [*S′*(spectral TD)] were measured at the peak of the Doppler spectrum with a low gain setting (*Figure 1A*). Peak systolic mitral annular velocities were also measured by colour TD [*S′*(colour TD)] (*Figure 1B*). Systolic mitral annular excursion (MAE) was measured using anatomical M-mode echocardiography from the apical position [MAE (M-mode)] (*Figure 1C*) and from TD by integration of the velocity curves [MAE (colour TD)] (*Figure 1C*). The annular plane motion and velocity indices of the septal, lateral, inferior, and anterior walls were averaged to give global measurements of LV performance.

The LVOT peak velocity was measured from the LVOT spectrum using a low gain setting. The LVOT velocity time integral (vti) was measured by tracing the modal velocity throughout systole (*Figure 1D*). All indices reflected the average of three cardiac cycles during quiet respiration.

Analysis of deformation indices

Segmental longitudinal strain and strain rate were measured in the three standard apical views.

Longitudinal end-systolic strain was obtained by speckle tracking in grey-scale recordings by 2D speckle-tracking echocardiography (2D-ST) (Automated Function Imaging; EchoPAC PC version BT 09, GE Vingmed, Horten, Norway). The regions of interest (ROIs) were manually adjusted to include the entire LV myocardium and simultaneously avoid the pericardium (*Figure 1E*). Segments with poor tracking were excluded manually. End-systolic strain was measured at the automatically detected aortic valve closure (manually corrected if necessary).

Longitudinal strain rate was calculated from colour TD recordings, using the TD velocity gradient along the ultrasound beam (Q-Analysis; EchoPAC PC version BT 09, GE Vingmed). For each segment, a

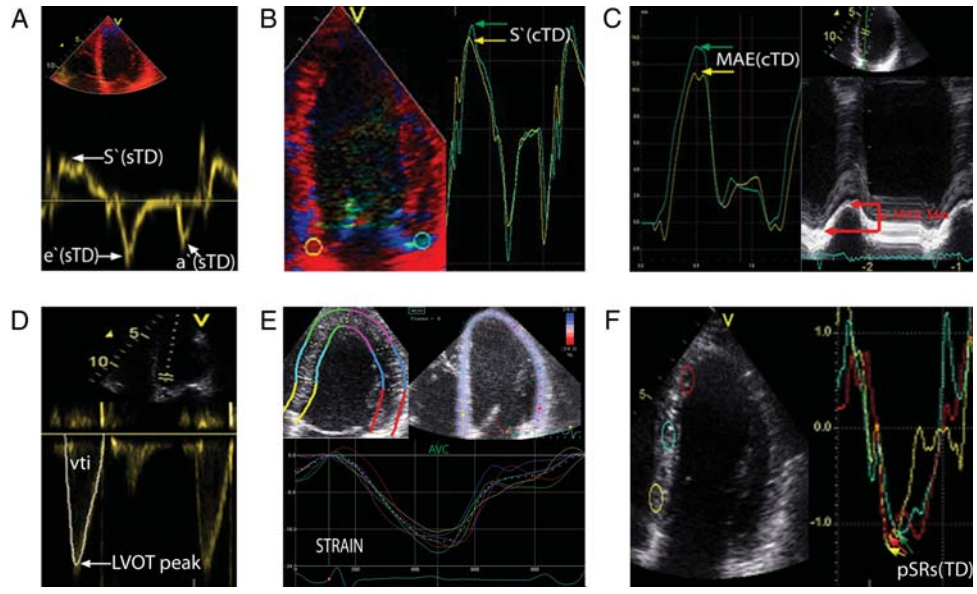

Figure 1 Representative measurements of left ventricular systolic performance obtained by different methods. (*A*) Spectral tissue Doppler (sTD)-derived septal mitral annulus velocities. Peak systolic velocity *S′*(sTD), early diastolic velocity [*e′*(sTD)], and late diastolic velocity *a′*(sTD) measured at the maximum of the Doppler spectrum with a low gain setting. (*B*) Velocity curves from colour tissue Doppler (cTD). Peak systolic mitral annulus velocity *S′*(cTD) measured at the peaks. (*C*) Measurements of systolic mitral annular excursion (MAE) by integrated velocity curves from colour tissue Doppler MAE (cTD) and by reconstructed M-mode MAE (Mm). (*D*) The left ventricular outflow tract (LVOT) peak velocity and velocity time integral (vti) measured by tracing the modal velocity. (*E*) Deformation indices obtained from two-dimensional speckle-tracking echocardiography with regions of interest and the corresponding traces of longitudinal strain. (*F*) Longitudinal peak systolic strain rate obtained from colour tissue Doppler recordings SR_S (TD).

stationary ROI with offset length 12 mm was manually positioned in the middle of the myocardium. The ROI was adjusted up to 10 mm longitudinally and 5 mm laterally in order to avoid noise. Peak systolic strain rate (SR_S) was measured as the maximal negative value during ejection time and reflected the average of three cardiac cycles.

Segmental longitudinal strain and SR_S (TD) were analysed in an 18-segment model of the LV, and global averages were calculated from the standard ASE 16-segment model.[5]

Statistics

Values are reported as mean and SD. Calculation of the relative change (the measured difference between rest and the different contractile states, divided by the measurement at rest) was done for all echocardiographic indices. For multiple comparisons, one-way ANOVA with *post hoc* Tukey's correction were used. The area under the receiver-operating characteristic (ROC) curve (AUC) for detection of different contractile states was also used for comparison of the methods. We also calculated the intervals given by mean $\pm$ 2SD for indices at rest and during the different contractile states and compared the percentage overlap relative to the mean at rest of these intervals.

Data reproducibility

Reproducibility was tested on a different population in relation to the HUNT study, and the results are published elsewhere.[6,7] The inter-observer mean error (the percentage difference between two experienced physician echocardiographers' measurements on separate recordings) was 7–10% for the peak systolic velocity indices and 4–14% for the end-systolic indices.

Table 1 Characteristics of the study population

Variable	Mean (SD)
Age (years)	25 (2.9)
Height (cm)	179 (6.5)
Weight (kg)	75 (12)
BMI (kg/m^2)	23 (3)
BSA (m^2)	1.9 (0.2)
LV mass (g)	180 (27)
LV volume (mL)	134 (27)

The parameters are displayed as mean (standard deviation). BMI, body mass index; BSA, body surface area; LV, left ventricular. LV mass and volume were obtained from real-time 3D echocardiography.

Results

Study population and feasibility

Table 1 shows the basic characteristics of the study population, and *Table 2* summarizes the haemodynamic response to low-dose dobutamine and metoprolol. All participants completed their pre-specified protocol. No participants had ST-segment changes, symptomatic blood pressure changes, or arrhythmias during any of the drug infusions. All subjects had synchronous LV activation assessed by visual assessment. Estimation of biplane 2D and 3D

Table 2 The haemodynamic response to dobutamine and metoprolol

	Rest ($n = 33$)	Dobutamine ($n = 20$)		Metoprolol					
				All metoprolol ($n = 20$)		Metoprolol after dobutamine ($n = 7$)		Only metoprolol ($n = 13$)	
	Mean (SD)	Mean (SD)	Mean change (%)	Mean (SD)	Mean change (%)	Mean (SD)	Mean change (%)	Mean (SD)	Mean change (%)
Heart rate (bpm)	61 (9)	67 (12)	13	51 (6)	−12	54 (5)	−9	49 (6)	−14
Systolic BP (mmHg)	118 (10)	135 (15)	14	98 (9)	−14	99 (10)	−16	98 (10)	−11
Diastolic BP (mmHg)	70 (9)	62 (9)	−9	55 (8)	−22	56 (7)	−18	55 (9)	−23

BP, blood pressure; SD, standard deviation.

Table 3 Systolic echocardiographic indices at rest and during dobutamine

	Mean (SD) at rest	Mean (SD) during stress	Mean change (95% CI)	Mean ± 2SD overlap rest vs. dobutamine (% overlap)	AUC (95% CI)
Peak systolic velocity indices					
S′(spectral TD)	9.4 (1.0) cm/s	15.1 (1.8) cm/s	62% (53–71)%	−0.10 cm/s (no overlap)	1.00 (1.00–1.00)
S′(colour TD)	7.6 (0.9) cm/s	11.5 (1.0) cm/s	52% (43–62)%	−0.06 cm/s (no overlap)	1.00 (1.00–1.00)
LVOT peak	1.0 (0.1) m/s	1.7 (0.2) m/s	60% (48–73)%	0.11 m/s (11%)	0.99 (0.99–1.00)
Global SRs (TD)	−1.2 (0.1) s^{-1}	−1.8 (0.1) s^{-1}	56% (50–61)%	0.2 s^{-1} (no overlap)	1.00 (1.00–1.00)
End-systolic indices					
Global strain (2D-ST)	−0.19 (0.02)	−0.23 (0.02)	21% (17–25)%	0.03 (18%)	0.95 (0.86–1.00)
LVOT vti	21 (4) cm	27 (4) cm	30% (20–40)%	8.6 cm (41%)	0.89 (0.79–1.00)
MAE (M-mode)	15 (2) mm	20 (2) mm	30% (25–36)%	2.8 (18%)	0.96 (0.91–1.00)
MAE (colour TD)	15 (2) mm	18 (2) mm	23% (17–29)%	3.4 mm (23%)	0.93 (0.85–1.00)
2D LVEF	0.57 (0.06)	0.70 (0.06)	25% (20–30)%	0.11 (21%)	0.95 (0.89–1.00)
3D LVEF	0.56 (0.04)	0.69 (0.04)	24% (21–27)%	0.03 (5%)	1.00 (1.00–1.00)
FS	0.32 (0.04)	0.42 (0.06)	31% (24–37)%	0.10 (32%)	0.89 (0.60–1.00)

AUC, area under the receiver-operating characteristic curve for detection of increased contraction; CI, confidence interval; FS, fractional shortening; LVEF, left ventricular ejection fraction; LVOT, left ventricular outflow tract; MAE, mitral annulus excursion; S′, mean peak systolic mitral annulus velocity; SD, standard deviation; SRs, peak systolic strain rate; ST, speckle tracking echocardiography; vti, velocity time integral; TD, tissue Doppler; 2D, two-dimensional; 3D, three-dimensional.

LVEF, mitral annulus velocity and -motion indices, and systolic flow indices were feasible in all recordings. Estimation of diastolic flow and TD indices and flow Doppler time intervals, presented in Supplementary data online, *Table S1*, were also feasible in all recordings. One thousand and eighty-four (83%) segments post-processed by 2D-ST and 1120 (85%) segments post-processed by the TD velocity gradient method were accepted for analysis. The rest of the segments were excluded because of reverberations, valvular interference, or tracking difficulties. The percentages of rejected segments were 14% at rest, 20% during dobutamine stress, and 15% after injection of metoprolol.

Systolic indices during low-dose dobutamine stress

Table 3 shows the mean (SD) at rest and during stress, and the effect of stress, for all the systolic indices of LV performance. All indices increased significantly (all $P < 0.001$) from rest to stress. The relative increase in the peak velocity indices ranged from 51 to 62%, and these changes were significantly higher (all $P < 0.05$) than the relative changes of all end-systolic indices which ranged from 21 to 31%. In the ROC analysis, the AUC was between 0.93 and 1.00 for all methods, and differences between peak velocity- and end-systolic indices were not significant. The range and the mean ± 2SD at rest and during stress overlapped for all indices except S′(spectral TD), S′(colour TD), and SR_S (TD) (*Table 3* and *Figure 2*).

Systolic indices after metoprolol

Table 4 shows the mean (SD) at rest and after injection of metoprolol for all systolic indices of LV performance. The absolute changes were significantly less pronounced (all $P < 0.001$) after injection of metoprolol compared with the change induced by

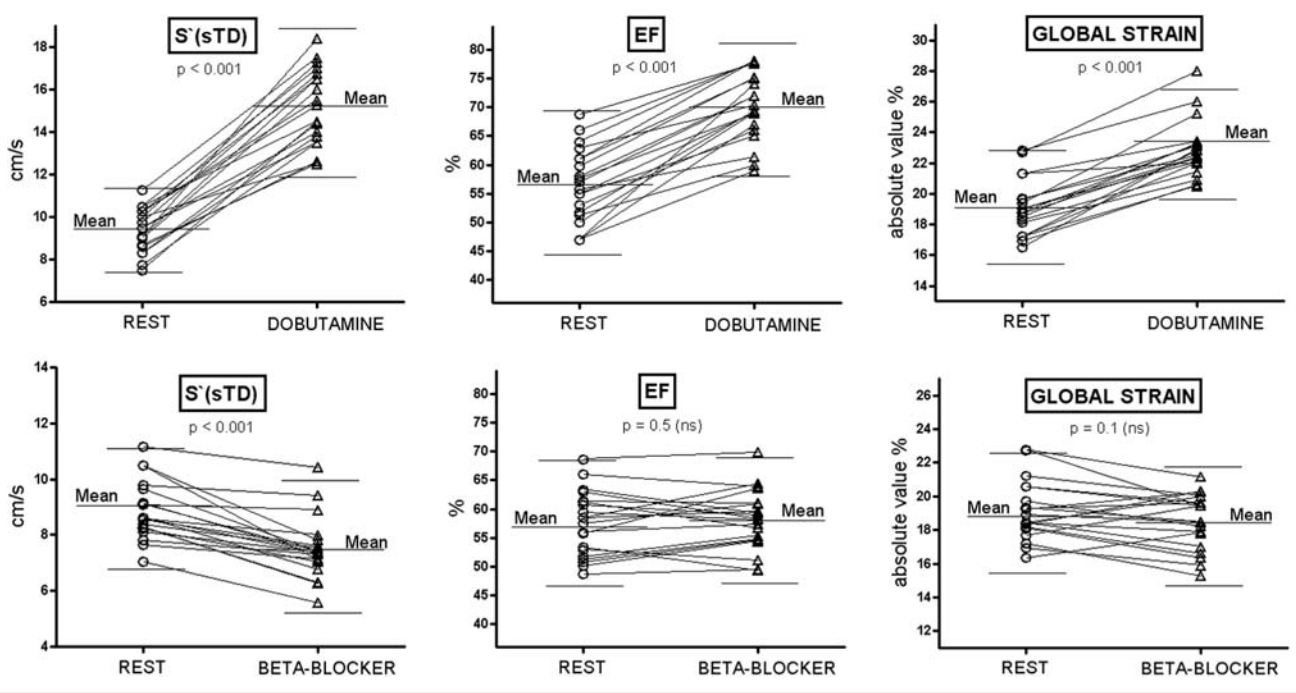

Figure 2 The response to dobutamine and β-blocker of peak systolic annulus velocity, ejection fraction, and global strain. Individual changes of peak systolic velocity spectral tissue Doppler mitral annulus velocities [*S′*(sTD)], ejection fraction (EF), and global strain at rest, during low-dose dobutamine (upper panels), and after injection of metoprolol (lower panels). The mean (wide line), the mean ± 2SD (narrow line), and the *P*-value of the change are displayed for each variable. The relative change during stress and after injection of metoprolol was highest for *S′*(sTD).

low-dose dobutamine. All indices decreased significantly after injection of metoprolol (all $P < 0.05$), except global strain, MAE (M-mode), and 2D LVEF. The relative changes of the peak velocity indices ranged from −15 to −11% and the relative changes of all end-systolic indices ranged from −5 to 1%. There was a trend for all peak systolic indices to have higher AUC for detection of decreased contraction compared with the end-systolic indices, and this was significant for SR_S (TD) compared with all end-systolic indices and for *S′*(spectral TD) compared with global strain, MAE (M-mode), and 2D LVEF. The range and the mean ± 2SD at rest and after injection of metoprolol overlapped for all indices.

Discussion

To our knowledge, this is the first study that directly compares the influence of contractility changes on LVEF, traditional Doppler indices, TD indices, and newer speckle-tracking-based indices in the same human data set. In this study, peak systolic velocity indices exhibited greater variation than end-systolic indices during inotropic alterations. We suggest from this that the peak systolic velocity indices better reflected LV contraction.

Study population and study design

We randomly selected a study population from a relatively homogenous sample of young and healthy subjects. The population was chosen in order to induce uniform alterations in contraction and avoid any pathological response to dobutamine or metoprolol. The main effect of dobutamine at low dose is increased inotropy without a profound effect on heart rate,[8] and it is thus well suited for studying changes in contraction. In line with previous studies, low-dose dobutamine increased the heart rate by 13%[9,10] and metoprolol reduced the heart rate by 12%. No invasive reference method was used, but dobutamine and metoprolol have well-documented positive and negative inotropic effects, and has previously been used to define inotropic states in several studies.[3,8,10,11] Low-dose dobutamine has previously induced >50% increase in the maximal first derivative of LV pressure (LV dP/dt_{max}) obtained by cardiac catheterization in different populations,[12–14] which is in the same range as the measured increase in peak systolic velocity indices during low-dose dobutamine in this study.

Peak systolic vs. end-systolic indices

The study shows a significantly different response to positive and negative inotropic stimulation between peak systolic velocity indices and end-systolic indices. This is supported by findings in several previous studies: inotropic alterations affected the peak velocity considerably more than the velocity time integral of LVOT and aortic blood velocity waveform in two studies.[8,15] In studies of patients with heart disease, *S′* had a better correlation to LV pressure development than LVEF, MAE, and LVOT vti.[16,17] *S′*

Table 4 Systolic echocardiographic indices at rest and after metoprolol

	Mean (SD) at rest	Mean (SD) after metoprolol	Mean change (95% CI)	Mean ± 2SD overlap rest vs. metoprolol (% overlap)	AUC (95% CI)
Peak systolic velocity indices					
S′(spectral TD)	8.9 (1.0) cm/s	7.5 (1.1) cm/s	−15% (−19 to −11)%	2.9 cm/s (33%)	0.85 (0.72–0.98)
S′(colour TD)	7.5 (1.0) cm/s	6.5 (0.7) cm/s	−13% (−16 to −10)%	2.3 cm/s (30%)	0.78 (0.63–0.92)
LVOT peak	1.0 (0.1) m/s	0.9 (0.1) m/s	−11% (−15 to −6)%	0.6 m/s (56%)	0.77 (0.62–0.92)
Global SRs (TD)	1.2 (0.1) s^{-1}	1.1 (0.1) s^{-1}	−11% (−14 to −8)%	0.2 s^{-1} (14%)	0.91 (0.83–1.0)
End-systolic indices					
Global strain (2D-ST)	−0.19 (0.02)	−0.19 (0.02)	−3% (−6 to 1)%	0.06 (33%)	0.53 (0.35–0.71)
LVOT vti	20 (3) cm	19 (3) cm	−5% (−10 to 0)%	11 cm 57%	0.62 (0.44–0.79)
MAE (M-mode)	16 (2) mm	16 (2) mm	−1% (−6 to 4)%	9 mm (56%)	0.53 (0.35–0.72)
MAE (colour TD)	15 (2) mm	14 (1) mm	−5% (−8 to −1)%	6 mm 42%	0.63 (0.44–0.81)
2D LVEF	0.57 (0.06)	0.58 (0.05)	+1% (−2 to 4)%	0.22 (39%)	0.48 (0.29–0.66)
3D LVEF	0.56 (0.04)	0.54 (0.04)	−4% (−7 to −2)%	0.10 (18%)	0.68 (0.52–0.85)
FS	0.32 (0.04)	0.32 (0.04)	−1% (−4 to 3)%	0.16 (51%)	0.54 (0.36–0.72

AUC, area under the receiver-operating characteristic curve for detection of decreased contraction; CI, confidence interval; FS, fractional shortening; LVEF, left ventricular ejection fraction; LVOT, left ventricular outflow tract; MAE, mitral annulus excursion; S′, mean peak systolic mitral annulus velocity; SD, standard deviation; SRs, peak systolic strain rate; ST, speckle tracking echocardiography; vti, velocity time integral; TD, tissue Doppler; 2D, two-dimensional; 3D, three-dimensional.

increased considerably more than LVEF, FS, and e′ during low-dose dobutamine in a study on healthy humans.[9]

S′, LVOT peak, and peak SR_S are almost simultaneous events in the heart cycle,[18] and their timing corresponds well to the timing of peak force development on a myocyte level, which occurs in the first part of systole.[19] End-systolic indices are much less dependent of the temporal component of deformation compared with peak systolic indices, and end-systolic indices are more related to stroke volume, i.e. the total amount of work performed by the ventricle during systole. This is influenced not only by contractility (force), but also by afterload, as well as the total time span of the work. Thus, end-systolic indices are more heart rate-sensitive than peak systolic indices, and the modest changes in heart rate induced by inotropic alterations in this study could partly explain the less pronounced changes of the end-systolic indices. However, according to other studies, such modest changes in heart rate have negligible influence on Doppler myocardial imaging parameters.[20,21] Furthermore, SR_S showed larger variation and better correlation to LV pressure development compared with end-systolic strain during inotropic alterations independent of heart rate in the study of atrial paced pigs.[3]

Clinical implications of our study

LVEF is a key functional and prognostic marker of LV function. However, LVEF overestimates the myocardial function in small hypertrophic hearts, has limited reproducibility, and is a poor indicator of the contractile properties of the myocardium.[1] The present and other studies[22–24] indicate that peak systolic velocity indices give important supplementary information to LVEF and global strain. In this study, peak systolic velocity indices were more sensitive in detecting contraction changes, and therefore, it may be suggested that peak systolic velocity indices are more sensitive to detect changes of cardiac function also in clinical practice. However, this has to be tested in a clinical setting. Compared with deformation imaging, indices of annular tissue velocities appear superior with respect to feasibility and time efficiency. Thus, the average peak systolic mitral annulus tissue velocity currently seems to be the preferred marker of contraction among frequently used echocardiographic methods in everyday clinical practice. As real-time 3D echocardiography with low frame rate is now available in clinical practice, it is important to keep in mind that peak systolic indices require higher frame rate than end-systolic indices.

Limitations

The subjects were fairly young and without heart disease, which probably gave a more homogenous response to inotropic alterations than would have been expected in a general population. It remains to be tested whether our results could be extrapolated to a more general population of patients with heart disease or whether our results are useful for predicting outcomes during longer-term follow-up in patients with heart disease. In addition, the present study addresses only global indices, and regional indices may perform better in conditions with regional dysfunction. In seven subjects, recordings under the influence of metoprolol were obtained after infusion of dobutamine. Although metoprolol was given at least 20 min after dobutamine was discontinued, there was a trend ($P = 0.10$) for a smaller decrease in heart rate among these seven subjects. However, the effect of metoprolol on any of the echocardiographic indices did not differ significantly (all $P > 0.12$) in these 7 subjects compared with the 13 subjects who did not receive dobutamine before metoprolol. Parameters of twist and torsion were not available in the present study. Only longitudinal, not circumferential or radial, strain and SRs were calculated. LVEF was obtained from echocardiography only and not from other imaging modalities such as magnetic resonance imaging or

nuclear imaging. The subjects were not examined during changes in loading conditions.

Conclusion

Peak systolic velocity indices (peak systolic mitral annulus tissue velocities, ejection velocities, and peak systolic strain rate) exhibited greater variation than end-systolic indices during inotropic alterations from which it is assumed that they better reflected LV contraction. Considering feasibility and time efficiency, peak systolic annulus tissue velocity seems to be the preferred marker of contraction among frequently used echocardiographic methods.

Supplementary data

Supplementary data are available at *European Journal of Echocardiography* online.

Conflict of interest: none declared.

Funding

The study has been supported by a grant from the Norwegian Research Council, through the centre for research-based innovation, MI Lab.

References

1. Bijnens BH, Cikes M, Claus P, Sutherland GR. Velocity and deformation imaging for the assessment of myocardial dysfunction. *Eur J Echocardiogr* 2009;**10**:216–26.
2. Marwick TH. Measurement of strain and strain rate by echocardiography: ready for prime time? *J Am Coll Cardiol* 2006;**47**:1313–27.
3. Weidemann F, Jamal F, Sutherland GR, Claus P, Kowalski M, Hatle L *et al.* Myocardial function defined by strain rate and strain during alterations in inotropic states and heart rate. *Am J Physiol Heart Circ Physiol* 2002;**283**:H792–9.
4. Nagueh SF, Appleton CP, Gillebert TC, Marino PN, Oh JK, Smiseth OA *et al.* Recommendations for the evaluation of left ventricular diastolic function by echocardiography. *J Am Soc Echocardiogr* 2009;**22**:107–33.
5. Lang RM, Bierig M, Devereux RB, Flachskampf FA, Foster E, Pellikka PA *et al.* Recommendations for chamber quantification: a report from the American Society of Echocardiography's Guidelines and Standards Committee and the Chamber Quantification Writing Group, developed in conjunction with the European Association of Echocardiography, a branch of the European Society of Cardiology. *J Am Soc Echocardiogr* 2005;**18**:1440–63.
6. Thorstensen A, Dalen H, Amundsen BH, Aase SA, Stoylen A. Reproducibility in echocardiographic assessment of the left ventricular global and regional function, the HUNT study. *Eur J Echocardiogr* 2010;**11**:149–56.
7. Dalen H, Thorstensen A, Romundstad PR, Aase SA, Stoylen A, Vatten LJ. Cardiovascular risk factors and systolic and diastolic cardiac function: a tissue doppler and speckle tracking echocardiographic study. *J Am Soc Echocardiogr* 2011;**24**:322–32.e6.
8. Singer M, Allen MJ, Webb AR, Bennett ED. Effects of alterations in left ventricular filling, contractility, and systemic vascular resistance on the ascending aortic blood velocity waveform of normal subjects. *Crit Care Med* 1991;**19**:1138–45.
9. Gorcsan J 3rd, Deswal A, Mankad S, Mandarino WA, Mahler CM, Yamazaki N *et al.* Quantification of the myocardial response to low-dose dobutamine using tissue Doppler echocardiographic measures of velocity and velocity gradient. *Am J Cardiol* 1998;**81**:615–23.
10. Greenberg NL, Firstenberg MS, Castro PL, Main M, Travaglini A, Odabashian JA *et al.* Doppler-derived myocardial systolic strain rate is a strong index of left ventricular contractility. *Circulation* 2002;**105**:99–105.
11. Vogel M, Cheung MM, Li J, Kristiansen SB, Schmidt MR, White PA *et al.* Noninvasive assessment of left ventricular force-frequency relationships using tissue Doppler-derived isovolumic acceleration: validation in an animal model. *Circulation* 2003;**107**:1647–52.
12. Kobayashi M, Izawa H, Cheng XW, Asano H, Hirashiki A, Unno K *et al.* Dobutamine stress testing as a diagnostic tool for evaluation of myocardial contractile reserve in asymptomatic or mildly symptomatic patients with dilated cardiomyopathy. *JACC Cardiovasc Imaging* 2008;**1**:718–26.
13. Lenihan DJ, Gerson MC, Dorn GW 2nd, Hoit BD, Walsh RA. Effects of changes in atrioventricular gradient and contractility on left ventricular filling in human diastolic cardiac dysfunction. *Am Heart J* 1996;**132**:1179–88.
14. Mak S, Newton GE. Vitamin C augments the inotropic response to dobutamine in humans with normal left ventricular function. *Circulation* 2001;**103**:826–30.
15. Bauer F, Jones M, Shiota T, Firstenberg MS, Qin JX, Tsujino H *et al.* Left ventricular outflow tract mean systolic acceleration as a surrogate for the slope of the left ventricular end-systolic pressure–volume relationship. *J Am Coll Cardiol* 2002;**40**:1320–7.
16. Lindqvist P, Waldenstrom A, Wikstrom G, Kazzam E. Potential use of isovolumic contraction velocity in assessment of left ventricular contractility in man: a simultaneous pulsed Doppler tissue imaging and cardiac catheterization study. *Eur J Echocardiogr* 2007;**8**:252–8.
17. Bach DS. Quantitative Doppler tissue imaging as a correlate of left ventricular contractility. *Int J Card Imaging* 1996;**12**:191–5.
18. Marsan NA, Tops LF, Westenberg JJ, Delgado V, de Roos A, van der Wall EE *et al.* Usefulness of multimodality imaging for detecting differences in temporal occurrence of left ventricular systolic mechanical events in healthy young adults. *Am J Cardiol* 2009;**104**:440–6.
19. Chirinos JA, Segers P, Gupta AK, Swillens A, Rietzschel ER, De Buyzere ML *et al.* Time-varying myocardial stress and systolic pressure–stress relationship: role in myocardial–arterial coupling in hypertension. *Circulation* 2009;**119**:2798–807.
20. Boettler P, Hartmann M, Watzl K, Maroula E, Schulte-Moenting J, Knirsch W *et al.* Heart rate effects on strain and strain rate in healthy children. *J Am Soc Echocardiogr* 2005;**18**:1121–30.
21. Weytjens C, D'Hooge J, Droogmans S, Van den Bergh A, Cosyns B, Lahoutte T *et al.* Influence of heart rate reduction on Doppler myocardial imaging parameters in a small animal model. *Ultrasound Med Biol* 2009;**35**:30–5.
22. Mogelvang R, Sogaard P, Pedersen SA, Olsen NT, Marott JL, Schnohr P *et al.* Cardiac dysfunction assessed by echocardiographic tissue Doppler imaging is an independent predictor of mortality in the general population. *Circulation* 2009;**119**:2679–85.
23. Yu CM, Sanderson JE, Marwick TH, Oh JK. Tissue Doppler imaging a new prognosticator for cardiovascular diseases. *J Am Coll Cardiol* 2007;**49**:1903–14.
24. Yip G, Wang M, Zhang Y, Fung JW, Ho PY, Sanderson JE. Left ventricular long axis function in diastolic heart failure is reduced in both diastole and systole: time for a redefinition? *Heart* 2002;**87**:121–5.

European Heart Journal - Cardiovascular Imaging Advance Access published April 12, 2012

European Heart Journal – Cardiovascular Imaging
doi:10.1093/ehjci/jes070

Strain rate imaging combined with wall motion analysis gives incremental value in direct quantification of myocardial infarct size

Anders Thorstensen[1,2]*, Brage Høyem Amundsen[1,2], Håvard Dalen[1,3], Pavel Hala[4], Gabriel Kiss[1], Svein Arne Aase[1], Hans Torp[1], and Asbjørn Støylen[1,2]

[1]MI Lab and Department of Circulation and Medical Imaging, Norwegian University of Science and Technology, MTFS, Postboks 8905, NO-7491, Trondheim, Norway; [2]Department of Cardiology, St Olavs Hospital/Trondheim University Hospital, Trondheim, Norway; [3]Department of Medicine, Levanger Hospital, Nord-Trøndelag Health Trust, Levanger, Norway; and [4]Homolka Hospital, Prague, Czech Republic

Received 6 January 2012; accepted after revision 13 March 2012

Background The study aimed to evaluate the diagnostic accuracy of a new method for direct echocardiographic quantification of the myocardial infarct size, using late enhancement magnetic resonance imaging (LE-MRI) as a reference method.

Methods and results Echocardiography and LE-MRI were performed on average 31 days after first-time myocardial infarction in 58 patients. Echocardiography was also performed on 35 healthy controls. Direct echocardiographic quantification of the infarct size was based on automated selection and quantification of areas with hypokinesia and akinesia from colour-coded strain rate data, with manual correction based on visual wall motion analysis. The left ventricular (LV) ejection fraction, speckle-tracking-based longitudinal global strain, wall motion score index (WMSI), longitudinal systolic motion and velocity, and the ratio of early mitral inflow velocity to mitral annular early diastolic velocity were also measured by echocardiography. The area under the receiver-operating characteristic curves for the identification of the infarct size >12% by LE-MRI was 0.84, using the new method for direct echocardiographic quantification of the infarct size. The new method showed significantly a higher correlation with the infarct size by LE-MRI both at the global ($r = 0.81$) and segmental ($r = 0.59$) level compared with other indices of LV function.

Conclusion Direct quantification of the percentage infarct size by strain rate imaging combined with wall motion analysis yields high diagnostic accuracy and better correlation to LE-MRI compared with other echocardiographic indices of global LV function. Echocardiography performed ~1 month after myocardial infarction showed ability to identify the patients with the infarct size >12%.

Keywords Late gadolinium enhancement • Myocardial infarction • Speckle tracking • Strain rate • Tissue Doppler • Area measurement

Introduction

The infarct size assessed by late enhancement magnetic resonance imaging (LE-MRI) is a powerful predictor of the outcome after myocardial infarction (MI),[1–3] but LE-MRI is less available than echocardiography in most clinical settings. Echocardiography has been extensively validated in patients with MI, but most echocardiographic methods are measurements of global left ventricular (LV) function, where the degree of reduced function may serve as an indirect estimate of the infarct size. The global end-systolic longitudinal strain (GLS) by speckle tracking as well as the wall motion score index (WMSI) has demonstrated ability to differentiate between smaller and larger MIs and to predict the transmurality of the scar burden.[4–7] Other studies have indicated independent incremental prognostic and diagnostic information when the tissue Doppler (TD)-based systolic strain rate (SR) is combined with the WMSI.[8,9] The colour TD-based SR displayed as the semi-quantitative-curved motion mode (M-mode) or bull's eye view allows quick visual identification of MI, and artefacts are often easier to detect with these techniques compared with

* Corresponding author. Tel: +47 72 82 85 46, +47 97 69 07 31, Fax: +47 72 82 83 72, Email: anders.thorstensen@ntnu.no

trace analyses.[10,11] In this study, we present a new method for direct quantification of the infarct size based on area measurement by TD-based colour-coded SR data corrected by visual wall motion analysis (WMA), and we aimed to test whether this approach gives higher diagnostic accuracy compared with other echocardiographic techniques, using LE-MRI as a reference method.

Methods

Study population and study design

The study was conducted in a single-tertiary coronary care centre. Seventy-one consecutive patients with documented first-time non-ST-segment-elevation myocardial infarction (NSTEMI) or ST-segment-elevation myocardial infarction (STEMI) and peak cardiac troponin T measurement >0.5 μg/L were prospectively enrolled from April 2008 to June 2009. Exclusion criteria were prior MI, bundle-branch block with QRS duration >130 ms, significant valvular disease, previous heart surgery, age >75 years, extensive co-morbidity with short life expectancy, chronic atrial fibrillation, and contraindications to MRI. No patients were excluded because of impaired echocardiographic image quality. Written informed consent was obtained. Patients were examined with LE-MRI and echocardiography on the same day in average 31 ± 11 days the index MI. Five patients were excluded because they were not able to complete the LE-MRI examinations due to claustrophobia. Another eight patients were excluded due to sub-optimal LE-MRI image quality. Thus the final patient population was 58.

The control group consisted of 35 age- and sex-matched participants in the Echocardiography in the Nord-Trøndelag Health Survey (HUNT) who were free from known cardiovascular disease, diabetes, and hypertension.[12] Validation of the normality of the control group was performed by the physician echocardiographer (H.D.) and based on self-filled questionnaires, careful medical history, and examinations. The control group was not examined by LE-MRI and their infarction size was assumed to be 0%. Of the final 58 patients with full LE-MRI, 46 (79%) had STEMI, whereas 12 (21%) had NSTEMI. Coronary angiography identified a coronary culprit lesion in all patients. Percutaneous coronary intervention (PCI) of the culprit coronary lesion was performed during the hospital stay in all patients except three patients in whom the defined culprit lesion was not amenable to PCI. The median time from the onset of symptoms to PCI was 3.0 h (range 0.6–140 h). The study was approved by the Regional Committee for Medical Research Ethics, and conducted according to the second Helsinki Declaration.

Echocardiographic image acquisition

One operator (A.T.) performed all the analyses, and two operators (A.T. and H.D.) performed all echocardiographic examinations (A.T.; the MI group and H.D.; the control group). A Vivid 7 (80%) or a Vivid E9 (20%) scanner (GE Vingmed, Horten, Norway) with a phased array transducer (M3S) was used. For each two-dimensional (2D) view, three consecutive cardiac cycles were recorded during quiet respiration. From the three apical views (four chamber, two chamber, and long axis), separate B-mode acquisitions (mean frame rate 61 ± 15 s^{-1}), and colour TD acquisitions (mean frame rate 123 ± 24 s^{-1}) were recorded, and from the parasternal view, three short-axis planes (mitral, papillary and apex) were recorded in B-mode. Loops were digitally stored and later analysed off-line using EchoPAC version BT11 (GE Vingmed Ultrasound, Horten, Norway). Pulsed wave Doppler mitral flow velocities were recorded from the apical four-chamber view with the sample volume between the leaflet tips. Spectral TD mitral annular velocities were acquired with a 6 mm sample volume positioned at the base of the septal, lateral, inferior, and anterior walls.

Quantification of the infarct size by SR and WMA (the new method)

Longitudinal SR was obtained from colour TD recordings by calculating the velocity gradient. The cine loops were post-processed by in-house software (GC lab, ELVIZ). The regions of interest (ROIs) were tracked with TD along the ultrasound beam and grey-scale speckles perpendicular to the ultrasound beam, and the velocity gradient was sampled along curved M-modes drawn along the LV walls. SR data in the areas between the three standard planes were applied by cubic spline interpolation, assuming 60° rotation angle between the three apical planes and displayed as semi-quantitative colour-coded SR in a conventional bull's eye view, as comprehensively described previously.[11] The mid-systolic frame was selected for the analysis, and on the sub segmental level, areas with SR < −0.5 s^{-1} were automatically marked as normal, areas with SR −0.5 to −0.25 s^{-1} were automatically marked as hypokinesia, and areas with SR > −0.25 s^{-1} were automatically marked as akinesia.[11,13] SR data in the apical one-fourth of the apical segments were automatically discarded. Based on combined judgement of the colour-coded SR data and WMA in the grey-scale recordings, the areas with marked hypokinesia and akinesia were manually corrected, but in the apical one-fourth of the apical segments or in case of obvious artefacts in the SR analysis, the judgement of LV function was based on WMA in grey-scale recordings only. The areas of all the sub segments with hypokinesia and akinesia were divided by the total myocardial area and the total segmental area for estimation of global and segmental area fractions of hypokinesia and akinesia (*Figure 1*). Based on the previously reported relationship between the infarct size and the WMSI,[6] the transmurality of the hypokinetic and akinetic areas were defined as 50 and 100%, respectively. Thus, the described area-based method gives a direct estimate of the infarct size by echocardiography which can be directly compared with the infarct volume fraction given by LE-MRI.

Other echocardiographic methods

The wall motion score (WMS) was assessed in a 16-segment model.[14] Segmental wall motion was judged as normal, 1; hypokinetic, 2; akinetic, 3; and dyskinetic, 4. WMSI represents the average value of analysed segments.

The longitudinal end-systolic strain was obtained by speckle tracking in grey-scale recordings by 2D speckle-tracking echocardiography (2D-ST) (automated function imaging; EchoPAC PC version BT 11, GE Vingmed, Horten, Norway). The ROIs were manually adjusted to include the entire LV myocardium and simultaneously avoid the pericardium. Location of end-systole was manually corrected if necessary. The GLS was calculated by averaging at least 12 accepted end-systolic strain values in the standard ASE 16 segment mode.[14]

LV volumes and LV ejection fraction (LVEF) were measured by biplane Simpson's method from the apical four- and two-chamber views. End-diastolic volume was measured at the time of mitral valve closure, and end-systolic volume was measured on the image with the smallest LV cavity.

From the spectral TD recordings, peak systolic (*S′*) and peak early (*e′*) diastolic mitral annular velocities were measured at the peak of the Doppler spectrum with a low gain setting. Systolic mitral annular excursion (MAE), measured by anatomical M-mode echocardiography

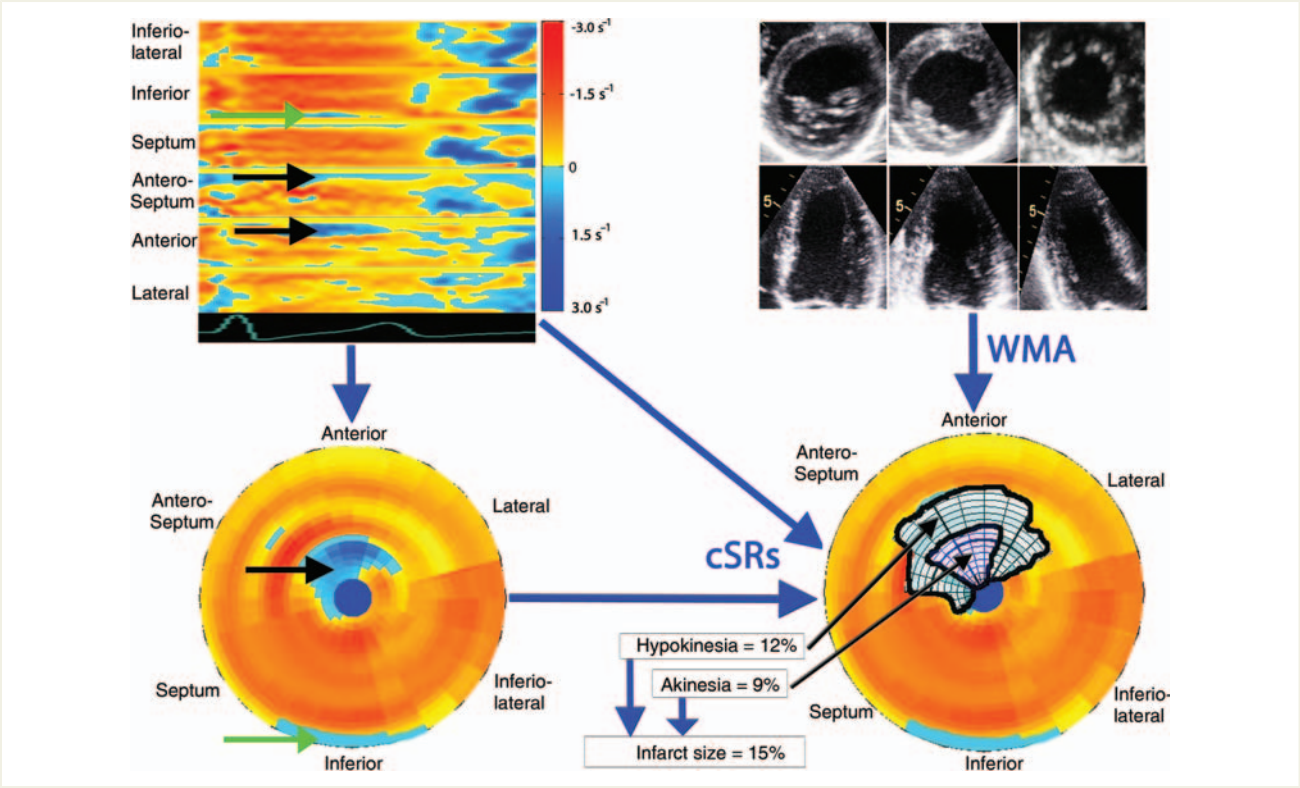

Figure 1 Composite figure displaying the direct quantification of the infarct size by cSR combined with WMA. Upper left: curved anatomic motion mode of cSR during systole and early diastole. Lower left: bull's eye view of cSR during mid-systole. Arrows are indicating areas of suspected artefact and akinesia. Upper right: Three short-axis views and three apical views of the left ventricle in B-mode recordings indicating WMA. Lower right: Based on combined judgement of cSR and WMA, areas of hypokinesia and akinesia are marked and displayed as percentages of the total left ventricle area. Infarct size estimated assuming 50% infarct volume fraction in the hypokinetic areas and 100% infarct volume fraction in the akinetic areas. cSR, tissue Doppler-based colour-coded systolic strain rate data; WMA, wall motion analysis.

from the apical position, and the length of the LV measured as the end-diastolic distance from the epicardial apex to the mitral annulus, were obtained from the septal, lateral, inferior, and anterior site. Measurements from the four sites were averaged for S', e', MAE and LV length. S' corrected for the left ventricle length (S'/LV length) and the fractional shortening of the myocardium in long axis (FS_L) were calculated by dividing S' and MAE by the end-diastolic length of the left ventricle.

Magnetic resonance imaging

Examinations were performed on a 1.5 T Siemens Avanto (Siemens Medical, Erlangen, Germany) with a six-element body matrix coil. Late-enhancement (LE) images were obtained 10–20 min after i.v. injection of 0.15 mmol/kg gadodiamide (Omniscan, GE Healthcare, Oslo, Norway) in multiple short-axis slices covering the LV. A balanced steady-state-free precision inversion recovery sequence was used, with ECG-triggered data acquisition in mid-diastole. Typical image parameters were: matrix 176 × 256, in-plane resolution 1.3 × 1.3 mm, slice thickness 8 mm; inter slice gap 2 mm; flip angle 45°; and inversion time 280–350 ms. Images were acquired during end-expiratory breath hold. The LE-MRI analyses were performed by two operators (P.H. and B.H.A.), using Segment v1.7.[15] On each short-axis image, the total myocardial area as well as the area of infarcted myocardium was semi-automatically drawn. Areas with signal intensity >2 SD above normal myocardium in the same slice were considered infarcted. The infarct size was calculated as infarct volume in percentage of total myocardial volume. As short- and long-term mortality rates have been demonstrated to be increased in patients with the infarct size >12%,[1,16] patients were divided in small and large MIs using 12% as cut-off. Segments with percentage infarct volume fraction >50% were classified as transmurally infracted.[17,18]

All echocardiographic and LE-MRI analyses were performed separately and blinded to other analyses and participant's data. For the echocardiographic analyses, the patients and healthy controls were re-named, mixed, and analysed in random order.

Statistical analyses

Continuous variables are presented as mean ± SD. Categorical variables are presented as numbers (%). Differences between small and large MIs and the healthy controls were analysed by independent samples t-test. The relationship between the infarct size assessed by LE-MRI and each global echocardiographic index was analysed by bivariate correlation based on normal distribution among the final 58 patients. Pearson's correlation coefficient (r) is reported. For the segmental indices, the relationship between each echocardiographic index and the segmental percentage infarct volume fraction assessed by LE-MRI was analysed by bivariate rank correlations and reported as Spearman's correlation coefficient (r). The method described by Meng *et al.*[19] was used to compare the correlation coefficients.[19] The area under the receiver-operating characteristic curves (AUC) for the identification of small and large MIs is reported. Cut-off values that gave the largest sum of sensitivity and specificity are reported. Comparison between AUC for the different methods was

Table 1 Patient characteristics, risk factors, angiographic findings, and medications

	Large MIs (n = 25)	Small MIs (n = 33)	Healthy controls (n = 35)
LE-MRI infarct size (infarct volume fraction)	19.5 ± 5.7%*	5.3 ± 3.2%	Not available
Age, years	56.7 ± 13.6	54.9 ± 12.9	56.9 ± 13.0
BMI, kg/m^2	26.1 ± 6.0	25.4 ± 5.4	26.1 ± 5.2
Male sex, n (%)	19 (76)	25 (76)	28 (80)
Heart rate, bpm	64 (11)	60 (11)*	67 (11)
Current smoker, n (%)	12 (48)	17 (52)	—
Creatinine, μmol/L	68.5 ± 7.1***	70.5 ± 17.2*	88.0 ± 19.1
Peak troponin T, μg/L	7.7 ± 5.7*	3.2 ± 2.4	Not available
Hypertension, n (%)	5 (20)	5 (15)	—
Diabetes mellitus, n (%)	4 (16)	2 (6)	—
STEMI, n (%)	22 (88)	24 (73)	—
Single vessel disease, n (%)	14 (56)	25 (76)	Not available
LAD culprit, n (%)	10 (40)	13 (39)	—
CX culprit, n (%)	7 (28)	6 (18)	—
RCA culprit, n (%)	8 (32)	14 (42)	—
Aspirin, n (%)	25 (100)	33 (100)	—
Clopidogrel, n (%)	25 (100)	33 (100)	—
Beta-blocker, n (%)	23 (92)	29 (88)	—
Statin, n (%)	25 (100)	33 (100)	—
ACEi or ARB, n (%)	7 (28)	8 (24)	—

ACEi, angiotensin-converting enzyme inhibitors; ARB, angiotensin II receptor blockers; bpm, beats per minute; BMI, body mass index; LE-MRI, late enhancement magnetic resonance imaging; CX, circumflex artery; LAD, left anterior descending artery; MI, myocardial infarction; RCA, right coronary artery; STEMI, ST-segment-elevation myocardial infarction. Continuous variables displayed as mean ± SD. Categorical variables are displayed as numbers (percentage).
*$P < 0.001$ for large MIs vs. small MIs.
**$P < 0.05$ for small MIs vs. healthy controls.
***$P < 0.001$ for large MIs vs. healthy controls.

performed according to the method described by Hanley and McNeil.[20] The reproducibility, expressed by the coefficient of repeatability was calculated as 2 × SD of the differences in repeated measurements. All statistical analyses were performed on SPSS version 17 (SPSS, Inc, Chicago, IL, USA).

Results

Study population and feasibility

Patient characteristics are listed in *Table 1*. Direct quantification of infarct size by SR and WMA (the new method), estimation of WMSI, biplane LVEF, and mitral annulus velocity and -displacement were feasible in all the subjects. The feasibility of GLS was 95% (>12 segments accepted for analysis in 88/93 subjects). The calculation of the WMSI and the GLS was based on 1455 (98%) and 1288 (87%) segments, respectively. Segments were excluded because of drop outs, reverberations, valvular interference, or tracking difficulties.

Infarct size by LE-MRI

Evidence of MI by LE was detected in all patients. The mean (SD) infarct size was 11.4 (8.1)% of the total LV myocardial volume (*Figure 2*). Thirty-three patients (57%) had calculated the infarct size <12% and 25 patients (43%) had calculated the infarct size >12%. Evidence of infarction by LE was detected in 387 (42%) segments with transmural extension (>50% LE) in 74 (8%) segments.

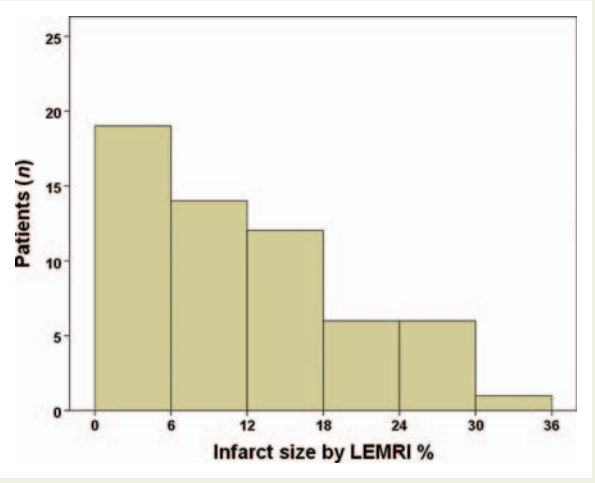

Figure 2 Histogram demonstrating the distribution of the infarct size by LE-MRI. LE-MRI, late enhancement magnetic resonance imaging.

Table 2 Echocardiographic findings of the controls and the patients by the infarct size

	Large MIs ($n = 25$)	Small MIs ($n = 33$)	Healthy controls ($n = 35$)
Infarct size by the new method	13.2 ± 10.1%*	2.7% ± 3.5%‡	0.2% ± 0.9%
WMSI	1.33 ± 0.26*	1.09 ± 0.11***	1.01 ± 0.02
GLS	−15.5 ± 3.0%*	−18.5 ± 2.1%	−19.3 ± 2.2%
FS_L	11.5 ± 2.1%*	13.7 ± 1.6%	14.1 ± 1.9%
LVEF	49.2 ± 5.7%*	55.9 ± 6.2%	58.1 ± 5.9%
S′/LV length	0.71 ± 0.15 s^{-1}**	0.80 ± 0.11 s^{-1}	0.80 ± 0.16 s^{-1}
E/*e′*	10.0 ± 2.2**	8.5 ± 2.2	7.5 ± 2.2

E, peak early diastolic mitral inflow velocity; *e′*, mean peak early diastolic mitral annular velocity; FS_L, fractional shortening of the long axis; GLS, global end-systolic longitudinal strain; LV, left ventricular; LVEF, left ventricular ejection fraction; MI, myocardial infarction; *S′*, peak systolic mitral annular velocity; new method, combined judgement of colour-coded strain rate data and wall motion analysis; SD, standard deviation; WMSI, wall motion score index.
Mean ± SD of different echocardiographic findings of the healthy controls and the patients by infarct size are shown.
*$P < 0.001$ for large MIs vs. small MIs and large MIs vs. healthy controls.
**$P < 0.05$ for large MIs vs. small MIs and large MIs vs. healthy controls.
***$P < 0.001$ for small MIs vs. healthy controls.

Echocardiography and infarct size

There were significant differences between the patients with large MIs compared with those with small MIs or healthy controls for all the indices (*Table 2*). Patients with small MIs also had a significantly larger infarct size by the new method and the WMSI compared with the healthy controls ($P < 0.001$).

There were significant correlations between the global infarct size assessed by LE-MRI and all the echocardiographic indices of LV global function: $r = 0.81$ for the infarct size by the new method, 0.74 for WMSI, 0.67 for GLS, 0.61 for FS_L, 0.55 for LVEF, 0.44 for *S′*/LV length, and 0.41 for *E*/*e′* (*Figure 3*). The correlation coefficient of the new method was significantly higher ($P < 0.05$) than all the other echocardiographic indices. There was a strong correlation between the new method and the WMSI ($r = 0.85$). The GLS was most closely correlated to FS_L ($r = 0.64$).

The new method also demonstrated the highest AUC for separation of small vs. large MIs, large MIs vs. healthy controls, and small MIs vs. healthy controls, but the differences between methods were not statistically significant for most of the comparisons (*Table 3*). A cut-off value of 7.0%, by the new method, had a sensitivity of 72% and a specificity of 88% for separating small and large MIs. WMSI of 1.14 and GLS of −16.6% had a sensitivity of 72 and 68% and a specificity of 75 and 85%, respectively, to separate small and large MIs. Of the 19 patients with LE-MRI infarct size <6%, hypokinetic or akinetic areas were only identified in six patients (32%) by the infarct size by the new method and in five patients (26%) by WMSI. For the group of 58 MI patients, the infarct size by the new method underestimated the infarct size by 4.2% (95% limits of agreement −14.3 to 5.9%) compared with LE-MRI (*Figure 4*).

Segmental indices and identification of transmurality

The correlations of the segmental indices with segmental infarct volume fractions assessed by LE-MRI were: $r = 0.59$ for SR and WMA (the new method), $r = 0.53$ for WMS, and $r = 0.48$ for segmental longitudinal strain by speckle tracking (all $P < 0.01$). The correlation of the new method with LE-MRI was significantly higher compared with WMS and segmental longitudinal strain (all $P < 0.02$). The echocardiographic indices showed generally excellent ability to identify transmurally infarcted segments with >50% contrast enhancement by LE-MRI. Segmental infarct fraction >36% by the new method had a sensitivity of 85% and a specificity of 95% for the identification of transmurally infarcted segments, while WMS >1 and segmental longitudinal strain > −14.1% had a sensitivity of 79 and 82%, and a specificity of 93 and 82%, respectively, for the identification of transmurally infarcted segments.

Data reproducibility

One of the co-authors reanalysed 20 randomly selected recordings to assess the reproducibility of the infarct size by the new method, the WMSI, and the GLS. In addition, comprehensive reproducibility data are recently published.[21] Coefficient of repeatability was 9.7% for the infarct size by the new method, 0.19 for WMSI, 2.2% for GLS, 1.7% for FS_L, 8.2% for LVEF, 0.08 s^{-1} for *S′*/LV length, and 1.1 for *E*/*e′*.

Discussion

This study is, to our knowledge, the first to validate an echocardiographic method for direct quantification of the infarct size. The new method yields high diagnostic accuracy and better correlation to LE-MRI compared with the WMSI, GLS, FS_L, LVEF, *S′*/LV length, and *E*/*e′*.

The WMSI also measures the extent of infarction in terms of the number of segments affected and the degree of segmental functional impairment. However, these measurements are only semi-quantitative. All the other methods used in our study are measurements of the global LV function, where the degree of reduced function only may serve as an indirect estimate of the infarct size. The GLS, FS_L, LVEF, *S′*/LV length, and *E*/*e* may yield measurements that are in the border zone between normal and decreased LV function, whereas the new method and the WMSI dichotomize each

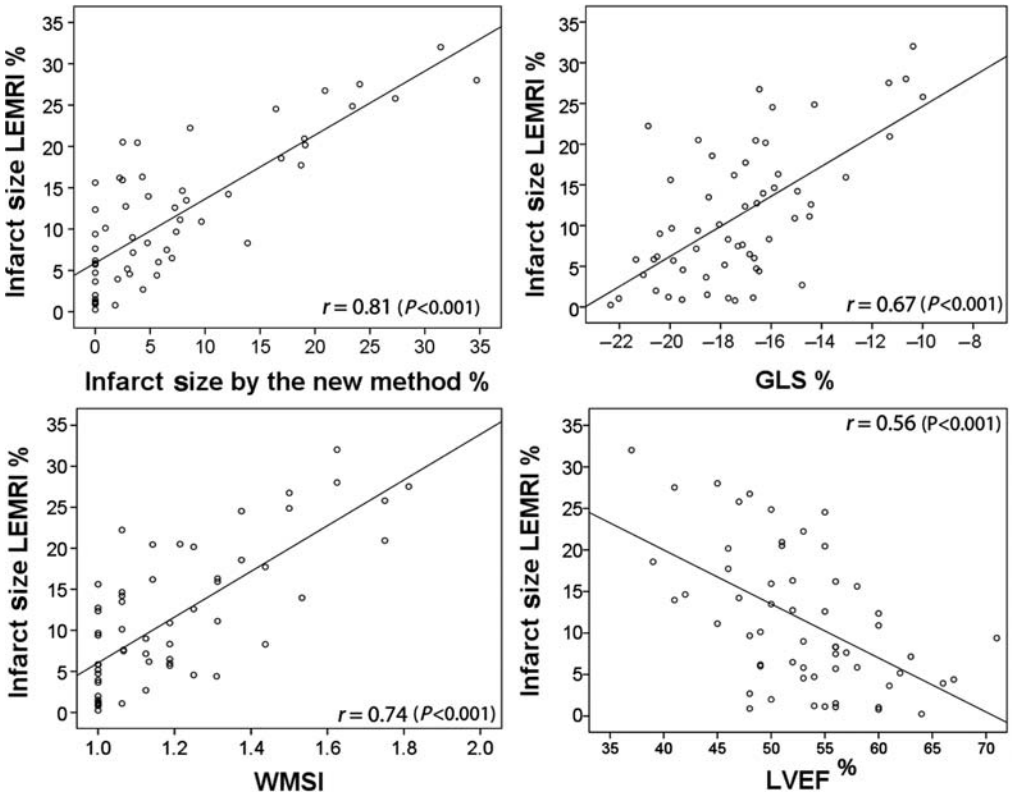

Figure 3 Scatter plots with regression line of the infarct size by LE-MRI and global echocardiographic indices of LV function. The infarct size by the new method was based on combined judgement of the colour-coded stain rate data and wall motion analysis. Pearson's correlation coefficients (*r*) are reported in the figure. GLS, global end-systolic longitudinal strain; LE-MRI, contrast enhanced magnetic resonance imaging; LV, left ventricular; WMSI, wall motion score index.

Table 3 AUC of the different echocardiographic indices

	AUC (95% CI) for separation of large MIs and healthy controls	AUC (95% CI) for separation of large and small MIs	AUC (95% CI) for separation of small MIs and healthy controls
Infarct size by the new method	0.95[a] (0.90–1.00)	0.84[b] (0.73–0.94)	0.73[c] (0.60–0.85)
WMSI	0.92[d] (0.84–1.00)	0.79 (0.67–0.91)	0.73[c] (0.60–0.85)
GLS	0.87[b] (0.77–0.96)	0.80 (0.68–0.92)	0.62 (0.49–0.75)
FS_L	0.82[e] (0.71–0.92)	0.78 (0.65–0.91)	0.54 (0.39–0.67)
LVEF	0.86[e] (0.77–0.96)	0.78 (0.66–0.89)	0.62 (0.52–0.76)
S′/LV length	0.68 (0.53–0.82)	0.72 (0.57–0.85)	0.46 (0.32–0.60)
E/*e′*	0.75 (0.62–0.88)	0.66 (0.52–0.81)	0.63 (0.50–0.77)

AUC, area under the receiver-operating characteristic curve; CI, confidence interval; *E*, peak early diastolic velocity; *e′*, mean peak early diastolic mitral annular velocity; FS_L, fractional shortening of the long axis; GLS, global end-systolic longitudinal strain; LV, left ventricular; LVEF, left ventricular ejection fraction; MI, myocardial infarction; new method, combined judgement of colour-coded strain rate data and wall motion analysis; *S′*, peak systolic mitral annulus velocity; WMSI, wall motion score index.
[a]AUC significantly ($P \leq 0.02$) higher than GLS, FS_L, LVEF, *S′*/LV length and *E*/*e′*.
[b]AUC significantly ($P < 0.05$) higher than *S′*/LV length and *E*/*e′*.
[c]AUC significantly ($P < 0.05$) higher than FS_L and *S′*/LV length.
[d]AUC significantly ($P \leq 0.03$) higher than FS_L, *S′*/LV length and *E*/*e′*.
[e]AUC significantly ($P < 0.05$) higher than *S′*/LV length.

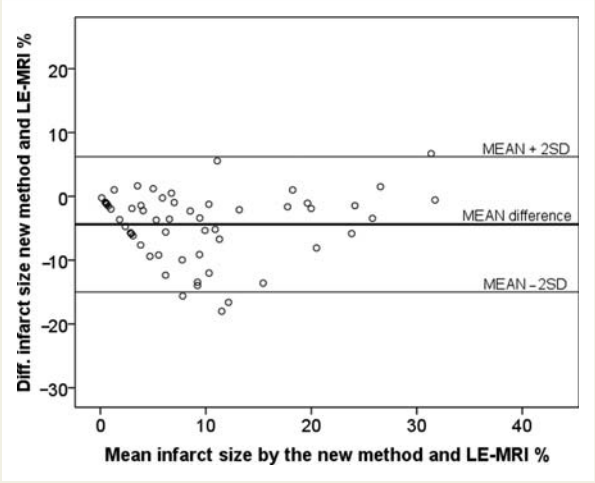

Figure 4 Bland–Altman plot displaying 95% limits of agreement between the infarct size assessed by the new method and LE-MRI. The infarct size by the new method was based on combined judgement of the colour-coded stain rate data and wall motion analysis. Diff., difference; LE-MRI, contrast enhanced magnetic resonance imaging; SD, standard deviation.

segment or sub segment as either healthy or diseased, and infarct size >0 or WMSI >1.0 are more conclusive indications of visible MI.

In the present study, the new infarct size method yielded the highest correlation with LE-MRI both at the global and segmental level. A possible explanation to the difference between the WMSI and the new method is that the areas of hypokinesia and akinesia are classified on a sub-segment level and reported as continuous data by the new method. This may increase the diagnostic accuracy compared with the WMSI, which dichotomizes each segment into ordinal data. In addition, the new method corrects for the area distortion in the bull's eye view, whereas the WMSI has no correction for the unequal segment size, apart from the reduced number of segments in the apex. The new method is not a replacement of WMS, as WMS can still be said to be part of the new method. TD-based SR is sensitive to signal noise and acoustic artefacts, and the segmental 95% confidence interval of a healthy population is rather wide.[12] Thus, the usefulness of TD-based SR obtained from trace analysis seems limited, when being used independently. However, judgement of SR data counteracts potential misinterpretations of WMA due to passive motion caused by tethering. Furthermore, the identification of MI and artefacts is often easy when TD-based SR is displayed as semi-quantitative colour information in curved M-mode or bull's eye views.[10,11]

Mid-systolic SR was used for unadjusted automatic detection of hypokinesia and akinesia as the measurements have to be simultaneous in a bull's eye view. This may explain the differences in the cut-off values in this study compared with other studies that uses peak SR.[6,9] The cut-off values of the WMSI (1.14) and the GLS (−16.5%) for separation of small and large MIs presented are in line with others.[4,6] Sjølie *et al.*[4] presented a cut-off value of −15.0% for the GLS for the identification of the infarct size >20% in a study of 39 STEMI patients in whom echocardiography was performed ~10 days after hospital admittance. As expected due to acute stunning effects, the cut-off values were different in a study where echocardiography was performed immediately before revascularization.[5] Compared with the longitudinal strain by speckle tracking, the new method showed higher correlations with LE-MRI both at the global and segmental level, but the accuracy of the longitudinal strain by speckle tracking in separation of small and large MIs and identification of transmurally infarcted segments were still comparable with the new method.

To avoid variability due to ventricular size, MAE, and *S′* were divided by the end-diastolic length of the left ventricle.[22] However, correcting for the end-diastolic length led only to a trend towards increase in the diagnostic accuracy which was not statistically significant (data not shown). However, it may be noted that the variability in the LV size was small, as 80% of the subjects were men. FS_L is a measurement of the LV global longitudinal strain, and as expected, FS_L and GLS showed high mutual correlation and similar diagnostic accuracy.

Clinical implications of the study

In this study, ~70% of the patients with LE-MRI infarct size <6% did not have visible hypokinesia or akinesia by echocardiography, whereas most patients with visible hypokinesia or akinesia did have LE-MRI infarct size >12%. The infarct size by the new method underestimated the infarct size assessed by LE-MRI. This may to some degree be explained by lack of echocardiographic detectable hypokinesia in MIs with low degree of transmurality.

In line with previous studies,[4–6] the sensitivity and specificity for detecting large MIs were higher for global averages of regional indices compared with strictly global indices of LV performance (FS_L, LVEF, *S′*/LV length, and *E*/e). The present study also indicates that SR data yield additive diagnostic information to WMA. Similar results have been reported previously[8,23] and underscore the versatility of echocardiography and the advantage of performing an integrated judgment, using more than one echocardiographic method.

Direct quantification of the percentage infarct size by echocardiography may be particularly attractive for patients and health workers who are not familiar with the terminology of advanced echocardiography. In contrast, the GLS, WMSI, FS_L, LVEF, *S′*/LV length, and *E*/*e′* have units and magnitude that may be difficult to relate to the infarct size.

Limitations

Both the presented method for direct quantification of the infarct size and the WMSI are highly subjective, and its accuracy depends on the skills of the user. However, all echocardiographic methods are operator dependent, and in particular deformation analysis by speckle tracking echocardiography requires experienced critical judgement of the tracking of each segment. The healthy controls were not examined by LE-MRI. Therefore, the LE-MRI analyses were, in contrast to the echocardiographic analyses, performed without mixing healthy controls and MI patients.

Conclusions

The presented new method combining strain rate imaging and WMA enables direct quantification of the percentage infarct size with high diagnostic accuracy and better correlation to LE-MRI compared with other echocardiographic indices of global LV function. Thus, the method adds incremental diagnostic value to the WMS in the B-mode. Echocardiography performed ~1 month after MI showed ability to identify the patients with the infarct size >12%, whereas most patients with the infarct size <6% did not have echocardiographic indices of impaired LV function.

Conflict of interest: none declared.

Funding

The study has been supported by a grant from the Norwegian Research Council, through the centre for research based innovation; MI Lab. GE Healthcare Ultrasound is a partner in MI lab. S.A.A. was previously employed by MI Lab, but is now employed by GE Healthcare Ultrasound. H.T. holds a 10% position in GE Healthcare Ultrasound.

References

1. Burns RJ, Gibbons RJ, Yi Q, Roberts RS, Miller TD, Schaer GL *et al.* The relationships of left ventricular ejection fraction, end-systolic volume index and infarct size to six-month mortality after hospital discharge following myocardial infarction treated by thrombolysis. *J Am Coll Cardiol* 2002;**39**:30–6.
2. Bello D, Einhorn A, Kaushal R, Kenchaiah S, Raney A, Fieno D *et al.* Cardiac magnetic resonance imaging: infarct size is an independent predictor of mortality in patients with coronary artery disease. *Magn Reson Imaging* 2011;**29**:50–6.
3. Wu E, Ortiz JT, Tejedor P, Lee DC, Bucciarelli-Ducci C, Kansal P *et al.* Infarct size by contrast enhanced cardiac magnetic resonance is a stronger predictor of outcomes than left ventricular ejection fraction or end-systolic volume index: prospective cohort study. *Heart* 2008;**94**:730–6.
4. Sjoli B, Orn S, Grenne B, Vartdal T, Smiseth OA, Edvardsen T *et al.* Comparison of left ventricular ejection fraction and left ventricular global strain as determinants of infarct size in patients with acute myocardial infarction. *J Am Soc Echocardiogr* 2009;**22**:1232–8.
5. Eek C, Grenne B, Brunvand H, Aakhus S, Endresen K, Hol PK *et al.* Strain echocardiography and wall motion score index predicts final infarct size in patients with non-ST-segment-elevation myocardial infarction. *Circ Cardiovasc Imaging* 2010;**3**:187–94.
6. Gjesdal O, Helle-Valle T, Hopp E, Lunde K, Vartdal T, Aakhus S *et al.* Noninvasive separation of large, medium, and small myocardial infarcts in survivors of reperfused ST-elevation myocardial infarction: a comprehensive tissue Doppler and speckle-tracking echocardiography study. *Circ Cardiovasc Imaging* 2008;**1**:189–96, 2 p following 96.
7. Kansal MM, Panse PM, Abe H, Caracciolo G, Wilansky S, Tajik AJ *et al.* Relationship of contrast-enhanced magnetic resonance imaging-derived intramural scar distribution and speckle tracking echocardiography-derived left ventricular two-dimensional strains. *Eur Heart J Cardiovasc Imaging* 2012;**13**:152–8.
8. Bjork Ingul C, Rozis E, Slordahl SA, Marwick TH. Incremental value of strain rate imaging to wall motion analysis for prediction of outcome in patients undergoing dobutamine stress echocardiography. *Circulation* 2007;**115**:1252–9.
9. Zhang Y, Chan AK, Yu CM, Yip GW, Fung JW, Lam WW *et al.* Strain rate imaging differentiates transmural from non-transmural myocardial infarction: a validation study using delayed-enhancement magnetic resonance imaging. *J Am Coll Cardiol* 2005;**46**:864–71.
10. Stoylen A, Heimdal A, Bjornstad K, Wiseth R, Vik-Mo H, Torp H *et al.* Strain rate imaging by ultrasonography in the diagnosis of coronary artery disease. *J Am Soc Echocardiogr* 2000;**13**:1053–64.
11. Stoylen A, Ingul CB, Torp H. Strain and strain rate parametric imaging. A new method for post processing to 3-/4-dimensional images from three standard apical planes. Preliminary data on feasibility, artefact and regional dyssynergy visualisation. *Cardiovasc Ultrasound* 2003;**1**:11.
12. Dalen H, Thorstensen A, Aase SA, Ingul CB, Torp H, Vatten LJ *et al.* Segmental and global longitudinal strain and strain rate based on echocardiography of 1266 healthy individuals: the HUNT study in Norway. *Eur J Echocardiogr* 2010;**11**:176–83.
13. Ingul CB, Stoylen A, Slordahl SA. Recovery of stunned myocardium in acute myocardial infarction quantified by strain rate imaging: a clinical study. *J Am Soc Echocardiogr* 2005;**18**:401–10.
14. Lang RM, Bierig M, Devereux RB, Flachskampf FA, Foster E, Pellikka PA *et al.* Recommendations for chamber quantification. *Eur J Echocardiogr* 2006;**7**:79–108.
15. Heiberg E, Engblom H, Engvall J, Hedstrom E, Ugander M, Arheden H. Semi-automatic quantification of myocardial infarction from delayed contrast enhanced magnetic resonance imaging. *Scand Cardiovasc J* 2005;**39**:267–75.
16. Miller TD, Christian TF, Hodge DO, Hopfenspirger MR, Gersh BJ, Gibbons RJ. Comparison of acute myocardial infarct size to two-year mortality in patients <65 to those ≥65 years of age. *Am J Cardiol* 1999;**84**:1170–5.
17. Kim RJ, Wu E, Rafael A, Chen EL, Parker MA, Simonetti O *et al.* The use of contrast-enhanced magnetic resonance imaging to identify reversible myocardial dysfunction. *New Eng J Med* 2000;**343**:1445–53.
18. Thiele H, Kappl MJ, Linke A, Erbs S, Boudriot E, Lembcke A *et al.* Influence of time-to-treatment, TIMI-flow grades, and ST-segment resolution on infarct size and infarct transmurality as assessed by delayed enhancement magnetic resonance imaging. *Eur Heart J* 2007;**28**:1433–9.
19. Meng X-l, Rosenthal R, Rubin DB. Comparing correlated correlation coefficients. *Psychol Bull* 1992;**111**:172–5.
20. Hanley JA, McNeil BJ. A method of comparing the areas under receiver operating characteristic curves derived from the same cases. *Radiology* 1983;**148**:839–43.
21. Thorstensen A, Dalen H, Amundsen BH, Aase SA, Stoylen A. Reproducibility in echocardiographic assessment of the left ventricular global and regional function, the HUNT study. *Eur J Echocardiogr* 2010;**11**:149–56.
22. Nestaas E, Stoylen A, Brunvand L, Fugelseth D. Longitudinal strain and strain rate by tissue Doppler are more sensitive indices than fractional shortening for assessing the reduced myocardial function in asphyxiated neonates. *Cardiol Young* 2011;**21**:1–7.
23. Ingul CB, Stoylen A, Slordahl SA, Wiseth R, Burgess M, Marwick TH. Automated analysis of myocardial deformation at dobutamine stress echocardiography: an angiographic validation. *J Am Coll Cardiol* 2007;**49**:1651–9.

3D echocardiography in the evaluation of global and regional function in patients with recent myocardial infarction – a comparison with magnetic resonance imaging

Authors

Thorstensen, Anders, MD[*†] Dalen, Håvard, MD, PhD[*†] Hala, Pavel, MD[‡]

Kiss, Gabriel, MSc, PhD[*†]

D'hooge, Jan, MSc, PhD[*§]

Torp, Hans, MSc, Dr.Techn. Professor[*]

Støylen, Asbjørn, MD, Dr.Med. Associate Professor[*†]

Amundsen, Brage H, MD, PhD[*†]

[*] MI Lab and Department of Circulation and Medical Imaging, Norwegian University of Science and Technology, Trondheim, Norway

[†] Department of Cardiology, St Olavs Hospital/Trondheim University Hospital, Trondheim, Norway

[†] Department of Medicine, Levanger Hospital, Nord-Trøndelag Health Trust, Norway

[‡] Homolka Hospital, Prague, Czech Republic

[§] Division of Imaging and Cardiovascular Dynamics, University of Leuven, Leuven, Belgium

Address for correspondence

Dr Anders Thorstensen

Department of Circulation and Medical imaging, NTNU MTFS, Postboks 8905

NO-7491 Trondheim, Norway

Fax: +47 72 82 83 72

Phone: +47 72 82 85 46 or +47 97 69 07 31

E-mail: anders.thorstensen@ntnu.no

Abstract

Objective

We aimed to compare three-dimensional (3D) and two-dimensional (2D) echocardiography in the evaluation of patients with recent myocardial infarction (MI), using late enhancement magnetic resonance imaging (LE-MRI) as a reference method.

Methods

Echocardiography and LE-MRI were performed approximately one month after first-time myocardial infarction in 58 patients. Echocardiography was also performed on 35 healthy controls. Left ventricular (LV) ejection fraction by 3D echocardiography (3D-LVEF), 3D- wall motion score (WMS), 2D-WMS, 3D speckle-tracking-based longitudinal, circumferential, transmural and area strain, and 2D speckle tracking based longitudinal strain were measured.

Results

The global correlations to infarct size by LE-MRI were significantly higher ($P<0.03$) for 3D-WMS and 2D-WMS compared to 3D-LVEF and the four different measurements of 3D strain, and 2D global longitudinal strain was more closely correlated to LE-MRI than 3D global longitudinal strain ($P<0.03$). The segmental correlations to infarct size by LE-MRI were also significantly higher ($P<0.04$) for 3D-WMS, 2D-WMS, and 2D longitudinal strain compared to the other indices. Three-dimensional WMS showed a sensitivity of 76% and a specificity of 72% for identification of LV infarct size >12%, and a sensitivity of 73% and a specificity of 95% for identification of segments with transmural infarct extension.

Conclusions

Three-dimensional WMS and 2D grey-scale echocardiography showed the strongest correlations to LE-MRI. The tested 3D strain method suffers from low temporal and spatial resolution in 3D acquisitions and added diagnostic value could not be proven.

Key words:

Coronary artery disease, late gadolinium enhancement, myocardial infarction, speckle tracking, strain, wall motion score

Abbreviation list

AS = area strain

AUC = area under the receiver operating characteristic curves

CS = circumferential strain

GLS = global longitudinal strain

LE-MRI = late enhancement magnetic resonance imaging

LS = longitudinal strain

LV = left ventricular

LVEF = left ventricular ejection fraction

MI = myocardial infarction

ST = speckle tracking TMS = transmural strain

WMS = wall motion score

2D = two-dimensional

3D = three-dimensional.

Introduction

Prognosis and clinical improvement following acute myocardial infarction (MI) are closely related to infarct size and the transmural distribution of necrosis (1, 2). Echocardiographic measurements of left ventricular (LV) function are indirect estimates of infarct size, and two dimensional (2D) speckle tracking (ST) echocardiography, 2D tissue Doppler based deformation indices, and 2D wall motion analyses are validated indices of global and regional systolic LV function (3-8). However, the standard planes of 2D echocardiography do not encompass the entire left ventricle, resulting in a potential risk of missing deformation abnormalities between the planes. Real time three-dimensional (3D) echocardiography can be displayed as multiple 2D short-axis slices covering the entire LV, and automated tracking of the long-axis motion can reduce out-of-plane motion, which may cause misinterpretations in 2D analysis. Three-dimensional measurements of the regional myocardial deformation in several orientations have the potential to overcome errors caused by misalignment and out-of- plane motion in 2D echocardiography, and speckle tracking-based methods have recently been introduced (9). The aim of the present study was to compare the diagnostic accuracy of wall motion analysis by 3D dynamic multi-slice echocardiography, 3D speckle tracking echocardiography and 2D echocardiography for the assessment of regional and global LV function in patients with recent MI, using late enhancement magnetic resonance imaging (LE- MRI) as reference method.

Methods

Study population and study design

The study was conducted in a single tertiary coronary care centre. Seventy-one consecutive patients with documented first-time non–ST-segment–elevation myocardial infarction (NSTEMI) or ST-segment–elevation myocardial infarction (STEMI) and peak cardiac troponin T measurement >0.5 µg/L were prospectively enrolled from April 2008 to June 2009. Exclusion criteria were prior MI, QRS duration >130 ms, significant valvular disease, previous heart surgery, age >75 years, extensive co-morbidity, chronic atrial fibrillation and contraindications to MRI. No patients were excluded because of impaired echocardiographic image quality. Written informed consent was obtained. Patients were examined with LE-MRI and echocardiography on the same day, on average 31 ± 11 days after hospital admission of the index MI. Five patients were excluded because they were not able to complete the LE- MRI examinations due to claustrophobia. Another eight patients were excluded due to sub-optimal LE-MRI image quality. Of the final 58 patients with full LE-MRI, 46 (79%) had STEMI, whereas 12 (21%) had NSTEMI. Coronary angiography identified a coronary culprit lesion in all patients. Percutaneous

coronary intervention (PCI) of the lesion was performed during the hospital stay in all patients, except in three patients in whom the lesion was not amenable to PCI. The median time from the onset of symptoms to PCI was 3.0 hours (range 0.6-140 hours).

The control group consisted of 35 age- and sex-matched participants from the Echocardiography in the Nord-Trøndelag Health Study (HUNT) who were free from known cardiovascular disease, diabetes and hypertension (10). Validation of the normality of the control group was based on self-filled questionnaires, careful medical history, electrocardiogram, and clinical examinations. The control group was not examined by LE- MRI. The study was approved by the Regional Committee for Medical Research Ethics, and conducted according to the second Helsinki Declaration.

Magnetic resonance imaging

Examinations were performed on a 1.5 T Siemens Avanto (Siemens Medical, Erlangen, Germany) with a six-element body matrix coil. Late-enhancement images were obtained 10-20 minutes after intravenous injection of 0.15 mmol/kg gadodiamide (Omniscan, GE Healthcare, Oslo, Norway) in multiple short-axis slices covering the LV. A balanced steady- state free precision inversion recovery sequence was used, with ECG-triggered data acquisition in mid-diastole. Typical image parameters were: matrix 176x256, in-plane resolution 1.3x1.3 mm, slice thickness 8 mm, gap 2 mm, flip angel°, and inversion time 280-350 ms. The LE-MRI analyses were performed by two operators (PH and BHA), using Segment v1.7 (11). On each short-axis image, the total myocardial area as well as the area of infarcted myocardium was semi-automatically drawn. Areas with signal intensity more than two standard deviations (SD) above normal myocardium were considered infarcted. The infarct size was calculated as infarct volume in percentage of total myocardial volume. As short- and long-term mortality rates have been demonstrated to be increased in patients with infarct size >12% (12), patients were divided in small and large MI, using 12% as cut-off. Segments with infarct volume fraction >50% were classified as transmurally infarcted, while segments with infarct volume 1-50% were classified as sub-endocardially infarcted (13, 14). All echocardiographic and LE-MRI analyses were performed separately and blinded to other analyses and participant's data. For the echocardiographic analyses, the patients and healthy controls were renamed, mixed, and analysed in random order.

Echocardiographic image acquisition

One operator (AT) performed all the analyses, and two operators (AT and HD) performed all echocardiographic examinations (AT; the MI group and HD; the control group). A Vivid 7 (80%) or a Vivid E9 (20%) scanner was used (GE Vingmed, Horten, Norway), with a phased- array (M3S) or matrix-array (3V) transducer for the 2D and 3D recordings, respectively. Three consecutive cycles in B-mode acquisitions (mean frame rate 61 ± 15 s^{-1}) were recorded from the three apical views (4-chamber, 2-chamber and long-axis) and from the parasternal view (mitral valve, papillary muscle, and apical short-axis planes). Images were analyzed off- line using EchoPAC version BT11 (GE Vingmed Ultrasound,

Horten, Norway). Three-dimensional recordings were acquired from the apical window, and 4-6 consecutive ECG- gated subvolumes were acquired during end-expiratory apnoea to generate a full-volume data set (volume rate 26 ± 4 s^{-1}). Care was taken to encompass the entire LV cavity and, if unsatisfactory, the data set was re-acquired (15).

3D Echocardiographic analyses

Three-dimensional wall motion score (WMS) was analyzed in dynamic multi-slice view, ensuring continuous visualization of the same cardiac structures throughout the cardiac cycle (Figure 1). The slices were automatically updated after tracking in each frame to correct for out-of-plane motion caused by longitudinal shortening of the left ventricle. WMS for 2D and 3D echocardiography was assessed in a 16-segment model. Segmental WMS was graded as 1; normal, 2; hypokinetic, 3; akinetic, and 4; dyskinetic. Wall motion score index (WMSI) was calculated by averaging the scored segments when ≥12 segments were accepted for analysis.

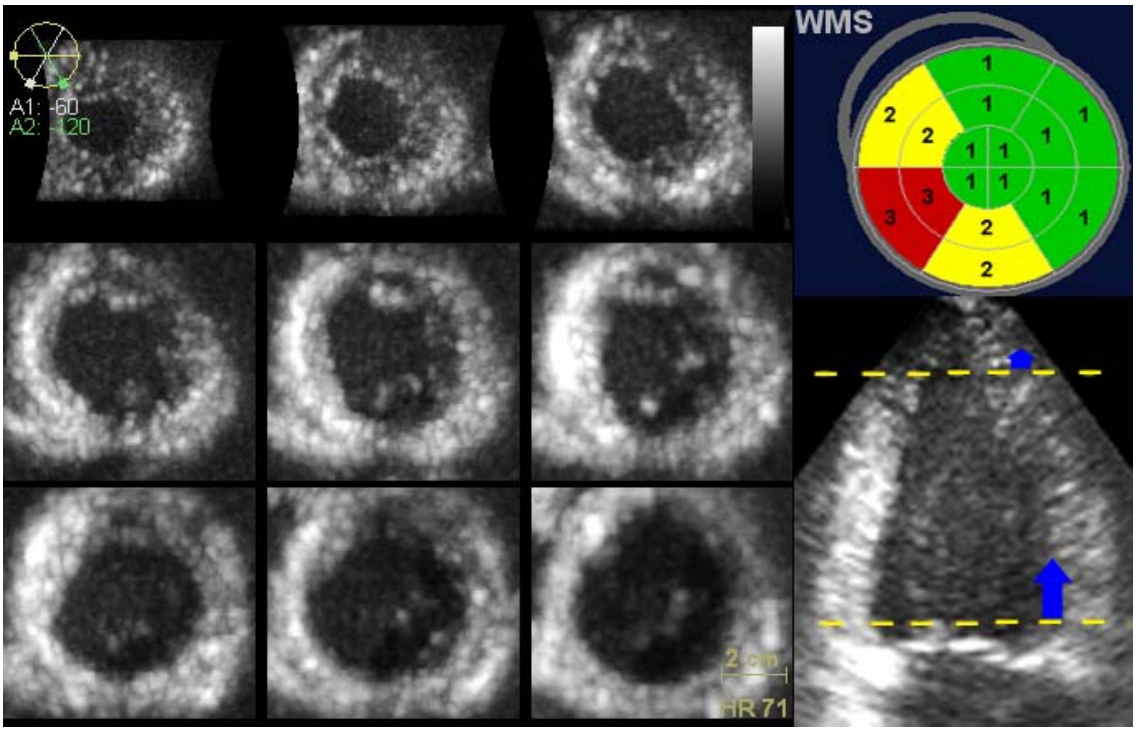

Figure 1 *Left: Three-dimensional wall motion analysis performed by dynamic multi-slice short axis views. Upper right: Bulls-eye presentation of wall motion scores (WMS) indicating inferoseptal myocardial infarction in a 16-segment model. Lower right: Two-chamber view with blue arrows indicating correction for out-of-plane motion caused by longitudinal shortening, which is more prominent at the basal level.*

Three-dimensional strain analysis was conducted using auto LV quantification (version BT11, GE Vingmed Ultrasound, Horten, Norway) (Figure 2). After manual alignment of the three apical views and the short axis view, points were placed in the mitral annulus plane and at the apex, in end-diastole and end-systole. End systole, which was defined as the frame with the smallest LV cavity, was automatically

detected by the software, but manually corrected if necessary. End-diastolic and end-systolic volumes were measured by semi-automatic detection of the endocardial surface, with manual adjustment, and 3D left ventricular ejection fraction (LVEF) was calculated. The epicardial border was automatically detected by the software and manually adjusted, in order to delineate the region of interest (ROI) for the analysis of end-systolic 3D longitudinal (3D-LS), circumferential (3D-CS), transmural (3D-TMS) and area strain (3D-AS). The strain values were obtained by a midwall tracking algorithm based on frame-to-frame block matching in three dimensions. Area strain was calculated as the percentage variation in the midwall surface area. Finally, the tracking of each segment was manually controlled, and segments with sub-optimal tracking were manually rejected. Measurements of 3D global longitudinal strain (3D-GLS), 3D global circumferential strain (3D-GCS), 3D global transmural strain (3D-GTMS), and 3D global area strain (3D-GAS) were calculated by averaging the end-systolic segmental values when ≥12 segments had acceptable tracking.

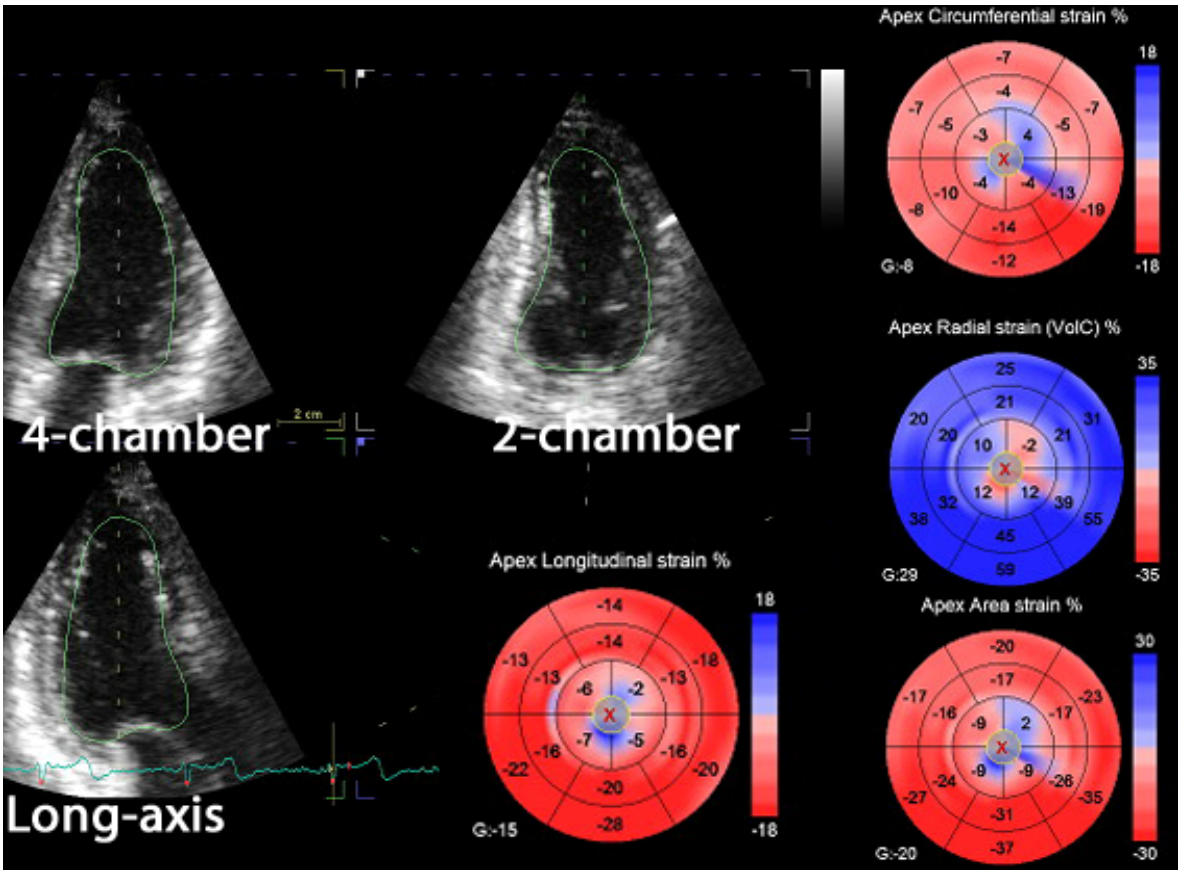

Figure 2: *Analyses of global and segmental three-dimensional longitudinal, circumferential, radial (transmural), and 3D area strain in a patient with an apical anterior myocardial infarction. The regions of interest were delineated after semi-automatic detection of the endocardial surface and the epicardial borders in end-diastole and end-systole.*

2D Echocardiographic analyses

Two-dimensional longitudinal end-systolic strain (2D-LS) was obtained by ST in 2D grey- scale recordings (Automated Function Imaging; EchoPAC PC version BT 11, GE, Horten, Norway). The ROIs were manually adjusted to include the entire LV myocardium and simultaneously avoid the pericardium. Location of end-systole was manually corrected if necessary. Two-dimensional global longitudinal strain (2D-GLS) was calculated by averaging end-systolic values when ≥12 segments had acceptable tracking.

Statistical analyses.

Continuous variables are presented as mean ± SD. Categorical variables are presented as numbers (%). Differences between small and large MIs and healthy controls were analyzed by independent samples *t*-test. For global indices, the relationship between the infarct size assessed by LE-MRI and each echocardiographic index was analyzed by bivariate correlation based on normal distribution among the final 58 patients and reported as Pearson's correlation coefficient (*r*). For the segmental indices, the relationship between each echocardiographic index and the segmental percentage infarct volume fraction assessed by LE-MRI was analyzed by bivariate rank correlations and reported as Spearman's correlation coefficient (*r*). Correlation coefficients were compared according to the method described by Meng et al (16). The area under the receiver-operating characteristic curves (AUC) for the identification of small and large MIs is reported. AUC for the different methods was compared according to the method described by Hanley and McNeil (17). Cut-off values giving the largest sum of sensitivity and specificity are reported. Reproducibility was assessed by one of the authors' reanalysis of 20 randomly selected recordings, and expressed as the coefficient of repeatability (COR) for continuous variables or the weighted kappa coefficient for segmental WMS. Statistical analyses were performed in SPSS version 17 (SPSS Inc, Chicago, Ill).

Results

Study population and feasibility.

Patient characteristics are listed in Table 1. Estimation of 3D-LVEF and 2D-WMSI were feasible (≥12 accepted segments) in all the recordings. The feasibility of the other global indices was: 98% (91/93) for 3D-WMSI, 62% (58/93) for the four different global 3D strain components, and 95% (88/93) for 2D-GLS. Segmental analysis was feasible in 1050 (71%) segments by Auto LV quantification, and 1288 (87%) segments by 2D ST. The calculation of 2D and 3D WMSI was based on 1455 (98%) and 1405 (95%) segments, respectively. The rest of the segments were excluded because of drop outs, reverberations, valvular interference, or tracking difficulties. There were significantly more discarded segments in the perfusion territory of the left anterior descending artery.

Table 1 Patient characteristics, risk factors, angiographic findings and medications.

	Infarct Size >12% (n=25)	Infarct Size 12% (n=33)	Healthy controls
LE-MRI infarct size (infarct volume fraction)	19.5 ± 5.7% *	5.3 ± 3.2%	not available
Age, years	56.7 ± 13.6	54.9 ± 12.9	56.9 ± 13.0
BMI, kg/m2	26.1 ± 6.0	25.4 ± 5.4	26.1 ± 5.2
Male sex, n (%)	19 (76)	25 (76)	28 (80)
Heart rate, bpm	64 (11)	60 (11) †	67 (11)
Current smoker, n (%)	12 (48)	17 (52)	-
Creatinine, µmol/L	68.5 1 ± 7.1 ‡	70.5 ± 17.2 †	88.0 ± 19.1
Peak Troponin T, µg/L	7.7 ± 5.7 *	3.2 ± 2.4	not available
Hypertension, n (%)	5 (20)	5 (15)	-
Diabetes mellitus, n (%)	4 (16)	2 (6)	-
STEMI, n (%)	22 (88)	24 (73)	-
Single vessel disease, n (%)	14 (56)	25 (76)	not available
LAD culprit, n (%)	10 (40)	13 (39)	-
CX culprit, n (%)	7 (28)	6 (18)	-
RCA culprit, n (%)	8 (32)	14 (42)	-
Aspirin, n (%)	25 (100)	33 (100)	-
Clopidogrel, n (%)	25 (100)	33 (100)	-
Beta-blocker, n (%)	23 (92)	29 (88)	-
Statin, n (%)	25 (100)	33 (100)	-
ACEi or ARB, n (%)	7 (28)	8 (24)	-

Table 2: *Continuous variables displayed as mean ± SD. Categorical variables are displayed as numbers (percentage). * P<0.001 for large MI vs. small MI; † P<0.05 for small MI vs. healthy controls; ‡ P<0.001 for large MI vs. healthy controls. Abbreviations: ACEi = angiotensin-converting enzyme inhibitors; ARB = angiotensin II receptor blockers; bpm = beats per minute; BMI = body mass index; LE-MRI = late enhancement magnetic resonance imaging; CX = circumflex artery; LAD = left anterior descending artery; RCA = right coronary artery; STEMI = ST-segment–elevation myocardial infarction.*

Infarct Size by LE-MRI

Evidence of MI was detected by LE-MRI in all patients. The mean (SD) infarct size was 11.4% (8.1%) of the total LV myocardial volume (Figure 3). Thirty-three patients (57%) had calculated the infarct size <12% and 25 patients (43%) had infarct size >12%. Evidence of infarction by LE-MRI was detected in 387 (42%) segments, with transmural extension (>50% late enhancement) in 74 (8%) segments.

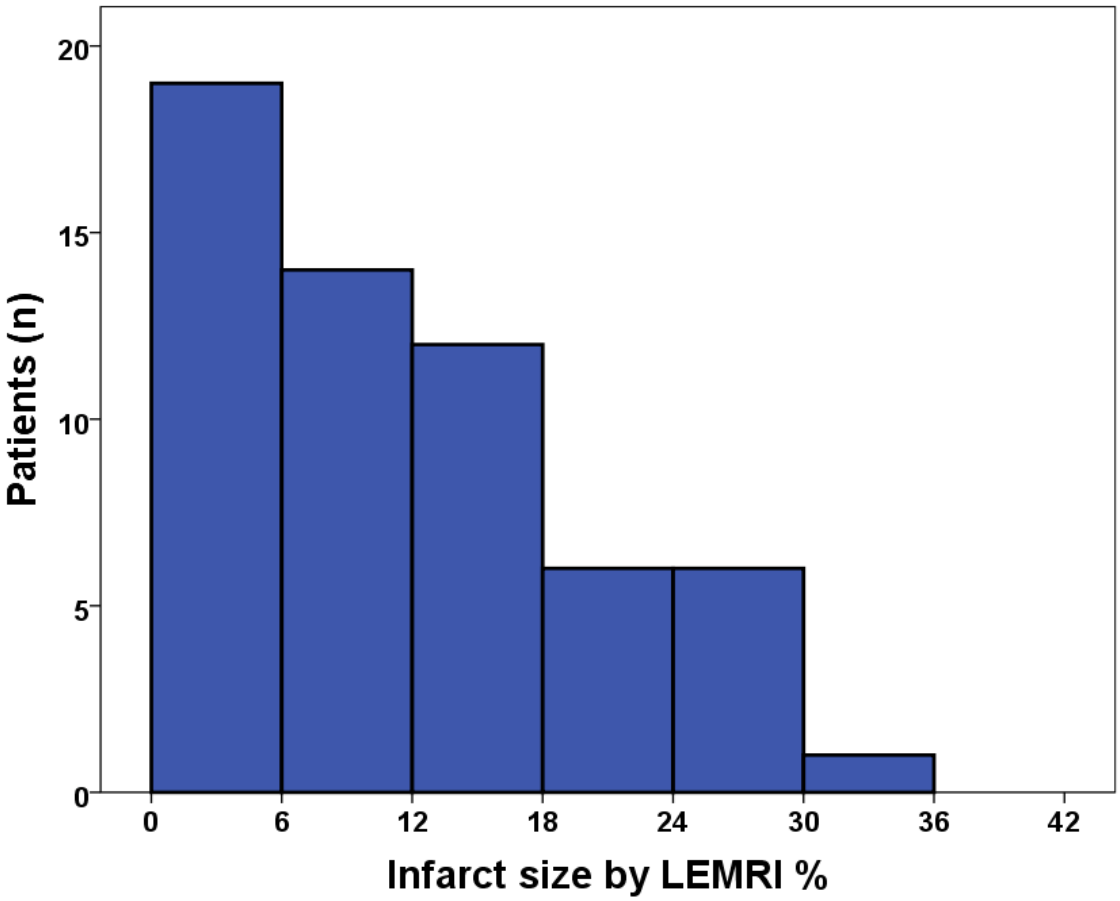

Figure 3: *Histogram demonstrating the distribution of infarct size by LE-MRI. Abbreviations: LE-MRI = late enhancement magnetic resonance imaging.*

Echocardiography - Global indices

There were significant differences between the patients with large MIs compared with those with small MIs or healthy controls for all the indices (Table 2). In patients with small MIs, the 3D-LVEF was significantly lower (P<0.02) and 2D- and 3D-WMSI were significantly higher (P<0.03) compared with the healthy controls.

Table 2 Global echocardiographic indices of healthy controls and patients by infarct size

	Large MI (n =	**Small MI (n = 33)**	**Healthy controls**
3D-LVEF	48.2 ± 6.7% *	55.3 ± 6.1% †	58.1 ± 5.4%
3D-WMSI	1.30 ± 0.23 *	1.08 ± 0.13 †	1.01 ± 0.02
3D global longitudinal	-16.0 ± 2.9% *	-18.0 ± 2.6%	-19.4 ± 3.0%
3D global area strain	-27.3 ± 3.9% *	-30.6 ± 4.4%	-32.3 ± 3.1%
3D global	-14.5 ± 3.2% *	-16.4 ± 3.1%	-17.2 ± 2.0%
3D global transmural	41.0 ± 8.5% *	47.5 ± 9.5%	49.7 ± 7.0%
2D-WMSI	1.33 ± 0.26 *	1.09 ± 0.11 †	1.01 ± 0.02
2D global longitudinal	-15.4 ± 3.0% *	-18.6 ± 2.0%	-19.4 ± 2.2%

Table 2: *Mean ± SD of different of global echocardiographic indices of the patients stratified by infarct size and the healthy controls are shown. Large MI was defined as total infarct volume fraction >12 % by LE-MRI and small MI was defined as total infarct volume fraction <12%. * Significant difference (all P<0.01) between large and small MIs, and large MIs and the healthy controls. † Significant difference (all P<0.03) between small MI and the healthy controls. Abbreviations: LE-MRI = late enhancement magnetic resonance imaging; LVEF = left ventricular ejection fraction; MI = myocardial infarction; WMSI = wall motion score index; 2D = two-dimensional; 3D = three-dimensional.*

There were significant correlations between global infarct size assessed by LE-MRI and all the echocardiographic indices of LV global function with r = 0.51 for 3D-LVEF, 0.72 for 3D-WMSI, 0.74 for 2D-WMSI, 0.42 for 3D- GLS, 0.47 for 3D-GCS, 0.48 for 3D-GTMS, 0.50 for 3D-GAS, and 0.67 for 2D-GLS (Figure 4). The correlations with LE-MRI were higher (P<0.03) for 3D- and 2D-WMSI compared to the other echocardiographic indices, except 2D-GLS. Furthermore, 2D-GLS was more closely correlated to LE-MRI than 3D-GLS (P<0.03).

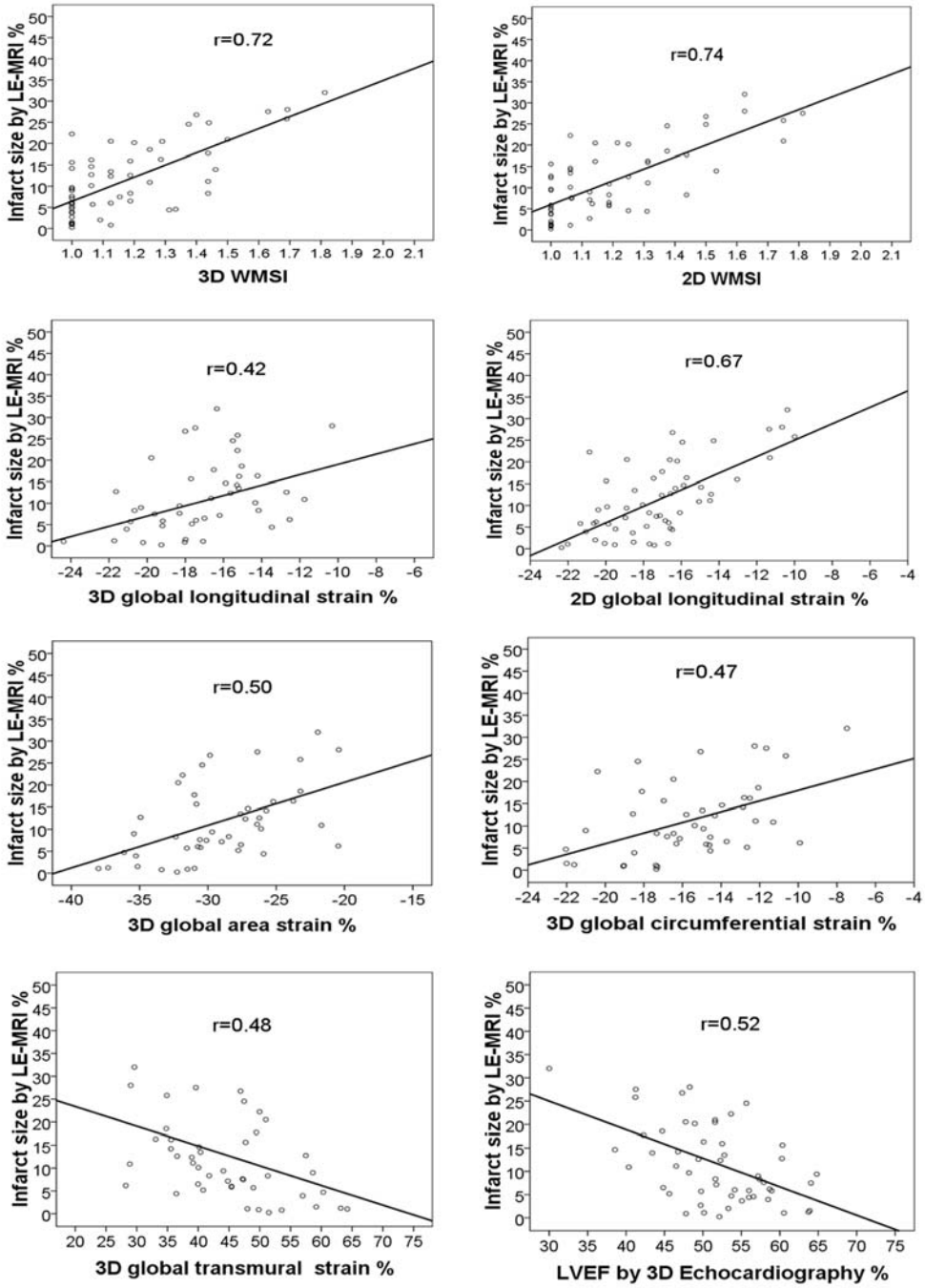

Figure 4: *Scatter plots with regression lines of infarct size by LE-MRI and global echocardiographic indices of LV function. Pearson's correlation coefficients (r) are reported in the figures. Abbreviations: LE-MRI = late enhancement magnetic resonance imaging; LVEF = left ventricular ejection fraction; WMSI = wall motion score index; 2D = two-dimensional; 3D = three-dimensional.*

The AUC for identification of large MIs ranged from 0.69 to 0.80 (Table 3). Although 3D-WMSI, 2D-WMSI, and 2D-GLS were the only methods with AUC >0.75, the differences between methods were not statistically significant. Three-dimensional WMSI >1.11 and 2D- WMSI >1.14 had a sensitivity of 76% and 72% and a specificity of 72% and 74%, respectively, to separate small and large MI, while 2D-GLS >-16.5% had a sensitivity of 68% and a specificity of 85% to separate small and large MIs. Abnormal 2D or 3D WMS was only identified in 5 (26%) of the patients with LE-MRI infarct size <6%.

Table 3 AUC for identification of large MI and transmurally infarcted segments of the different echocardiographic indices of global and segmental LV function

	AUC (95% CI) of global indices for separation of large and small MIs	**AUC (95 % CI) of segmental indices for identification of transmurally infarcted**
3D-LVEF	0.74	-
3D-WMS	0.80	-
3D longitudinal strain	0.72	0.73
3D area strain	0.72	0.85 *
3D circumferential strain	0.69	0.87 *
3D transmural strain	0.71	0.86 *
2D-WMS	0.79	-
2D longitudinal strain	0.80	0.88 *

Table 3: *Large MI: total infarct volume fraction >12% by LE-MRI. Small MI: total infarct volume fraction <12% by LE-MRI. Transmurally infarcted segments: segmental infarct volume fraction >50%. The differences in AUC for separation of large and small MIs were not statistical significant.* ******* *= AUC significantly (P≤0.01) higher than 3D longitudinal strain; Abbreviations: AUC = area under the receiver operating characteristic curve; CI = confidence interval; LE-MRI = late enhancement magnetic resonance imaging; LVEF = left ventricular ejection fraction; MI = myocardial infarction; WMS = wall motion score; 2D = two- dimensional; 3D = three-dimensional.*

Segmental indices

The mean segmental values of the non-infarcted, sub-endocardial infarcted and transmurally infarcted segments were significantly different for all the echocardiographic methods (Table 4).

Table 4 Segmental values of echocardiographic indices in infarcted and non-infarcted segments.

	Transmurally infarcted segments (>50% by LE-MRI)	Sub-endocardial infarcted segments (1-50 % by LE-MRI)	Non-infarcted segments
3D-WMS	2.10 ± 0.80	1.23 ± 0.47	1.02 ± 0.16
3D longitudinal strain	-13.6 ± 5.2%	-15.9 ± 5.7%	-18.3 ± 5.5%
3D area strain	-20.4 ± 7.0%	-27.0 ± 7.2%	-31.2 ± 8.4%
3D circumferential strain	-8.3 ± 5.4%	-14.1 ± 5.3%	-17.2 ± 5.7%
3D transmural strain	27.6 ± 11.3%	39.5 ± 16.0%	48.4 ± 16.0%
2D-WMS	2.14 ± 0.76	1.26 ± 0.53	1.02 ± 0.17
2D longitudinal strain	-10.5 ± 5.1%	-15.4 ± 4.2%	-19.1 ± 3.8%

Table 4: *Mean ± SD of different segmental echocardiographic indices of transmurally, sub-endocardial, and non-infarcted segments. The differences were significant (all P<0.001) between non-infarcted segments, sub-endocardial infarcted segments, and transmurally infarcted segments for all methods. Abbreviations: LE-MRI = late enhancement magnetic resonance imaging; WMSI = wall motion score index; 2D = two-dimensional; 3D = three- dimensional.*

There were significant correlations between segmental infarct volume fraction assessed by LE-MRI and all the segmental echocardiographic indices with $r = 0.53$ for 3D-WMS, 0.53 for 2D-WMS, 0.25 for 3D-LS, 0.40 for 3D-CS, 0.40 for 3D-TMS, 0.40 for 3D-AS, and 0.48 for 2D-LS (Figure 5). The correlations of 3D-WMS, 2D-WMS and 2D-LS with segmental infarct volume fraction were significantly higher compared to the other echocardiographic indices (all P<0.04). In addition, the correlation coefficients for 3D-CS, 3D-TMS, and 3D-AS were significantly higher than for 3D-LS (all P<0.03). The correlation coefficient between 3D- WMS and 2D-WMS was 0.74. The correlations between the four different measurements of segmental 3D strain were generally strong (all $r>0.79$), except the correlation between 3D-LS and 3D-CS ($r = 0.43$).

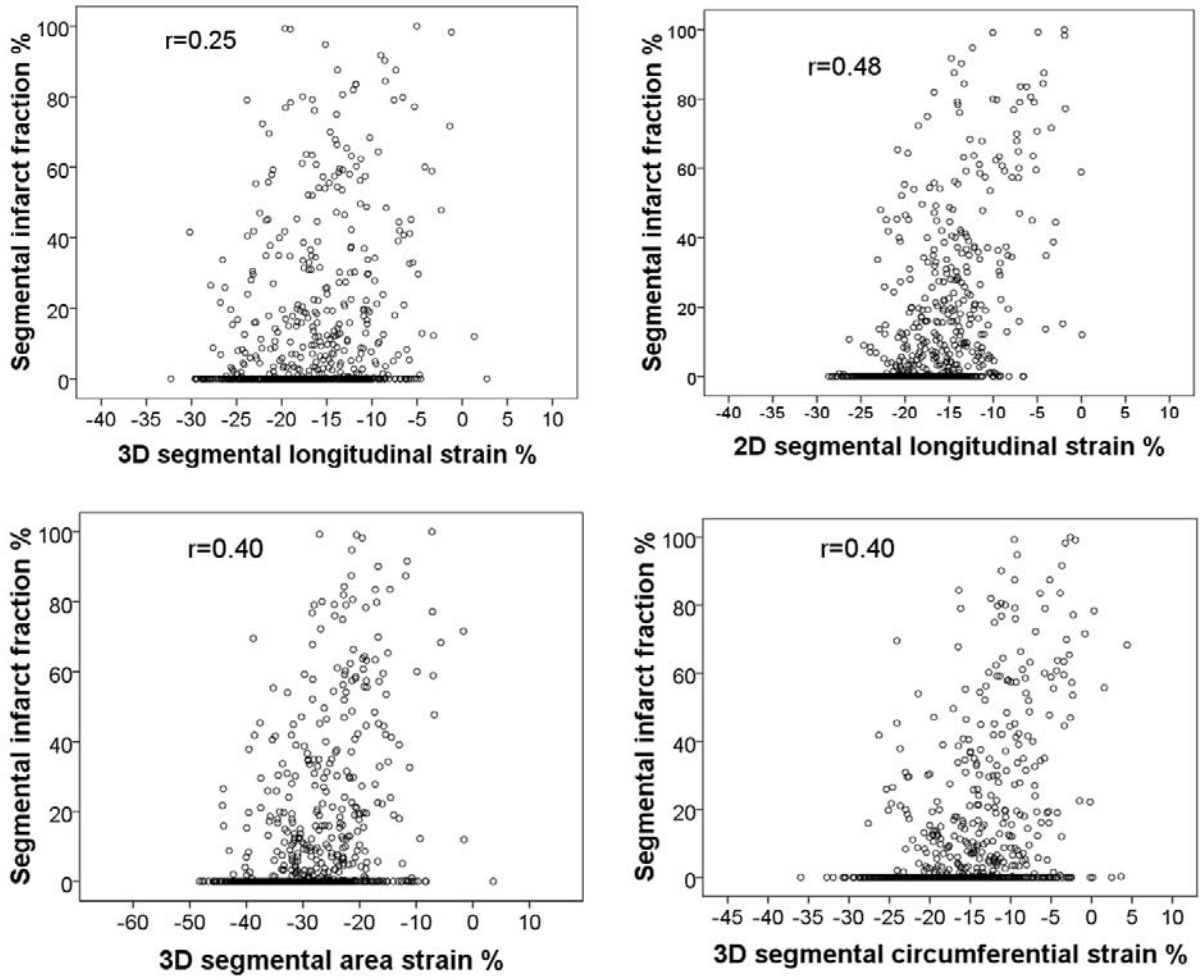

Figure 5: *Scatter plots of segmental percentage infarct volume fraction by LE-MRI and segmental end-systolic strain measurements. Spearman's correlation coefficients (r) are reported in the figures. Abbreviations: LE-MRI = late enhancement magnetic resonance imaging; 2D = two- dimensional; 3D = three-dimensional.*

All the segmental echocardiographic indices showed generally good ability to identify transmurally infarcted segments with more than 50% contrast enhancement by LE-MRI (Table 3). However, the AUC for 3D-LS was significant lower (all $P<0.01$) than the other echocardiographic indices. Otherwise, the differences in AUC of the echocardiographic indices were not statistically significant. Three-dimensional-WMS and 2D-WMS >1 had a sensitivity of 73% and 77% and a specificity of 95% and 94%, respectively, for identification of transmurally infarcted segments, while 2D-LS >-14.4% had a sensitivity of 80% and a specificity of 85% for identification of transmurally infarcted segments.

Data reproducibility

For the global echocardiographic indices the COR was 0.21 for 3D WMSI, 0.19 for 2D WMSI, 4.1% for 3D-GLS, 5.7% for 3D-GCS, 12.2% for 3D-GTMS, 6.1% for 3D-GAS, and 2.2% for 2D-GLS. For the segmental echocardiographic indices the weighted kappa coefficient was 0.72 for 3D WMS and 0.67 for 2D WMS. COR was 8.3% for 3D-LS, 10.3% for 3D-CS, 25.2% for 3D-TMS, 11.9% for 3D-AS, and 6.6% for 2D-LS. In addition, comprehensive reproducibility data are recently published (18).

Discussion

The present study shows that both 2D- and 3D- echocardiography performed one month after a myocardial infarction were able to identify patients with infarct size >12%, while most patients with infarct size <6% did not have echocardiographic indices of impaired LV function. WMS by 2D and 3D echocardiography and 2D speckle tracking echocardiography showed the strongest correlations to LE-MRI both at the global and segmental level.

3D strain analyses

The four different measurements of 3D strain were able to identify most patients with infarct size >12%, but considering the lower feasibility and more moderate correlations to LE-MRI of 3D strain compared with wall motion analysis and 2D ST echocardiography, added diagnostic value of the tested implementation of 3D strain could not be proven. ST-echocardiography and other quantitative deformation analyses are sensitive to low frame rate, signal noise, and artefacts. Despite acquiring the 3D recordings over four to six consecutive heart beats, both the temporal and spatial resolutions were considerably lower in 3D than in 2D. This is probably the cause of the low correlation between longitudinal 3D strain and LE- MRI; longitudinal motion is higher at the base, where resolution is lower. Furthermore, stitching artefacts in 3D recordings are more likely to cause misinterpretation in speckle tracking than in visual wall motion analysis. A recent publication reported accurate and reproducible 3D strain measurements in a study which mainly included healthy subjects and patients with ischemic and non-ischemic cardiomyopathy (19), but this study population was selected on the basis of image quality and their results were not validated by MRI.

3D versus 2D wall motion analyses

Our results show that 3D-WMS by dynamic multi-slice obtained from only one 3D recording provides a quick and reliable view of the LV function. Wall motion score in 2D can be difficult due to in- and out-of-plane motion, tethering and the limited coverage of the LV. In some cases with better apical acoustic window, 3D-WMS showed added diagnostic value, but as 2D echocardiography performed better in subjects with better parasternal acoustic window, the overall accuracy of 3D-WMS and 2D

echocardiography did not differ significantly. Comparing the entire LV circumference in dynamic short-axis slices from a 3D recording makes it easier to separate areas with reduced function, and this may compensate for the lower temporal resolution and larger voxel size in 3D. In daily routine, this would be a clear advantage in patients with limited parasternal acoustic window, where short-axis images are hard to get. Furthermore, our data suggest that a frame rate of 20-25 s^{-1} is sufficient for 3D wall motion analysis at normal resting heart rates.

Similar diagnostic accuracy of WMS and 2D ST echocardiography in patients with MI has also been shown by others (20, 21). Thus, there are still potential for further technological development of quantitative deformation imaging. The cut-off values of 2D-WMSI (1.14) and GLS (-16.5%) for separation of small and large MIs in our study are similar to previous studies (13, 22). As expected due to the effects of acute stunning, the cut-off values in these studies are different from the cut-off values reported in a study where echocardiography was performed immediately before revascularization (20). In the acute setting, the regions with reduced function reflects stunning as well as necrosis, and thus, area at risk more than the actual area of infarction.

Limitations

WMS and deformation analyses are operator dependent, and in particular ST echocardiography require experienced critical judgement of the tracking of each segment. The 3D recordings were acquired with a 3V transducer. Later hardware versions have improved both volume rate and resolution, and this would probably have improved the 3D strain results. We have only tested one 3D strain method, and, as for 2D strain measurements, the results should not be generalized to other 3D strain methods.

Prior MI was an exclusion criterion in this study. Distinguishing between acute and chronic MI is clinically important, but was not the aim of this study. The healthy controls were not examined by LE-MRI. Therefore, the LE-MRI analyses were, in contrast to the echocardiographic analyses, performed without mixing healthy controls and MI patients. The pixel intensity cut-off for identification of infarcted myocardium by LE-MRI is not thoroughly validated, and using the usual cut-off of 2 SD above the mean pixel intensity may result in overestimation of the true infarct size (23).

Conclusions

WMS by 2D and 3D echocardiography and 2D speckle tracking echocardiography showed the strongest correlations to LE-MRI both at the global and segmental level. Dynamic multi- slice short-axis obtained from only one 3D recording gives a quick and reliable view of the LV regional function. Added diagnostic value of the tested implementation of 3D strain could not be proven.

References

1. Burns RJ, Gibbons RJ, Yi Q, Roberts RS, Miller TD, Schaer GL, et al. The relationships of left ventricular ejection fraction, end-systolic volume index and infarct size to six-month mortality after hospital discharge following myocardial infarction treated by thrombolysis. J Am Coll Cardiol 2002;39:30-6.

2. Wu E, Ortiz JT, Tejedor P, Lee DC, Bucciarelli-Ducci C, Kansal P, et al. Infarct size by contrast enhanced cardiac magnetic resonance is a stronger predictor of outcomes than left ventricular ejection fraction or end-systolic volume index: prospective cohort study. Heart 2008;94:730-6.

3. Amundsen BH, Helle-Valle T, Edvardsen T, Torp H, Crosby J, Lyseggen E, et al. Noninvasive myocardial strain measurement by speckle tracking echocardiography: validation against sonomicrometry and tagged magnetic resonance imaging. J Am Coll Cardiol 2006;47:789-93.

4. Stanton T, Leano R, Marwick TH. Prediction of All-Cause Mortality From Global Longitudinal Speckle Strain. Circulation: Cardiovascular Imaging 2009;2:356-64.

5. Stoylen A, Heimdal A, Bjornstad K, Torp HG, Skjaerpe T. Strain Rate Imaging by Ultrasound in the Diagnosis of Regional Dysfunction of the Left Ventricle. Echocardiography 1999;16:321-9.

6. Stoylen A, Heimdal A, Bjornstad K, Wiseth R, Vik-Mo H, Torp H, et al. Strain rate imaging by ultrasonography in the diagnosis of coronary artery disease. J Am Soc Echocardiogr 2000;13:1053-64.

7. Bansal M, Cho GY, Chan J, Leano R, Haluska BA, Marwick TH. Feasibility and accuracy of different techniques of two-dimensional speckle based strain and validation with harmonic phase magnetic resonance imaging. J Am Soc Echocardiogr 2008;21:1318-25.

8. Grenne B, Eek C, Sjoli B, Dahlslett T, Hol PK, Orn S, et al. Mean strain throughout the heart cycle by longitudinal two-dimensional speckle-tracking echocardiography enables early prediction of infarct size. J Am Soc Echocardiogr 2011;24:1118-25.

9. Kleijn SA, Aly MF, Terwee CB, van Rossum AC, Kamp O. Three-dimensional speckle tracking echocardiography for automatic assessment of global and regional left ventricular function based on area strain. J Am Soc Echocardiogr 2011;24:314-21.

10. Dalen H, Thorstensen A, Aase SA, Ingul CB, Torp H, Vatten LJ, et al. Segmental and global longitudinal strain and strain rate based on echocardiography of 1266 healthy individuals: the HUNT study in Norway. Eur J Echocardiogr 2010;11:176-83.

11. Heiberg E, Engblom H, Engvall J, Hedstrom E, Ugander M, Arheden H. Semi- automatic quantification of myocardial infarction from delayed contrast enhanced magnetic resonance imaging. Scand Cardiovasc J 2005;39:267-75.

12. Miller TD, Christian TF, Hodge DO, Hopfenspirger MR, Gersh BJ, Gibbons RJ. Comparison of

acute myocardial infarct size to two-year mortality in patients <65 to those >=65 years of age. The American Journal of Cardiology 1999;84:1170-5.

13. Gjesdal O, Helle-Valle T, Hopp E, Lunde K, Vartdal T, Aakhus S, et al. Noninvasive separation of large, medium, and small myocardial infarcts in survivors of reperfused ST- elevation myocardial infarction: a comprehensive tissue Doppler and speckle-tracking echocardiography study. Circ Cardiovasc Imaging 2008;1:189-96, 2 p following 96.

14. Kim RJ, Wu E, Rafael A, Chen EL, Parker MA, Simonetti O, et al. The use of contrast-enhanced magnetic resonance imaging to identify reversible myocardial dysfunction. N Engl J Med 2000;343:1445-53.

15. Lang RM, Badano LP, Tsang W, Adams DH, Agricola E, Buck T, et al. EAE/ASE recommendations for image acquisition and display using three-dimensional echocardiography. J Am Soc Echocardiogr 2012;25:3-46.

16. Meng X-l, Rosenthal R, Rubin DB. Comparing correlated correlation coefficients. Psychological Bulletin 1992;111:172-5.

17. Hanley JA, McNeil BJ. A method of comparing the areas under receiver operating characteristic curves derived from the same cases. Radiology 1983;148:839-43.

18. Thorstensen A, Dalen H, Amundsen BH, Aase SA, Stoylen A. Reproducibility in echocardiographic assessment of the left ventricular global and regional function, the HUNT study. Eur J Echocardiogr 2010;11:149-56.

19. Reant P, Barbot L, Touche C, Dijos M, Arsac F, Pillois X, et al. Evaluation of Global Left Ventricular Systolic Function Using Three-Dimensional Echocardiography Speckle- Tracking Strain Parameters. J Am Soc Echocardiogr 2011.

20. Eek C, Grenne B, Brunvand H, Aakhus S, Endresen K, Hol PK, et al. Strain echocardiography and wall motion score index predicts final infarct size in patients with non- ST-segment-elevation myocardial infarction. Circ Cardiovasc Imaging 2010;3:187-94.

21. Mistry N, Beitnes JO, Halvorsen S, Abdelnoor M, Hoffmann P, Kjeldsen SE, et al. Assessment of left ventricular function in ST-elevation myocardial infarction by global longitudinal strain: a comparison with ejection fraction, infarct size, and wall motion score index measured by non-invasive imaging modalities. Eur J Echocardiogr 2011;12:678-83.

22. Sjoli B, Orn S, Grenne B, Vartdal T, Smiseth OA, Edvardsen T, et al. Comparison of left ventricular ejection fraction and left ventricular global strain as determinants of infarct size in patients with acute myocardial infarction. J Am Soc Echocardiogr 2009;22:1232-8.

23. Flett AS, Hasleton J, Cook C, Hausenloy D, Quarta G, Ariti C, et al. Evaluation of techniques for the quantification of myocardial scar of differing etiology using cardiac magnetic resonance. JACC Cardiovasc Imaging 2011;4:150-6.

Funding sources & disclosures

The study has been supported by a grant from the Norwegian Research Council, through the centre for research based innovation; MI Lab. MI Lab has an annual total budget of ≈ 33.5 million NOK. GE Healthcare Ultrasound is one of the industry partners in MI lab, and the annual contribution from GE Healthcare Ultrasound to this budget is ≈ 8.5 million NOK (≈ 25%).

Dissertations at the Faculty of Medicine, NTNU

1977

1. Knut Joachim Berg: EFFECT OF ACETYLSALICYLIC ACID ON RENAL FUNCTION
2. Karl Erik Viken and Arne Ødegaard: STUDIES ON HUMAN MONOCYTES CULTURED *IN VITRO*

1978

3. Karel Bjørn Cyvin: CONGENITAL DISLOCATION OF THE HIP JOINT.
4. Alf O. Brubakk: METHODS FOR STUDYING FLOW DYNAMICS IN THE LEFT VENTRICLE AND THE AORTA IN MAN.

1979

5. Geirmund Unsgaard: CYTOSTATIC AND IMMUNOREGULATORY ABILITIES OF HUMAN BLOOD MONOCYTES CULTURED IN VITRO

1980

6. Størker Jørstad: URAEMIC TOXINS
7. Arne Olav Jenssen: SOME RHEOLOGICAL, CHEMICAL AND STRUCTURAL PROPERTIES OF MUCOID SPUTUM FROM PATIENTS WITH CHRONIC OBSTRUCTIVE BRONCHITIS

1981

8. Jens Hammerstrøm: CYTOSTATIC AND CYTOLYTIC ACTIVITY OF HUMAN MONOCYTES AND EFFUSION MACROPHAGES AGAINST TUMOR CELLS *IN VITRO*

1983

9. Tore Syversen: EFFECTS OF METHYLMERCURY ON RAT BRAIN PROTEIN.
10. Torbjørn Iversen: SQUAMOUS CELL CARCINOMA OF THE VULVA.

1984

11. Tor-Erik Widerøe: ASPECTS OF CONTINUOUS AMBULATORY PERITONEAL DIALYSIS.
12. Anton Hole: ALTERATIONS OF MONOCYTE AND LYMPHOCYTE FUNCTIONS IN REALTION TO SURGERY UNDER EPIDURAL OR GENERAL ANAESTHESIA.
13. Terje Terjesen: FRACTURE HEALING AND STRESS-PROTECTION AFTER METAL PLATE FIXATION AND EXTERNAL FIXATION.
14. Carsten Saunte: CLUSTER HEADACHE SYNDROME.
15. Inggard Lereim: TRAFFIC ACCIDENTS AND THEIR CONSEQUENCES.
16. Bjørn Magne Eggen: STUDIES IN CYTOTOXICITY IN HUMAN ADHERENT MONONUCLEAR BLOOD CELLS.
17. Trond Haug: FACTORS REGULATING BEHAVIORAL EFFECTS OG DRUGS.

1985

18. Sven Erik Gisvold: RESUSCITATION AFTER COMPLETE GLOBAL BRAIN ISCHEMIA.
19. Terje Espevik: THE CYTOSKELETON OF HUMAN MONOCYTES.
20. Lars Bevanger: STUDIES OF THE Ibc (c) PROTEIN ANTIGENS OF GROUP B STREPTOCOCCI.
21. Ole-Jan Iversen: RETROVIRUS-LIKE PARTICLES IN THE PATHOGENESIS OF PSORIASIS.
22. Lasse Eriksen: EVALUATION AND TREATMENT OF ALCOHOL DEPENDENT BEHAVIOUR.
23. Per I. Lundmo: ANDROGEN METABOLISM IN THE PROSTATE.

1986

24. Dagfinn Berntzen: ANALYSIS AND MANAGEMENT OF EXPERIMENTAL AND CLINICAL PAIN.
25. Odd Arnold Kildahl-Andersen: PRODUCTION AND CHARACTERIZATION OF MONOCYTE-DERIVED CYTOTOXIN AND ITS ROLE IN MONOCYTE-MEDIATED CYTOTOXICITY.
26. Ola Dale: VOLATILE ANAESTHETICS.

1987

27. Per Martin Kleveland: STUDIES ON GASTRIN.
28. Audun N. Øksendal: THE CALCIUM PARADOX AND THE HEART.
29. Vilhjalmur R. Finsen: HIP FRACTURES

1988

30. Rigmor Austgulen: TUMOR NECROSIS FACTOR: A MONOCYTE-DERIVED REGULATOR OF CELLULAR GROWTH.
31. Tom-Harald Edna: HEAD INJURIES ADMITTED TO HOSPITAL.
32. Joseph D. Borsi: NEW ASPECTS OF THE CLINICAL PHARMACOKINETICS OF METHOTREXATE.
33. Olav F. M. Sellevold: GLUCOCORTICOIDS IN MYOCARDIAL PROTECTION.
34. Terje Skjærpe: NONINVASIVE QUANTITATION OF GLOBAL PARAMETERS ON LEFT VENTRICULAR FUNCTION: THE SYSTOLIC PULMONARY ARTERY PRESSURE AND CARDIAC OUTPUT.
35. Eyvind Rødahl: STUDIES OF IMMUNE COMPLEXES AND RETROVIRUS-LIKE ANTIGENS IN PATIENTS WITH ANKYLOSING SPONDYLITIS.
36. Ketil Thorstensen: STUDIES ON THE MECHANISMS OF CELLULAR UPTAKE OF IRON FROM TRANSFERRIN.
37. Anna Midelfart: STUDIES OF THE MECHANISMS OF ION AND FLUID TRANSPORT IN THE BOVINE CORNEA.
38. Eirik Helseth: GROWTH AND PLASMINOGEN ACTIVATOR ACTIVITY OF HUMAN GLIOMAS AND BRAIN METASTASES - WITH SPECIAL REFERENCE TO TRANSFORMING GROWTH FACTOR BETA AND THE EPIDERMAL GROWTH FACTOR RECEPTOR.
39. Petter C. Borchgrevink: MAGNESIUM AND THE ISCHEMIC HEART.
40. Kjell-Arne Rein: THE EFFECT OF EXTRACORPOREAL CIRCULATION ON SUBCUTANEOUS TRANSCAPILLARY FLUID BALANCE.
41. Arne Kristian Sandvik: RAT GASTRIC HISTAMINE.
42. Carl Bredo Dahl: ANIMAL MODELS IN PSYCHIATRY.

1989

43. Torbjørn A. Fredriksen: CERVICOGENIC HEADACHE.
44. Rolf A. Walstad: CEFTAZIDIME.
45. Rolf Salvesen: THE PUPIL IN CLUSTER HEADACHE.
46. Nils Petter Jørgensen: DRUG EXPOSURE IN EARLY PREGNANCY.
47. Johan C. Ræder: PREMEDICATION AND GENERAL ANAESTHESIA IN OUTPATIENT GYNECOLOGICAL SURGERY.
48. M. R. Shalaby: IMMUNOREGULATORY PROPERTIES OF TNF-α AND THE RELATED CYTOKINES.
49. Anders Waage: THE COMPLEX PATTERN OF CYTOKINES IN SEPTIC SHOCK.
50. Bjarne Christian Eriksen: ELECTROSTIMULATION OF THE PELVIC FLOOR IN FEMALE URINARY INCONTINENCE.
51. Tore B. Halvorsen: PROGNOSTIC FACTORS IN COLORECTAL CANCER.

1990

52. Asbjørn Nordby: CELLULAR TOXICITY OF ROENTGEN CONTRAST MEDIA.
53. Kåre E. Tvedt: X-RAY MICROANALYSIS OF BIOLOGICAL MATERIAL.
54. Tore C. Stiles: COGNITIVE VULNERABILITY FACTORS IN THE DEVELOPMENT AND MAINTENANCE OF DEPRESSION.
55. Eva Hofsli: TUMOR NECROSIS FACTOR AND MULTIDRUG RESISTANCE.
56. Helge S. Haarstad: TROPHIC EFFECTS OF CHOLECYSTOKININ AND SECRETIN ON THE RAT PANCREAS.
57. Lars Engebretsen: TREATMENT OF ACUTE ANTERIOR CRUCIATE LIGAMENT INJURIES.
58. Tarjei Rygnestad: DELIBERATE SELF-POISONING IN TRONDHEIM.
59. Arne Z. Henriksen: STUDIES ON CONSERVED ANTIGENIC DOMAINS ON MAJOR OUTER MEMBRANE PROTEINS FROM ENTEROBACTERIA.
60. Steinar Westin: UNEMPLOYMENT AND HEALTH: Medical and social consequences of a factory closure in a ten-year controlled follow-up study.
61. Ylva Sahlin: INJURY REGISTRATION, a tool for accident preventive work.
62. Helge Bjørnstad Pettersen: BIOSYNTHESIS OF COMPLEMENT BY HUMAN ALVEOLAR MACROPHAGES WITH SPECIAL REFERENCE TO SARCOIDOSIS.
63. Berit Schei: TRAPPED IN PAINFUL LOVE.
64. Lars J. Vatten: PROSPECTIVE STUDIES OF THE RISK OF BREAST CANCER IN A COHORT OF NORWEGIAN WOMAN.

1991

65. Kåre Bergh: APPLICATIONS OF ANTI-C5a SPECIFIC MONOCLONAL ANTIBODIES FOR THE ASSESSMENT OF COMPLEMENT ACTIVATION.
66. Svein Svenningsen: THE CLINICAL SIGNIFICANCE OF INCREASED FEMORAL ANTEVERSION.
67. Olbjørn Klepp: NONSEMINOMATOUS GERM CELL TESTIS CANCER: THERAPEUTIC OUTCOME AND PROGNOSTIC FACTORS.
68. Trond Sand: THE EFFECTS OF CLICK POLARITY ON BRAINSTEM AUDITORY EVOKED POTENTIALS AMPLITUDE, DISPERSION, AND LATENCY VARIABLES.
69. Kjetil B. Åsbakk: STUDIES OF A PROTEIN FROM PSORIATIC SCALE, PSO P27, WITH RESPECT TO ITS POTENTIAL ROLE IN IMMUNE REACTIONS IN PSORIASIS.
70. Arnulf Hestnes: STUDIES ON DOWN´S SYNDROME.
71. Randi Nygaard: LONG-TERM SURVIVAL IN CHILDHOOD LEUKEMIA.
72. Bjørn Hagen: THIO-TEPA.
73. Svein Anda: EVALUATION OF THE HIP JOINT BY COMPUTED TOMOGRAMPHY AND ULTRASONOGRAPHY.

1992

74. Martin Svartberg: AN INVESTIGATION OF PROCESS AND OUTCOME OF SHORT-TERM PSYCHODYNAMIC PSYCHOTHERAPY.
75. Stig Arild Slørdahl: AORTIC REGURGITATION.
76. Harold C Sexton: STUDIES RELATING TO THE TREATMENT OF SYMPTOMATIC NON-PSYCHOTIC PATIENTS.
77. Maurice B. Vincent: VASOACTIVE PEPTIDES IN THE OCULAR/FOREHEAD AREA.
78. Terje Johannessen: CONTROLLED TRIALS IN SINGLE SUBJECTS.
79. Turid Nilsen: PYROPHOSPHATE IN HEPATOCYTE IRON METABOLISM.
80. Olav Haraldseth: NMR SPECTROSCOPY OF CEREBRAL ISCHEMIA AND REPERFUSION IN RAT.
81. Eiliv Brenna: REGULATION OF FUNCTION AND GROWTH OF THE OXYNTIC MUCOSA.

1993

82. Gunnar Bovim: CERVICOGENIC HEADACHE.
83. Jarl Arne Kahn: ASSISTED PROCREATION.
84. Bjørn Naume: IMMUNOREGULATORY EFFECTS OF CYTOKINES ON NK CELLS.
85. Rune Wiseth: AORTIC VALVE REPLACEMENT.
86. Jie Ming Shen: BLOOD FLOW VELOCITY AND RESPIRATORY STUDIES.
87. Piotr Kruszewski: SUNCT SYNDROME WITH SPECIAL REFERENCE TO THE AUTONOMIC NERVOUS SYSTEM.
88. Mette Haase Moen: ENDOMETRIOSIS.
89. Anne Vik: VASCULAR GAS EMBOLISM DURING AIR INFUSION AND AFTER DECOMPRESSION IN PIGS.
90. Lars Jacob Stovner: THE CHIARI TYPE I MALFORMATION.
91. Kjell Å. Salvesen: ROUTINE ULTRASONOGRAPHY IN UTERO AND DEVELOPMENT IN CHILDHOOD.

1994

92. Nina-Beate Liabakk: DEVELOPMENT OF IMMUNOASSAYS FOR TNF AND ITS SOLUBLE RECEPTORS.
93. Sverre Helge Torp: *erb*B ONCOGENES IN HUMAN GLIOMAS AND MENINGIOMAS.
94. Olav M. Linaker: MENTAL RETARDATION AND PSYCHIATRY. Past and present.
95. Per Oscar Feet: INCREASED ANTIDEPRESSANT AND ANTIPANIC EFFECT IN COMBINED TREATMENT WITH DIXYRAZINE AND TRICYCLIC ANTIDEPRESSANTS.
96. Stein Olav Samstad: CROSS SECTIONAL FLOW VELOCITY PROFILES FROM TWO-DIMENSIONAL DOPPLER ULTRASOUND: Studies on early mitral blood flow.
97. Bjørn Backe: STUDIES IN ANTENATAL CARE.
98. Gerd Inger Ringdal: QUALITY OF LIFE IN CANCER PATIENTS.
99. Torvid Kiserud: THE DUCTUS VENOSUS IN THE HUMAN FETUS.
100. Hans E. Fjøsne: HORMONAL REGULATION OF PROSTATIC METABOLISM.
101. Eylert Brodtkorb: CLINICAL ASPECTS OF EPILEPSY IN THE MENTALLY RETARDED.
102. Roar Juul: PEPTIDERGIC MECHANISMS IN HUMAN SUBARACHNOID HEMORRHAGE.
103. Unni Syversen: CHROMOGRANIN A. Phsysiological and Clinical Role.

1995

104. Odd Gunnar Brakstad: THERMOSTABLE NUCLEASE AND THE *nuc* GENE IN THE DIAGNOSIS OF *Staphylococcus aureus* INFECTIONS.
105. Terje Engan: NUCLEAR MAGNETIC RESONANCE (NMR) SPECTROSCOPY OF PLASMA IN MALIGNANT DISEASE.
106. Kirsten Rasmussen: VIOLENCE IN THE MENTALLY DISORDERED.
107. Finn Egil Skjeldestad: INDUCED ABORTION: Timetrends and Determinants.
108. Roar Stenseth: THORACIC EPIDURAL ANALGESIA IN AORTOCORONARY BYPASS SURGERY.
109. Arild Faxvaag: STUDIES OF IMMUNE CELL FUNCTION *in mice infected with* MURINE RETROVIRUS.

1996

110. Svend Aakhus: NONINVASIVE COMPUTERIZED ASSESSMENT OF LEFT VENTRICULAR FUNCTION AND SYSTEMIC ARTERIAL PROPERTIES. Methodology and some clinical applications.
111. Klaus-Dieter Bolz: INTRAVASCULAR ULTRASONOGRAPHY.
112. Petter Aadahl: CARDIOVASCULAR EFFECTS OF THORACIC AORTIC CROSS-CLAMPING.
113. Sigurd Steinshamn: CYTOKINE MEDIATORS DURING GRANULOCYTOPENIC INFECTIONS.
114. Hans Stifoss-Hanssen: SEEKING MEANING OR HAPPINESS?
115. Anne Kvikstad: LIFE CHANGE EVENTS AND MARITAL STATUS IN RELATION TO RISK AND PROGNOSIS OF CANCER.
116. Torbjørn Grøntvedt: TREATMENT OF ACUTE AND CHRONIC ANTERIOR CRUCIATE LIGAMENT INJURIES. A clinical and biomechanical study.
117. Sigrid Hørven Wigers: CLINICAL STUDIES OF FIBROMYALGIA WITH FOCUS ON ETIOLOGY, TREATMENT AND OUTCOME.
118. Jan Schjøtt: MYOCARDIAL PROTECTION: Functional and Metabolic Characteristics of Two Endogenous Protective Principles.
119. Marit Martinussen: STUDIES OF INTESTINAL BLOOD FLOW AND ITS RELATION TO TRANSITIONAL CIRCULATORY ADAPATION IN NEWBORN INFANTS.
120. Tomm B. Müller: MAGNETIC RESONANCE IMAGING IN FOCAL CEREBRAL ISCHEMIA.
121. Rune Haaverstad: OEDEMA FORMATION OF THE LOWER EXTREMITIES.
122. Magne Børset: THE ROLE OF CYTOKINES IN MULTIPLE MYELOMA, WITH SPECIAL REFERENCE TO HEPATOCYTE GROWTH FACTOR.
123. Geir Smedslund: A THEORETICAL AND EMPIRICAL INVESTIGATION OF SMOKING, STRESS AND DISEASE: RESULTS FROM A POPULATION SURVEY.

1997

124. Torstein Vik: GROWTH, MORBIDITY, AND PSYCHOMOTOR DEVELOPMENT IN INFANTS WHO WERE GROWTH RETARDED *IN UTERO*.
125. Siri Forsmo: ASPECTS AND CONSEQUENCES OF OPPORTUNISTIC SCREENING FOR CERVICAL CANCER. Results based on data from three Norwegian counties.
126. Jon S. Skranes: CEREBRAL MRI AND NEURODEVELOPMENTAL OUTCOME IN VERY LOW BIRTH WEIGHT (VLBW) CHILDREN. A follow-up study of a geographically based year cohort of VLBW children at ages one and six years.
127. Knut Bjørnstad: COMPUTERIZED ECHOCARDIOGRAPHY FOR EVALUTION OF CORONARY ARTERY DISEASE.
128. Grethe Elisabeth Borchgrevink: DIAGNOSIS AND TREATMENT OF WHIPLASH/NECK SPRAIN INJURIES CAUSED BY CAR ACCIDENTS.
129. Tor Elsås: NEUROPEPTIDES AND NITRIC OXIDE SYNTHASE IN OCULAR AUTONOMIC AND SENSORY NERVES.
130. Rolf W. Gråwe: EPIDEMIOLOGICAL AND NEUROPSYCHOLOGICAL PERSPECTIVES ON SCHIZOPHRENIA.
131. Tonje Strømholm: CEREBRAL HAEMODYNAMICS DURING THORACIC AORTIC CROSSCLAMPING. An experimental study in pigs

1998

132. Martinus Bråten: STUDIES ON SOME PROBLEMS REALTED TO INTRAMEDULLARY NAILING OF FEMORAL FRACTURES.

133. Ståle Nordgård: PROLIFERATIVE ACTIVITY AND DNA CONTENT AS PROGNOSTIC INDICATORS IN ADENOID CYSTIC CARCINOMA OF THE HEAD AND NECK.
134. Egil Lien: SOLUBLE RECEPTORS FOR **TNF** AND **LPS**: RELEASE PATTERN AND POSSIBLE SIGNIFICANCE IN DISEASE.
135. Marit Bjørgaas: HYPOGLYCAEMIA IN CHILDREN WITH DIABETES MELLITUS
136. Frank Skorpen: GENETIC AND FUNCTIONAL ANALYSES OF DNA REPAIR IN HUMAN CELLS.
137. Juan A. Pareja: SUNCT SYNDROME. ON THE CLINICAL PICTURE. ITS DISTINCTION FROM OTHER, SIMILAR HEADACHES.
138. Anders Angelsen: NEUROENDOCRINE CELLS IN HUMAN PROSTATIC CARCINOMAS AND THE PROSTATIC COMPLEX OF RAT, GUINEA PIG, CAT AND DOG.
139. Fabio Antonaci: CHRONIC PAROXYSMAL HEMICRANIA AND HEMICRANIA CONTINUA: TWO DIFFERENT ENTITIES?
140. Sven M. Carlsen: ENDOCRINE AND METABOLIC EFFECTS OF METFORMIN WITH SPECIAL EMPHASIS ON CARDIOVASCULAR RISK FACTORES.

1999

141. Terje A. Murberg: DEPRESSIVE SYMPTOMS AND COPING AMONG PATIENTS WITH CONGESTIVE HEART FAILURE.
142. Harm-Gerd Karl Blaas: THE EMBRYONIC EXAMINATION. Ultrasound studies on the development of the human embryo.
143. Noèmi Becser Andersen:THE CEPHALIC SENSORY NERVES IN UNILATERAL HEADACHES. Anatomical background and neurophysiological evaluation.
144. Eli-Janne Fiskerstrand: LASER TREATMENT OF PORT WINE STAINS. A study of the efficacy and limitations of the pulsed dye laser. Clinical and morfological analyses aimed at improving the therapeutic outcome.
145. Bård Kulseng: A STUDY OF ALGINATE CAPSULE PROPERTIES AND CYTOKINES IN RELATION TO INSULIN DEPENDENT DIABETES MELLITUS.
146. Terje Haug: STRUCTURE AND REGULATION OF THE HUMAN UNG GENE ENCODING URACIL-DNA GLYCOSYLASE.
147. Heidi Brurok: MANGANESE AND THE HEART. A Magic Metal with Diagnostic and Therapeutic Possibilites.
148. Agnes Kathrine Lie: DIAGNOSIS AND PREVALENCE OF HUMAN PAPILLOMAVIRUS INFECTION IN CERVICAL INTRAEPITELIAL NEOPLASIA. Relationship to Cell Cycle Regulatory Proteins and HLA DQBI Genes.
149. Ronald Mårvik: PHARMACOLOGICAL, PHYSIOLOGICAL AND PATHOPHYSIOLOGICAL STUDIES ON ISOLATED STOMACS.
150. Ketil Jarl Holen: THE ROLE OF ULTRASONOGRAPHY IN THE DIAGNOSIS AND TREATMENT OF HIP DYSPLASIA IN NEWBORNS.
151. Irene Hetlevik: THE ROLE OF CLINICAL GUIDELINES IN CARDIOVASCULAR RISK INTERVENTION IN GENERAL PRACTICE.
152. Katarina Tunòn: ULTRASOUND AND PREDICTION OF GESTATIONAL AGE.
153. Johannes Soma: INTERACTION BETWEEN THE LEFT VENTRICLE AND THE SYSTEMIC ARTERIES.
154. Arild Aamodt: DEVELOPMENT AND PRE-CLINICAL EVALUATION OF A CUSTOM-MADE FEMORAL STEM.
155. Agnar Tegnander: DIAGNOSIS AND FOLLOW-UP OF CHILDREN WITH SUSPECTED OR KNOWN HIP DYSPLASIA.
156. Bent Indredavik: STROKE UNIT TREATMENT: SHORT AND LONG-TERM EFFECTS
157. Jolanta Vanagaite Vingen: PHOTOPHOBIA AND PHONOPHOBIA IN PRIMARY HEADACHES

2000

158. Ola Dalsegg Sæther: PATHOPHYSIOLOGY DURING PROXIMAL AORTIC CROSS-CLAMPING CLINICAL AND EXPERIMENTAL STUDIES
159. xxxxxxxxx (blind number)
160. Christina Vogt Isaksen: PRENATAL ULTRASOUND AND POSTMORTEM FINDINGS – A TEN YEAR CORRELATIVE STUDY OF FETUSES AND INFANTS WITH DEVELOPMENTAL ANOMALIES.
161. Holger Seidel: HIGH-DOSE METHOTREXATE THERAPY IN CHILDREN WITH ACUTE LYMPHOCYTIC LEUKEMIA: DOSE, CONCENTRATION, AND EFFECT CONSIDERATIONS.

162. Stein Hallan: IMPLEMENTATION OF MODERN MEDICAL DECISION ANALYSIS INTO CLINICAL DIAGNOSIS AND TREATMENT.
163. Malcolm Sue-Chu: INVASIVE AND NON-INVASIVE STUDIES IN CROSS-COUNTRY SKIERS WITH ASTHMA-LIKE SYMPTOMS.
164. Ole-Lars Brekke: EFFECTS OF ANTIOXIDANTS AND FATTY ACIDS ON TUMOR NECROSIS FACTOR-INDUCED CYTOTOXICITY.
165. Jan Lundbom: AORTOCORONARY BYPASS SURGERY: CLINICAL ASPECTS, COST CONSIDERATIONS AND WORKING ABILITY.
166. John-Anker Zwart: LUMBAR NERVE ROOT COMPRESSION, BIOCHEMICAL AND NEUROPHYSIOLOGICAL ASPECTS.
167. Geir Falck: HYPEROSMOLALITY AND THE HEART.
168. Eirik Skogvoll: CARDIAC ARREST Incidence, Intervention and Outcome.
169. Dalius Bansevicius: SHOULDER-NECK REGION IN CERTAIN HEADACHES AND CHRONIC PAIN SYNDROMES.
170. Bettina Kinge: REFRACTIVE ERRORS AND BIOMETRIC CHANGES AMONG UNIVERSITY STUDENTS IN NORWAY.
171. Gunnar Qvigstad: CONSEQUENCES OF HYPERGASTRINEMIA IN MAN
172. Hanne Ellekjær: EPIDEMIOLOGICAL STUDIES OF STROKE IN A NORWEGIAN POPULATION. INCIDENCE, RISK FACTORS AND PROGNOSIS
173. Hilde Grimstad: VIOLENCE AGAINST WOMEN AND PREGNANCY OUTCOME.
174. Astrid Hjelde: SURFACE TENSION AND COMPLEMENT ACTIVATION: Factors influencing bubble formation and bubble effects after decompression.
175. Kjell A. Kvistad: MR IN BREAST CANCER – A CLINICAL STUDY.
176. Ivar Rossvoll: ELECTIVE ORTHOPAEDIC SURGERY IN A DEFINED POPULATION. Studies on demand, waiting time for treatment and incapacity for work.
177. Carina Seidel: PROGNOSTIC VALUE AND BIOLOGICAL EFFECTS OF HEPATOCYTE GROWTH FACTOR AND SYNDECAN-1 IN MULTIPLE MYELOMA.

2001

178. Alexander Wahba: THE INFLUENCE OF CARDIOPULMONARY BYPASS ON PLATELET FUNCTION AND BLOOD COAGULATION – DETERMINANTS AND CLINICAL CONSEQUENSES
179. Marcus Schmitt-Egenolf: THE RELEVANCE OF THE MAJOR hISTOCOMPATIBILITY COMPLEX FOR THE GENETICS OF PSORIASIS
180. Odrun Arna Gederaas: BIOLOGICAL MECHANISMS INVOLVED IN 5-AMINOLEVULINIC ACID BASED PHOTODYNAMIC THERAPY
181. Pål Richard Romundstad: CANCER INCIDENCE AMONG NORWEGIAN ALUMINIUM WORKERS
182. Henrik Hjorth-Hansen: NOVEL CYTOKINES IN GROWTH CONTROL AND BONE DISEASE OF MULTIPLE MYELOMA
183. Gunnar Morken: SEASONAL VARIATION OF HUMAN MOOD AND BEHAVIOUR
184. Bjørn Olav Haugen: MEASUREMENT OF CARDIAC OUTPUT AND STUDIES OF VELOCITY PROFILES IN AORTIC AND MITRAL FLOW USING TWO- AND THREE-DIMENSIONAL COLOUR FLOW IMAGING
185. Geir Bråthen: THE CLASSIFICATION AND CLINICAL DIAGNOSIS OF ALCOHOL-RELATED SEIZURES
186. Knut Ivar Aasarød: RENAL INVOLVEMENT IN INFLAMMATORY RHEUMATIC DISEASE. A Study of Renal Disease in Wegener's Granulomatosis and in Primary Sjögren's Syndrome
187. Trude Helen Flo: RESEPTORS INVOLVED IN CELL ACTIVATION BY DEFINED URONIC ACID POLYMERS AND BACTERIAL COMPONENTS
188. Bodil Kavli: HUMAN URACIL-DNA GLYCOSYLASES FROM THE UNG GENE: STRUCTRUAL BASIS FOR SUBSTRATE SPECIFICITY AND REPAIR
189. Liv Thommesen: MOLECULAR MECHANISMS INVOLVED IN TNF- AND GASTRIN-MEDIATED GENE REGULATION
190. Turid Lingaas Holmen: SMOKING AND HEALTH IN ADOLESCENCE; THE NORD-TRØNDELAG HEALTH STUDY, 1995-97
191. Øyvind Hjertner: MULTIPLE MYELOMA: INTERACTIONS BETWEEN MALIGNANT PLASMA CELLS AND THE BONE MICROENVIRONMENT

192. Asbjørn Støylen: STRAIN RATE IMAGING OF THE LEFT VENTRICLE BY ULTRASOUND. FEASIBILITY, CLINICAL VALIDATION AND PHYSIOLOGICAL ASPECTS
193. Kristian Midthjell: DIABETES IN ADULTS IN NORD-TRØNDELAG. PUBLIC HEALTH ASPECTS OF DIABETES MELLITUS IN A LARGE, NON-SELECTED NORWEGIAN POPULATION.
194. Guanglin Cui: FUNCTIONAL ASPECTS OF THE ECL CELL IN RODENTS
195. Ulrik Wisløff: CARDIAC EFFECTS OF AEROBIC ENDURANCE TRAINING: HYPERTROPHY, CONTRACTILITY AND CALCUIM HANDLING IN NORMAL AND FAILING HEART
196. Øyvind Halaas: MECHANISMS OF IMMUNOMODULATION AND CELL-MEDIATED CYTOTOXICITY INDUCED BY BACTERIAL PRODUCTS
197. Tore Amundsen: PERFUSION MR IMAGING IN THE DIAGNOSIS OF PULMONARY EMBOLISM
198. Nanna Kurtze: THE SIGNIFICANCE OF ANXIETY AND DEPRESSION IN FATIQUE AND PATTERNS OF PAIN AMONG INDIVIDUALS DIAGNOSED WITH FIBROMYALGIA: RELATIONS WITH QUALITY OF LIFE, FUNCTIONAL DISABILITY, LIFESTYLE, EMPLOYMENT STATUS, CO-MORBIDITY AND GENDER
199. Tom Ivar Lund Nilsen: PROSPECTIVE STUDIES OF CANCER RISK IN NORD-TRØNDELAG: THE HUNT STUDY. Associations with anthropometric, socioeconomic, and lifestyle risk factors
200. Asta Kristine Håberg: A NEW APPROACH TO THE STUDY OF MIDDLE CEREBRAL ARTERY OCCLUSION IN THE RAT USING MAGNETIC RESONANCE TECHNIQUES

2002

201. Knut Jørgen Arntzen: PREGNANCY AND CYTOKINES
202. Henrik Døllner: INFLAMMATORY MEDIATORS IN PERINATAL INFECTIONS
203. Asta Bye: LOW FAT, LOW LACTOSE DIET USED AS PROPHYLACTIC TREATMENT OF ACUTE INTESTINAL REACTIONS DURING PELVIC RADIOTHERAPY. A PROSPECTIVE RANDOMISED STUDY.
204. Sylvester Moyo: STUDIES ON STREPTOCOCCUS AGALACTIAE (GROUP B STREPTOCOCCUS) SURFACE-ANCHORED MARKERS WITH EMPHASIS ON STRAINS AND HUMAN SERA FROM ZIMBABWE.
205. Knut Hagen: HEAD-HUNT: THE EPIDEMIOLOGY OF HEADACHE IN NORD-TRØNDELAG
206. Li Lixin: ON THE REGULATION AND ROLE OF UNCOUPLING PROTEIN-2 IN INSULIN PRODUCING ß-CELLS
207. Anne Hildur Henriksen: SYMPTOMS OF ALLERGY AND ASTHMA VERSUS MARKERS OF LOWER AIRWAY INFLAMMATION AMONG ADOLESCENTS
208. Egil Andreas Fors: NON-MALIGNANT PAIN IN RELATION TO PSYCHOLOGICAL AND ENVIRONTENTAL FACTORS. EXPERIENTAL AND CLINICAL STUDES OF PAIN WITH FOCUS ON FIBROMYALGIA
209. Pål Klepstad: MORPHINE FOR CANCER PAIN
210. Ingunn Bakke: MECHANISMS AND CONSEQUENCES OF PEROXISOME PROLIFERATOR-INDUCED HYPERFUNCTION OF THE RAT GASTRIN PRODUCING CELL
211. Ingrid Susann Gribbestad: MAGNETIC RESONANCE IMAGING AND SPECTROSCOPY OF BREAST CANCER
212. Rønnaug Astri Ødegård: PREECLAMPSIA – MATERNAL RISK FACTORS AND FETAL GROWTH
213. Johan Haux: STUDIES ON CYTOTOXICITY INDUCED BY HUMAN NATURAL KILLER CELLS AND DIGITOXIN
214. Turid Suzanne Berg-Nielsen: PARENTING PRACTICES AND MENTALLY DISORDERED ADOLESCENTS
215. Astrid Rydning: BLOOD FLOW AS A PROTECTIVE FACTOR FOR THE STOMACH MUCOSA. AN EXPERIMENTAL STUDY ON THE ROLE OF MAST CELLS AND SENSORY AFFERENT NEURONS

2003

216. Jan Pål Loennechen: HEART FAILURE AFTER MYOCARDIAL INFARCTION. Regional Differences, Myocyte Function, Gene Expression, and Response to Cariporide, Losartan, and Exercise Training.

217. Elisabeth Qvigstad: EFFECTS OF FATTY ACIDS AND OVER-STIMULATION ON INSULIN SECRETION IN MAN
218. Arne Åsberg: EPIDEMIOLOGICAL STUDIES IN HEREDITARY HEMOCHROMATOSIS: PREVALENCE, MORBIDITY AND BENEFIT OF SCREENING.
219. Johan Fredrik Skomsvoll: REPRODUCTIVE OUTCOME IN WOMEN WITH RHEUMATIC DISEASE. A population registry based study of the effects of inflammatory rheumatic disease and connective tissue disease on reproductive outcome in Norwegian women in 1967-1995.
220. Siv Mørkved: URINARY INCONTINENCE DURING PREGNANCY AND AFTER DELIVERY: EFFECT OF PELVIC FLOOR MUSCLE TRAINING IN PREVENTION AND TREATMENT
221. Marit S. Jordhøy: THE IMPACT OF COMPREHENSIVE PALLIATIVE CARE
222. Tom Christian Martinsen: HYPERGASTRINEMIA AND HYPOACIDITY IN RODENTS – CAUSES AND CONSEQUENCES
223. Solveig Tingulstad: CENTRALIZATION OF PRIMARY SURGERY FOR OVARAIN CANCER. FEASIBILITY AND IMPACT ON SURVIVAL
224. Haytham Eloqayli: METABOLIC CHANGES IN THE BRAIN CAUSED BY EPILEPTIC SEIZURES
225. Torunn Bruland: STUDIES OF EARLY RETROVIRUS-HOST INTERACTIONS – VIRAL DETERMINANTS FOR PATHOGENESIS AND THE INFLUENCE OF SEX ON THE SUSCEPTIBILITY TO FRIEND MURINE LEUKAEMIA VIRUS INFECTION
226. Torstein Hole: DOPPLER ECHOCARDIOGRAPHIC EVALUATION OF LEFT VENTRICULAR FUNCTION IN PATIENTS WITH ACUTE MYOCARDIAL INFARCTION
227. Vibeke Nossum: THE EFFECT OF VASCULAR BUBBLES ON ENDOTHELIAL FUNCTION
228. Sigurd Fasting: ROUTINE BASED RECORDING OF ADVERSE EVENTS DURING ANAESTHESIA – APPLICATION IN QUALITY IMPROVEMENT AND SAFETY
229. Solfrid Romundstad: EPIDEMIOLOGICAL STUDIES OF MICROALBUMINURIA. THE NORD-TRØNDELAG HEALTH STUDY 1995-97 (HUNT 2)
230. Geir Torheim: PROCESSING OF DYNAMIC DATA SETS IN MAGNETIC RESONANCE IMAGING
231. Catrine Ahlén: SKIN INFECTIONS IN OCCUPATIONAL SATURATION DIVERS IN THE NORTH SEA AND THE IMPACT OF THE ENVIRONMENT
232. Arnulf Langhammer: RESPIRATORY SYMPTOMS, LUNG FUNCTION AND BONE MINERAL DENSITY IN A COMPREHENSIVE POPULATION SURVEY. THE NORD-TRØNDELAG HEALTH STUDY 1995-97. THE BRONCHIAL OBSTRUCTION IN NORD-TRØNDELAG STUDY
233. Einar Kjelsås: EATING DISORDERS AND PHYSICAL ACTIVITY IN NON-CLINICAL SAMPLES
234. Arne Wibe: RECTAL CANCER TREATMENT IN NORWAY – STANDARDISATION OF SURGERY AND QUALITY ASSURANCE

2004

235. Eivind Witsø: BONE GRAFT AS AN ANTIBIOTIC CARRIER
236. Anne Mari Sund: DEVELOPMENT OF DEPRESSIVE SYMPTOMS IN EARLY ADOLESCENCE
237. Hallvard Lærum: EVALUATION OF ELECTRONIC MEDICAL RECORDS – A CLINICAL TASK PERSPECTIVE
238. Gustav Mikkelsen: ACCESSIBILITY OF INFORMATION IN ELECTRONIC PATIENT RECORDS; AN EVALUATION OF THE ROLE OF DATA QUALITY
239. Steinar Krokstad: SOCIOECONOMIC INEQUALITIES IN HEALTH AND DISABILITY. SOCIAL EPIDEMIOLOGY IN THE NORD-TRØNDELAG HEALTH STUDY (HUNT), NORWAY
240. Arne Kristian Myhre: NORMAL VARIATION IN ANOGENITAL ANATOMY AND MICROBIOLOGY IN NON-ABUSED PRESCHOOL CHILDREN
241. Ingunn Dybedal: NEGATIVE REGULATORS OF HEMATOPOIETEC STEM AND PROGENITOR CELLS
242. Beate Sitter: TISSUE CHARACTERIZATION BY HIGH RESOLUTION MAGIC ANGLE SPINNING MR SPECTROSCOPY
243. Per Arne Aas: MACROMOLECULAR MAINTENANCE IN HUMAN CELLS – REPAIR OF URACIL IN DNA AND METHYLATIONS IN DNA AND RNA

244. Anna Bofin: FINE NEEDLE ASPIRATION CYTOLOGY IN THE PRIMARY INVESTIGATION OF BREAST TUMOURS AND IN THE DETERMINATION OF TREATMENT STRATEGIES
245. Jim Aage Nøttestad: DEINSTITUTIONALIZATION AND MENTAL HEALTH CHANGES AMONG PEOPLE WITH MENTAL RETARDATION
246. Reidar Fossmark: GASTRIC CANCER IN JAPANESE COTTON RATS
247. Wibeke Nordhøy: MANGANESE AND THE HEART, INTRACELLULAR MR RELAXATION AND WATER EXCHANGE ACROSS THE CARDIAC CELL MEMBRANE

2005

248. Sturla Molden: QUANTITATIVE ANALYSES OF SINGLE UNITS RECORDED FROM THE HIPPOCAMPUS AND ENTORHINAL CORTEX OF BEHAVING RATS
249. Wenche Brenne Drøyvold: EPIDEMIOLOGICAL STUDIES ON WEIGHT CHANGE AND HEALTH IN A LARGE POPULATION. THE NORD-TRØNDELAG HEALTH STUDY (HUNT)
250. Ragnhild Støen: ENDOTHELIUM-DEPENDENT VASODILATION IN THE FEMORAL ARTERY OF DEVELOPING PIGLETS
251. Aslak Steinsbekk: HOMEOPATHY IN THE PREVENTION OF UPPER RESPIRATORY TRACT INFECTIONS IN CHILDREN
252. Hill-Aina Steffenach: MEMORY IN HIPPOCAMPAL AND CORTICO-HIPPOCAMPAL CIRCUITS
253. Eystein Stordal: ASPECTS OF THE EPIDEMIOLOGY OF DEPRESSIONS BASED ON SELF-RATING IN A LARGE GENERAL HEALTH STUDY (THE HUNT-2 STUDY)
254. Viggo Pettersen: FROM MUSCLES TO SINGING: THE ACTIVITY OF ACCESSORY BREATHING MUSCLES AND THORAX MOVEMENT IN CLASSICAL SINGING
255. Marianne Fyhn: SPATIAL MAPS IN THE HIPPOCAMPUS AND ENTORHINAL CORTEX
256. Robert Valderhaug: OBSESSIVE-COMPULSIVE DISORDER AMONG CHILDREN AND ADOLESCENTS: CHARACTERISTICS AND PSYCHOLOGICAL MANAGEMENT OF PATIENTS IN OUTPATIENT PSYCHIATRIC CLINICS
257. Erik Skaaheim Haug: INFRARENAL ABDOMINAL AORTIC ANEURYSMS – COMORBIDITY AND RESULTS FOLLOWING OPEN SURGERY
258. Daniel Kondziella: GLIAL-NEURONAL INTERACTIONS IN EXPERIMENTAL BRAIN DISORDERS
259. Vegard Heimly Brun: ROUTES TO SPATIAL MEMORY IN HIPPOCAMPAL PLACE CELLS
260. Kenneth McMillan: PHYSIOLOGICAL ASSESSMENT AND TRAINING OF ENDURANCE AND STRENGTH IN PROFESSIONAL YOUTH SOCCER PLAYERS
261. Marit Sæbø Indredavik: MENTAL HEALTH AND CEREBRAL MAGNETIC RESONANCE IMAGING IN ADOLESCENTS WITH LOW BIRTH WEIGHT
262. Ole Johan Kemi: ON THE CELLULAR BASIS OF AEROBIC FITNESS, INTENSITY-DEPENDENCE AND TIME-COURSE OF CARDIOMYOCYTE AND ENDOTHELIAL ADAPTATIONS TO EXERCISE TRAINING
263. Eszter Vanky: POLYCYSTIC OVARY SYNDROME – METFORMIN TREATMENT IN PREGNANCY
264. Hild Fjærtoft: EXTENDED STROKE UNIT SERVICE AND EARLY SUPPORTED DISCHARGE. SHORT AND LONG-TERM EFFECTS
265. Grete Dyb: POSTTRAUMATIC STRESS REACTIONS IN CHILDREN AND ADOLESCENTS
266. Vidar Fykse: SOMATOSTATIN AND THE STOMACH
267. Kirsti Berg: OXIDATIVE STRESS AND THE ISCHEMIC HEART: A STUDY IN PATIENTS UNDERGOING CORONARY REVASCULARIZATION
268. Björn Inge Gustafsson: THE SEROTONIN PRODUCING ENTEROCHROMAFFIN CELL, AND EFFECTS OF HYPERSEROTONINEMIA ON HEART AND BONE

2006

269. Torstein Baade Rø: EFFECTS OF BONE MORPHOGENETIC PROTEINS, HEPATOCYTE GROWTH FACTOR AND INTERLEUKIN-21 IN MULTIPLE MYELOMA
270. May-Britt Tessem: METABOLIC EFFECTS OF ULTRAVIOLET RADIATION ON THE ANTERIOR PART OF THE EYE
271. Anne-Sofie Helvik: COPING AND EVERYDAY LIFE IN A POPULATION OF ADULTS WITH HEARING IMPAIRMENT

272. Therese Standal: MULTIPLE MYELOMA: THE INTERPLAY BETWEEN MALIGNANT PLASMA CELLS AND THE BONE MARROW MICROENVIRONMENT
273. Ingvild Saltvedt: TREATMENT OF ACUTELY SICK, FRAIL ELDERLY PATIENTS IN A GERIATRIC EVALUATION AND MANAGEMENT UNIT – RESULTS FROM A PROSPECTIVE RANDOMISED TRIAL
274. Birger Henning Endreseth: STRATEGIES IN RECTAL CANCER TREATMENT – FOCUS ON EARLY RECTAL CANCER AND THE INFLUENCE OF AGE ON PROGNOSIS
275. Anne Mari Aukan Rokstad: ALGINATE CAPSULES AS BIOREACTORS FOR CELL THERAPY
276. Mansour Akbari: HUMAN BASE EXCISION REPAIR FOR PRESERVATION OF GENOMIC STABILITY
277. Stein Sundstrøm: IMPROVING TREATMENT IN PATIENTS WITH LUNG CANCER – RESULTS FROM TWO MULITCENTRE RANDOMISED STUDIES
278. Hilde Pleym: BLEEDING AFTER CORONARY ARTERY BYPASS SURGERY - STUDIES ON HEMOSTATIC MECHANISMS, PROPHYLACTIC DRUG TREATMENT AND EFFECTS OF AUTOTRANSFUSION
279. Line Merethe Oldervoll: PHYSICAL ACTIVITY AND EXERCISE INTERVENTIONS IN CANCER PATIENTS
280. Boye Welde: THE SIGNIFICANCE OF ENDURANCE TRAINING, RESISTANCE TRAINING AND MOTIVATIONAL STYLES IN ATHLETIC PERFORMANCE AMONG ELITE JUNIOR CROSS-COUNTRY SKIERS
281. Per Olav Vandvik: IRRITABLE BOWEL SYNDROME IN NORWAY, STUDIES OF PREVALENCE, DIAGNOSIS AND CHARACTERISTICS IN GENERAL PRACTICE AND IN THE POPULATION
282. Idar Kirkeby-Garstad: CLINICAL PHYSIOLOGY OF EARLY MOBILIZATION AFTER CARDIAC SURGERY
283. Linn Getz: SUSTAINABLE AND RESPONSIBLE PREVENTIVE MEDICINE. CONCEPTUALISING ETHICAL DILEMMAS ARISING FROM CLINICAL IMPLEMENTATION OF ADVANCING MEDICAL TECHNOLOGY
284. Eva Tegnander: DETECTION OF CONGENITAL HEART DEFECTS IN A NON-SELECTED POPULATION OF 42,381 FETUSES
285. Kristin Gabestad Nørsett: GENE EXPRESSION STUDIES IN GASTROINTESTINAL PATHOPHYSIOLOGY AND NEOPLASIA
286. Per Magnus Haram: GENETIC VS. AQUIRED FITNESS: METABOLIC, VASCULAR AND CARDIOMYOCYTE ADAPTATIONS
287. Agneta Johansson: GENERAL RISK FACTORS FOR GAMBLING PROBLEMS AND THE PREVALENCE OF PATHOLOGICAL GAMBLING IN NORWAY
288. Svein Artur Jensen: THE PREVALENCE OF SYMPTOMATIC ARTERIAL DISEASE OF THE LOWER LIMB
289. Charlotte Björk Ingul: QUANITIFICATION OF REGIONAL MYOCARDIAL FUNCTION BY STRAIN RATE AND STRAIN FOR EVALUATION OF CORONARY ARTERY DISEASE. AUTOMATED VERSUS MANUAL ANALYSIS DURING ACUTE MYOCARDIAL INFARCTION AND DOBUTAMINE STRESS ECHOCARDIOGRAPHY
290. Jakob Nakling: RESULTS AND CONSEQUENCES OF ROUTINE ULTRASOUND SCREENING IN PREGNANCY – A GEOGRAPHIC BASED POPULATION STUDY
291. Anne Engum: DEPRESSION AND ANXIETY – THEIR RELATIONS TO THYROID DYSFUNCTION AND DIABETES IN A LARGE EPIDEMIOLOGICAL STUDY
292. Ottar Bjerkeset: ANXIETY AND DEPRESSION IN THE GENERAL POPULATION: RISK FACTORS, INTERVENTION AND OUTCOME – THE NORD-TRØNDELAG HEALTH STUDY (HUNT)
293. Jon Olav Drogset: RESULTS AFTER SURGICAL TREATMENT OF ANTERIOR CRUCIATE LIGAMENT INJURIES – A CLINICAL STUDY
294. Lars Fosse: MECHANICAL BEHAVIOUR OF COMPACTED MORSELLISED BONE – AN EXPERIMENTAL IN VITRO STUDY
295. Gunilla Klensmeden Fosse: MENTAL HEALTH OF PSYCHIATRIC OUTPATIENTS BULLIED IN CHILDHOOD
296. Paul Jarle Mork: MUSCLE ACTIVITY IN WORK AND LEISURE AND ITS ASSOCIATION TO MUSCULOSKELETAL PAIN

297. Björn Stenström: LESSONS FROM RODENTS: I: MECHANISMS OF OBESITY SURGERY – ROLE OF STOMACH. II: CARCINOGENIC EFFECTS OF *HELICOBACTER PYLORI* AND SNUS IN THE STOMACH

2007

298. Haakon R. Skogseth: INVASIVE PROPERTIES OF CANCER – A TREATMENT TARGET ? IN VITRO STUDIES IN HUMAN PROSTATE CANCER CELL LINES
299. Janniche Hammer: GLUTAMATE METABOLISM AND CYCLING IN MESIAL TEMPORAL LOBE EPILEPSY
300. May Britt Drugli: YOUNG CHILDREN TREATED BECAUSE OF ODD/CD: CONDUCT PROBLEMS AND SOCIAL COMPETENCIES IN DAY-CARE AND SCHOOL SETTINGS
301. Arne Skjold: MAGNETIC RESONANCE KINETICS OF MANGANESE DIPYRIDOXYL DIPHOSPHATE (MnDPDP) IN HUMAN MYOCARDIUM. STUDIES IN HEALTHY VOLUNTEERS AND IN PATIENTS WITH RECENT MYOCARDIAL INFARCTION
302. Siri Malm: LEFT VENTRICULAR SYSTOLIC FUNCTION AND MYOCARDIAL PERFUSION ASSESSED BY CONTRAST ECHOCARDIOGRAPHY
303. Valentina Maria do Rosario Cabral Iversen: MENTAL HEALTH AND PSYCHOLOGICAL ADAPTATION OF CLINICAL AND NON-CLINICAL MIGRANT GROUPS
304. Lasse Løvstakken: SIGNAL PROCESSING IN DIAGNOSTIC ULTRASOUND: ALGORITHMS FOR REAL-TIME ESTIMATION AND VISUALIZATION OF BLOOD FLOW VELOCITY
305. Elisabeth Olstad: GLUTAMATE AND GABA: MAJOR PLAYERS IN NEURONAL METABOLISM
306. Lilian Leistad: THE ROLE OF CYTOKINES AND PHOSPHOLIPASE A_2s IN ARTICULAR CARTILAGE CHONDROCYTES IN RHEUMATOID ARTHRITIS AND OSTEOARTHRITIS
307. Arne Vaaler: EFFECTS OF PSYCHIATRIC INTENSIVE CARE UNIT IN AN ACUTE PSYCIATHRIC WARD
308. Mathias Toft: GENETIC STUDIES OF LRRK2 AND PINK1 IN PARKINSON'S DISEASE
309. Ingrid Løvold Mostad: IMPACT OF DIETARY FAT QUANTITY AND QUALITY IN TYPE 2 DIABETES WITH EMPHASIS ON MARINE N-3 FATTY ACIDS
310. Torill Eidhammer Sjøbakk: MR DETERMINED BRAIN METABOLIC PATTERN IN PATIENTS WITH BRAIN METASTASES AND ADOLESCENTS WITH LOW BIRTH WEIGHT
311. Vidar Beisvåg: PHYSIOLOGICAL GENOMICS OF HEART FAILURE: FROM TECHNOLOGY TO PHYSIOLOGY
312. Olav Magnus Søndenå Fredheim: HEALTH RELATED QUALITY OF LIFE ASSESSMENT AND ASPECTS OF THE CLINICAL PHARMACOLOGY OF METHADONE IN PATIENTS WITH CHRONIC NON-MALIGNANT PAIN
313. Anne Brantberg: FETAL AND PERINATAL IMPLICATIONS OF ANOMALIES IN THE GASTROINTESTINAL TRACT AND THE ABDOMINAL WALL
314. Erik Solligård: GUT LUMINAL MICRODIALYSIS
315. Elin Tollefsen: RESPIRATORY SYMPTOMS IN A COMPREHENSIVE POPULATION BASED STUDY AMONG ADOLESCENTS 13-19 YEARS. YOUNG-HUNT 1995-97 AND 2000-01; THE NORD-TRØNDELAG HEALTH STUDIES (HUNT)
316. Anne-Tove Brenne: GROWTH REGULATION OF MYELOMA CELLS
317. Heidi Knobel: FATIGUE IN CANCER TREATMENT – ASSESSMENT, COURSE AND ETIOLOGY
318. Torbjørn Dahl: CAROTID ARTERY STENOSIS. DIAGNOSTIC AND THERAPEUTIC ASPECTS
319. Inge-Andre Rasmussen jr.: FUNCTIONAL AND DIFFUSION TENSOR MAGNETIC RESONANCE IMAGING IN NEUROSURGICAL PATIENTS
320. Grete Helen Bratberg: PUBERTAL TIMING – ANTECEDENT TO RISK OR RESILIENCE ? EPIDEMIOLOGICAL STUDIES ON GROWTH, MATURATION AND HEALTH RISK BEHAVIOURS; THE YOUNG HUNT STUDY, NORD-TRØNDELAG, NORWAY
321. Sveinung Sørhaug: THE PULMONARY NEUROENDOCRINE SYSTEM. PHYSIOLOGICAL, PATHOLOGICAL AND TUMOURIGENIC ASPECTS
322. Olav Sande Eftedal: ULTRASONIC DETECTION OF DECOMPRESSION INDUCED VASCULAR MICROBUBBLES
323. Rune Bang Leistad: PAIN, AUTONOMIC ACTIVATION AND MUSCULAR ACTIVITY RELATED TO EXPERIMENTALLY-INDUCED COGNITIVE STRESS IN HEADACHE PATIENTS

324. Svein Brekke: TECHNIQUES FOR ENHANCEMENT OF TEMPORAL RESOLUTION IN THREE-DIMENSIONAL ECHOCARDIOGRAPHY
325. Kristian Bernhard Nilsen: AUTONOMIC ACTIVATION AND MUSCLE ACTIVITY IN RELATION TO MUSCULOSKELETAL PAIN
326. Anne Irene Hagen: HEREDITARY BREAST CANCER IN NORWAY. DETECTION AND PROGNOSIS OF BREAST CANCER IN FAMILIES WITH *BRCA1*GENE MUTATION
327. Ingebjørg S. Juel : INTESTINAL INJURY AND RECOVERY AFTER ISCHEMIA. AN EXPERIMENTAL STUDY ON RESTITUTION OF THE SURFACE EPITHELIUM, INTESTINAL PERMEABILITY, AND RELEASE OF BIOMARKERS FROM THE MUCOSA
328. Runa Heimstad: POST-TERM PREGNANCY
329. Jan Egil Afset: ROLE OF ENTEROPATHOGENIC *ESCHERICHIA COLI* IN CHILDHOOD DIARRHOEA IN NORWAY
330. Bent Håvard Hellum: *IN VITRO* INTERACTIONS BETWEEN MEDICINAL DRUGS AND HERBS ON CYTOCHROME P-450 METABOLISM AND P-GLYCOPROTEIN TRANSPORT
331. Morten André Høydal: CARDIAC DYSFUNCTION AND MAXIMAL OXYGEN UPTAKE MYOCARDIAL ADAPTATION TO ENDURANCE TRAINING

2008

332. Andreas Møllerløkken: REDUCTION OF VASCULAR BUBBLES: METHODS TO PREVENT THE ADVERSE EFFECTS OF DECOMPRESSION
333. Anne Hege Aamodt: COMORBIDITY OF HEADACHE AND MIGRAINE IN THE NORD-TRØNDELAG HEALTH STUDY 1995-97
334. Brage Høyem Amundsen: MYOCARDIAL FUNCTION QUANTIFIED BY SPECKLE TRACKING AND TISSUE DOPPLER ECHOCARDIOGRAPHY – VALIDATION AND APPLICATION IN EXERCISE TESTING AND TRAINING
335. Inger Anne Næss: INCIDENCE, MORTALITY AND RISK FACTORS OF FIRST VENOUS THROMBOSIS IN A GENERAL POPULATION. RESULTS FROM THE SECOND NORD-TRØNDELAG HEALTH STUDY (HUNT2)
336. Vegard Bugten: EFFECTS OF POSTOPERATIVE MEASURES AFTER FUNCTIONAL ENDOSCOPIC SINUS SURGERY
337. Morten Bruvold: MANGANESE AND WATER IN CARDIAC MAGNETIC RESONANCE IMAGING
338. Miroslav Fris: THE EFFECT OF SINGLE AND REPEATED ULTRAVIOLET RADIATION ON THE ANTERIOR SEGMENT OF THE RABBIT EYE
339. Svein Arne Aase: METHODS FOR IMPROVING QUALITY AND EFFICIENCY IN QUANTITATIVE ECHOCARDIOGRAPHY – ASPECTS OF USING HIGH FRAME RATE
340. Roger Almvik: ASSESSING THE RISK OF VIOLENCE: DEVELOPMENT AND VALIDATION OF THE BRØSET VIOLENCE CHECKLIST
341. Ottar Sundheim: STRUCTURE-FUNCTION ANALYSIS OF HUMAN ENZYMES INITIATING NUCLEOBASE REPAIR IN DNA AND RNA
342. Anne Mari Undheim: SHORT AND LONG-TERM OUTCOME OF EMOTIONAL AND BEHAVIOURAL PROBLEMS IN YOUNG ADOLESCENTS WITH AND WITHOUT READING DIFFICULTIES
343. Helge Garåsen: THE TRONDHEIM MODEL. IMPROVING THE PROFESSIONAL COMMUNICATION BETWEEN THE VARIOUS LEVELS OF HEALTH CARE SERVICES AND IMPLEMENTATION OF INTERMEDIATE CARE AT A COMMUNITY HOSPITAL COULD PROVIDE BETTER CARE FOR OLDER PATIENTS. SHORT AND LONG TERM EFFECTS
344. Olav A. Foss: "THE ROTATION RATIOS METHOD". A METHOD TO DESCRIBE ALTERED SPATIAL ORIENTATION IN SEQUENTIAL RADIOGRAPHS FROM ONE PELVIS
345. Bjørn Olav Åsvold: THYROID FUNCTION AND CARDIOVASCULAR HEALTH
346. Torun Margareta Melø: NEURONAL GLIAL INTERACTIONS IN EPILEPSY
347. Irina Poliakova Eide: FETAL GROWTH RESTRICTION AND PRE-ECLAMPSIA: SOME CHARACTERISTICS OF FETO-MATERNAL INTERACTIONS IN DECIDUA BASALIS
348. Torunn Askim: RECOVERY AFTER STROKE. ASSESSMENT AND TREATMENT; WITH FOCUS ON MOTOR FUNCTION
349. Ann Elisabeth Åsberg: NEUTROPHIL ACTIVATION IN A ROLLER PUMP MODEL OF CARDIOPULMONARY BYPASS. INFLUENCE ON BIOMATERIAL, PLATELETS AND COMPLEMENT

350. Lars Hagen: REGULATION OF DNA BASE EXCISION REPAIR BY PROTEIN INTERACTIONS AND POST TRANSLATIONAL MODIFICATIONS
351. Sigrun Beate Kjøtrød: POLYCYSTIC OVARY SYNDROME – METFORMIN TREATMENT IN ASSISTED REPRODUCTION
352. Steven Keita Nishiyama: PERSPECTIVES ON LIMB-VASCULAR HETEROGENEITY: IMPLICATIONS FOR HUMAN AGING, SEX, AND EXERCISE
353. Sven Peter Näsholm: ULTRASOUND BEAMS FOR ENHANCED IMAGE QUALITY
354. Jon Ståle Ritland: PRIMARY OPEN-ANGLE GLAUCOMA & EXFOLIATIVE GLAUCOMA. SURVIVAL, COMORBIDITY AND GENETICS
355. Sigrid Botne Sando: ALZHEIMER'S DISEASE IN CENTRAL NORWAY. GENETIC AND EDUCATIONAL ASPECTS
356. Parvinder Kaur: CELLULAR AND MOLECULAR MECHANISMS BEHIND METHYLMERCURY-INDUCED NEUROTOXICITY
357. Ismail Cüneyt Güzey: DOPAMINE AND SEROTONIN RECEPTOR AND TRANSPORTER GENE POLYMORPHISMS AND EXTRAPYRAMIDAL SYMPTOMS. STUDIES IN PARKINSON'S DISEASE AND IN PATIENTS TREATED WITH ANTIPSYCHOTIC OR ANTIDEPRESSANT DRUGS
358. Brit Dybdahl: EXTRA-CELLULAR INDUCIBLE HEAT-SHOCK PROTEIN 70 (Hsp70) – A ROLE IN THE INFLAMMATORY RESPONSE ?
359. Kristoffer Haugarvoll: IDENTIFYING GENETIC CAUSES OF PARKINSON'S DISEASE IN NORWAY
360. Nadra Nilsen: TOLL-LIKE RECEPTOR 2 –EXPRESSION, REGULATION AND SIGNALING
361. Johan Håkon Bjørngaard: PATIENT SATISFACTION WITH OUTPATIENT MENTAL HEALTH SERVICES – THE INFLUENCE OF ORGANIZATIONAL FACTORS.
362. Kjetil Høydal : EFFECTS OF HIGH INTENSITY AEROBIC TRAINING IN HEALTHY SUBJECTS AND CORONARY ARTERY DISEASE PATIENTS; THE IMPORTANCE OF INTENSITY,, DURATION AND FREQUENCY OF TRAINING.
363. Trine Karlsen: TRAINING IS MEDICINE: ENDURANCE AND STRENGTH TRAINING IN CORONARY ARTERY DISEASE AND HEALTH.
364. Marte Thuen: MANGANASE-ENHANCED AND DIFFUSION TENSOR MR IMAGING OF THE NORMAL, INJURED AND REGENERATING RAT VISUAL PATHWAY
365. Cathrine Broberg Vågbø: DIRECT REPAIR OF ALKYLATION DAMAGE IN DNA AND RNA BY 2-OXOGLUTARATE- AND IRON-DEPENDENT DIOXYGENASES
366. Arnt Erik Tjønna: AEROBIC EXERCISE AND CARDIOVASCULAR RISK FACTORS IN OVERWEIGHT AND OBESE ADOLESCENTS AND ADULTS
367. Marianne W. Furnes: FEEDING BEHAVIOR AND BODY WEIGHT DEVELOPMENT: LESSONS FROM RATS
368. Lene N. Johannessen: FUNGAL PRODUCTS AND INFLAMMATORY RESPONSES IN HUMAN MONOCYTES AND EPITHELIAL CELLS
369. Anja Bye: GENE EXPRESSION PROFILING OF *INHERITED* AND *ACQUIRED* MAXIMAL OXYGEN UPTAKE – RELATIONS TO THE METABOLIC SYNDROME.
370. Oluf Dimitri Røe: MALIGNANT MESOTHELIOMA: VIRUS, BIOMARKERS AND GENES. A TRANSLATIONAL APPROACH
371. Ane Cecilie Dale: DIABETES MELLITUS AND FATAL ISCHEMIC HEART DISEASE. ANALYSES FROM THE HUNT1 AND 2 STUDIES
372. Jacob Christian Hølen: PAIN ASSESSMENT IN PALLIATIVE CARE: VALIDATION OF METHODS FOR SELF-REPORT AND BEHAVIOURAL ASSESSMENT
373. Erming Tian: THE GENETIC IMPACTS IN THE ONCOGENESIS OF MULTIPLE MYELOMA
374. Ole Bosnes: KLINISK UTPRØVING AV NORSKE VERSJONER AV NOEN SENTRALE TESTER PÅ KOGNITIV FUNKSJON
375. Ola M. Rygh: 3D ULTRASOUND BASED NEURONAVIGATION IN NEUROSURGERY. A CLINICAL EVALUATION
376. Astrid Kamilla Stunes: ADIPOKINES, PEROXISOME PROFILERATOR ACTIVATED RECEPTOR (PPAR) AGONISTS AND SEROTONIN. COMMON REGULATORS OF BONE AND FAT METABOLISM
377. Silje Engdal: HERBAL REMEDIES USED BY NORWEGIAN CANCER PATIENTS AND THEIR ROLE IN HERB-DRUG INTERACTIONS
378. Kristin Offerdal: IMPROVED ULTRASOUND IMAGING OF THE FETUS AND ITS CONSEQUENCES FOR SEVERE AND LESS SEVERE ANOMALIES

379. Øivind Rognmo: HIGH-INTENSITY AEROBIC EXERCISE AND CARDIOVASCULAR HEALTH
380. Jo-Åsmund Lund: RADIOTHERAPY IN ANAL CARCINOMA AND PROSTATE CANCER

2009

381. Tore Grüner Bjåstad: HIGH FRAME RATE ULTRASOUND IMAGING USING PARALLEL BEAMFORMING
382. Erik Søndenaa: INTELLECTUAL DISABILITIES IN THE CRIMINAL JUSTICE SYSTEM
383. Berit Rostad: SOCIAL INEQUALITIES IN WOMEN'S HEALTH, HUNT 1984-86 AND 1995-97, THE NORD-TRØNDELAG HEALTH STUDY (HUNT)
384. Jonas Crosby: ULTRASOUND-BASED QUANTIFICATION OF MYOCARDIAL DEFORMATION AND ROTATION
385. Erling Tronvik: MIGRAINE, BLOOD PRESSURE AND THE RENIN-ANGIOTENSIN SYSTEM
386. Tom Christensen: BRINGING THE GP TO THE FOREFRONT OF EPR DEVELOPMENT
387. Håkon Bergseng: ASPECTS OF GROUP B STREPTOCOCCUS (GBS) DISEASE IN THE NEWBORN. EPIDEMIOLOGY, CHARACTERISATION OF INVASIVE STRAINS AND EVALUATION OF INTRAPARTUM SCREENING
388. Ronny Myhre: GENETIC STUDIES OF CANDIDATE TENE3S IN PARKINSON'S DISEASE
389. Torbjørn Moe Eggebø: ULTRASOUND AND LABOUR
390. Eivind Wang: TRAINING IS MEDICINE FOR PATIENTS WITH PERIPHERAL ARTERIAL DISEASE
391. Thea Kristin Våtsveen: GENETIC ABERRATIONS IN MYELOMA CELLS
392. Thomas Jozefiak: QUALITY OF LIFE AND MENTAL HEALTH IN CHILDREN AND ADOLESCENTS: CHILD AND PARENT PERSPECTIVES
393. Jens Erik Slagsvold: N-3 POLYUNSATURATED FATTY ACIDS IN HEALTH AND DISEASE – CLINICAL AND MOLECULAR ASPECTS
394. Kristine Misund: A STUDY OF THE TRANSCRIPTIONAL REPRESSOR ICER. REGULATORY NETWORKS IN GASTRIN-INDUCED GENE EXPRESSION
395. Franco M. Impellizzeri: HIGH-INTENSITY TRAINING IN FOOTBALL PLAYERS. EFFECTS ON PHYSICAL AND TECHNICAL PERFORMANCE
396. Kari Hanne Gjeilo: HEALTH-RELATED QUALITY OF LIFE AND CHRONIC PAIN IN PATIENTS UNDERGOING CARDIAC SURGERY
397. Øyvind Hauso: NEUROENDOCRINE ASPECTS OF PHYSIOLOGY AND DISEASE
398. Ingvild Bjellmo Johnsen: INTRACELLULAR SIGNALING MECHANISMS IN THE INNATE IMMUNE RESPONSE TO VIRAL INFECTIONS
399. Linda Tømmerdal Roten: GENETIC PREDISPOSITION FOR DEVELOPMENT OF PREEMCLAMPSIA – CANDIDATE GENE STUDIES IN THE HUNT (NORD-TRØNDELAG HEALTH STUDY) POPULATION
400. Trude Teoline Nausthaug Rakvåg: PHARMACOGENETICS OF MORPHINE IN CANCER PAIN
401. Hanne Lehn: MEMORY FUNCTIONS OF THE HUMAN MEDIAL TEMPORAL LOBE STUDIED WITH fMRI
402. Randi Utne Holt: ADHESION AND MIGRATION OF MYELOMA CELLS – IN VITRO STUDIES –
403. Trygve Solstad: NEURAL REPRESENTATIONS OF EUCLIDEAN SPACE
404. Unn-Merete Fagerli: MULTIPLE MYELOMA CELLS AND CYTOKINES FROM THE BONE MARROW ENVIRONMENT; ASPECTS OF GROWTH REGULATION AND MIGRATION
405. Sigrid Bjørnelv: EATING– AND WEIGHT PROBLEMS IN ADOLESCENTS, THE YOUNG HUNT-STUDY
406. Mari Hoff: CORTICAL HAND BONE LOSS IN RHEUMATOID ARTHRITIS. EVALUATING DIGITAL X-RAY RADIOGRAMMETRY AS OUTCOME MEASURE OF DISEASE ACTIVITY, RESPONSE VARIABLE TO TREATMENT AND PREDICTOR OF BONE DAMAGE
407. Siri Bjørgen: AEROBIC HIGH INTENSITY INTERVAL TRAINING IS AN EFFECTIVE TREATMENT FOR PATIENTS WITH CHRONIC OBSTRUCTIVE PULMONARY DISEASE
408. Susanne Lindqvist: VISION AND BRAIN IN ADOLESCENTS WITH LOW BIRTH WEIGHT
409. Torbjørn Hergum: 3D ULTRASOUND FOR QUANTITATIVE ECHOCARDIOGRAPHY

410. Jørgen Urnes: PATIENT EDUCATION IN GASTRO-OESOPHAGEAL REFLUX DISEASE. VALIDATION OF A DIGESTIVE SYMPTOMS AND IMPACT QUESTIONNAIRE AND A RANDOMISED CONTROLLED TRIAL OF PATIENT EDUCATION
411. Elvar Eyjolfsson: 13C NMRS OF ANIMAL MODELS OF SCHIZOPHRENIA
412. Marius Steiro Fimland: CHRONIC AND ACUTE NEURAL ADAPTATIONS TO STRENGTH TRAINING
413. Øyvind Støren: RUNNING AND CYCLING ECONOMY IN ATHLETES; DETERMINING FACTORS, TRAINING INTERVENTIONS AND TESTING
414. Håkon Hov: HEPATOCYTE GROWTH FACTOR AND ITS RECEPTOR C-MET. AUTOCRINE GROWTH AND SIGNALING IN MULTIPLE MYELOMA CELLS
415. Maria Radtke: ROLE OF AUTOIMMUNITY AND OVERSTIMULATION FOR BETA-CELL DEFICIENCY. EPIDEMIOLOGICAL AND THERAPEUTIC PERSPECTIVES
416. Liv Bente Romundstad: ASSISTED FERTILIZATION IN NORWAY: SAFETY OF THE REPRODUCTIVE TECHNOLOGY
417. Erik Magnus Berntsen: PREOPERATIV PLANNING AND FUNCTIONAL NEURONAVIGATION – WITH FUNCTIONAL MRI AND DIFFUSION TENSOR TRACTOGRAPHY IN PATIENTS WITH BRAIN LESIONS
418. Tonje Strømmen Steigedal: MOLECULAR MECHANISMS OF THE PROLIFERATIVE RESPONSE TO THE HORMONE GASTRIN
419. Vidar Rao: EXTRACORPOREAL PHOTOCHEMOTHERAPY IN PATIENTS WITH CUTANEOUS T CELL LYMPHOMA OR GRAFT-vs-HOST DISEASE
420. Torkild Visnes: DNA EXCISION REPAIR OF URACIL AND 5-FLUOROURACIL IN HUMAN CANCER CELL LINES

2010

421. John Munkhaugen: BLOOD PRESSURE, BODY WEIGHT, AND KIDNEY FUNCTION IN THE NEAR-NORMAL RANGE: NORMALITY, RISK FACTOR OR MORBIDITY ?
422. Ingrid Castberg: PHARMACOKINETICS, DRUG INTERACTIONS AND ADHERENCE TO TREATMENT WITH ANTIPSYCHOTICS: STUDIES IN A NATURALISTIC SETTING
423. Jian Xu: BLOOD-OXYGEN-LEVEL-DEPENDENT-FUNCTIONAL MAGNETIC RESONANCE IMAGING AND DIFFUSION TENSOR IMAGING IN TRAUMATIC BRAIN INJURY RESEARCH
424. Sigmund Simonsen: ACCEPTABLE RISK AND THE REQUIREMENT OF PROPORTIONALITY IN EUROPEAN BIOMEDICAL RESEARCH LAW. WHAT DOES THE REQUIREMENT THAT BIOMEDICAL RESEARCH SHALL NOT INVOLVE RISKS AND BURDENS DISPROPORTIONATE TO ITS POTENTIAL BENEFITS MEAN?
425. Astrid Woodhouse: MOTOR CONTROL IN WHIPLASH AND CHRONIC NON-TRAUMATIC NECK PAIN
426. Line Rørstad Jensen: EVALUATION OF TREATMENT EFFECTS IN CANCER BY MR IMAGING AND SPECTROSCOPY
427. Trine Moholdt: AEROBIC EXERCISE IN CORONARY HEART DISEASE
428. Øystein Olsen: ANALYSIS OF MANGANESE ENHANCED MRI OF THE NORMAL AND INJURED RAT CENTRAL NERVOUS SYSTEM
429. Bjørn H. Grønberg: PEMETREXED IN THE TREATMENT OF ADVANCED LUNG CANCER
430. Vigdis Schnell Husby: REHABILITATION OF PATIENTS UNDERGOING TOTAL HIP ARTHROPLASTY WITH FOCUS ON MUSCLE STRENGTH, WALKING AND AEROBIC ENDURANCE PERFORMANCE
431. Torbjørn Øien: CHALLENGES IN PRIMARY PREVENTION OF ALLERGY. THE PREVENTION OF ALLERGY AMONG CHILDREN IN TRONDHEIM (PACT) STUDY.
432. Kari Anne Indredavik Evensen: BORN TOO SOON OR TOO SMALL: MOTOR PROBLEMS IN ADOLESCENCE
433. Lars Adde: PREDICTION OF CEREBRAL PALSY IN YOUNG INFANTS. COMPUTER BASED ASSESSMENT OF GENERAL MOVEMENTS
434. Magnus Fasting: PRE- AND POSTNATAL RISK FACTORS FOR CHILDHOOD ADIPOSITY
435. Vivi Talstad Monsen: MECHANISMS OF ALKYLATION DAMAGE REPAIR BY HUMAN AlkB HOMOLOGUES
436. Toril Skandsen: MODERATE AND SEVERE TRAUMATIC BRAIN INJURY. MAGNETIC RESONANCE IMAGING FINDINGS, COGNITION AND RISK FACTORS FOR DISABILITY

437. Ingeborg Smidesang: ALLERGY RELATED DISORDERS AMONG 2-YEAR OLDS AND ADOLESCENTS IN MID-NORWAY – PREVALENCE, SEVERITY AND IMPACT. THE PACT STUDY 2005, THE YOUNG HUNT STUDY 1995-97
438. Vidar Halsteinli: MEASURING EFFICIENCY IN MENTAL HEALTH SERVICE DELIVERY: A STUDY OF OUTPATIENT UNITS IN NORWAY
439. Karen Lehrmann Ægidius: THE PREVALENCE OF HEADACHE AND MIGRAINE IN RELATION TO SEX HORMONE STATUS IN WOMEN. THE HUNT 2 STUDY
440. Madelene Ericsson: EXERCISE TRAINING IN GENETIC MODELS OF HEART FAILURE
441. Marianne Klokk: THE ASSOCIATION BETWEEN SELF-REPORTED ECZEMA AND COMMON MENTAL DISORDERS IN THE GENERAL POPULATION. THE HORDALAND HEALTH STUDY (HUSK)
442. Tomas Ottemo Stølen: IMPAIRED CALCIUM HANDLING IN ANIMAL AND HUMAN CARDIOMYOCYTES REDUCE CONTRACTILITY AND INCREASE ARRHYTHMIA POTENTIAL – EFFECTS OF AEROBIC EXERCISE TRAINING
443. Bjarne Hansen: ENHANCING TREATMENT OUTCOME IN COGNITIVE BEHAVIOURAL THERAPY FOR OBSESSIVE COMPULSIVE DISORDER: THE IMPORTANCE OF COGNITIVE FACTORS
444. Mona Løvlien: WHEN EVERY MINUTE COUNTS. FROM SYMPTOMS TO ADMISSION FOR ACUTE MYOCARDIAL INFARCTION WITH SPECIAL EMPHASIS ON GENDER DIFFERECES
445. Karin Margaretha Gilljam: DNA REPAIR PROTEIN COMPLEXES, FUNCTIONALITY AND SIGNIFICANCE FOR REPAIR EFFICIENCY AND CELL SURVIVAL
446. Anne Byriel Walls: NEURONAL GLIAL INTERACTIONS IN CEREBRAL ENERGY – AND AMINO ACID HOMEOSTASIS – IMPLICATIONS OF GLUTAMATE AND GABA
447. Cathrine Fallang Knetter: MECHANISMS OF TOLL-LIKE RECEPTOR 9 ACTIVATION
448. Marit Følsvik Svindseth: A STUDY OF HUMILIATION, NARCISSISM AND TREATMENT OUTCOME IN PATIENTS ADMITTED TO PSYCHIATRIC EMERGENCY UNITS
449. Karin Elvenes Bakkelund: GASTRIC NEUROENDOCRINE CELLS – ROLE IN GASTRIC NEOPLASIA IN MAN AND RODENTS
450. Kirsten Brun Kjelstrup: DORSOVENTRAL DIFFERENCES IN THE SPATIAL REPRESENTATION AREAS OF THE RAT BRAIN
451. Roar Johansen: MR EVALUATION OF BREAST CANCER PATIENTS WITH POOR PROGNOSIS
452. Rigmor Myran: POST TRAUMATIC NECK PAIN. EPIDEMIOLOGICAL, NEURORADIOLOGICAL AND CLINICAL ASPECTS
453. Krisztina Kunszt Johansen: GENEALOGICAL, CLINICAL AND BIOCHEMICAL STUDIES IN *LRRK2* – ASSOCIATED PARKINSON'S DISEASE
454. Pål Gjerden: THE USE OF ANTICHOLINERGIC ANTIPARKINSON AGENTS IN NORWAY. EPIDEMIOLOGY, TOXICOLOGY AND CLINICAL IMPLICATIONS
455. Else Marie Huuse: ASSESSMENT OF TUMOR MICROENVIRONMENT AND TREATMENT EFFECTS IN HUMAN BREAST CANCER XENOGRAFTS USING MR IMAGING AND SPECTROSCOPY
456. Khalid S. Ibrahim: INTRAOPERATIVE ULTRASOUND ASSESSMENT IN CORONARY ARTERY BYPASS SURGERY – WITH SPECIAL REFERENCE TO CORONARY ANASTOMOSES AND THE ASCENDING AORTA
457. Bjørn Øglænd: ANTHROPOMETRY, BLOOD PRESSURE AND REPRODUCTIVE DEVELOPMENT IN ADOLESCENCE OF OFFSPRING OF MOTHERS WHO HAD PREECLAMPSIA IN PREGNANCY
458. John Olav Roaldset: RISK ASSESSMENT OF VIOLENT, SUICIDAL AND SELF-INJURIOUS BEHAVIOUR IN ACUTE PSYCHIATRY – A BIO-PSYCHO-SOCIAL APPROACH
459. Håvard Dalen: ECHOCARDIOGRAPHIC INDICES OF CARDIAC FUNCTION – NORMAL VALUES AND ASSOCIATIONS WITH CARDIAC RISK FACTORS IN A POPULATION FREE FROM CARDIOVASCULAR DISEASE, HYPERTENSION AND DIABETES: THE HUNT 3 STUDY
460. Beate André: CHANGE CAN BE CHALLENGING. INTRODUCTION TO CHANGES AND IMPLEMENTATION OF COMPUTERIZED TECHNOLOGY IN HEALTH CARE
461. Latha Nrugham: ASSOCIATES AND PREDICTORS OF ATTEMPTED SUICIDE AMONG DEPRESSED ADOLESCENTS – A 6-YEAR PROSPECTIVE STUDY

462. Håvard Bersås Nordgaard: TRANSIT-TIME FLOWMETRY AND WALL SHEAR STRESS ANALYSIS OF CORONARY ARTERY BYPASS GRAFTS – A CLINICAL AND EXPERIMENTAL STUDY

Cotutelle with University of Ghent: Abigail Emily Swillens: A MULTIPHYSICS MODEL FOR IMPROVING THE ULTRASONIC ASSESSMENT OF LARGE ARTERIES

2011

463. Marte Helene Bjørk: DO BRAIN RHYTHMS CHANGE BEFORE THE MIGRAINE ATTACK? A LONGITUDINAL CONTROLLED EEG STUDY
464. Carl-Jørgen Arum: A STUDY OF UROTHELIAL CARCINOMA: GENE EXPRESSION PROFILING, TUMORIGENESIS AND THERAPIES IN ORTHOTOPIC ANIMAL MODELS
465. Ingunn Harstad: TUBERCULOSIS INFECTION AND DISEASE AMONG ASYLUM SEEKERS IN NORWAY. SCREENING AND FOLLOW-UP IN PUBLIC HEALTH CARE
466. Leif Åge Strand: EPIDEMIOLOGICAL STUDIES AMONG ROYAL NORWEGIAN NAVY SERVICEMEN. COHORT ESTABLISHMENT, CANCER INCIDENCE AND CAUSE-SPECIFIC MORTALITY
467. Katrine Høyer Holgersen: SURVIVORS IN THEIR THIRD DECADE AFTER THE NORTH SEA OIL RIG DISASTER OF 1980. LONG-TERM PERSPECTIVES ON MENTAL HEALTH
468. MarianneWallenius: PREGNANCY RELATED ASPECTS OF CHRONIC INFLAMMATORY ARTHRITIDES: DISEASE ONSET POSTPARTUM, PREGNANCY OUTCOMES AND FERTILITY. DATA FROM A NORWEGIAN PATIENT REGISTRY LINKED TO THE MEDICAL BIRTH REGISTRY OF NORWAY
469. Ole Vegard Solberg: 3D ULTRASOUND AND NAVIGATION – APPLICATIONS IN LAPAROSCOPIC SURGERY
470. Inga Ekeberg Schjerve: EXERCISE-INDUCED IMPROVEMENT OF MAXIMAL OXYGEN UPTAKE AND ENDOTHELIAL FUNCTION IN OBESE AND OVERWEIGHT INDIVIDUALS ARE DEPENDENT ON EXERCISE-INTENSITY
471. Eva Veslemøy Tyldum: CARDIOVASCULAR FUNCTION IN PREECLAMPSIA – WITH REFERENCE TO ENDOTHELIAL FUNCTION, LEFT VENTRICULAR FUNCTION AND PRE-PREGNANCY PHYSICAL ACTIVITY
472. Benjamin Garzón Jiménez de Cisneros: CLINICAL APPLICATIONS OF MULTIMODAL MAGNETIC RESONANCE IMAGING
473. Halvard Knut Nilsen: ASSESSING CODEINE TREATMENT TO PATIENTS WITH CHRONIC NON-MALIGNANT PAIN: NEUROPSYCHOLOGICAL FUNCTIONING, DRIVING ABILITY AND WEANING
474. Eiliv Brenner: GLUTAMATE RELATED METABOLISM IN ANIMAL MODELS OF SCHIZOPHRENIA
475. Egil Jonsbu: CHEST PAIN AND PALPITATIONS IN A CARDIAC SETTING; PSYCHOLOGICAL FACTORS, OUTCOME AND TREATMENT
476. Mona Høysæter Fenstad: GENETIC SUSCEPTIBILITY TO PREECLAMPSIA : STUDIES ON THE NORD-TRØNDELAG HEALTH STUDY (HUNT) COHORT, AN AUSTRALIAN/NEW ZEALAND FAMILY COHORT AND DECIDUA BASALIS TISSUE
477. Svein Erik Gaustad: CARDIOVASCULAR CHANGES IN DIVING: FROM HUMAN RESPONSE TO CELL FUNCTION
478. Karin Torvik: PAIN AND QUALITY OF LIFE IN PATIENTS LIVING IN NURSING HOMES
479. Arne Solberg: OUTCOME ASSESSMENTS IN NON-METASTATIC PROSTATE CANCER
480. Henrik Sahlin Pettersen: CYTOTOXICITY AND REPAIR OF URACIL AND 5-FLUOROURACIL IN DNA
481. Pui-Lam Wong: PHYSICAL AND PHYSIOLOGICAL CAPACITY OF SOCCER PLAYERS: EFFECTS OF STRENGTH AND CONDITIONING
482. Ole Solheim: ULTRASOUND GUIDED SURGERY IN PATIENTS WITH INTRACRANIAL TUMOURS
483. Sten Roar Snare: QUANTITATIVE CARDIAC ANALYSIS ALGORITHMS FOR POCKET-SIZED ULTRASOUND DEVICES
484. Marit Skyrud Bratlie: LARGE-SCALE ANALYSIS OF ORTHOLOGS AND PARALOGS IN VIRUSES AND PROKARYOTES
485. Anne Elisabeth F. Isern: BREAST RECONSTRUCTION AFTER MASTECTOMY – RISK OF RECURRENCE AFTER DELAYED LARGE FLAP RECONSTRUCTION – AESTHETIC OUTCOME, PATIENT SATISFACTION, QUALITY OF LIFE AND SURGICAL RESULTS;

HISTOPATHOLOGICAL FINDINGS AND FOLLOW-UP AFTER PROPHYLACTIC MASTECTOMY IN HEREDITARY BREAST CANCER

486. Guro L. Andersen: CEREBRAL PALSY IN NORWAY – SUBTYPES, SEVERITY AND RISK FACTORS
487. Frode Kolstad: CERVICAL DISC DISEASE – BIOMECHANICAL ASPECTS
488. Bente Nordtug: CARING BURDEN OF COHABITANTS LIVING WITH PARTNERS SUFFERING FROM CHRONIC OBSTRUCTIVE PULMONARY DISEASE OR DEMENTIA
489. Mariann Gjervik Heldahl: EVALUATION OF NEOADJUVANT CHEMOTHERAPY IN LOCALLY ADVANCED BREAST CANCER BASED ON MR METHODOLOGY
490. Lise Tevik Løvseth: THE SUBJECTIVE BURDEN OF CONFIDENTIALITY
491. Marie Hjelmseth Aune: INFLAMMATORY RESPONSES AGAINST GRAM NEGATIVE BACTERIA INDUCED BY TLR4 AND NLRP12
492. Tina Strømdal Wik: EXPERIMENTAL EVALUATION OF NEW CONCEPTS IN HIP ARTHROPLASTY
493. Solveig Sigurdardottir: CLINICAL ASPECTS OF CEREBRAL PALSY IN ICELAND. A POPULATION-BASED STUDY OF PRESCHOOL CHILDREN
494. Arne Reimers: CLINICAL PHARMACOKINETICS OF LAMOTRIGINE
495. Monica Wegling: KULTURMENNESKETS BYRDE OG SYKDOMMENS VELSIGNELSE. KAN MEDISINSK UTREDNING OG INTERVENSJON HA EN SELVSTENDIG FUNKSJON UAVHENGIG AV DET KURATIVE?
496. Silje Alvestad: ASTROCYTE-NEURON INTERACTIONS IN EXPERIMENTAL MESIAL TEMPORAL LOBE EPILEPSY – A STUDY OF UNDERLYING MECHANISMS AND POSSIBLE BIOMARKERS OF EPILEPTOGENESIS
497. Javaid Nauman: RESTING HEART RATE: A MATTER OF LIFE OR DEATH – PROSPECTIVE STUDIES OF RESTING HEART RATE AND CARDIOVASCULAR RISK (THE HUNT STUDY, NORWAY)
498. Thuy Nguyen: THE ROLE OF C-SRC TYROSINE KINASE IN ANTIVIRAL IMMUNE RESPONSES
499. Trine Naalsund Andreassen: PHARMACOKINETIC, PHARMACODYNAMIC AND PHARMACOGENETIC ASPECTS OF OXYCODONE TREATMENT IN CANCER PAIN
500. Eivor Alette Laugsand: SYMPTOMS IN PATIENTS RECEIVING OPIOIDS FOR CANCER PAIN – CLINICAL AND PHARMACOGENETIC ASPECTS
501. Dorthe Stensvold: PHYSICAL ACTIVITY, CARDIOVASCULAR HEALTH AND LONGEVITY IN PATIENTS WITH METABOLIC SYNDROME
502. Stian Thoresen Aspenes: PEAK OXYGEN UPTAKE AMONG HEALTHY ADULTS – CROSS-SECTIONAL DESCRIPTIONS AND PROSPECTIVE ANALYSES OF PEAK OXYGEN UPTAKE, PHYSICAL ACTIVITY AND CARDIOVASCULAR RISK FACTORS IN HEALTHY ADULTS (20-90 YEARS)
503. Reidar Alexander Vigen: PATHOBIOLOGY OF GASTRIC CARCINOIDS AND ADENOCARCINOMAS IN RODENT MODELS AND PATIENTS. STUDIES OF GASTROCYSTOPLASTY, GENDER-RELATED FACTORS, AND AUTOPHAGY
504. Halvard Høilund-Kaupang: MODELS AND METHODS FOR INVESTIGATION OF REVERBERATIONS IN NONLINEAR ULTRASOUND IMAGING
505. Audhild Løhre: WELLBEING AMONG SCHOOL CHILDREN IN GRADES 1-10: PROMOTING AND ADVERSE FACTORS
506. Torgrim Tandstad: VOX POPULI. POPULATION-BASED OUTCOME STUDIES IN TESTICULAR CANCER
507. Anna Brenne Grønskag: THE EPIDEMIOLOGY OF HIP FRACTURES AMONG ELDERLY WOMEN IN NORD-TRØNDELAG. HUNT 1995-97, THE NORD-TRØNDELAG HEALTH STUDY
508. Kari Ravndal Risnes: BIRTH SIZE AND ADULT MORTALITY: A SYSTEMATIC REVIEW AND A LONG-TERM FOLLOW-UP OF NEARLY 40 000 INDIVIDUALS BORN AT ST. OLAV UNIVERSITY HOSPITAL IN TRONDHEIM 1920-1960
509. Hans Jakob Bøe: LONG-TERM POSTTRAUMATIC STRESS AFTER DISASTER – A CONTROLLED STUDY OF SURVIVORS' HEALTH 27 YEARS AFTER THE CAPSIZED NORTH SEA OIL RIG
510. Cathrin Barbara Canto, Cotutelle with University of Amsterdam: LAYER SPECIFIC INTEGRATIVE PROPERTIES OF ENTORHINAL PRINCIPAL NEURONS
511. Ioanna Sandvig: THE ROLE OF OLFACTORY ENSHEATHING CELLS, MRI, AND BIOMATERIALS IN TRANSPLANT-MEDIATED CNS REPAIR

512. Karin Fahl Wader: HEPATOCYTE GROWTH FACTOR, C-MET AND SYNDECAN-1 IN MULTIPLE MYELOMA
513. Gerd Tranø: FAMILIAL COLORECTAL CANCER
514. Bjarte Bergstrøm: INNATE ANTIVIRAL IMMUNITY – MECHANISMS OF THE RIG-I-MEDIATED RESPONSE
515. Marie Søfteland Sandvei: INCIDENCE, MORTALITY, AND RISK FACTORS FOR ANEURYSMAL SUBARACHNOID HEMORRHAGE. PROSPECTIVE ANALYZES OF THE HUNT AND TROMSØ STUDIES
516. Mary-Elizabeth Bradley Eilertsen: CHILDREN AND ADOLESCENTS SURVIVING CANCER: PSYCHOSOCIAL HEALTH, QUALITY OF LIFE AND SOCIAL SUPPORT
517. Takaya Saito: COMPUTATIONAL ANALYSIS OF REGULATORY MECHANISM AND INTERACTIONS OF MICRORNAS

Godkjent for disputas, publisert post mortem: Eivind Jullumstrø: COLORECTAL CANCER AT LEVANGER HOSPITAL 1980-2004

518. Christian Gutvik: A PHYSIOLOGICAL APPROACH TO A NEW DECOMPRESSION ALGORITHM USING NONLINEAR MODEL PREDICTIVE CONTROL
519. Ola Storrø: MODIFICATION OF ADJUVANT RISK FACTOR BEHAVIOURS FOR ALLERGIC DISEASE AND ASSOCIATION BETWEEN EARLY GUT MICROBIOTA AND ATOPIC SENSITIZATION AND ECZEMA. EARLY LIFE EVENTS DEFINING THE FUTURE HEALTH OF OUR CHILDREN
520. Guro Fanneløb Giskeødegård: IDENTIFICATION AND CHARACTERIZATION OF PROGNOSTIC FACTORS IN BREAST CANCER USING MR METABOLOMICS
521. Gro Christine Christensen Løhaugen: BORN PRETERM WITH VERY LOW BIRTH WEIGHT – NEVER ENDING COGNITIVE CONSEQUENCES?
522. Sigrid Nakrem: MEASURING QUALITY OF CARE IN NURSING HOMES – WHAT MATTERS?
523. Brita Pukstad: CHARACTERIZATION OF INNATE INFLAMMATORY RESPONSES IN ACUTE AND CHRONIC WOUNDS

2012

524. Hans H. Wasmuth: ILEAL POUCHES
525. Inger Økland: BIASES IN SECOND-TRIMESTER ULTRASOUND DATING RELATED TO PREDICTION MODELS AND FETAL MEASUREMENTS
526. Bjørn Mørkedal: BLOOD PRESSURE, OBESITY, SERUM IRON AND LIPIDS AS RISK FACTORS OF ISCHAEMIC HEART DISEASE
527. Siver Andreas Moestue: MOLECULAR AND FUNCTIONAL CHARACTERIZATION OF BREAST CANCER THROUGH A COMBINATION OF MR IMAGING, TRANSCRIPTOMICS AND METABOLOMICS
528. Guro Aune: CLINICAL, PATHOLOGICAL, AND MOLECULAR CLASSIFICATION OF OVARIAN CARCINOMA
529. Ingrid Alsos Lian: MECHANISMS INVOLVED IN THE PATHOGENESIS OF PRE-ECLAMPSIA AND FETAL GROWTH RESTRICTION. TRANSCRIPTIONAL ANALYSES OF PLACENTAL AND DECIDUAL TISSUE
530. Karin Solvang-Garten: X-RAY REPAIR CROSS-COMPLEMENTING PROTEIN 1 – THE ROLE AS A SCAFFOLD PROTEIN IN BASE EXCISION REPAIR AND SINGLE STRAND BREAK REPAIR
531. Toril Holien: BONE MORPHOGENETIC PROTEINS AND MYC IN MULTIPLE MYELOMA
532. Rooyen Mavenyengwa: *STREPTOCOCCUS AGALACTIAE* IN PREGNANT WOMEN IN ZIMBABWE: EPIDEMIOLOGY AND SEROTYPE MARKER CHARACTERISTICS
533. Tormod Rimehaug: EMOTIONAL DISTRESS AND PARENTING AMONG COMMUNITY AND CLINIC PARENTS
534. Maria Dung Cao: MR METABOLIC CHARACTERIZATION OF LOCALLY ADVANCED BREAST CANCER – TREATMENT EFFECTS AND PROGNOSIS
535. Mirta Mittelstedt Leal de Sousa: PROTEOMICS ANALYSIS OF PROTEINS INVOLVED IN DNA BASE REPAIR AND CANCER THERAPY
536. Halfdan Petursson: THE VALIDITY AND RELEVANCE OF INTERNATIONAL CARDIOVASCULAR DISEASE PREVENTION GUIDELINES FOR GENERAL PRACTICE
537. Marit By Rise: LIFTING THE VEIL FROM USER PARTICIPATION IN CLINICAL WORK – WHAT IS IT AND DOES IT WORK?

538. Lene Thoresen: NUTRITION CARE IN CANCER PATIENTS. NUTRITION ASSESSMENT: DIAGNOSTIC CRITERIA AND THE ASSOCIATION TO SURVIVAL AND HEALTH-RELATED QUALITY OF LIFE IN PATIENTS WITH ADVANCED COLORECTAL CARCINOMA
539. Berit Doseth: PROCESSING OF GENOMIC URACIL IN MAN AND MOUSE
540. Gro Falkenér Bertheussen: PHYSICAL ACTIVITY AND HEALTH IN A GENERAL POPULATION AND IN CANCER SURVIVORS – METHODOLOGICAL, OBSERVATIONAL AND CLINICAL ASPECTS
541. Anne Kari Knudsen: CANCER PAIN CLASSIFICATION
542. Sjur Urdson Gjerald: A FAST ULTRASOUND SIMULATOR
543. Harald Edvard Mølmen Hansen: CARDIOVASCULAR EFFECTS OF HIGH INTENSITY AEROBIC INTERVAL TRAINING IN HYPERTENSITIVE PATIENTS, HEALTHY AGED AND YOUNG PERSONS
544. Sasha Gulati: SURGICAL RESECTION OF HIGH-GRADE GLIOMAS
545. John Chr. Fløvig: FREQUENCY AND EFFECT OF SUBSTANCES AND PSYCHOACTIVE MEDICATIONS THE WEEK BEFORE ADMISSION TO AN ACUTE PSYCHIATRIC DEPARTMENT
546. Kristin Moksnes Husby: OPTIMIZING OPIOID TREATMENT FOR CANCER PAIN – CLINICAL AND PHARMACOLOGICAL ASPECTS
547. Audun Hanssen-Bauer: X-RAY REPAIR CROSS-COMPLEMENTING PROTEIN 1 ASSOCIATED MULTIPROTEIN COMPLEXES IN BASE EXCISION REPAIR
548. Marit Saunes: ECZEMA IN CHILDREN AND ADOLESCENTS – EPIDEMIOLOGY, COURSE AND IMPACT. THE PREVENTION OF ALLERGY AMONG CHILDREN IN TRONDHEIM (PACT) STUDY, YOUNG-HUNT 1995-97
549. Guri Kaurstad: CARDIOMYOCYTE FUNCTION AND CALCIUM HANDLING IN ANIMAL MODELS OF INBORN AND ACQUIRED MAXIMAL OXYGEN UPTAKE
550. Kristian Svendsen: METHODOLOGICAL CHALLENGES IN PHARMACOEPIDEMIOLOGICAL STUDIES OF OPIOID CONSUMPTION
551. Signe Nilssen Stafne: EXERCISE DURING PREGNANCY
552. Marius Widerøe: MAGNETIC RESONANCE IMAGING OF HYPOXIC-ISCHEMIC BRAIN INJURY DEVELOPMENT IN THE NEWBORN RAT – MANGANESE AND DIFFUSION CONTRASTS
553. Andreas Radtke: MOLECULAR METHODS FOR TYPING *STREPTOCOCCUS AGALACTIAE* WITH SPECIAL EMPHASIS ON THE DEVELOPMENT AND VALIDATION OF A MULTI-LOCUS VARIABLE NUMBER OF TANDEM REPEATS ASSAY (MLVA)
554. Thor Wilhelm Bjelland: PHARMACOLOGICAL ASPECTS OF THERAPEUTIC HYPOTHERMIA
555. Caroline Hild Hakvåg Pettersen: THE EFFECT OF OMEGA-3 POLYUNSATURATED FATTY ACIDS ON HUMAN CANCER CELLS – MOLECULAR MECHANISMS INVOLVED
556. Inga Thorsen Vengen: INFLAMMATION AND ATHEROSCLEROSIS – RISK ASSOCIATIONS IN THE HUNT SURVEYS
557. Elisabeth Balstad Magnussen: PREECLAMPSIA, PRETERM BIRTH AND MATERNAL CARDIOVASCULAR RISK FACTORS
558. Monica Unsgaard-Tøndel: MOTOR CONTROL EXERCISES FOR PATIENTS WITH LOW BACK PAIN
559. Lars Erik Sande Laugsand: INSOMNIA AND RISK FOR CARDIOVASCULAR DISEASE
560. Kjersti Grønning: PATIENT EDUCATION AND CHRONIC INFLAMMATORY POLYARTHRITIS – COPING AND EFFECT
561. Hanne Gro Wenzel: PRE AND POST-INJURY HEALTH IN PERSONS WITH WHIPLASH: THE HUNT STUDY. EXPLORATION OF THE FUNCTIONAL SOMATIC MODEL FOR CHRONIC WHIPLASH
562. Øystein Grimstad: TOLL-LIKE RECEPTOR-MEDIATED INFLAMMATORY RESPONSES IN KERATINOCYTES
563. Håkon Olav Leira: DEVELOPMENT OF AN IMAGE GUIDANCE RESEARCH SYSTEM FOR BRONCHOSCOPY
564. Michael A. Lang: DIVING IN EXTREME ENVIRONMENTS: THE SCIENTIFIC DIVING EXPERIENCE

565. Helena Bertilsson: PROSTATE CANCER-TRANSLATIONAL RESEARCH. OPTIMIZING TISSUE SAMPLING SUITABLE FOR HISTOPATHOLOGIC, TRANSCRIPTOMIC AND METABOLIC PROFILING
566. Kirsten M. Selnæs: MR IMAGING AND SPECTROSCOPY IN PROSTATE AND COLON CANCER DIAGNOSTICS
567. Gunvor Steine Fosnes: CONSTIPATION AND DIARRHOEA. EFFECTIVENESS AND ADVERSE EFFECTS OF DRUGS
568. Areej Elkamil: SPASTIC CEREBRAL PALSY: RISK FACTORS, BOTULINUM TOXIN USE AND PREVENTION OF HIP DISLOCATION
569. Ruth Derdikman Eiron: SYMPTOMS OF ANXIETY AND DEPRESSION AND PSYCHOSOCIAL FUNCTION IN MALES AND FEMALES FROM ADOLESCENCE TO ADULTHOOD: LONGITUDINAL FINDINGS FROM THE NORD-TRØNDELAG HEALTH STUDY
570. Constantin Sergiu Jianu: PROTON PUMP INHIBITORS AND GASTRIC NEOPLASIA IN MAN
571. Øystein Finset Sørdal: THE ROLE OF GASTRIN AND THE ECL CELL IN GASTRIC CARCINOGENESIS
572. Lisbeth Østgaard Rygg: GROUP EDUCATION FOR PATIENTS WITH TYPE 2 DIABETES – NEEDS, EXPERIENCES AND EFFECTS
573. Viola Lobert: IDENTIFICATION OF NOVEL REGULATORS OF EPITHELIAL POLARITY AND CELL MIGRATION
574. Maria Tunset Grinde: CHARACTERIZATION OF BREAST CANCER USING MR METABOLOMICS AND GENE EXPRESSION ANALYSIS
575. Grete Kjelvik: HUMAN ODOR IDENTIFICATION STUDIES IN HEALTHY INDIVIDUALS, MILD COGNITIVE IMPAIRMENT AND ALZHEIMER'S DISEASE
576. Tor Eivind Bernstein: RECTAL CANCER SURGERY. PROGNOSTIC FACTORS RELATED TO TREATMENT
577. Kari Sand: INFORMED CONSENT DOCUMENTS FOR CANCER RESEARCH: TEXTUAL AND CONTEXTUAL FACTORS OF RELEVANCE FOR UNDERSTANDING
578. Laurent Francois Thomas: EFFECTS OF SINGLE-NUCLEOTIDE POLYMORPHISMS ON microRNA-BASED GENE REGULATION AND THEIR ASSOCIATION WITH DISEASE
579. Øystein Sandanger: THE INNATE IMMUNE SYSTEM: A PARADOXICAL MEDIATOR OF HOST DEFENSE, TISSUE REPAIR AND COLLATERAL DAMAGE
580. Line Knutsen Lund: MENTAL HEALTH IN LOW BIRTH WEIGHT INDIVIDUALS APPROACHING ADULTHOOD
581. Nils Kristian Skjærvold: AUTOMATED BLOOD GLUCOSE CONTROL – DEVELOPMENT AND TESTING OF AN ARTIFICIAL ENDOCRINE PANCREAS USING AV NOVEL INTRAVASCULAR GLUCOSE MONITOR AND A NEW APPROACH TO INSULIN PHARMACOLOGY
582. Håvard Kallestad: SLEEP DISTURBANCE: CLINICAL SIGNIFICANCE IN MENTAL HEALTH CARE AND COGNITIVE FACTORS
583. Anders Wallenius: URACIL-DNA GLYCOSYLASE, ACTIVATION-INDUCED DEAMINASE AND REGULATION OF ADAPTIVE IMMUNE RESPONSES
584. Gry Børmark Hoftun: CHRONIC NON-SPECIFIC PAIN IN ADOLESCENCE PREVALENCE, DISABILITY, AND ASSOCIATED FACTORS – YOUNG-HUNT AND HUNT 3, 2006-2008
585. Elisabeth Hansen: THE SIGNIFICANCE OF RESISTANCE TRAINING AND PSYCHOBIOLOGY IN PRIMARY PREVENTION OF TYPE 2 DIABETES AMONG PEOPLE WITH IMPAIRED GLUCOSE TOLERANCE
586. Ragnhild Omli: URINARY INCONTINENCE AND URINARY TRACT INFECTIONS IN THE ELDERLY: RISK FACTORS AND CONSEQUENCES
587. Christina Sæten Fjeldbo: GASTRIN-MEDIATED REGULATION OF GENE EXPRESSION; A SYSTEMS BIOLOGY APPROACH
588. Yunita Widyastuti: RISK FACTORS FOR COMMON COMPLICATIONS FOLLOWING ADULT HEART SURGERY
589. Anders Thorstensen: 2D AND 3D ECHOCARDIOGRAPHY DURING INOTROPIC ALTERATIONS AND AFTER RECENT MYOCARDIAL INFARCTION